



UNIVERSITÀ
DEGLI STUDI
DI PADOVA

Sede Amministrativa: Università degli Studi di Padova

Dipartimento di Biologia

SCUOLA DI DOTTORATO DI RICERCA IN : BIOSCIENZE E BIOTECHNOLOGIE

INDIRIZZO: GENETICA E BIOLOGIA MOLECOLARE DELLO SVILUPPO

CICLO XXVI

***Drosophila melanogaster* AS A MODEL OF MITOCHONDRIAL BIOLOGY, MITOCHONDRIAL
DISEASE AND NEUROLOGICAL DISORDERS**

Direttore della Scuola : Ch.mo Prof. Giuseppe Zanotti

Coordinatore d'indirizzo: Ch.mo Prof. Rodolfo Costa

Supervisore :Ch.mo Prof. Mauro A. Zordan

Dottorando : Antonia Piazzesi

TABLE OF CONTENTS

List Of Abbreviations	1
Abstract (English)	3
Abstract (Italiano)	5
GENERAL ASSUMPTIONS: The use of <i>Drosophila melanogaster</i> as an animal model	7
<i>i.i</i> : The Use of <i>Drosophila melanogaster</i> : a Brief History	9
<i>i.ii</i> : The Molecular Techniques Available in <i>Drosophila</i>	10
<i>i.ii.a</i> : The UAS-GAL4 System.....	10
<i>i.ii.b</i> : The FRT-FLP System.....	12
<i>i.ii.c</i> : Balancer Chromosomes	13
<i>i.iii</i> : Biology of <i>Drosophila melanogaster</i> and its Relevance as a Model.....	14
<i>i.iii.a</i> : <i>Drosophila</i> Life Cycle.....	15
<i>i.iii.b</i> : <i>Drosophila</i> Morphology.....	16
<i>i.iii.c</i> : The <i>Drosophila</i> Neuromuscular Junction.....	17
CHAPTER I: <i>drim2</i>	19
Abstract: <i>drim2</i> is essential for correct mitochondrial function in <i>Drosophila melanogaster</i>	21
INTRODUCTION	23
1.1 Mitochondrial Biogenesis and Function	25
1.1.1: Mitochondrial DNA Replication	26
1.1.2: Mitochondrial dNTP Synthesis	27
1.1.3: Mitochondria and Iron Homeostasis	29
1.2 Mitochondrial Diseases in Humans	30

1.2.1: Mitochondrial Diseases of mtDNA Replication.....	30
1.2.2: Mitochondrial Diseases Related to dNTP Metabolism	31
1.2.3: Mitochondrial Diseases Related to Mitochondrial Carriers	31
1.3: <i>Drosophila melanogaster</i> as a model for mitochondrial disease.....	32
1.4: RIM2 in <i>Saccharomyces cerevisiae</i>	33
1.4.1: Discovery and Characterization of <i>RIM2</i>	33
1.4.2: <i>RIM2</i> and Iron Transport	34
1.5: Mitochondrial Carriers in Humans.....	35
1.5.1: The Mitochondrial Carrier Family	35
1.5.2: <i>PNC-1</i>	36
1.5.3: <i>PNC-1</i> and Disease.....	37
1.5.4: <i>SLC25A36</i>	38
MATERIALS AND METHODS.....	39
2.1: Maintenance of Fly Stocks	41
2.2: <i>In vivo</i> Characterization of <i>drim2</i>	41
2.2.1: <i>drim2</i> K.O. Line.....	41
2.2.2: Characterization of Mutant Larval Size.....	42
2.2.3: Larval Locomotor Activity	43
2.2.4: Larval Behaviour	43
2.2.5: Characterization of the Neuromuscular Junction	44
2.2.6: Analysis of Muscle Mitochondrial Pattern.....	44
2.2.7: Mitochondrial Respiration of Mutant Larvae	45
2.3: <i>In vitro</i> Analysis of <i>drim2</i> Expression.....	46

2.3.1: RNA Extraction and Retrotranscription	46
2.3.2: Cloning PCR of <i>drim2</i> Gene	47
2.3.3: Cloning into pGEM [®] -T Easy Vector.....	48
2.3.4: Cloning in pACT Vector	49
2.3.5: Maintaining <i>Drosophila</i> S2R+ cells in Culture.....	50
2.3.6: Transfecting <i>Drosophila</i> S2R+ Cells	51
2.3.7: Quantitative Real-Time PCR of <i>drim2</i>	52
2.3.8: Western Blot Analysis of <i>drim2</i>	53
2.3.9: Immunolocalization of <i>drim2</i>	54
2.4: Rescuing the <i>drim2</i> K.O. Phenotype.....	54
2.4.1: Generating Rescue Lines	54
2.4.2: DNA Extraction from Flies	55
2.4.3: Screening of Rescue Lines by PCR.....	55
2.4.4: Using UAS/GAL4 System to Express “Rescue” Construct.....	57
2.4.5: Testing qRT-PCR Primer Efficiency.....	57
2.4.6: Verification of Presence of Construct mRNA.....	58
2.4.7: Verification of Presence of Construct Protein.....	58
2.4.8: Vitality Analysis of “Rescued” Flies.....	59
2.4.9: <i>In vivo</i> Analysis of “Rescued” Larvae.....	59
2.4.10: Generation of “Double Rescue” Lines	59
2.4.11: Phylogenetic Analysis of <i>PNC-1</i> and <i>SLC25A36</i>	60
RESULTS.....	61
3.1: Characterization of <i>drim2</i> K.O. Line	63

3.1.1: Initial Observations.....	63
3.1.2: Characterization of Mutant Larval Size.....	63
3.1.3: Locomotor Activity of <i>drim2</i> Mutant Larvae.....	65
3.1.4: Analysis of Mitochondrial Muscle Pattern.....	66
3.1.5: Mitochondrial Respiration in <i>drim2</i> K.O.Larvae	67
3.1.6: Mitochondrial Gene Transcription in <i>drim2</i> Mutants.....	68
3.1.7: Characterization of the Neuromuscular Junction in <i>drim2</i> Mutant Larvae .	69
3.1.8: Analysis of Sensory Capabilities in Mutant Larvae	73
3.1.9: Evaluating Iron Content in Mutant Larval Proteins	75
3.2: <i>In vitro</i> Localization of <i>drim2</i> Protein	76
3.2.1: Expression of Tagged <i>drim2</i> <i>in vitro</i>	76
3.2.2: Immunolocalization of <i>drim2</i> Protein.....	78
3.3: Rescuing the <i>drim2</i> Mutant Phenotype	78
3.3.1: Final Crosses and PCR Confirmation of Rescue Lines.....	79
3.3.2: Expressing <i>drim2</i> , <i>PNC-1</i> and <i>SLC25A36</i> in a Mutant Background.....	79
3.3.3: Verification of Presence of Construct	81
3.3.4: Vitality Analysis of Rescued Flies	82
3.3.5: Locomotor Activity of Rescued Larvae	83
3.3.6: Neuromuscular Junction Morphology of Rescued Larvae	84
3.3.7: Mitochondrial Respiration of Rescued Larvae	86
3.3.8: Transcription of Mitochondrial Genes in Rescued Larvae.....	87
3.3.9: Protein Iron Content of Rescued Larvae	87
3.3.10: Phylogenetic Analysis of <i>PNC-1</i> and <i>SLC25A36</i>	88

DISCUSSION	93
4.1: Characterization of <i>drim2</i> in <i>Drosophila melanogaster</i>	95
4.1.1: <i>drim2</i> is Essential for <i>Drosophila melanogaster</i> Survival	95
4.1.2: <i>drim2</i> is a Mitochondrial Protein and is Essential for Correct Mitochondrial Function in <i>Drosophila melanogaster</i>	96
4.1.3: Mitochondrial DNA Integrity is Compromised in <i>drim2</i> Mutants.....	97
4.1.4: Evidence that <i>drim2</i> is a Mitochondrial dNTP Transporter	97
4.1.5: There is No Evidence that <i>drim2</i> is an Iron Transporter in <i>Drosophila melanogaster</i>	98
4.1.6: Knock-out of <i>drim2</i> Causes Severe Secondary Effects in <i>Drosophila melanogaster</i>	98
4.2: Characterization of <i>drim2</i>, <i>PNC-1</i> and <i>SLC25A36</i> Expression in a <i>drim2</i> K.O. Background	100
4.2.1: <i>drim2</i> Mutants Expressing Any of the Three Genes Reach Adulthood ...	100
4.2.2: <i>PNC-1</i> and <i>SLC25A36</i> Can Rescue Mitochondrial Function in the Absence of <i>drim2</i>	101
4.2.3: Is There Any Indication of What <i>SLC25A36</i> Function Might Be in Human Cells?.....	101
4.2.4: Evolutionary History of <i>PNC-1</i> and <i>SLC25A36</i>	102
4.3: Concluding Remarks	103
<i>Functional characterization of <i>drim2</i>, the <i>Drosophila melanogaster</i> homolog of the yeast mitochondrial deoxynucleotide transporter</i>	105
CHAPTER II: <i>dTTC19</i>	149
Abstract: Further characterization of the <i>Drosophila dTTC19</i> mutant, a model for mitochondrial disease of the ETC	151
INTRODUCTION	153

1.1 The Electron Transport Chain	155
1.1.1: Complex III Structure and Function	156
1.1.2: Complex III Assembly	157
1.2 Complex III Dysfunction and Disease	157
1.2.1: Mitochondrial Diseases Tied to Mutations in Complex III-encoding Genes	158
1.2.2: Complex III Assembly Factors and Disease	159
1.3: Tetratricopeptide 19	159
1.3.1: Human TTC19	160
1.3.2: TTC19 and Mitochondrial Disease	160
1.3.3: <i>dTTC19</i> in <i>Drosophila</i>	160
MATERIALS AND METHODS	163
2.1: Generating “Rescue” Lines for the dTTC19 Mutant	165
2.1.1: Cloning the <i>dTTC19</i> Gene	165
2.1.2: Cloning <i>dTTC19</i> into pUAST Vector	165
2.1.3: Screening for Positive pUAST Colonies	166
2.1.4: Creating Rescue lines in a <i>dTTC19</i> K.O. Background	166
2.2: Locomotor Activity of <i>dTTC19</i> Mutant Larvae and Adults	167
2.3: Visual Capacity of <i>dTTC19</i> Mutant Flies	168
2.4: Sensory Capabilities of <i>dTTC19Δ</i> Larvae	168
RESULTS	171
3.1: Characterization of <i>dTTC19Δ</i> Larvae	173
3.1.1: Larval Locomotor Activity	173
3.1.2: Larval Behaviour.....	174

3.2 Characterization of <i>dTTC19</i> Mutant Adults	176
3.2.1: In Depth Analysis of Locomotor Activity	176
3.2.2: Visual Acuity in <i>dTTC19</i> Mutant Adults	178
3.3: Generation of <i>dTTC19</i> Rescue Line	180
DISCUSSION	183
4.1: Characterization of <i>dTTC19</i> Mutant Larvae	185
4.1.1: <i>dTTC19</i> Mutant Larvae Have a Previously Unnoticed Mutant Phenotype	185
4.1.2: Possible Effect of Heteroplasmy in <i>dTTC19</i> Mutants?	185
4.2: Characterization of <i>dTTC19</i> Mutant Adults	187
4.2.1: <i>dTTC19</i> Mutant Adults Exhibit Visual Defects Similar to <i>white</i> ¹¹¹⁸ flies	187
4.2.2: <i>dTTC19</i> Mutant Adults have Defects in Locomotor Activity Independent of Exploratory Tendencies.....	188
4.3: Future Prospects for <i>dTTC19</i> Rescue Lines	188
4.3.1: Generation of <i>Drosophila</i> Rescue Lines.....	188
4.3.2: Generation of Human TTC19 Rescue Lines was Unsuccessful	189
 CHAPTER III: A NEW PROTOCOL FOR STUDYING SOCIAL BEHAVIOUR IN <i>DROSOPHILA</i>	 191
Abstract: A new protocol for using social behaviour in <i>Drosophila melanogaster</i> as a model for neurological disorders with antisocial behaviour	193
INTRODUCTION	195
1.1: Neurotransmission	197
1.1.1: Neurotransmission: An Overview.....	197
1.1.2: Dopamine	198
1.1.3: SNAP-25	199

1.2: Neurological Disorders Involving Sociality Problems	200
1.2.1: Dopamine and Disease.....	201
1.2.2: SNAP-25 and Disease.....	202
1.2.3: Neurological Disorders of Childhood Deprivation.....	203
1.3: Social Behaviour in <i>Drosophila</i>	204
1.3.1: SNAP-25 and <i>Drosophila</i>	205
1.3.1.1: The <i>Drosophila</i> SNAP-25 Mutant.....	206
1.3.2: Dopamine Dysfunction and <i>Drosophila</i> Behaviour.....	206
1.3.2.1: The <i>pale</i> ⁴ Mutant.....	207
1.3.2.2: The <i>ebony</i> Mutant.....	207
MATERIALS AND METHODS	209
2.1: Maintaining Fly Stocks	211
2.1.1: SNAP-25 Mutants.....	211
2.1.2: <i>e</i> ¹ ; <i>pale</i> ⁴ /TM3 Mutant Line.....	211
2.2: Adult Locomotor Activity	212
2.3: Testing Visual Acuity in <i>Drosophila</i>	213
2.4: Analyzing Social Behavior in Flies	213
RESULTS	217
3.1: Social Behaviour in <i>Drosophila melanogaster</i>	219
3.1.1: Social Behaviour in wild-type Flies.....	220
3.1.2: Social Behaviour in <i>white</i> ¹¹¹⁸ and <i>sine oculis</i> Flies.....	221
3.1.3: The Effect of Isolation on Social Behaviour.....	224
3.1.4: Differences Between wild-type Lines.....	225

3.2: Dopamine Dysregulation and Social Behaviour	226
3.2.1: Visual Acuity in Dopamine Mutants	227
3.2.2: Social Behaviour in Dopamine Mutants	228
3.3: Characterization of SNAP-25^{R206D} Mutants	230
3.3.1: Locomotor Activity of SNAP-25 Mutants.....	230
3.3.2: Social Behaviour in SNAP-25 Mutants	232
3.3.3: Marking Flies for Mixed Social Groups	234
DISCUSSION	237
4.1: Social Behaviour in <i>Drosophila melanogaster</i>	239
4.1.1: <i>Drosophila melanogaster</i> Exhibit Social Behaviour	239
4.1.2: <i>Drosophila</i> Social Behaviour Relies on Visual Acuity	239
4.1.3: Previous Social Contact can Affect Social Behaviour in <i>Drosophila</i>	240
4.1.4: Circadian Rhythms Probably Affect Social Behaviour	241
4.1.5: Why are there Differences Between wild-type Lines?	242
4.2 <i>Drosophila melanogaster</i> as a Model for Antisocial Behaviour	243
4.2.1: Mutants Heterozygous for <i>pale</i> ⁴ Mutation are Antisocial	243
4.2.2: Decreased Dopamine has an Effect on Social Behaviour.....	244
4.2.3: Stubble Phenotype has no Effect on Social Behaviour.....	244
4.2.4: Both <i>pale</i> ⁴ /+ and TM3/+ Flies have Normal Visual Acuity	245
4.2.5: <i>ebony</i> Mutants have Social Defects	247
4.3: The Effect of the SNAP-25^{R206D} Point-Mutation on <i>Drosophila</i> Behaviour	247
4.3.1: SNAP-25 Mutants Socialize as <i>white</i> ¹¹¹⁸ Flies do	248
4.3.2: SNAP-25 Mutants have Locomotor Activity Defects	249

4.3.3: Flies can be Marked on the Abdomen but not on the Scutellum	249
4.4: Concluding Remarks	250
BIBLIOGRAPHY	251
APPENDIX I: Solution Recipes	269
APPENDIX II: Vector Maps.....	277

LIST OF ABBREVIATIONS:

ADHD – Attention Deficit Hyperactivity Disorder
adPEO – autosomal-dominant progressive external ophthalmoplegia
BSA – bovine serum albumin
CDS – coding DNA sequence
CNS – central nervous system
COX – cytochrome *c* oxidase
CSA – congenital sideroblastic anaemia
DA – dopamine
d.f. – degrees of freedom
dGK – deoxyguanosine kinase
DNC – deoxynucleotide carrier
dNTP – deoxynucleotide triphosphates
DTH – *Drosophila* tyrosine hydroxylase
EM – electron microscopy
EMT – epithelial-to-mesenchymal transition
ETC – electron transport chain
FBS – fetal bovine serum
fps – frames per second
GFP – green fluorescent protein
IMM – inner mitochondrial membrane
ISCs – iron sulphur-containing clusters
K. D. – knock-down
K. O. – knock-out
LHON – Leber Hereditary Optic Neuropathy
LS – Leigh Syndrome
MCF – Mitochondrial Carrier Family
MCPHA – Amish lethal microcephaly
MDS – mitochondrial depletion syndrome
mEPSP – miniature excitatory postsynaptic potentials
MNGIE – mitochondrial neurogastrointestinal encephalomyopathy
MS – multiple sclerosis

mtDNA – mitochondrial DNA
mt-dNTPs – mitochondrial deoxynucleotide triphosphates
NBAD – N- β -alanyl dopamine
NCBI – National Centre for Biotechnology Information
nf – not fluorescent
NMJ – neuromuscular junction
ns – not significant
NT – neurotransmitter
OCR – oxygen consumption rate
O_H – heavy strand origin of replication
O_L – light strand origin of replication
OMM – outer mitochondrial membrane
OXPHOS – Oxidative Phosphorylation
PCR – Polymerase Chain Reaction
PD – Parkinson's Disease
PEO – progressive external ophthalmoplegia
Q – Ubiquinone
qRT-PCR – Quantitative Real-Time Polymerase Chain Reaction
ROS – Reactive Oxygen Species
RT – room temperature
S. E. – standard error
SNc – substantia nigra pars compacta
TCA – tricarboxylic acid cycle
TK2 – Thymidine kinase-2
TH – tyrosine hydroxylase
UAS – Upstream Activating Sequence
UQH₂ – ubiquinol
WT – wild-type
ZT – zeitgeber time

***Drosophila melanogaster* as a model for mitochondrial biology, mitochondrial disease and neurological disorders.**

Drosophila melanogaster has a long history of being used as an animal model for a wide variety of human diseases, including genetic diseases, neurodegeneration and alcoholism. Despite the fact that *Drosophila* was first used as an animal model over 100 years ago, it still remains an extremely relevant model today, thanks to its short life cycle, its low cost ease to rear in laboratory conditions and the sophistication of the molecular tools available for genetic manipulation in *Drosophila melanogaster*. This model also has far less genetic redundancy with respect to mammals, making the study of the role of certain genes far more straightforward, and yet despite this, still possesses an ortholog for 75% of human disease-causing genes. All of these properties contribute to the relevance of this model and were taken advantage of during this project.

In the first part of this project, *Drosophila melanogaster* was used as a model for mitochondrial deoxynucleotide transport. The *Drosophila* homolog CG18317 of the yeast gene *RIM2*, which was previously reported to be a pyrimidine dNTP transporter, was characterized. Knock-out (K.O.) flies for gene CG18317, here referred to as *drim2*, were characterized for mitochondrial function and mtDNA integrity. The two human homologs for this gene, *PNC-1* and *SLC25A36* were also expressed in this mutant background, in order to investigate the functional homology of these genes and confirm the validity of this model for human mitochondrial dNTP transport.

This project also focuses on further characterizing a K.O. fly line for *dTTC19*, a gene whose human homolog has already been tied to mitochondrial encephalopathy and psychosis in humans. This characterization was also accompanied by the generation of three K.O. lines which express the *dTTC19* gene in a mutant background, in order to finally confirm that the entirety of the mutant phenotype is due to the absence of transcription of the *dTTC19* gene.

Finally, this project attempts to propose a new protocol which will enable researchers to use *Drosophila melanogaster* as a model for neurological disorders which present with antisocial symptoms. A protocol was developed to investigate social behaviour in *Drosophila melanogaster* and to demonstrate that subtle changes in either dopamine levels or previous social contact can have dramatic effects on their social interactions. We therefore propose that *Drosophila* can also be a useful model for the investigation of the genetic factors involved in

diseases which present with antisocial behaviour such as autism, obsessive compulsive disorder, depression and so forth.

In conclusion, this project takes full advantage of *Drosophila melanogaster* as an animal model for mitochondrial biology and disease. Furthermore, it proposes yet another way in which *Drosophila* can be used as a model which has not yet been done.

***Drosophila melanogaster* come animale modello per la biologia mitocondriale, le malattie mitocondriali e i disturbi neurologici**

Drosophila melanogaster ha una lunga storia come animale modello per tante malattie umane, incluse le malattie genetiche, la neurodegenerazione e l'alcolismo. Anche se *Drosophila* fu inizialmente utilizzata come animale modello più di 100 anni fa, rimane comunque un modello rilevante oggi grazie al suo ciclo vitale breve, il suo basso costo e la sofisticazione degli attrezzi molecolari disponibili per la sua manipolazione genetica. Questo modello ha anche meno ridondanza genetica rispetto ai mammiferi, rendendo lo studio della funzione di questi geni molto più diretto, ma malgrado questo possiede un ortologo per 75% dei geni legati a malattie umane. Tutte queste proprietà contribuiscono alla sua rilevanza come modello e sono state sfruttate durante questo progetto.

In primis, *Drosophila melanogaster* è stata usata come modello per il trasporto mitocondriale di deossinucleotidi. Il gene *RIM2* in lievito, che è stato precedentemente caratterizzato come trasportatore mitocondriale di deossinucleotidi pirimidinici, ha un omologo in *Drosophila*: CG18317, qui chiamato *drim2*, che è stato caratterizzato in questo progetto. Questo gene è stato rimosso *in vivo* e la funzione mitocondriale e l'integrità del mtDNA sono state caratterizzate. I due omologhi umani per questo gene, *PNC-1* e *SLC25A36*, sono stati espressi nel mutante, per determinare l'omologia funzionale di questi geni e per confermare la validità di questo mutante come modello per il trasporto mitocondriale umano di deossinucleotidi.

Questo progetto si è anche focalizzato su una caratterizzazione più approfondita di una linea mutante per *dTTC19*, un omologo di un gene umano che è già stato collegato alla encefalopatia mitocondriale e la psicosi. Questa caratterizzazione è stata accompagnata dalla generazione di tre linee mutanti che esprimono *dTTC19*, per confermare che il fenotipo mutante osservato sia dovuto alla mancata trascrizione di *dTTC19*.

In fine, questo progetto propone un nuovo protocollo che, nella nostra opinione, permetterà di utilizzare *Drosophila melanogaster* come modello per disturbi neurologici che presentano con sintomi asociali. Un protocollo è stato sviluppato per studiare il comportamento sociale in *Drosophila melanogaster* e per dimostrare che piccole differenze nei livelli di dopamina o nel contatto sociale dopo l'eclosione possono avere effetti drammatici sulle interazioni sociali in *Drosophila*. Proponiamo che *Drosophila* può essere un modello utile per lo studio dei fattori

genici coinvolti nelle malattie che presentano con comportamento asociale come l'autismo, il disturbo ossessivo compulsivo, la depressione eccetera.

In conclusione, questo progetto sfrutta interamente *Drosophila melanogaster* come animale modello per la biologia e le malattie mitocondriali. In più, propone un nuovo modo per utilizzare *Drosophila* come modello che non è stato finora sfruttato.

GENERAL ASSUMPTIONS

General Assumptions: The use of *Drosophila melanogaster* as an animal model*i.i: The Use of *Drosophila melanogaster*: a Brief History*

Drosophila melanogaster is one of the oldest model organisms which still has an enormous relevance today. In the early 1900s, during which time the scientific method was being developed and genetics research was the new *mode*, the need for a model organism for such research was acknowledged. At the time, *Drosophila melanogaster* was already being bred at many universities, as its simplicity and rapid life cycle made it an incredibly popular model for the study of everything from embryology to insect behaviour (Allen, 1975). Given the low-cost ease with which it is raised and the large numbers which can be produced in short periods of time, it was thus proposed as a potential model for the new emerging field of genetics.

Foremost in this field was Thomas Hunt Morgan, whose experiments in *Drosophila* won him the 1933 Nobel Prize in Physiology or Medicine for his discovery of chromosomes as the basic unit of inheritance (nobelprize.org). Thomas Hunt Morgan was also the first to demonstrate sex-linked heredity with his study of the heritability of the *white* mutation in the fruit fly (Morgan, 1910). *Drosophila* was also the model used in the discovery of gene linkage (Morgan, 1911), homologous recombination (Bridges and Anderson, 1925), x-ray induced mutations (Muller, 1928) and the first tumour suppressor gene (Gateff and Schneiderman, 1967).

Notwithstanding its historical importance, *Drosophila* remains an extremely relevant model organism today. A quick search in PubMed yields 3754 papers published in 2012 involving *Drosophila* and, despite the relative “evolutionary distance” between humans and flies, approximately 75% of human disease-causing genes have an ortholog in *Drosophila melanogaster* (Reiter *et. al.*, 2001). There are many reasons for its continued success as a model organism, not the least of which include the fact that it has a fully sequenced genome, that its relative lack of genetic redundancy (compared to vertebrates) makes the functional study of certain genes far more straightforward, and that there are a variety of very sophisticated molecular techniques currently available in *Drosophila melanogaster*.

i.ii: The Molecular Techniques Available in Drosophila

The use of *Drosophila melanogaster* as a model organism for the study of genetics has kept up with modern research thanks to the sophistication of the molecular tools that have been developed for its use. Thanks to the versatility of these tools it is possible to conduct a wide range of knock-down, knock-out, over-expression and transgenic experiments with extensive spatiotemporal control. One of the most versatile of these tools is the UAS-GAL4 system.

i.ii.a: The UAS-GAL4 System

The UAS-GAL4 system is one of the most versatile genetic tools available to the *Drosophila melanogaster* researcher. It is based on a *Saccharomyces cerevisiae* binary system, whereby the 881 amino acid transcription factor GAL4 recognizes and binds the *Upstream Activating Sequence*, or *UAS*, activating transcription of whatever lies downstream of it (Fig *i.ii.a*; Duffy, 2002). The expression of *GAL4* itself also does not seem to cause any overt defects in *Drosophila*, although this is not true if flies are kept at higher temperatures (as *GAL4* expression is also temperature sensitive) (Kramer and Staveley, 2003). UAS lines are generated by cloning the gene of interest downstream of the *Upstream Activating Sequence* and then microinjecting this construct into *Drosophila* embryos so as to have it recombine in the genome. GAL4 lines are generated by cloning *GAL4* downstream of a gene promoter, depending on when and where one wants to express *GAL4*.

Flies harbouring the *UAS* and *GAL4* sequences are kept as separate parental lines in order to ensure full control over the expression of the sequence of interest. The two lines are then crossed, yielding F1 progeny harbouring both the *GAL4* protein and the *UAS*, thereby activating transcription of the gene of interest (Fig *i.ii.a*).

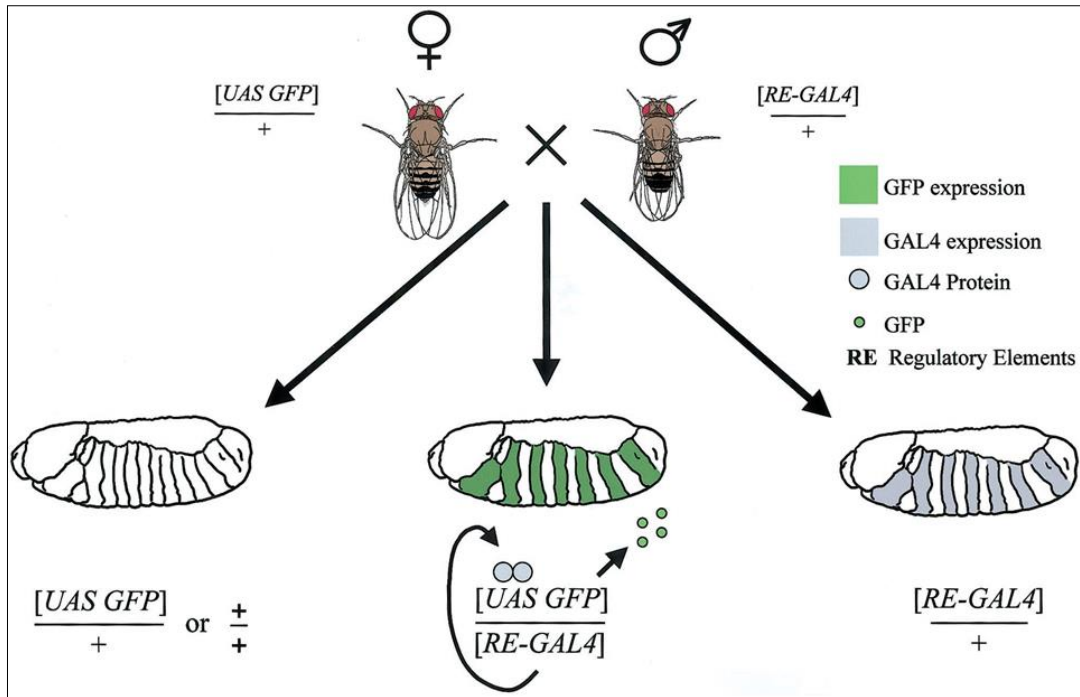


Fig i.ii.a: Schematic representation of the UAS-GAL4 system in *Drosophila*. Source: Duffy, 2002.

This binary system holds enormous potential for genetic manipulation of *Drosophila melanogaster*. First of all, various lines exist with *GAL4* expression under the control of a wide range of promoters, also called drivers. This allows the researcher to express their gene of interest either constitutively, as is the case with the *Act5c* driver, tissue specifically, like the *elav* driver which expresses *GAL4* only in the nervous system, or time-specifically, with the use of drivers that are expressed only at certain stages of the *Drosophila* life cycle. One can also use *heat shock* or *Gene-Switch* drivers, which only express *GAL4* when the flies are heat shocked at 37°C for one hour or fed progesterone-fortified food, respectively (McGuire *et. al.*, 2004).

The use of a fly line harbouring a gene under UAS control also allows for very creative genetic manipulation. Fly lines with miRNAs under UAS control give the researcher the ability to knock down a gene of interest in the tissue and/or at the time they choose by crossing them with one of the aforementioned *GAL4* drivers. It is also possible to clone any sequenced gene from any organism under *UAS* control and recombine these constructs in the *Drosophila* genome, in order to observe the effect of the overexpression of such gene either ubiquitously or tissue-specifically. This can also be done with a mutated version of the gene of interest, or one can observe the effect of the expression of any gene in any *Drosophila* mutant background. The bipartite approach also allows for the study of the expression of genes with toxic effects, or which can cause lethality at early stages (Duffy, 2002).

i.ii.b: The FRT-FLP System

Drosophila melanogaster is a model organism in which it is possible to create a clean knock-out mutant for a specific gene. This is immensely useful, as there is no possibility for residual expression of the gene of interest, as is the case with the knock-down. It also allows for much more specific deletions, avoiding secondary effects when more than one gene is mutated, as can happen with chemical or irradiation mutagenesis (Parks *et. al.*, 2004). In *Drosophila*, this technique involves the FRT-FLP System discovered in *Saccharomyces cerevisiae*, which is in many ways analogous to the Cre-lox system for conditional knock-out available in mice.

In 2004, researchers were able to generate 29,682 lines stably harbouring either an XP or *PiggyBac* transposon (Thibault *et. al.*, 2004) at various positions distributed throughout the genome, which are now available on order from Bloomington Stock Centre at Indiana University. These transposons contain a series of repeated and inverted sequences known as FRT sites. Two *Drosophila* lines, one harbouring a transposon upstream and the other downstream of the gene of interest, can then be crossed in order to obtain a fly line in which the genomic region is flanked by FRT sequences. If these lines are then crossed with a fly line expressing FLP-recombinase, the enzyme will recognize the FRT sites within the p-elements and will catalyse a recombination event between them, effectively excising the intermediate genomic region (Fig *i.ii.b*).

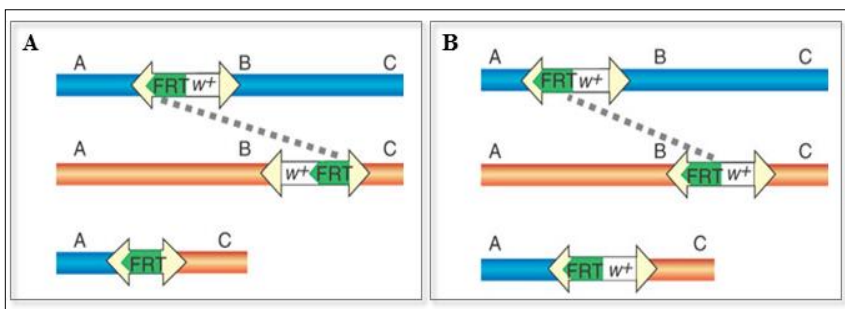


Fig *i.ii.b:* Schematic representation of FRT-FLP knock-out system generating (A) progeny without *white⁺* (*w⁺*) marker or (B) progeny with *white⁺* marker. Source: Parks *et. al.*, 2004.

Drosophila transgenic lines usually take advantage of *white¹¹¹⁸* flies as a useful way to see whether or not the recombination event was successful. *White* mutants lack a gene encoding for an ATP-binding cassette (ABC) transporter, which is responsible for transporting the precursors for eye pigment to the *Drosophila* eye (Mackenzie *et. al.*, 1999), resulting in flies with white eyes. To generate these XP/*PiggyBac* lines, transposons harbouring *white⁺* (*w⁺*) markers alongside the FRT sequences, which encode for the ABC transporter, were inserted into the

genomes of *white* mutants (Parks *et. al.*, 2004). Therefore, the presence of red-eyed flies in the progeny indicated the successful insertion of the transposon into the genome. Depending on the position of the w^+ marker in relation to the FRT sites recognized by FLP recombinase, flies which had successfully excised the genomic region between the two transposons either lost (Fig *i.ii.b* A) or kept (Fig *i.ii.b* B) their w^+ marker.

Once a portion of the fly genome is successfully removed, the effects of such a deletion can be studied thoroughly. However, there is always the possibility that flies homozygous for this mutation have severely reduced vitality, fertility or even high lethality at embryonic or larval stages, depending on the deleted gene(s) in question. For this reason it is necessary to be able to keep such a mutation in stable heterozygosity if one wishes to continue to investigate the effects of the removal of their gene of interest. This is also possible in *Drosophila* with the use of balancer chromosomes.

i.ii.c: Balancer Chromosomes

Since homologous recombination is a very frequent event in *Drosophila*, fly lines with balancer chromosomes are available, which effectively maintain a genetic mutation or transgene which is homozygous lethal in heterozygosity, without running the risk of the mutated chromosome recombining with the unmutated one. Balancer chromosomes contain a series of short, repeated and inverted sequences which prevent homologous recombination with the second chromosome.

The *Drosophila* genome contains three pairs of autosomes, and balancer chromosomes exist for all three. These balancers all produce phenotypic effects, in order to be able to immediately identify their presence in the *Drosophila* genome without the need for molecular confirmation. They are additionally useful in that they are embryonic lethal when in the homozygous state, therefore one never runs the risk of performing analyses on flies homozygous for the balancer and therefore lacking in their genetic mutation. Table *iv.ii.c* includes a list of some of the most common balancer chromosomes available in *Drosophila*, including their phenotypic effects.







Chromosome	Balancer	Phenotypic Effect	
II	L ₂ PIN ₁	Adults with reduced eyes	
II	CyO	Adults with “curly” wings	
II	ScO	Adults without bristles on the scutellum	
III	TM6b,Tb	Short, thick larvae/pupae, adults with tufts of bristles instead of three above the first pair of legs (*)	
III	MKRS	Adults with short bristles	
III	TM3	Adults with short bristles	

Table i.ii.c: List of some of the most commonly used balancer chromosomes available, with their corresponding phenotypic effects. Source of images: flybase.org; (*) image courtesy of Dr. Paola Cisotto, Biology Department, University of Padua, Italy.

Some balancer chromosomes have phenotypic effects at both the larval and adult stages, while the chromosome II balancers only exhibit phenotypic effects at the adult stage. Therefore, if one needs to study a mutation on chromosome II which requires the identification of larvae which are either homozygous or heterozygous for the given mutation, an additional balancer chromosome which takes advantage of the previously described UAS-GAL4 system is available. The balancer *Kr-GAL4,UAS-GFP,CyO* expresses green fluorescent protein (GFP) under the control of the promoter for *Kruppel*, a developmental gene expressed in all larval stages. This balancer also contains *CyO*, which causes the curly-winged phenotype in adults (Table i.ii.c).

i.iii: Biology of *Drosophila melanogaster* and its Relevance as a Model

The molecular tools available in *Drosophila* have enabled it to keep up with the sophistication of the rapidly evolving field of genetics research. However, there are some critical aspects of the inherent biology of *Drosophila melanogaster* which in themselves make this an extremely popular model organism.

i.iii.a: Drosophila Life Cycle

Some of the most critical aspects of *Drosophila melanogaster* which have contributed to its success as a model organism involve its small size, low-cost-to-rear and short life cycle, all of which allow for the ability to raise large numbers in relatively small amounts of space and relatively little money. This rapid life cycle is one of the principle reasons why it was selected as a model organism for genetics research in the first place, and continues to be one of its most valuable qualities as an animal model today.

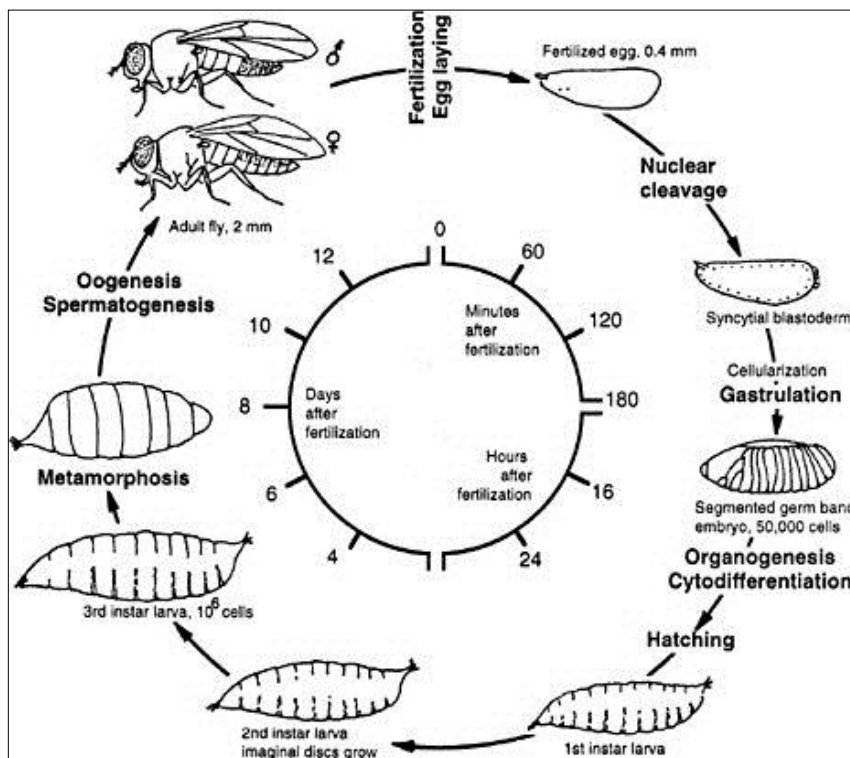


Fig i.ii.a: Life Cycle of *Drosophila melanogaster*, with times given when raised at 25°C. Source: National Research Council, 2000.

The life cycle of *Drosophila melanogaster* begins with the deposition of the fertilized egg on a food medium. After embryogenesis is completed the 1st instar larva hatches, after which it undergoes a moult, becoming a 2nd instar larva and then immersing itself in the food medium provided. There the larvae undergoes another moult, and finally as a 3rd instar larvae enters the “wandering” stage, whereby it leaves the food medium and crawls in search of an acceptable place to begin pupation. It then stops moving, the cuticle hardens and metamorphosis can begin. Once metamorphosis is complete, an adult hatches from the pupae and the life cycle begins again (Fig *i.iii.a*). At 25°C the entire cycle takes no more than 12 days, which makes it very easy to rear large numbers in a very short period of time. If fly lines need to be stocked for later use, on

the other hand, they can be kept in an incubator at 18°C, which doubles the length of the life cycle.

i.iii.b: Drosophila Morphology

The life cycle of *Drosophila* and the nature of metamorphosis allow for the same organism to present with very distinct morphologies, the two most utilized in research being the adult and third instar larval stages (Fig. *i.iii.b*). Adult *Drosophila melanogaster* exhibit the typical 3-part body structure of members of the Class Insecta: their body plan consists of a head, thorax and abdomen and they possess three pairs of legs (Fig *i.iii.b* A). Third instar larvae also have a typical segmented body plan, with a total of 11 segments, 8 of which containing hemi segmentally repeated body wall muscle fibres which are numbered and readily identifiable (Fig *i.iii.b* B).

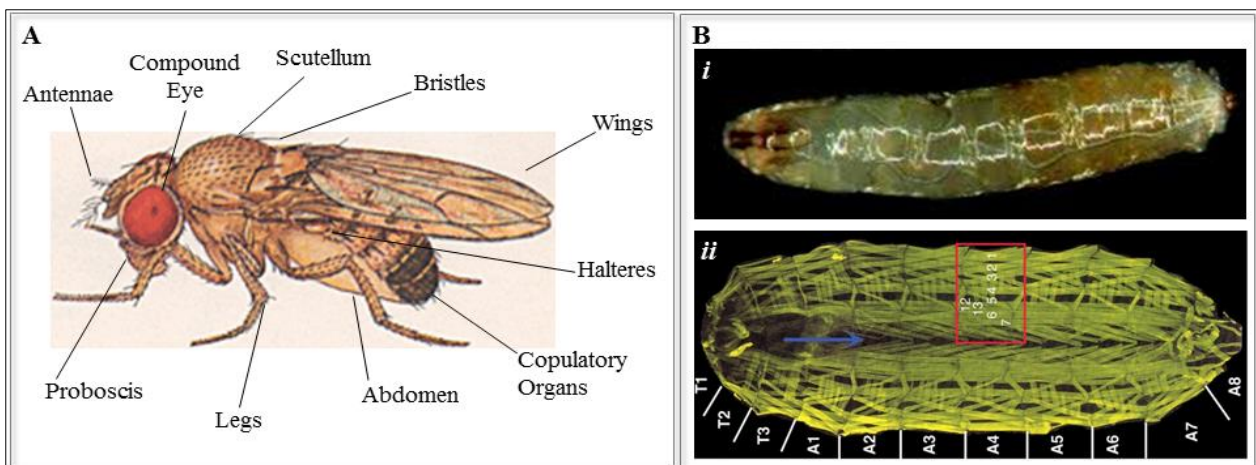


Fig. *i.iii.b*: (A) Labeled diagram of an adult *Drosophila melanogaster*. Source: flybase.org. (Bi) External view of third instar larva of *Drosophila melanogaster*. Source: Egli *et. al.*, 2003. (Bii) Larval body wall preparation exposing the repeated muscle pattern, with segments and muscle identity labelled. Source: Zhang and Stewart, 2010.

These two commonly used life stages in *Drosophila* provide advantages for certain types of research. The adult stage is often used in research involving behaviour, including mate choice (Byrne and Rice, 2006), alcohol addiction (Kaun *et. al.*, 2011) and drug use (McClung and Hirsh, 1998). Its short life cycle also means that vitality and toxicity experiments are also often conducted in this model organism. Third instar larvae, on the other hand, can be dissected to yield a body wall preparation (Fig *i.iii.b* Bii), i.e. muscular tissue rich in readily accessible mitochondria which can be used for a variety of biochemical experiments. Third instar larvae are

also very important for research into neurotransmission, due to their large and accessible neuromuscular junctions.

i.iii.c: The Drosophila Neuromuscular Junction

There are other aspects of *Drosophila melanogaster* biology, other than its small size and rapid life cycle, which make it a popular model organism. The relatively large size of third instar larvae and thus the ease with which it is possible to access its nervous system makes the *Drosophila* neuromuscular junction (NMJ) an extremely popular model for synaptic function, development and plasticity (Collins and DiAntonio, 2007). Unlike vertebrates, *Drosophila melanogaster* has glutamatergic NMJs, making it a highly accessible model for central glutamatergic vertebrate synapses which are relatively difficult to access (Collins and DiAntonio, 2007). The development and identity of each *Drosophila* NMJ is stereotyped and has been well characterized, and yet they also show very robust plasticity, making them a useful intermediate between the overly simple *C. elegans* and the very complex mouse model (Collins and DiAntonio, 2007). There are also a wide range of experimental procedures available for the *Drosophila* NMJ, from electrophysiology to live imaging, which when coupled with the finesse of the aforementioned genetic and molecular tools available make it an extremely attractive and extensively used synaptic model.

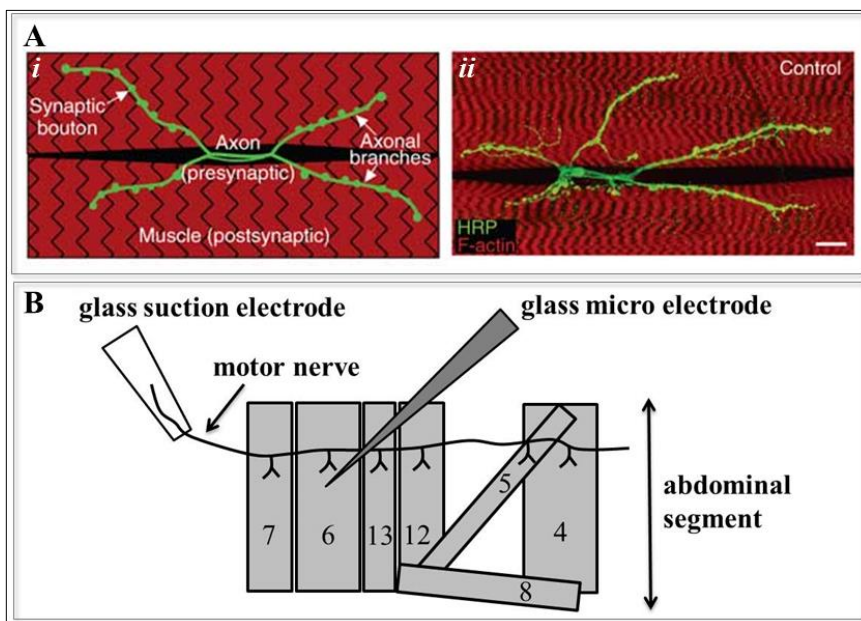


Fig. i.iii.c: (A) *Drosophila* NMJ of muscle 6/7 in third instar larvae. Source: Loya *et. al.*, 2009. (Ai) Labeled diagram of muscle 6/7 NMJ. (Aii) Muscle 6/7 NMJ immunostained with α -HRP (green). Scale bar: 20 μ m. (B) Diagram of method of measuring electrophysiology in *Drosophila* larval NMJ Source: Zhang and Stewart, 2010.

Both the history and the sophistication of *Drosophila melanogaster* have rendered it a very versatile animal model, for everything from alcoholism, Parkinson's disease and drug addiction to fragile X syndrome and neurodegenerative diseases. In this project, we will take full advantage of this versatility, using this organism as a model for mitochondrial biology, mitochondrial disease and, potentially, for neurological disorders.

CHAPTER I:

drim2

drim2* is essential for correct mitochondrial function in *Drosophila melanogaster

A balanced pool of deoxyribonucleotide triphosphates (dNTPs) is essential for correct mitochondrial DNA synthesis and mitochondrial function. In yeast a protein responsible specifically for the transport of pyrimidine dNTPs has been identified and is coded for by the *RIM2* gene. Based on homology, one *Drosophila melanogaster* gene (CG18317, here referred to as *drim2*) and two human genes (*SLC25A33*, or *PNC-1*, and *SLC25A36*) code for putative mitochondrial carrier proteins. This project focuses on the characterization of the *Drosophila drim2* gene.

A strain of *D. melanogaster* knockout (K.O.) for the *drim2* gene was previously generated in our lab, using the FLP/FRT system, which we then used to investigate the potential function of *drim2* in *Drosophila*. Also, rescue experiments were attempted by expressing either the *Drosophila drim2* gene or one of the human homologues in a *drim2* K.O. background.

drim2 K.O. individuals were 100% lethal at the 3rd instar stage and were visibly smaller than controls. Larval locomotor behaviour, sensory capabilities and neuromuscular junction morphology and activity were also analysed. Mitochondrial morphology and DNA integrity, biochemical activity of respiratory chain complexes and cellular respiration of whole tissues were also determined. *drim2* K.O. larvae show a significantly reduced locomotor behaviour compared to heterozygous larvae and controls. Also, mutant larval tissues show severely reduced cellular respiration, and mitochondrial patterning in muscles seems to be altered in mutant larvae. Neuromuscular junction morphology and function are significantly affected in *drim2* K.O. larvae, while mutant larvae do not show any obvious deficiencies in sensory capabilities. However, real-time PCR analysis reveals that mutant larvae have higher levels of expression of mitochondrial genes than their heterozygous counterparts, suggesting a possible compensation mechanism. Taken together, these results suggest that the *drim2* protein has a crucial role in *Drosophila melanogaster*, particularly in the maintenance of correct mitochondrial function. Also, rescue experiments conducted with both human genes result in adult flies with normal longevity and locomotor activity, suggesting a very high functional homology between the *Drosophila* gene and the two human homologous counterparts.

CHAPTER I: **INTRODUCTION**

1.1 Mitochondrial Biogenesis and Function

Mitochondria are organelles measuring 0.5-2 μm in length, possessing two double phospholipid membranes and their own circular DNA (Fig 1.1 A). Mitochondria were first recognized as ubiquitous cellular structures in 1890 by Richard Altmann, who hypothesized that these “bioblasts” were actually “elementary organisms” living within cells (Ernster and Schatz, 1981). Several decades later this idea was revived, and it has now become widely accepted that mitochondria derive from a prokaryotic ancestor phagocytosed by a host cell and giving it the ability to perform aerobic respiration, wherein they evolved to perform several vital functions (Scheffler, 1999).

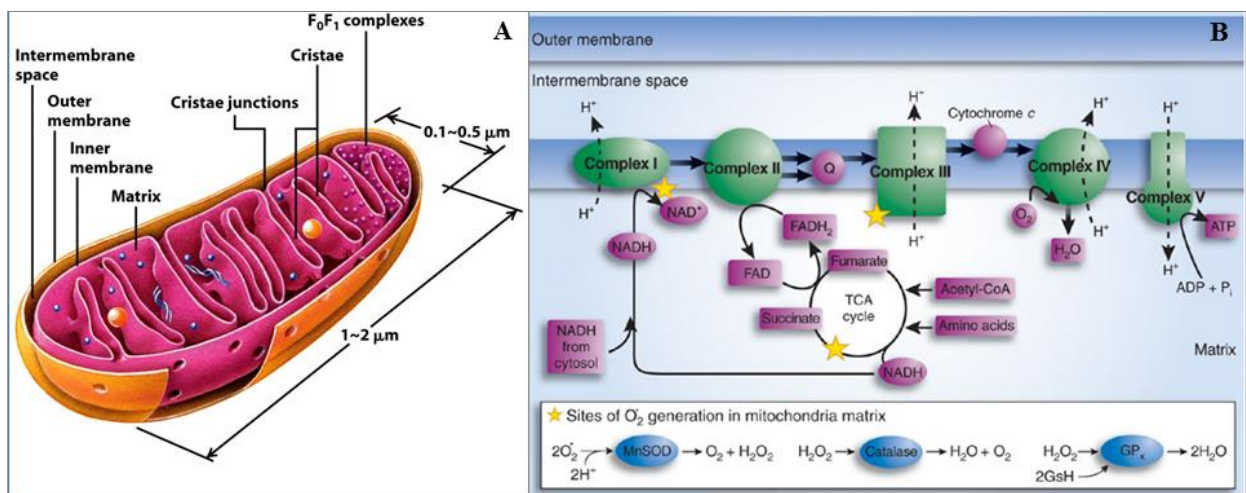


Fig 1.1: Diagram of (A) mitochondrial structure (Lodish *et. al.*, 2007) and (B) of the electron transport chain (Beal 2005).

The most well-studied and well appreciated function for mitochondria is oxidative phosphorylation, an aerobic process resulting in the production of chemical energy, in the form of ATP, from the tricarboxylic acid (TCA) cycle, fatty acid oxidation and amino acid oxidation (Fig 1.1 B). Five protein-lipid enzyme complexes embedded in the inner mitochondrial membrane are necessary to complete this process.

Oxidative phosphorylation begins with the oxidation of NADH at Complex I (NADH-Coenzyme Q reductase) and FADH₂ at Complex II (Nantes and Mugnol, 2008). Complex II then catalyzes electron transfer to ubiquinone (Q). This reduced Q then transfers its electron to Complex III (ubiquinol-cytochrome *c* oxidoreductase), which further catalyzes the electron transfer from Q to cytochrome *c*, a peripheral heme protein not associated with a respiratory complex, creating a transmembrane proton electrochemical potential (Nantes and Mugnol, 2008). Complex IV

(cytochrome *c* oxidase) then catalyzes the electron transfer from cytochrome *c* to O₂, which is thus converted to H₂O. The transmembrane proton electrochemical gradient that was created throughout this process then precipitates the production of ATP when the H⁺ protons flow back into the matrix through Complex V, or ATP Synthase (Smeitink *et. al.* 2001).

Except for Complex II, proteins for all of these complexes are, in part, encoded by the mitochondrial genome. Therefore mitochondria cannot properly perform this vital function without ensuring correct mitochondrial DNA replication.

1.1.1: Mitochondrial DNA Replication

The human mitochondrial genome, sequenced in 1981, is an approximately 16.5kb double-stranded circular structure (Anderson *et. al.*, 1981). It is an intron-less compact genome encoding for a total of 37 genes, of which 2 are ribosomal RNAs, 22 are transfer RNAs and 13 are proteins of the electron transport chain (Montoya *et. al.*, 2006). The two DNA strands in mammalian mtDNA are asymmetrical, named the “heavy” and “light” strands, based on their buoyancy densities (Garesse and Kaguni, 2005). There are currently two models for mtDNA replication (Fig 1.1.1), both ardously defended by their authors though no unanimous conclusion has been reached (Stumpf and Copeland, 2011). The first proposed model for mtDNA replication, known as the asynchronous model, posits that mtDNA replication commences with the heavy strand. Replication begins at the origin of replication, or O_H, displacing the parental strand in what is known as the displacement-loop, or D-loop (Brown *et. al.*, 2005). After approximately two-thirds of the mitochondrial genome is transcribed, this displacement exposes the site at which replication can commence on the light strand, or O_L, whereby transcription of this second stand begins in the opposite direction (Fig. 1.1.1; Brown *et. al.*, 2005).

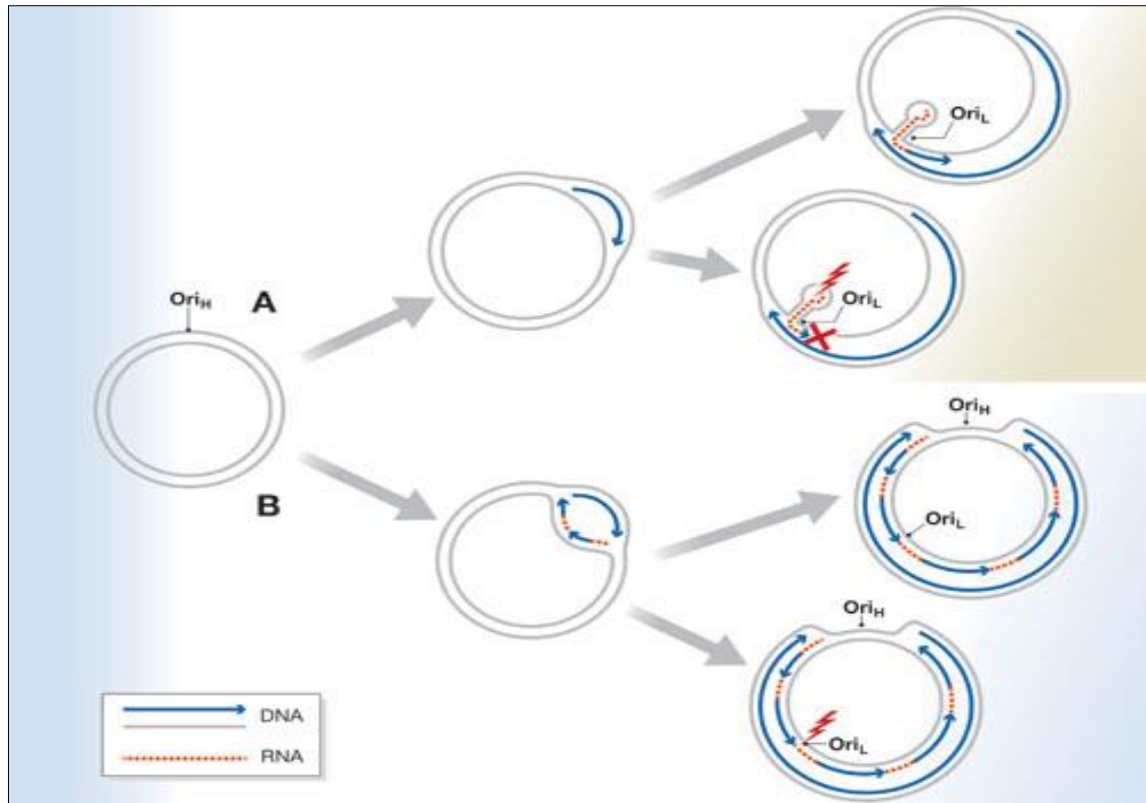


Fig 1.1.1: Two models of mtDNA replication: (A) asynchronous strand model (B) bidirectional model with discontinuous synthesis of the lagging strand. Source: Lightowlers and Chrzanowska-Lightowlers, 2012.

In 2000, evidence from 2D electrophoresis led to the proposition of the strand-coupled bidirectional model, which rejects the notion of asymmetrical replication, but rather proposes that replication begins near the O_H followed by two forks progressing around the circular mtDNA (Fig 1.1.1)(Holt *et. al.*, 2000).

While a consensus has yet to be reached on the method by which mtDNA is replicated, it is clear that mtDNA replication and repair relies on the presence of a balanced pool of dNTPs in order to avoid mtDNA mutations and/or depletion.

1.1.2: Mitochondrial dNTP Synthesis

In order for correct mitochondrial DNA replication to occur, a balanced pool of dNTPs needs to be present in the matrix. Since mtDNA replication is independent of S-phase, these pools must not rely on nucleotide production in the cell (Ferraro *et. al.*, 2006). There are thus two pathways

used by mitochondria for this purpose: (i) the synthesis of dNTPs within the mitochondria or (ii) the transport of dNTPs from the cytosol across the inner mitochondrial membrane (Fig 1.1.2).

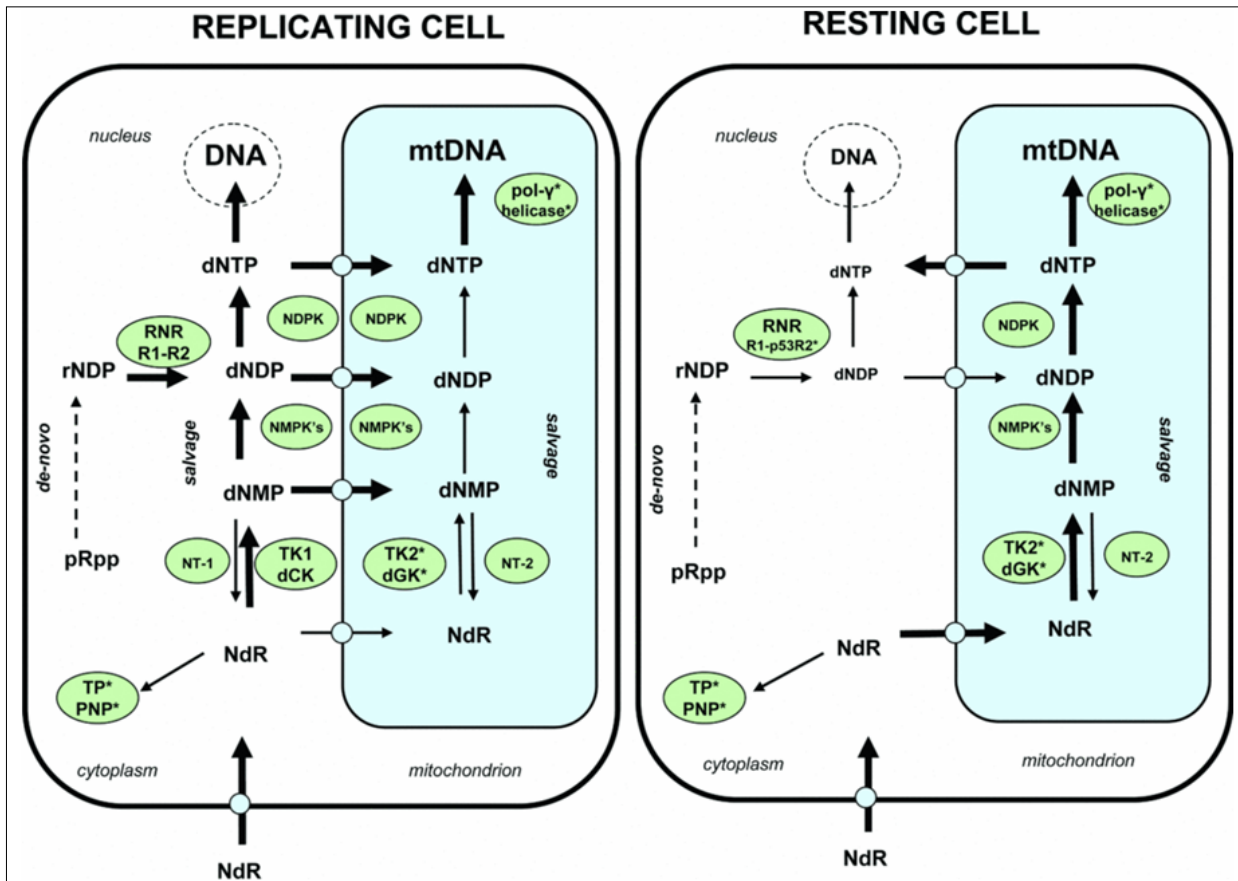


Fig 1.1.2.: Schematic representation of dNTP metabolism and transport in mitochondria in cycling and resting cells. Source: Saada, 2009.

Cytosolic and mitochondrial nucleotide and nucleoside pools are in constant communication via specialized mitochondrial membrane transporters (Saada, 2009). In 2001, the existence of a mitochondrial transporter capable of importing all four dNDPs (and, although less efficiently, dNTPs) was reported and called the deoxynucleotide carrier, or DNC (Dolce *et. al.*, 2001). Since then, however, many other transporter proteins have been either directly or indirectly implicated as nucleotide transporters in mitochondria (see below).

Deoxynucleotides can also be synthesized within the mitochondria, either via the mitochondrial deoxyribonucleoside salvage pathway (Saada, 2009), or possibly also by *de novo* synthesis (Mathews and Song, 2007). The thymidine kinase isoform TK2 is responsible for phosphorylating pyrimidines, while deoxyguanosine kinase (dGK) phosphorylates purine

deoxyribonucleosides to their monophosphates within mitochondria, and defects in either of these genes can result in very severe pathologies in humans (Mathews and Song, 2007). These monophosphates can then be converted to triphosphates needed for mtDNA replication by nucleoside diphosphate kinase (Mathews and Song, 2007).

1.1.3: Mitochondria and Iron Homeostasis

Mitochondria are less appreciated, though nonetheless essential for iron homeostasis and the biogenesis of heme and iron-containing clusters (ISCs) in eukaryotic cells (Richardson *et. al.*, 2010). Iron is highly versatile as a biological catalyst, but this very property also makes its metabolism very tricky. At pH 7.4, iron is readily oxidized, rendering it insoluble and potentially toxic due to its ability to catalyze reactive oxygen species (ROS), meaning it is in constant need of being chaperoned and stored (Richardson *et. al.*, 2010).

The details regarding iron uptake and metabolism in the mitochondria still remain to be fully elucidated. Mitochondrial iron transporters *MRS3* and *MRS4* were identified in yeast, when it was demonstrated that their inactivation lead to severe defects in iron metabolism and heme/Fe-S cluster biosynthesis (Mühlenhoff *et. al.*, 2003). In vertebrates two homologues were discovered: mitoferrin-1, encoded for by the gene *SLC25A37* is essential for iron uptake in erythroid cells, while mitoferrin-2 is encoded for by the gene *SLC25A28* and is essential in nonerythroid cells (Richardson *et. al.*, 2010).

Once inside the mitochondria iron can be stored, most likely by binding mitochondrial ferritin (Nie *et. al.*, 2004), or it can be used for either heme formation, which takes place exclusively within mitochondria (Ponka, 1997) or ISC biosynthesis, which are primarily synthesized in mitochondria (Lill and Kispal, 2000). Once synthesized, these clusters can be transported outside the mitochondria, where they can be incorporated into the necessary proteins.

Due to their integral importance, mitochondrial function is a tightly regulated process; leading to a wide range of disorders should any of these processes fail.

1.2 Mitochondrial Diseases in Humans

The heterogeneity of mitochondrial disease, as well as the fact that there is no universal consensus regarding the definition of mitochondrial disease, makes estimating its incidence in the population very difficult. If we consider mitochondrial disease to mean any disease which is precipitated by defects in the OXPHOS system, the incidence is estimated to be approximately 1:8500 (Sanchez-Martinez *et. al.*, 2006). Given the fact that mitochondria perform other vital functions in the cell, including Ca^{2+} homeostasis, apoptosis, ISC biosynthesis etc., the definition of mitochondrial disease could theoretically be expanded to include any disease precipitated by dysfunctional mitochondria, regardless of the involvement of the OXPHOS system, which would make this incidence much higher. Either way it is important to note that, despite the fact that the mitochondrial proteome contains approximately 1000 genes, mtDNA only encodes for 22 of them, making mitochondrial function heavily reliant on proteins encoded for by nuclear genes (Magnusson *et. al.*, 2003). Because of this it is important to note that many mitochondrial diseases can in fact be caused by genes that are nuclear in origin. In this study, particular attention will be given to mitochondrial diseases which involve defects in mtDNA replication and mt-dNTPs, given that our gene is hypothesized to be integral to the maintenance of mt-dNTP pools.

1.2.1: Mitochondrial Diseases of mtDNA Replication

Defects in genes responsible for correct mitochondrial DNA replication can lead to mitochondrial depletion syndrome (MDS), a group of symptoms associated with low mtDNA copy number. The various diseases and disorders related to this syndrome are highly heterogeneous, in that mutations in one gene can be associated with various different diseases, and one disease can be linked to mutations in numerous different genes. For example, *POLG*, the gene encoding for the catalytic subunit of the mitochondrial DNA polymerase poly, was first identified as causing progressive external ophthalmoplegia (PEO) (Van Goethem *et. al.*, 2001). Since then, however, mutations in *POLG* have also been associated with premature menopause, Alper's Syndrome, Parkinsonism and mitochondrial neurogastrointestinal encephalomyopathy (MNGIE) (Copeland, 2008). Conversely, mutations in more than one gene can be responsible for the same disorders. For example, MNGIE has been associated with mutations in *ECGF1* as well as in mutations in *POLG* (Copeland, 2008) and in *TYMP*, a gene integral in mitochondrial dNTP metabolism (González-Vioque *et. al.*, 2011). This heterogeneity, while complicating the matter

of studying the genetic basis of this subset of mitochondrial diseases, is not surprising. Given the fact that these genes are involved in mtDNA replication, defects in these genes can lead to secondary defects in the form of mutations in or depletion of mitochondrial genes, which in turn go on to affect the electron transport chain.

1.2.2: Mitochondrial Diseases Related to dNTP Metabolism

Another important category of genes to consider are genes which are involved in the generation and maintenance of mt-dNTP pools. Mitochondria require a balanced pool of dNTPs for proper mitochondrial DNA replication, so alterations in these can also lead to defects in mtDNA, which in turn can lead to a variety of OXPHOS-related pathologies. As described in section 1.1.2, thymidine kinase -2 (TK2), for example, is an enzyme responsible for phosphorylating deoxythymidine, deoxycytidine and deoxyuridine when cells are not replicating and therefore not producing dNTPs to be transported into the mitochondria (Wang et. al., 1999). It was later reported that four unrelated patients with fatal myopathy had mutations in this gene, as well as reduced ETC activity and mtDNA (Saada et. al., 2001). Deoxyguanosine kinase (dGK), on the other hand, phosphorylates purine nucleosides in the mitochondria of non-replicating cells (Copeland, 2008). Mutations in this gene have been associated with several different forms of MDS, from progressive liver failure (Salviati et. al., 2002) to infantile hepatoencephalopathy (Freisinger et. al., 2006).

1.2.3: Mitochondrial Diseases Related to Mitochondrial Carriers

Of particular interest to this study is the association of members of the mitochondrial carrier protein family with mitochondrial disease. In 2002, mutations in *SLC25A19* were associated with Amish lethal microcephaly (MCPHA), an autosomal recessive disease afflicting 1:500 Old Order Amish of Lancaster County, Pennsylvania, and characterized by severe congenital microcephaly and death, usually within the first year (Kelley *et al.*, 2002). Loss-of-function mutations in *SLC25A38*, a predicted mitochondrial amino acid carrier, were found to cause nonsyndromic autosomal-recessive congenital sideroblastic anaemia (CSA) (Guernsey *et. al.*, 2009), characterized by pathological iron deposits in erythroblast mitochondria (Bottomley, 2006). Mutations in the heart/muscle specific mitochondrial AAC1 carrier *SLC25A4* were found to be linked with autosomal dominant progressive external ophthalmoplegia (adPEO), characterized

by mtDNA deletions in post-mitotic tissues resulting in defective energy production (Palmieri, 2008). Neonatal myoclonic epilepsy, on the other hand, was found to be caused by mutations in *SLC25A22*, which encodes a mitochondrial glutamate/H⁺ symporter (Molinari *et. al.*, 2005). Taken together, these studies implicate defects in the mitochondrial carrier family as important contributors to mitochondrial disease.

1.3: *Drosophila melanogaster* as a Model for Mitochondrial Disease

Drosophila melanogaster is already a well-established model for a wide range of human disorders, including neurodegenerative disease, cancer and, most relevant to this project, mitochondrial diseases (Sánchez-Martínez *et. al.*, 2006), including mitochondrial depletion syndrome (MDS), mtDNA mutations and mitochondrial dysfunction related to mutations in nuclear genes.

One example of a generalized model for MDS is one in which the catalytic subunit of mtDNA polymerase poly- α is overexpressed in the nervous system of *Drosophila*, leading to depletion of mtDNA, thus a low mtDNA:nDNA ratio. These flies exhibit high mortality rates and an increase in apoptosis in the larval brain (Sánchez-Martínez *et al* 2006).

Often times, *Drosophila* is used because it is the model which most closely replicates the human disease symptoms. One example of this is a model for one of the most severe complications of the use of aminoglycoside antibiotics, which is irreversible deafness. One study in three unrelated Arab-Israeli families with aminoglycoside-induced deafness found that all of them had a mutation in the 12S rRNA gene, which encodes a mitochondrial ribosomal protein, demonstrating that the genetic susceptibility to this adverse reaction to antibiotics can itself be considered a mitochondrial disease (Prezant *et. al.* 1993). To model mitochondrial deafness, a *Drosophila* mutant line for the gene encoding mitochondrial ribosomal protein S12 *technical knockout (tko)* was generated (Toivonen *et. al.*, 2001). These flies exhibit developmental delay, bang sensitivity (a measure of defects in the signaling of motor neurons) and defects in the ability to perceive sound (Toivonen *et. al.*, 2001). Furthermore, this mutation causes these flies to be more sensitive to the mitochondrial translational inhibitor doxycyclin, while not exhibiting any ulterior defects when exposed to the eubacterial ribosome inhibitor streptomycin (Toivonen *et. al.*, 2001), resembling thus the symptoms of a human mutation in mitochondrial ribosomal RNA (Prezant *et. al.*, 1993).

Drosophila melanogaster is also often used as a model for a specific human mitochondrial disease. For example, a functional knock-down of the highly conserved *surf-1* gene in *Drosophila* has proven a useful model for Leigh Syndrome (LS), a progressive neurodegenerative disorder of infancy and childhood characterized by severe COX deficiency (Tiranti *et. al.*, 2001). Ubiquitous silencing of this gene in *Drosophila* causes larval lethality, while silencing in the CNS resulted in abnormal mitochondrial morphology, electrophysiological problems and decreased COX activity in cephalic regions, demonstrating the critical role of this gene in COX activity, organogenesis and development (Zordan *et. al.*, 2006).

The multifactorial origins of mitochondrial disease, combined with the fact that there are still many mitochondrial diseases of unknown genetic origin, makes the genetic basis of these diseases a very complicated and difficult area of study. In this project we attempt a different approach by first identifying genes which are crucial for mitochondrial maintenance and function, thus proposing them as interesting candidates for further study in the context of patients with mitochondrial disease. Here, we propose the *RIM2* gene, homolog of *SLC25A33* and *SLC25A36* in humans, as one such candidate.

1.4: RIM2 in *Saccharomyces cerevisiae*

1.4.1: Discovery and Characterization of *RIM2*

In 1993, the *RIM2* gene was sequenced and mapped to the right arm of chromosome II in *Saccharomyces cerevisiae* (Démolis *et. al.*, 1993). It was then demonstrated that this gene encodes for a 377 amino acid polypeptide with a typical triplicate structure, with two putative transmembrane segments separated by a hydrophobic loop in each repeat (Van Dyck *et. al.*, 1995). This protein was found to colocalize with mitochondria in yeast, and the inactivation of this protein resulted in colonies completely lacking mitochondrial DNA (Van Dyck *et. al.*, 1995). Furthermore, it was demonstrated that this gene could rescue the mitochondrial defects of both *pif1* and *mrs2* yeast mutants, characterized by complete lack of mitochondrial DNA and the absence of cytochrome *aa3*, respectively (Van Dyck *et al.*, 1995). Taken together, the researchers speculated that *RIM2* was a novel member of the mitochondrial carrier family (MCF), that it is involved in mitochondrial nucleic acid metabolism, and tentatively put forth the possibility that this protein is involved in dNTP transport across the inner mitochondrial membrane.

This theory was finally confirmed in 2006 when it was demonstrated that, when *RIM2* is overexpressed in bacteria and the protein reconstituted into liposomes, it is capable of transporting pyrimidine deoxyribonucleoside tri-, di- and (to a lesser extent) mono-phosphates (Marobbio *et al.*, 2006). Once this primary function was confirmed, further studies were conducted to elucidate the depth of the importance of this gene for mitochondrial biology and function.

1.4.2: *RIM2* and Iron Transport

Recently, this protein was also discovered to be involved in iron homeostasis in yeast mitochondria. Heme and Fe-S clusters are iron-containing cofactors which are needed by many enzymes to function properly, and the insertion of iron into these factors occurs within the mitochondria in the majority of eukaryotes (Richardson *et al.*, 2010). In yeast, mitochondrial carrier proteins Mrs3 and Mrs4 are responsible for transporting iron across the inner mitochondrial membrane, and double-deletion strains are very sensitive to iron deprivation (Mühlenhoff *et al.*, 2003). Overexpression of *RIM2* is able to enhance heme and Fe-S cluster synthesis in both wild-type and *mrs3/mrs4* K.O. strains (Yoon *et al.*, 2011). Also, expression of *RIM2* was shown to protect mutants of the vacuolar iron transporter *Ccc1* from iron toxicity (Lin *et al.*, 2011). Further analysis of *RIM2*-deficient cells also demonstrated a marked reduction in haem and Fe-S-containing proteins (Yoon *et al.*, 2011). Recently, it was conclusively demonstrated that *RIM2* co-transport iron and pyrimidine dNTPs in yeast mitochondria (Froschauer *et al.*, 2013). These results further indicate the importance of the *RIM2* protein by bringing to light a secondary yet essential function.

In this project, we focused on homologs of the yeast *RIM2* gene. In *Drosophila* a previously uncharacterized gene, *CG18317*, was identified as a *RIM2* homolog, thus it will be referred to here as *drim2*. In humans two members of the Mitochondrial Carrier Family *SLC25A33*, or *PNC-1*, and *SLC25A36* were also identified as *RIM2* homologs. This chapter will focus on these three genes in the context of the *Drosophila melanogaster* animal model.

1.5: Mitochondrial Carriers in Humans

1.5.1: The Mitochondrial Carrier Family

Due to their various complex roles in cellular function mirrored by a relatively small and simple genome, mitochondria require the transport of a variety of metabolites, nucleotides and cofactors across the inner mitochondrial membrane (IMM) (Palmieri, 2008). Their importance for mitochondrial function has led their sequences to be highly conserved across the eukaryotic kingdom, indicating their fundamental importance to eukaryotic organisms (Kunji and Robinson, 2006). In fact, homologs of these genes are present in all eukaryotes and have even been identified in some viruses and bacteria, most likely originating from horizontal gene transfer (Palmieri, 2013).

In humans, these mitochondrial carrier proteins are encoded by the *SLC25* gene family, which comprises 53 genes (Palmieri, 2013). These membrane-embedded proteins typically consist of three tandemly related 100 amino acid chains (Palmieri, 2004). Each chain contains two hydrophobic stretches which span the inner mitochondrial membrane, separated by hydrophilic regions, with the signature motif P-h-D/E-X-h-K/R-X-R/K-(20-30residues)-D/E-G-(4residues)-a-K/R-G, where “h” represents a hydrophobic stretch and “a” an aromatic residue (Palmieri, 2004) (Fig. 1.5.1.1).

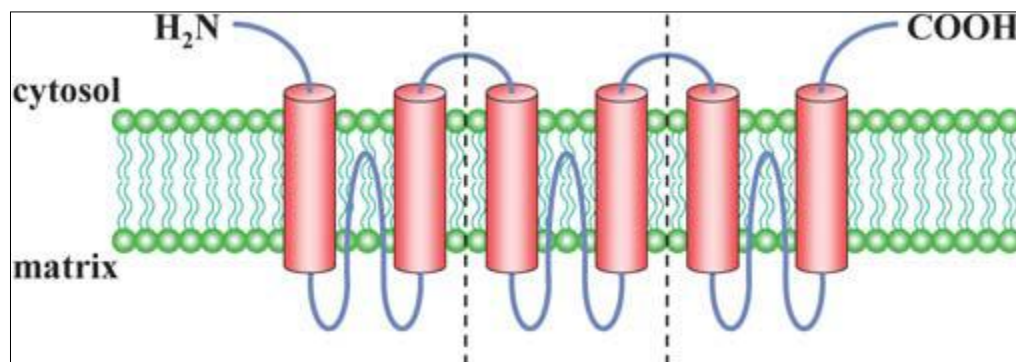


Fig 1.5.1.1.: Typical structure of a MCF protein. 6 α -helices span the inner mitochondrial membrane, while both C and N termini face the cytosol (Palmieri, 2004).

These transporters are involved in a wide variety of metabolic pathways, including gluconeogenesis, lipogenesis, the citric acid cycle, urea synthesis, iron metabolism, apoptosis, heat production and, of particular interest to this study, dNTP transport (Palmieri, 2013).

In this project, particular importance has been given to two members of this family: *SLC25A33*, or *PNC-1*, and *SLC25A36*. A phylogenetic analysis of the MCF in humans reveals that these two human genes (Fig 1.5.1.2, highlighted in red) are more closely related to each other than to any other member of the *SLC25* family (Palmieri, 2013). This evidence is consistent with a hypothesis that the two human homologs originated from a common RIM2-like ancestor, an idea which will be explored later in this study.

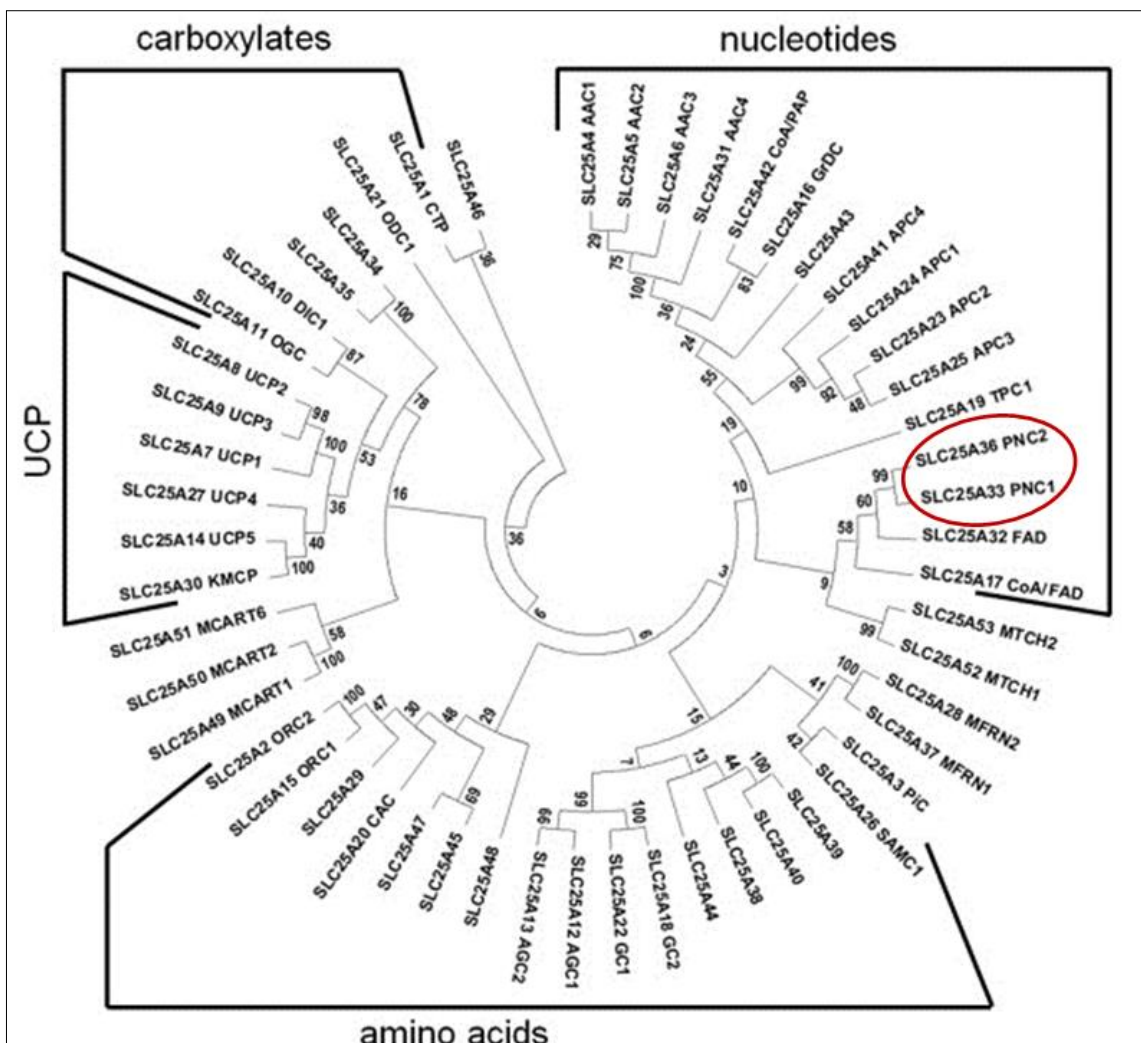


Fig 1.5.1.2.: Phylogenetic analysis of human *SLC25* family. Image from Palmieri, 2013, with a slight modification to highlight the two genes of particular importance to this project (red).

1.5.2: *PNC-1*

SLC25A33 was first identified as a mitochondrial carrier and member of the Solute Carrier 25 Family (*SLC25*) in 2006, with highest expression levels in the brainstem, coronal sections VIII and IV and the pineal gland (Haitina *et. al.*, 2006). This protein, whose encoding gene is located

on chromosome 1 at 1p36.22, has three homologous carrier repeats, each containing the signature motif P-X-[DE]-X-X-[KR], typical of mitochondrial carrier proteins (Fig 1.5.2).

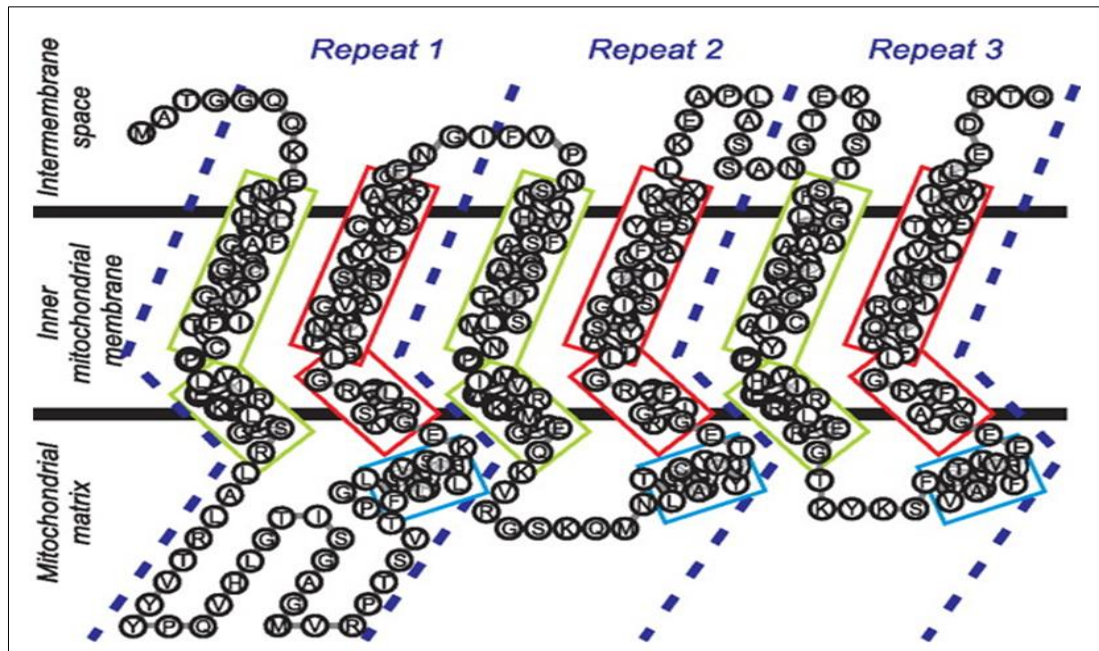


Fig 1.5.2: Schematic representation of putative *PNC-1* structure. Source: Floyd *et. al.*, 2007.

In 2007 it was demonstrated that expression of this gene is dependent on PI-3 kinase and mTOR activity (Floyd *et. al.*, 2007). Also, it was demonstrated that overexpressing it causes an increase in cell size, while its suppression results in lower mtUTP levels, earning it the name *Pyrimidine Nucleotide Carrier-1*, or *PNC-1* (Floyd *et. al.*, 2007). Later, it was demonstrated that knocking down of *PNC-1* leads to increased mitochondrial biogenesis and reduced mtDNA levels, while its overexpression leads to a reduction in mitochondrial biogenesis (Favre *et. al.*, 2010). Isotope-flow experiments confirmed that *PNC-1* can transport uridine nucleotides in cultured cells (Franzolin *et. al.*, 2012).

1.5.3: *PNC-1* and Disease

Alterations in mitochondrial DNA has long been linked to carcinogenesis, due to its relatively high probability of mutation compared to nuclear DNA, as well as the prevalence of mtDNA aberrations found in a wide range of tumors (reviewed in Penta *et. al.*, 2001). This, combined with a link between mitochondrial ROS production and carcinogenesis (Mori *et. al.*, 2004) as

well as metastasis (Ishikawa *et. al.*, 2008) make mitochondrial maintenance a significant factor in cancer prevention.

In keeping with this hypothesis *PNC-1*, which has not yet been linked to a specific mitochondrial disease, has been linked to certain types of cancer. Initially, *PNC-1* was identified as a candidate gene for cancer progression when mouse fibroblast cells from IGF-1R knock-out mice were transformed by overexpressing *IGF-1R* (Sell *et. al.*, 1994). It was then found that *PNC-1* is overexpressed in certain cancer cell lines and in primary prostate cancers, and that *IGF-1* expression, which is closely linked to cancer progression, also induces its rapid transcription (Floyd *et. al.*, 2007). Interestingly, it was also shown that *PNC-1* suppression in tumor cells initiated a ROS-dependent epithelial-to-mesenchymal transition (EMT) program, the first step in cancer metastasis (Favre *et. al.*, 2010). Also, suppression of *PNC-1* leads to an increase in ROS production (Floyd *et. al.*, 2007), most likely due to a leak of electrons at complex III (Favre *et. al.*, 2010).

Finally, *PNC-1* was also indirectly linked to the pathogenesis of trisomy 18, as it was found to be consistently down regulated in second trimester aneuploid fetuses, despite the fact that this gene is located on chromosome 1 (Koide *et. al.*, 2011).

1.5.4: *SLC25A36*

At this time, the function of *SLC25A36* still remains to be elucidated. Unlike *PNC-1*, mitochondrial transport of UTP was not affected when *SLC25A36* was silenced in Ost cells (Franzolin *et. al.*, 2012). Prof. Fernando Palmieri claims to have evidence that this gene is also a pyrimidine nucleotide transporter in human cells, but to date this data remains to be published (Palmieri, 2013).

The link between *SLC25A36* and disease is still tentative at best. A genome-wide association study linked *SLC25A36* with multiple sclerosis (MS) susceptibility (Baranzini *et. al.* 2009), although this association was not found to be statistically significant when replicated in a Spanish cohort of 2863 MS patients (Cavanillas *et. al.* 2011).

At this time, there is still a lot to be elucidated regarding the function of *SLC25A33* and *SLC25A36*. In this study, we will investigate the capabilities of these two genes to integrate in a *Drosophila melanogaster* mutant context.

CHAPTER I: **MATERIALS AND METHODS**

Recipes of all solutions used in this chapter are provided in Appendix I.

All primers used were ordered from BMR Genomics and provided by Invitrogen.

Maps of vectors are provided in Appendix II.

2.1: Maintenance of Fly Stocks

All fly lines originated from Bloomington Stock Centre at Indiana University unless otherwise stated.

Fly lines were maintained in standard fly culture tubes measuring 2.2cm in diameter and 9.5cm in length on cornmeal-yeast-agar medium. Lines in use were kept at 25°C, while stocked lines were kept at 18°C under a 12hr:12hr light:dark cycle.

2.2: *In vivo* Characterization of *drim2*

2.2.1: *drim2* K.O. Line

The *drim2* knock-out was previously generated in our lab. Two fly lines were ordered from Bloomington Stock Centre, one possessing a p-element at the 5' end and one possessing a p-element at the 3' end of our gene of interest *CG18317*, here referred to as *drim2* (Fig. 2.2.1). These two lines were crossed in order to obtain flies possessing both p-elements. These flies were then crossed with a line expressing FLP-Recombinase, an enzyme which catalyses a recombination event between the two p-elements, effectively excising our gene of interest. These mutants were then balanced with *Kr-GAL4,UAS-GFP,CyO* in order to discriminate between larvae and adults that were heterozygous and homozygous for the mutation. For clarity, $w^{1118};drim2\Delta/Kr-GAL4,UAS-GFP,CyO$ flies will be referred to as $drim2^{+/-}$, and $w^{1118};drim2\Delta/drim2\Delta$ larvae will be referred to as $drim2^{-/}$.



Figure 2.2.1: Map of CG18317 Fly lines harbouring each of the p-elements outlined in red were ordered to generate the *drim2* mutant line. Source: flybase.org

2.2.2: Characterization of Mutant Larval Size

As 100% of *drim2*^{-/-} larvae died before pupal formation, an analysis was done to determine whether there were significant differences in size between larvae that were heterozygous and homozygous for the mutation, both in crowded and uncrowded conditions.

In crowded conditions, >200 *drim2*^{+/-} adults were allowed to deposit in standard culture tubes over the course of 5 days. Adults were then removed and heterozygous and homozygous wandering third instar larvae were selected under a Leica MZ16 F fluorescent microscope. In uncrowded conditions, >200 *drim2*^{+/-} adults were allowed to deposit on 5cm plates containing standard fly medium for 2 hours. These plates were then incubated at 23°C overnight. First instar larvae were then removed from these plates and placed in standard culture tubes at densities of 20 larvae/tube. When wandering third instar larvae emerged they were again selected under a Leica MZ16 F fluorescent microscope in order to distinguish between heterozygous and homozygous mutants.

Larvae were then photographed on a plastic .5cm grid under a Leica S6D light microscope and the photographs were analysed with ImageJ software. Lengths and widths of larvae were recorded. Statistical analysis was performed using R x64 2.15.2 software.

2.2.3: Larval Locomotor Activity

Wandering third instar larvae were placed in the center of a 9.5cm plate coated with 1% agarose. This arena was placed in a light box on a Plexiglas 10.5cm raised pedestal, illuminated from underneath with a single LED light source. The larvae were then filmed with a Canon 2.0 megapixel camera and their movements were tracked by AnyMazeTM software over a 2-minute time period. This software analyzed their overall average speed and the total distance they travelled. A one-way ANOVA with Sidak correction was performed by the Any-MazeTM software to determine whether or not there were significant differences between genotypes.

2.2.4: Larval Behaviour

Mutant larvae were tested for their ability to distinguish between light/dark and salty/sweet cues in order to determine whether or not they had any obvious sensory deficiencies. 9.5cm plates filled with 1% agarose were prepared and separated into quarters. For light/dark experiments, two quarters were filled with 1% agarose containing red and blue tasteless food coloring, while the other two were filled with clear 1% agarose. The plate was then placed on a sheet of translucent paper with aluminum foil sections corresponding to the colored agarose sections, and then placed in the light box described in Section 2.2.3. 50 wandering third instar larvae were then placed in the center of these plates and their progress was filmed over a 5 minute period.

For salty/sweet experiments, 1% agarose plates were divided into quarters with the following concentrations of salt and/or sugar: 0.5M NaCl vs. neutral agarose, 1M NaCl vs. neutral agarose and 0.5M NaCl vs. 1M sucrose. All plates were prepared immediately before use to minimize diffusion of the substances between sections. For both salty/sweet and light/dark experiments, negative controls were performed by tracking the progress of 50 larvae over a 1% agarose plate which had been divided into sections but whose sections did not contain any additional substances. Chi-squared analysis was performed for each of the experiments using this negative control as the “expected” value.

2.2.5: Characterization of the Neuromuscular Junction

Larval body wall preparations were dissected as described in Zhang and Stewart, 2010. Briefly, larvae were placed in HL3A in a 3.5cm plate coated with SylGard. The larva was then pinned with 0.1mm stainless steel insect pins[®] (Austerlitz) at the top of the buccal apparatus and at the bottom between the spiracles, dorsal side up. The larva was then cut open with 2mm spring scissors and the cuticle was pinned open with four more pins. The interior organs were removed, while the ventral nerve cords were kept intact to prevent damaging the neuromuscular junction (NMJ).

The larvae were briefly washed in fresh HL3A, and then fixed in 4% PFA in PBS for 20 minutes. The larvae were then washed three times in 0.05% PBST and permeabilized for 30 minutes in 0.3% PBST at 4°C. Larvae were then blocked for one hour in 1% PBSTA to minimize aspecific binding of the antibody, then incubated ON at 4°C in 1:100 Cy3- conjugated goat α -HRP (Jackson ImmunoResearch) in 0.1% PBSTA. The following day the larvae were washed three times in 0.05% PBST, mounted in VectaShield[™] Mounting Medium (Vector Laboratories Inc.) on glass slides and stored at 4°C.

Scans of the NMJ of muscle 6/7 in the third segment were taken with a Leica SP5 confocal microscope. Stacks, measurements and analysis of the scans were done with ImageJ software. The NMJs were analyzed for number of boutons, average bouton size and the level of branching.

2.2.6: Analysis of Muscle Mitochondrial Pattern

Larval body walls were prepared as described in Section 2.2.5. Larvae were then washed briefly in PBS, and then incubated with 500nM MitoTracker[®] Red CMXRos in PBS (Life Technologies) for 40 minutes. Larvae were then washed 3 times in PBS, and then fixed for 20 minutes in 4% PFA in PBS. Larvae were washed 3 times in 0.05% PBST, then mounted in VectaShield[™] Mounting Medium (Vector Laboratories Inc.) on glass slides and stored at 4°C.

Scans of mitochondria in muscle 6 of the third segment were taken with a Leica SP5 confocal microscope. Final images were generated with ImageJ software.

2.2.7: Mitochondrial Respiration of Mutant Larvae

In order to directly determine mitochondrial dysfunction in mutant larvae, mitochondrial respiration of muscle tissue was measured with a Seahorse XF BioFlux Analyzer (Bioscience). Sensors of a Seahorse XF Calibration Plate (Bioscience) were hydrated overnight in 1mL XF Calibrant (Bioscience) as per the manufacturer's instructions. Third instar larvae were then placed in HL3A and snipped at the tail end, turned inside-out and their interior organs were removed. These muscle preparations were then placed in a Seahorse XF islet capture microplate (Bioscience), fixed in place with the small capture screens provided and placed in the Seahorse XF BioFlux Analyzer (Bioscience), which was set to follow the program listed in Appendix I. The oxygen consumption rate (OCR) was thus measured after mitochondrial respiration of muscle tissue preparations was first stimulated with the addition of 20mM glucose (in HL3A), and then inhibited with 5 μ M rotenone and antimycin A (in HL3A).

2.2.8: Determining Iron Content of Larval Proteins

In order to investigate whether or not *drim2* is also involved in iron transport into mitochondria, the FerroZine assay was used to determine the iron content of larval proteins as developed by Missirlis and colleagues (Missirlis *et. al.*, 2006) with some slight modifications. Each replica contained 13 larvae except for mutants, which due to their smaller size were increased to 16 per replica.

First, proteins were extracted from larvae by homogenizing them in Iron Extraction Buffer and centrifuging them for 15mins at 16,000g at 4°C. The supernatant was then transferred to a fresh tube and centrifuged for a further 5 minutes. Proteins thus extracted were quantified by Bradford assay. Briefly, 1 μ l of protein was added to 1ml of 1X BIO-RAD Bradford Dye Reagent, mixed and allowed to react at RT for 5 minutes. Absorbance was measured with a Beckman Coulter Life Science spectrophotometer at 595nm. Protein concentration was calculated by comparing the resulting absorbance to a standardized curve previously created with varying concentrations of Bovine Serum Albumin (BSA) between 1 and 10mg/ml.

To determine iron content of these proteins, 77 μ l of extracted protein was added to 17 μ l of concentrated HCl and boiled at 95°C for 20 minutes. The tubes were then centrifuged at 16,000g for 2 minutes, after which 50 μ l supernatant was added to 20 μ l of 75mM ascorbate (Sigma). 20 μ l of 10mM FerroZineTM Iron Reagent (Sigma) and 40 μ l of saturated ammonium acetate (Sigma)

were then added, the mixture was vortexed and the reaction was allowed to proceed for 5 minutes. Absorbance was measured with a Beckman Coulter Life Science spectrophotometer at 562nm. Iron concentration was calculated by comparing the resulting absorbance to a standardized curve generated by varying concentrations of ferric ammonium citrate (Sigma) between 0.005 and 0.15mM, which had previously been dissolved in Iron Extraction Buffer and had undergone a mock iron extraction procedure. Iron content was then normalized to protein concentration.

As a positive control for this protocol, flies were allowed to deposit on standard fly culture medium fortified with 10mM ferric ammonium citrate (Sigma) for 5 days. Third instar larvae emerging from this medium were then tested as above.

2.3: *In vitro* Analysis of *drim2* Expression

In order to determine the subcellular localization of the *drim2* protein in *Drosophila melanogaster*, cells expressing a tagged *drim2* protein were generated for immunohistochemical analysis.

2.3.1: RNA Extraction and Retrotranscription

RNA was extracted from *white*¹¹¹⁸ adult flies for the cloning of *drim2*. 10 adult flies were homogenized in 200µl of Trizol[®] Reagent (Life Technologies). The volume was then brought to 1ml and incubated at RT for 5 minutes. 200µl of Chloroform: Isoamyl Alcohol 24:1 (Sigma) was then added, the tube was shaken vigorously and placed on ice for 15 minutes. The mixture was centrifuged at 4°C for 15 minutes, the aqueous supernatant transferred to a clean tube and an isovolume of RNase-free Isopropanol (Life Technologies) was added. The tube was again shaken vigorously and incubated on ice for 15 minutes. The mixture was centrifuged at 4°C for 20 minutes, the supernatant was discarded and the pellet washed with 75% EtOH. After another 15 minute centrifuge at 4°C the pellet was dried, suspended in 55µl of RNase-free H₂O and 15µl of 8M LiCl, then left to precipitate overnight on ice at 4°C in order to eliminate the high carbohydrate contamination. The tubes were then centrifuged for 25 minutes at 4°C, the supernatant discarded and the pellet washed twice with 75% EtOH, centrifuging for 15 minutes at 4°C between each wash. The pellet was then dried, suspended in 15µl RNase-free H₂O and the

RNA concentration was determined with an RNA 6000 Nano LabChip[®] spectrophotometer (Agilent Technologies). RNA was stored at -80°C.

In order to generate the cDNA needed for cloning, 1µg of RNA was added to 1µl of 500µg/µl oligo-dT (Invitrogen) in a total of 5µl. The RNA was then denatured at 65°C for 6 minutes and then placed immediately on ice. 4µl of Retrotranscription Mix (Table 2.3.1) and 0.5µl of 200U/µl SuperScript[®] II Reverse Transcriptase (Life Technologies) was added and then placed in a thermoblock at 42°C for one hour. A further 0.5µl of 200U/µl SuperScript[®] II Reverse Transcriptase (Life Technologies) was added and the reaction was allowed to proceed for another hour. The reaction was terminated by bringing it to 65°C for 10 minutes, then cDNA was then stored at -20°C.

	Initial Concentration	Final Concentration	Source
5X First Strand Buffer	5X	1X	Invitrogen
DTT	0.1M	0.01M	Invitrogen
RNase OUT	400U/µl	20U/µl	Invitrogen
dNTPs	10mM	0.5mM	Promega

Table 2.3.1: Retrotranscription Mix

2.3.2: Cloning PCR of *drim2* Gene

The coding region of *drim2* was cloned using the primers listed in Table 2.3.2.1. Restriction enzymes which did not cleave the coding region of the gene were chosen with the Restriction Mapper program and their restriction sites were designed in the primers. An HA tag was also added at the 3' end.

Name	Sequence	Description
RIM2 F	5'-CCGGTACCATGGCCCAGAACACGGCCGACACTC-3'	Forward Primer Red: Restriction Site KpnI
RIM2 R	5'-GGGATATCTTAAGCGTAATCTGGAACATCGTATGGGTA AAAGTCGTAGAACTCGTTTCGATTTGTTGTTGAAGCGCC- 3'	Long Reverse Primer Red: Restriction Site EcoRV Blue: HA Tag
HA R	5'-GGGATATCTTAAGCGTAATCTGGAACATCG-3'	Short Reverse Primer Red: Restriction Site EcoRV Blue: HA Tag

Table 2.3.2.1: Primers used to clone *drim2*

2µl of cDNA was added to the Cloning PCR mix (Table 2.3.2.2) in a total of 50µl. The reaction was run as follows: 98°C for 30 sec, 35 cycles of 98°C for 20 sec, 58°C for 30 sec and 72°C for

45 sec, and then a final extension at 72°C for 10 minutes. After 10 cycles were completed, the short reverse primer (Table 2.3.2.1) was added to the reaction in order to facilitate the amplification.

	Initial Concentration	Final Concentration	Source
2X Phusion Mix	2X	1X	
Forward Primer (Table 2.3.2.1)	10mM	0.5mM	Invitrogen
Reverse Primer (Table 2.3.2.1)	10mM	0.5mM	Invitrogen
DNase- free H ₂ O	-	Tot Vol: 50µl	Life Technologies

Table 2.3.2.2: Cloning PCR Mix

A small 1% agarose gel was run at 150mA in an electrophoresis chamber filled with 1X TAE containing 5µl of PCR product to verify the reaction had succeeded. The PCR product was then tailed by adding 1µl 5U/µl GoTaq[®] DNA Polymerase (Promega) to the mixture and incubating it at 72° for 10 minutes. The cloned gene was then cleaned with a Promega Wizard[®] SV Gel and PCR Clean-Up System and stored at -20°C.

2.3.3: Cloning into pGEM[®]-T Easy Vector

In order to ensure maximum efficiency, the *drim2* PCR product was first cloned in a pGEM[®]-T Easy vector (Promega). 3µl of PCR product was added to 7µl of Ligation Mix (Table 2.3.3.1) and incubated overnight at 10°C.

Reagent	Initial Concentration	Final Concentration	Source
T4 Ligation Buffer	2X	1X	Promega
pGEM [®] -T Easy Vector	50ng/µl	5ng/µl	Promega
T4 DNA Ligase	400U/µl	40U/µl	Promega

Table 2.3.3.1: pGEM Ligation Mix

One-Shot[®] TOP10 Chemically Competent *E. coli* cells (Invitrogen) were defrosted on ice and 5µl of ligated pGEM-*drim2* was gently swirled into them. The cells were incubated on ice for 30 minutes, heat shocked in a 42°C water bath for 30 seconds then re-incubated on ice for 1 minute. 250µl of SOC medium was added and the cells were incubated in agitation at 37°C for 1 hour. 70µl and 230µl of cells were then plated on two plates containing LB Agar, 0.1mM IPTG,

20µg/ml X-gal and 50µg/ml Ampicillin and incubated overnight at 37°C. White colonies were selected and swirled into 120µl of LB Broth with 50µg/ml Ampicillin in a 96-well cell plate. The cells were left to grow overnight at 37°C.

Selected colonies were then screened for the construct by PCR. 1.5µl of cells were added to 23.5µl of Screening PCR Mix (Table 2.3.3.2) in each well of a 96-well PCR plate and placed in the following reaction: 95°C for 5 minutes, 30 cycles of 95°C for 30sec, 55°C for 30sec and 72°C for one minute, then a final extension of 72°C for 10 minutes. A gel was run with 20µl of PCR product to verify the presence of the gene.

Reagent	Initial Concentration	Final Concentration
dNTPs	10mM	0.2 mM
Primer F (Table 2.3.2.1)	100mM	0.5 mM
Primer R (Table 2.3.2.1)	100mM	0.5 mM
10X Buffer	10X	1X
MgCl ₂	100mM	2 mM
DNase-free H ₂ O		Tot Vol: 25µl

Table 2.3.3.2: Screening PCR Mix

6 colonies positive for *drim2* were selected. 30µl of each sample of bacteria were used to inoculate 4ml of LB Broth with 50µg/ml Ampicillin and left to grow overnight at 37°C. Plasmid DNA from 6 positive colonies was then extracted with a PureYield™ Plasmid Miniprep System (Promega) as per the manufacturer's instructions. 5µl of each was dried at 65°C for 30 minutes and sent to BMR Genomics for sequencing. The samples were analyzed for copying errors with SeqMan Pro software. *E. coli* colonies containing the *drim2* sequence free from copying errors were stored in 20% glycerol (Carlo Erba Reagents) at -80°C.

2.3.4: Cloning in pACT Vector

Tagged *drim2* was then cloned into a pACT vector for constitutive expression of the construct once transfected into *Drosophila* S2R+ cells (Life Technologies). The pGEM-*drim2* and the empty pACT vector were digested separately with EcoRV for 2 hours at 37°C (Table 2.3.3.1).

Reagent	pACT	pGEM-drim2	Source
Buffer 3 10X	1X	1X	NEB
EcoRV 20U/ μ l	1U/ μ l	1U/ μ l	NEB
BSA 100X	1X	1X	NEB
pACT 226ng/ μ l	4 μ g	-	-
pGEM-drim2 150 μ g/ μ l	-	4 μ g	-
DNase-free H ₂ O	Tot Vol: 80 μ l	Tot Vol: 80 μ l	Life Technologies

Table 2.3.4.1: EcoRV Digestion Mix

The mixture was then precipitated overnight at -20°C in 8 μ l 3M Na Acetate pH 5.2 and 176 μ l 100% EtOH. The digested mixture was centrifuged for 20 minutes at 4°C and the pellet was resuspended in KpnI mix (Table 2.3.3.2) and digested for 2 hours at 37°C.

Reagent	pACT	pGEM-drim2	Source
Buffer 1.1 10X	1X	1X	NEB
KpnI 20U/ μ l	1U/ μ l	1U/ μ l	NEB
BSA 100X	1X	1X	NEB
pACT	pellet	-	-
pGEM-drim2	-	pellet	-
DNase-free H ₂ O	Tot Vol: 80 μ l	Tot Vol: 80 μ l	Life Technologies

Table 2.3.4.2: KpnI Digestion Mix

The entire volume was run in a 0.8% UltraPure™ agarose (Life Technologies) gel at 100mA made with and run in modified TAE Buffer. The cut pACT plasmid and the *drim2* insert were cut out separately and the DNA was extracted with Millipore Centrifuge Filter Units as per the manufacturer's instructions. 117ng of pACT and 73ng of *drim2* were ligated as in Section 2.3.3.

One-Shot® TOP10 Chemically Competent *E. coli* cells (Life Technologies) were transformed, plated and screened for the construct as described in Section 2.3.3. Once the integrity of the construct was verified by sequencing, clones selected for transfection were stocked in 20% glycerol at -80°C, the vector was extracted and purified with a PureLink™ HiPure Plasmid MaxiPrep Kit (Invitrogen) and stored at -20°C for transfection.

2.3.5: Maintaining *Drosophila* S2R+ Cells in Culture

All experiments using *Drosophila* cells were performed under a sterile cell fume hood cleaned with alcohol and kept under constant UV light when not used.

Cells were grown in 75ml cell culture vessels in standard 1X Schneider's Drosophila Medium (Life Technologies) with 5% heat-inactivated Fetal Bovine Serum (FBS) at 25°C and changed every 4-5 days. Cells were split by tapping the flask and pipetting the solution a few times in order to detach adhering cells.

Cells were then counted by performing a 1:6 dilution in Trypan Blue and PBS, and then placed in a Bürker chamber. Cells lying along the diagonal squares of the chamber were counted and the following formula was applied:

$$\frac{\Sigma \text{cells} \times 10^6 \times \text{Dilution Factor}}{\text{no. diagonals} \times 12 \times \text{Bürker Factor}}$$

2 million cells were seeded in a total of 15mL of fresh Schneider's medium and kept at 25°C.

To stock cells, they were counted and centrifuged at 800g for 5 minutes. The supernatant was removed and set aside, while the cells were washed in PBS and pelleted again at 800g for 5 minutes. Freezing Medium was prepared by mixing 45% old Schneider's Medium, 45% Fresh Schneider's Medium and 10% DMSO. Cells were re-suspended in this medium and placed in 1mL cryovials, placed in a cryovial and kept at -80°C for 48 hours. Cells were then stored in liquid nitrogen.

2.3.6: Transfecting *Drosophila* S2R+ Cells

For western blot analysis, 2×10^6 S2R+ cells were seeded in each well of a 12-well plate and left to adhere overnight at 25°C. 230µl 1X Schneider's Drosophila Medium without serum was added to 20µl CellFectin® II Reagent (Life Technologies). Separately, 2.5µg pACT-*drim2* was added to 250µl of 1X Schneider's Drosophila Medium (Life Technologies) without serum, and both were left to rest for 20 minutes at RT. The two were then mixed together and left to equilibrate for a further 10 minutes at RT. The supernatant in the cell plate was pipetted away and kept aside, replaced with 500µl of the CellFectin® II Reagent/pACT-*drim2* mixture was carefully pipetted over the cells one drop at a time. The plate was then incubated at 25°C for 8 hours. The conditioned Schneider's Drosophila Medium taken from the cells was centrifuged at 800g for 10 minutes, and half of the supernatant was added to an isovolume of fresh 1X Schneider's Drosophila Medium with 5% heat-inactivated FBS. After the transfection was

complete, the CellFectin[®] II Reagent mixture was removed and the 1:1 conditioned:unconditioned 1X Schneider's Drosophila Medium was allowed to run down the side of the well over the transfected cells, which were then placed back in an incubator at 25°C.

Cells were collected 24, 48, 72 and 96 hours after transfection. The cells were centrifuged at 800g for 10 minutes, the supernatant discarded and the cell pellet stored at -80°C overnight.

Cells used for immunolocalization were instead seeded on round borosilicate coverslips in a 24well cell plate at 300,000, 500,000 and 700,000 cells/well and left to adhere for 12 hours. These cells were transfected with 375ng DNA, 625ng DNA and 875ng DNA, respectively, and collected 48 hours after transfection.

2.3.7: Quantitative Real-Time PCR of *drim2*

A Relative Quantitative Real-Time PCR (qRT-PCR) was performed on cells 24 hours, 48 hours and 96 hours after transfection with our construct in order to observe the expression levels over time. RNA was extracted and retrotranscribed from cells as described in Section 2.3.1, without the need for the LiCl precipitation step.

The cDNA for each time point was diluted to a final concentration of 25ng/μl. Four replicas were performed for each sample. 9μl of RT-PCR Mix (Table 2.3.6) and 1μl of sample was added to each well of a Primo[®] Framestar[®] 96 PCR Plate, closed with sealing tape and spun in a 5810R Eppendorf Centrifuge to remove all air bubbles. The plate was then run in a 7500 Real Time PCR System (Life Technologies) on the following program: 95°C for 2 minutes, 39 cycles of 95°C for 25 sec and 60°C for 1 minute, followed by a final extension at 72°C for 3 minutes. Results were analyzed with 7500 software (Life Technologies).

Reagent	Final Concentration	Source
2X GoTaq [®] qPCR Master Mix	1X	Promega
10mM Forward Primer (5'-TCGGTTACGGATCGAACAA-3')	0.15 mM	Invitrogen
10mM Reverse Primer (5'- TCGGTTACGGATCGAACAA-3')	0.15 mM	Invitrogen
DNase-free H ₂ O	Tot vol: 10μl	Life Technologies

Table 2.3.6: qRT-PCR Mix

2.3.8: Western Blot Analysis of *drim2*

Cell pellets from the three time points were suspended in 200µl RIPA Buffer and incubated on ice for 40 minutes. Cells were vortexed every 5 minutes of incubation, then centrifuged at 16,000g for 20 minutes at 4°C. The supernatant was then transferred to a clean tube and centrifuged again at 16,000g for 5 minutes. Protein concentration was quantified as described in Section 2.2.8. NuPAGE® LDS Sample Buffer (Life Technologies) and DTT (Sigma) added to a final concentration of 1X and 0.07M, respectively.

Proteins were denatured at 70°C for 10 minutes, then 20mg of protein was loaded in a NuPAGE 4-12% Bis-Tris Gel (Life Technologies) and run in MOPS Running Buffer at 80V for 2.5 hours in an XCell Sure Lock™ Electrophoresis Cell (Life Technologies). The gel casing was opened and the gel was gently placed between a piece of blotting paper and a Trans-Blot® Transfer nitrocellulose membrane (BIO-RAD). Another piece of blotting paper was placed over the membrane, sandwiched between sponges soaked in Transfer Buffer and placed in an X Cell™ Blot Module Chamber (Life Technologies). The chamber was filled with Transfer Buffer, placed in the XCell Sure Lock™ Electrophoresis Cell (Life Technologies) filled with dsH₂O and run at 30V for 1 hour. The membrane was then removed and stained with 0.1% Ponceau S in 5% acetic acid to verify the proteins were transferred correctly, then rinsed in H₂O and blocked for 1 hour in 5X blocking buffer to prevent aspecific binding of the antibody to the membrane. The membrane was then incubated with 1:2500 monoclonal mouse α-HA antibody (Sigma) in 1X blocking buffer overnight at 4°C in agitation.

The membrane was washed 3 times in TBST then incubated with 1:5000 rabbit α-mouse antibody (Sigma) in 1X blocking buffer for 2 hours at RT in agitation. The membrane was then washed another 3 times in TBST and incubated with ECL for 1 minute. Membrane was then wrapped in plastic, brought to a dark room and developed on Amersham high performance chemiluminescence Hyperfilm™ (Kodak). The film was pressed over the nitrocellulose membrane for 30 seconds – 2 minutes then placed in BIO-RAD Developing Solution until bands became visible. The film was then transferred to BIO-RAD Fixing Solution for 2-3 minutes. These were then rinsed and dried for analysis.

2.3.9: Immunolocalization of *drim2*

Cells were washed once in PBS and incubated with 100nM MitoTracker[®] Red CMXROS (Invitrogen) and 1 μ g/ml Cyclosporin H in Schneider's Medium without serum for 20 minutes at RT. Cells were then washed once with PBS and fixed for 20 minutes in 4% PFA in PBS. Cells were then washed 3 times in PBS and permeabilized with 50mM NH₄Cl and 0.1% Triton X-100 (Sigma) for 5 minutes. Cells were washed again in PBS and then blocked for 1 hour with 3% goat serum in PBS. Cells then incubated overnight in 1:100 Monoclonal mouse α -HA antibody (Sigma) and 2% goat serum in PBS at 4°C. Cells then washed 3 times in PBS and incubated with 1:500 FITC-conjugated rabbit α -mouse antibody (Santa Cruz Biotech) for 45 minutes at RT. Cells washed another 3 times in PBS then mounted in Movil on glass slides and stored at 4°C.

Images of immunolocalized cells were taken with a Leica SP5 confocal microscope and scans merged with ImageJ software.

2.4: Rescuing the *drim2* K.O. Phenotype

In order to validate this model, *drim2* mutant lines expressing either the *drim2* gene or one of its human homologs were generated and characterized.

2.4.1: Generating Rescue Lines

Coding regions of *drim2*, *PNC-1* and *SLC25A36* were previously cloned into a pUAST vector by Dr. Clara Benna in the lab and sent to BestGene Inc. for microinjection. The resulting flies harboring the constructs of interest were then crossed with *drim2*^{+/-} flies in order to obtain each of these genes under UAS-GAL4 control in a *drim2* K.O. background. Final crosses and PCR screenings were done during this project (Fig. 2.4.1).

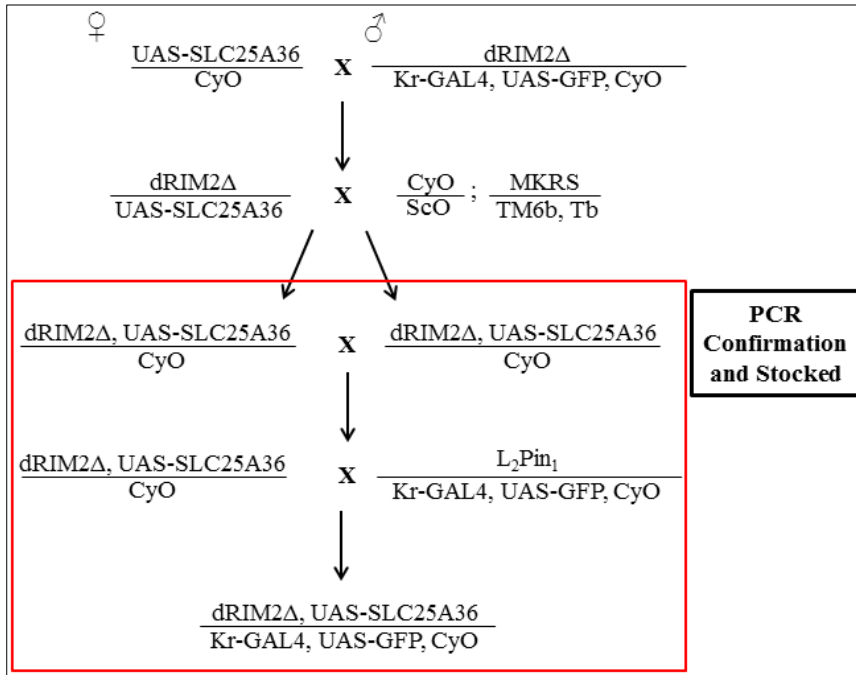


Fig. 2.4.1: Crosses done to obtain $drim2\Delta^{SLC36}$ line, with red box indicating crosses done during this project.

The final lines generated were as follows: $w^{1118}; drim2\Delta, UAS-drim2/Kr-GAL4, UAS-GFP, CyO$ for the *drim2* rescue line; $w^{1118}drim2\Delta, UAS-PNC-1/Kr-GAL4, UAS-GFP, CyO$ for the *PNC-1* rescue line and $w^{1118}drim2\Delta, UAS-SLC25A36/Kr-GAL4, UAS-GFP, CyO$ for the SLC25A36 rescue line. Also, a driver in a *drim2* mutant background was generated, with the genotype $w^{1118}; drim2\Delta, Act5c-GAL4/Kr-GAL4, UAS-GFP, CyO$. For clarity, the lines are referred to as $drim2\Delta^{drim2}$, $drim2\Delta^{PNC-1}$, $drim2\Delta^{SLC36}$ and $drim2^{+/-; Act-GAL4}$, respectively.

2.4.2: DNA Extraction from Flies

Individual flies were homogenized in 50 μ l DNA Extraction Buffer with a motorized pestle, after which 1 μ l of 20mg/ml Proteinase K was added. The extraction was then incubated at 37°C for 45 minutes, then at 100°C for 3 minutes to inactivate the proteinase. DNA was then stored at -20°C until needed.

2.4.3: Screening of Rescue Lines by PCR

Since the generation of these lines relied on homologous recombination, they had to be screened by PCR in order to verify whether or not the recombination event happened. Both p-elements and the rescue construct were screened for using the primers listed in Table 2.4.3.

Name	Sequence	Description
RB 5'	5'- TCCAAGCGGCGACTGAGATG -3'	Primer designed on p-element e00411
GEN R	5'- TATGCTTCCACAGTCGCAGT -3'	Primer designed downstream of e00411
RB 3'	5'- CCTCGATATACAGACCGATAA -3'	Primer designed on p-element e01575
GEN F	5'- AACTACGCCAGCGAACTCAC -3'	Primer designed upstream of e01575
UAS F	5'- GATCCAAGCTTGCATGCCTG -3'	Primer designed on UAS
RIM R	5'- TCCTTCCAAACAGTGTGCAG -3'	Primer designed on <i>drim2</i> gene
33 F	5'- CCGAATTCATGGCGACGGGCGG -3'	Primer designed on <i>PNC-1</i>
33 R	5'-GTACCTGTTAGAAGACCGTACTCAGTA-3'	Primer designed on <i>PNC-1</i>
36 F	5'- TGTGGGAATGATGCTAGCTG -3'	Primer designed on <i>SLC25A36</i>
36 R	5'- TGCCGCAGTCAGTGAAATAG -3'	Primer designed on <i>SLC25A36</i>

Table 2.4.3.1: Primers used to screen *drim2* Δ^{drim2} , *drim2* Δ^{PNC-1} , *drim2* Δ^{SLC36} lines

To perform the PCR confirmation, 2 μ l of DNA extract from adult flies (Section 2.4.3) was added to the PCR Mix described in Table 2.4.3.2, and run with the following program: 2mins at 95°C, then 35 cycles at 95°C for 30sec, 60°C for 30sec and 72°C for 1.5mins, finally at 72°C for 10 minutes for the final extension. DNA extractions from *white*¹¹¹⁸ adult flies were also run on the same program in order to confirm that there was no aspecific binding of the primers used at the annealing temperature chosen.

Reagent	Final Concentration	Source
5X GreenGoTaq [®] Reaction Buffer	1X	Promega
dNTP Mix (Appendix I)	0.25mM	Promega
Primer (Forward)	0.25mM	Invitrogen
Primer (Reverse)	0.25mM	Invitrogen
GoTaq [®] DNA Polymerase	0.5U	Promega
GIBCO H ₂ O	N/A	Life Technologies

Table 2.4.3.2: PCR Mix for confirming presence of p-elements and *drim2*, *PNC-1* and *SLC25A36* constructs.

7 μ l of DNA ladder was loaded in the first well of a 1% agarose gel, alongside 10 μ l of PCR product at 150mA for approximately 25 minutes, and observed under a transilluminator in order to both confirm the presence of the construct and to ensure that there was no aspecific binding of the primers.

2.4.4: Using UAS/GAL4 System to Express “Rescue” Construct

In order to determine whether or not the lines generated were capable of rescuing the *drim2* K.O. phenotype, the rescue lines *drim2* Δ^{drim2} , *drim2* Δ^{PNC-1} , *drim2* Δ^{SLC36} were each crossed with the *drim2*^{+/+;Act-GAL4} driver. Flies born with straight wings, therefore homozygous for the *drim2* mutation, were counted and their proportions were compared to flies born with curly wings. A chi-square test was performed to determine whether or not there is some mortality of “rescued” flies at an earlier stage.

2.4.5: Testing qRT-PCR Primer Efficiency

Primers for qRT-PCR were designed for the two human genes in order to determine whether or not the constructs were expressed in the lines which resulted positive from our screening. Once designed new qRT-PCR primers must be checked for efficiency, aspecificity and for the quantity of cDNA needed to give optimal results.

RNA from both larvae and adults was extracted and retrotranscribed as described in Section 2.3.1. cDNA of multiple samples containing the gene in question were combined and serial dilutions of 50ng/μl, 5ng/μl, 0.5ng/μl and 0.05ng/μl were made. Three replicates for each dilution were added to qRT-PCR Mix (Table 2.3.6) for a total volume of 10μl. Reaction was then run on a 7500 Real Time PCR System (Life Technologies) with the following program: 95°C for 2 minutes, then 38 cycles of 95°C for 20sec and 60° for 1 minute, then a final cycle of 95°C for 15sec, 60°C for 1min, 95°C for 15sec and 60°C for 15sec. This final cycle allows for problems with the primers such as dimerization or aspecificity to come out in the analysis.

Dissociation curves and amplification plots were analyzed in order to determine whether or not the primers dimerize, give aspecific binding and how many cycles of PCR are needed at a given concentration to reach saturation. A standard curve plotting log[C0] vs. Ct was then generated, and the slope of that line was used to determine the efficiency of the primers according to the following equation:

$$\% \text{ Efficiency} = -1 \times 10^{-1/\text{slope}}$$

The concentration of cDNA to use for the given pair of primers was then chosen based on the concentration at which 20-21 cycles amplified the signal well.

Once the parameters for the new primers were established, a relative qRT-PCR was performed for these genes as described in Section 2.3.6.

2.4.6: Verification of Presence of Construct mRNA

Expression levels of rescue constructs were verified by qRT-PCR in both larvae and adults. RNA from *white*¹¹¹⁸, *drim2* Δ ^{drim2}, *drim2* Δ ^{PNC-1} and *drim2* Δ ^{SLC36} larvae and adults was extracted and retrotranscribed as described in Section 2.3.1. qRT-PCR was performed with the primers listed in Table 2.4.8 as described in Section 2.3.6.

Primer	Sequence
drim2 F	5'-TCGGTTACGGATCGAACAA-3'
drim2 R	5'-TCGGTTACGGATCGAACAA-3'
SLC33 F	5'-GGTTCATCTGGGGACCATTA -3'
SLC33 R	5'-TCCAGGTGTCACGGATGTT -3'
SLC36 F	5'-CCTCAGAGCCTCCAAGGAAA -3'
SLC36 R	5'-TGTCTGGGGGACATGGTAGA -3'

Table 2.4.6: Primers used for qRT-PCR analysis of rescue constructs.

2.4.7: Verification of Presence of Construct Protein

The presence of the tagged construct in the rescue lines was verified by western blot. Proteins from adult *white*¹¹¹⁸, *drim2* Δ ^{drim2}, *drim2* Δ ^{PNC-1} and *drim2* Δ ^{SLC36} flies were extracted as described in Section 2.2.8, except that Protein Extraction Buffer was used instead of Iron Extraction Buffer. The rescue construct of *drim2* Δ ^{drim2} flies was tagged with a FLAG tag, the *drim2* Δ ^{PNC-1} rescue construct was tagged with an HA tag and the *drim2* Δ ^{SLC36} rescue construct was tagged with cMyc (Cell Signaling Technology). Western blot analysis of the three proteins was therefore conducted as in Section 2.3.7 with 1:1000 monoclonal mouse α -FLAG (Sigma) for *drim2* Δ ^{drim2} flies; 1:2500 monoclonal mouse α -HA (Sigma) for *drim2* Δ ^{PNC-1} flies; 1:2500 monoclonal mouse α -Myc (Cell Signaling Technology) for *drim2* Δ ^{SLC36} flies and 1:5000 goat α -mouse IgG (Sigma) as secondary antibody for all three.

2.4.8: Vitality Analysis of “Rescued” Flies

Once it was established that some lines were able to reach the adult stage, those flies were analyzed to see if they lived as long as controls. Male and female flies were separated and 10 individuals were placed in a standard size culture tube together, for a total of 12 replicas. Flies were placed in fresh culture tubes every 2-3 days, and the dead flies were counted. These results were plotted on a curve and an ANOVA test was performed to determine whether or not there were significant differences in mortality rates between *drim2* Δ^{drim2} , *drim2* Δ^{PNC-1} , *drim2* Δ^{SLC36} and *white*¹¹¹⁸ controls.

2.4.9: *In vivo* Analysis of “Rescued” Larvae

In order to test the extent to which the various lines were capable of rescuing the *drim2* K.O. phenotype, *drim2* Δ^{drim2} , *drim2* Δ^{PNC-1} , *drim2* Δ^{SLC36} larvae were tested for their locomotor activity, neuromuscular junction morphology, mitochondrial respiration, mitochondrial gene transcription, and protein iron content as described in Sections 2.2.3, 2.2.5, 2.2.7, 2.2.8 and 2.2.9, respectively.

2.4.10: Generation of “Double Rescue” Lines

In case the human genes were not able to completely rescue the *drim2* mutant phenotype, two K. O. lines expressing both human genes were generated by crossing *drim2* Δ^{PNC-1} and *drim2* Δ^{SLC36} lines (Fig. 2.4.11).

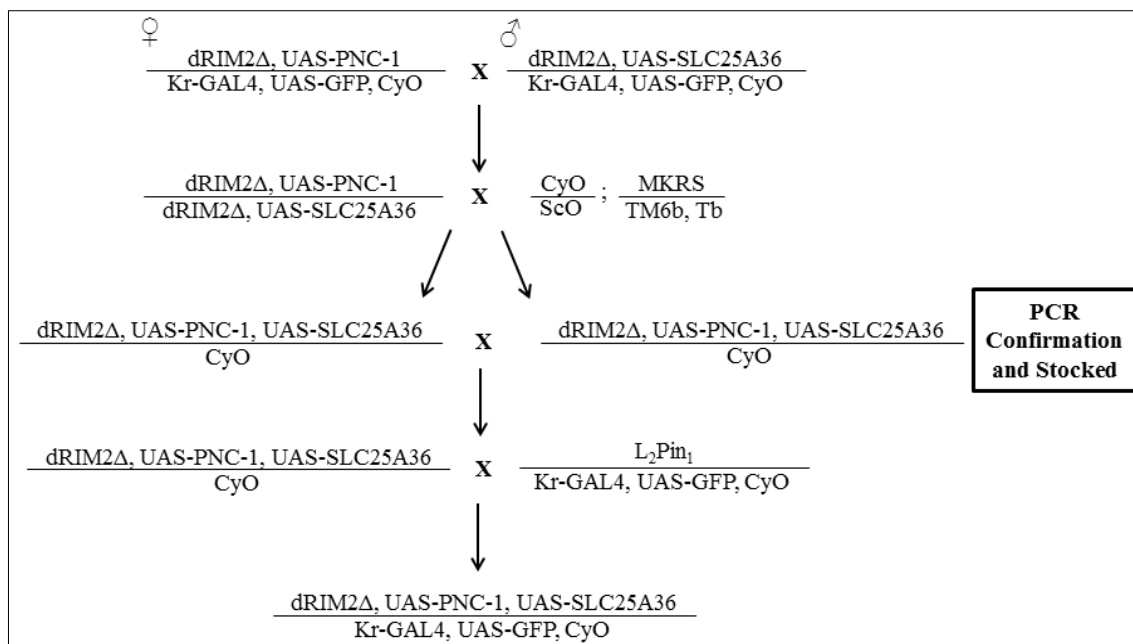


Fig. 2.4.10: Crosses done to generate *drim2* K. O. lines capable of expressing both human homologs, *PNC-1* and *SLC25A36* under UAS-GAL4 control.

This method relied on a recombination event happening in order to obtain both human homologs on chromosome II, and therefore the lines were confirmed by PCR as described in Section 2.4.2-2.4.3 with the primers listed in Table 2.4.3.

2.4.11: Phylogenetic Analysis of *PNC-1* and *SLC25A36*

In order to investigate the evolutionary history of the two putative human *RIM2* homologs, a phylogenetic analysis was conducted by Professor Alessandro Grapputo from the Department of Biology at the University of Padua, Italy, with mRNA sequences selected during this project.

Sequences for phylogenetic analysis were taken from the NCBI database using the blastx tool. Partial sequences or sequences with an e-value > e-5 were not taken into consideration. A total of 92 sequences were used for analysis. Sequences were then aligned with the use of MEGA 5.1 beta3 software, and then the translated proteins were aligned. The model for nucleotide substitution was chosen with jModelTest2 and the final phylogenetic tree was generated by Prof. Grapputo using MrBayes, a program which uses Bayesian inference and Markov chain Monte Carlo to calculate the posterior probabilities of trees (Huelsenbeck and Ronquist, 2001). Phylogenetic trees using both protein and the nucleotide sequences of the coding region of the mRNA were constructed in this fashion.

CHAPTER I: **RESULTS**

3.1: Characterization of *drim2* K.O. Line

This Chapter aims to investigate whether or not the *drim2* gene is integral to mitochondrial function to *Drosophila melanogaster*. In order to do this, the gene was knocked out *in vivo* and flies both homozygous and heterozygous for the mutation were characterized.

3.1.1: Initial Observations

100% of *drim2* K.O. larvae died before pupation, indicating that *drim2* expression is essential for metamorphosis to occur. Flies heterozygous for the mutation, on the other hand, survive to the adult stage. *drim2* mutant third instar larvae also appeared to be smaller than their heterozygous counterparts (Fig 3.1.1).

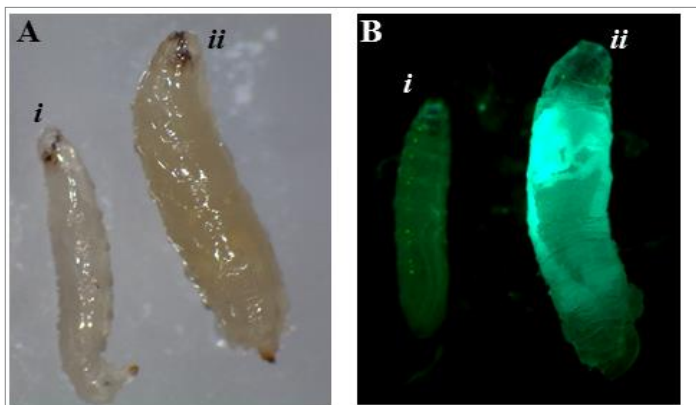


Fig. 3.1.1: Larvae heterozygous (*ii*) and homozygous (*i*) for the *drim2* mutation photographed under (A) visible and (B) fluorescent light.

In order to determine whether this difference in size was significant, and whether or not this was due to competition between larvae or due to an effect of the mutation itself, larval size was further characterized.

3.1.2: Characterization of Mutant Larval Size

Drosophila melanogaster is capable of reducing its size in response to a lack of resources, either as a result of poor food quality or heavy competition. Therefore, in order to investigate the effect of competition on mutant larval size, *drim2* K.O. larvae and *drim2*^{+/−} larvae were measured for length and width, both after being raised in crowded and uncrowded conditions. These data were

processed with R x64 2.15.2 software and an ANOVA with Tukey's post-hoc test was performed (Fig 3.1.2).

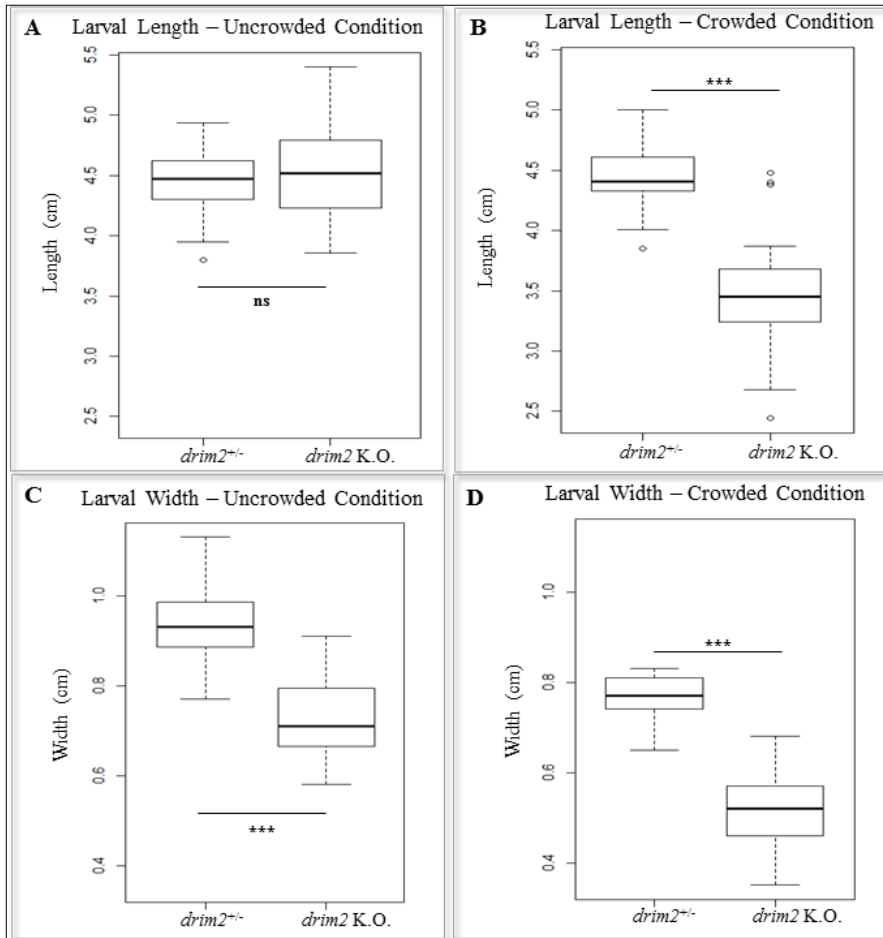


Fig 3.1.2: Boxplots of larval measurements. (A) Larval length in uncrowded conditions. (B) Larval length in crowded conditions. (C) Larval width in uncrowded conditions. (D) Larval width in crowded conditions. Statistical Analysis: ANOVA and Tukey's post hoc test (n=30). ***p<0.001 ns=not significant

When raised in crowded conditions, mutant larvae were significantly shorter (Fig 3.1.2 B) and thinner (Fig 3.1.2 D) than their heterozygous counterparts. When raised in uncrowded conditions, on the other hand, mutant larvae were still significantly thinner (Fig 3.1.2 C) but not shorter than heterozygous larvae (Fig 3.1.2 A), suggesting that part of the size discrepancy initially observed in mutant larvae could have been due to competition between larvae rather than an effect of the mutation itself. The mutation did have some effect on size however, since mutants remained significantly thinner. Whether or not the size discrepancy was due to competition, crowded conditions clearly had a much stronger effect on mutant larval size than it did on heterozygous controls.

3.1.3: Locomotor Activity of *drim2* Mutant Larvae

Since mitochondria are responsible for cellular ATP production in the cell, mitochondrial dysfunction often affects bodily functions which most rely on energy production, such as muscle movement. The locomotor activity of larvae heterozygous and homozygous for the *drim2* mutation was therefore evaluated and compared with *white*¹¹¹⁸ controls, as an indirect measure of energy production. The locomotor activity of mutant larvae raised in uncrowded conditions was also measured, in order to control for the effect of competition on locomotor activity.

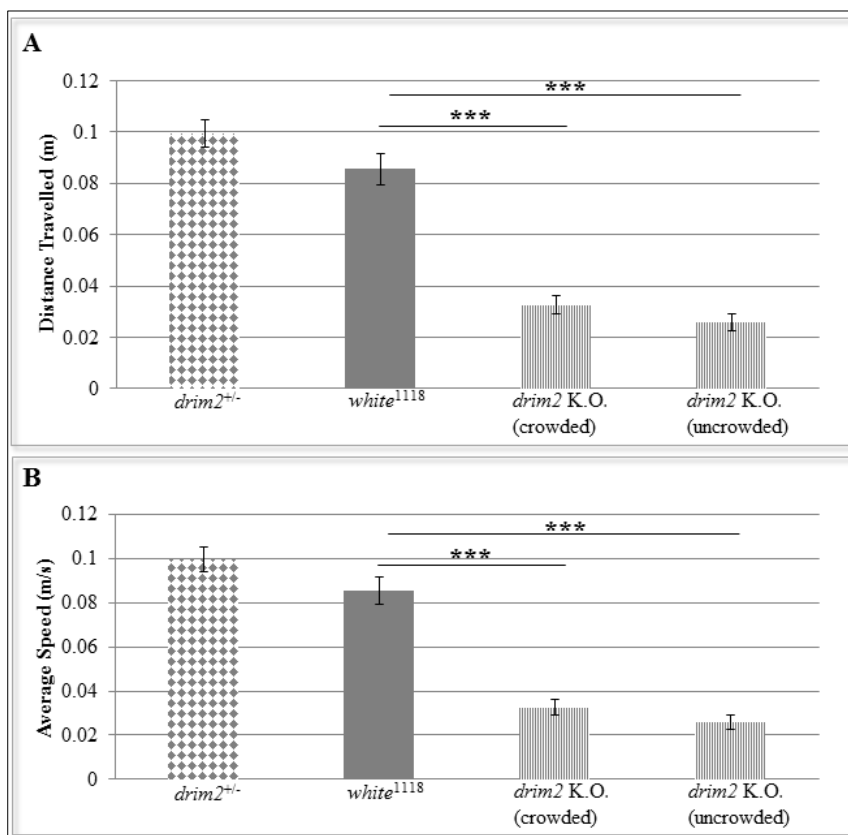


Fig. 3.1.3: Locomotor activity of mutant (lines), *drim2*^{+/-} (diamond) and *white*¹¹¹⁸ (matt) larvae over a 2 minute time period, measured in terms of (A) total distance travelled and (B) overall average speed. Mutant larvae moved significantly less compared to both *white*¹¹¹⁸ and *drim2*^{+/-} controls. Statistical analysis: one-way ANOVA with Sidak correction; n=50; ***p<0.001; Error bars= S.E.

The locomotor activity of *drim2* significantly reduced compared to both heterozygous and *white*¹¹¹⁸ controls, both terms of total distance travelled over a 2 minute period (Fig. 3.1.3 A) and overall average speed (Fig. 3.1.3 B), suggesting that mutants have muscular defects, possibly due to an impairment in energy production. This hypothesis is further supported by the fact that this defect is also observed in mutant larvae raised in uncrowded conditions, demonstrating that this locomotor deficiency is caused by the mutation rather than a side effect of competition. To investigate whether or not this locomotor activity deficit was due to mitochondrial dysfunction, *drim2* mutant mitochondria were characterized further.

3.1.4: Analysis of Mitochondrial Muscle Pattern

As a preliminary investigation of mutant mitochondria, MitoTracker[®] Staining of larval body wall muscles was performed in order to evaluate mitochondrial pattern, and as a primary indicator of mitochondrial size and number.

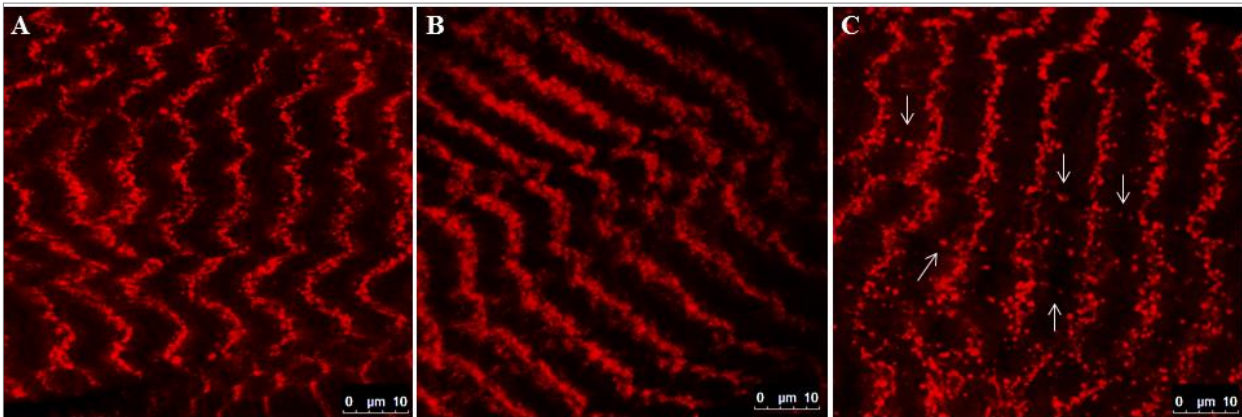


Fig 3.1.4.1: Coloration of mitochondria in muscle 6 of (A) *white*¹¹¹⁸, (B) *drim2*^{+/-} and (C) *drim2* K.O. third instar larvae. Arrows indicate mitochondria between z-bands.

Controls showed the typical muscular mitochondrial pattern, with organelles organized into parallel Z-bands along the muscle fiber (Fig. 3.1.4.1 A-B). Larvae homozygous for the *drim2* mutation (Fig 3.1.4.1 C), on the other hand, had a disorganized pattern of mitochondria in muscle 6, with some organelles scattered between z-bands (Fig 3.1.4.1 C, arrows). At first glance, these mutants also seemed to have smaller mitochondria than *white*¹¹¹⁸ controls (Fig 3.1.4.1 A), while heterozygous mutants (Fig 3.1.4.1 B) seemed to have larger mitochondria than controls. In order to verify this, larvae were sent to the MicroScoBio Research Center, Department of Experimental Medicine (DIMES) at the University of Genoa, Italy, in collaboration with Dr. Maria Cristina Gagliani and Prof. Carlo Tacchetti (Fig. 3.1.4.2).

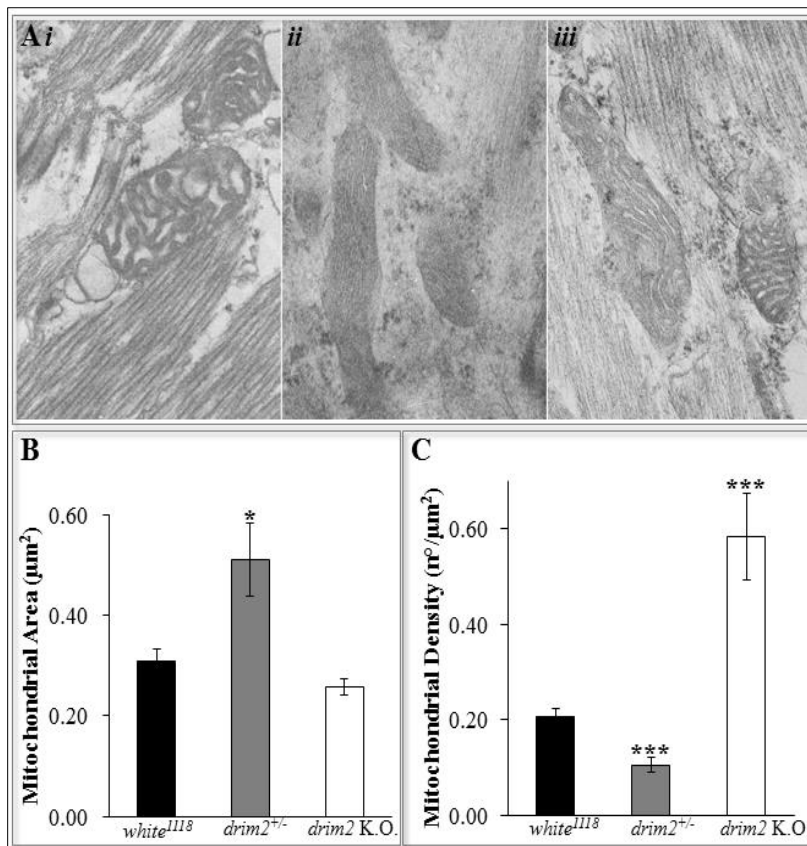
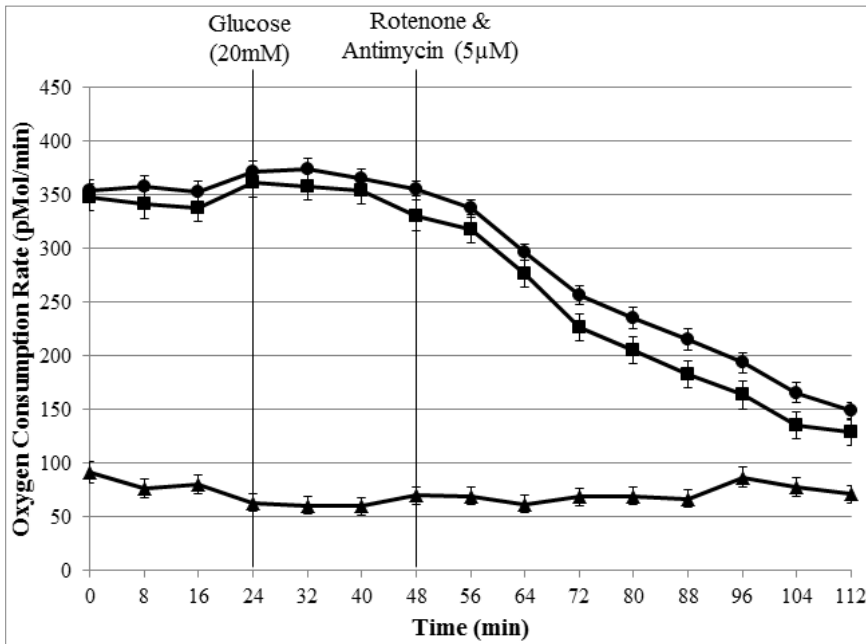


Fig. 3.1.4.2: (A) Electron microscopy scans of (i) *white*¹¹¹⁸ (ii) *drim2*^{+/-} and (iii) *drim2* mutant larval mitochondria. (B) Average mitochondrial area. Statistical analysis: Student's t-test; * $p < 0.05$. (C) Mitochondrial density in larval body wall muscle. Statistical analysis: Student's t-test; *** $p < 0.001$.

Electron microscopy analysis confirms that mitochondria are more dense in mutant larval body wall muscles (Fig. 3.1.4.2 C). While K.O. mitochondria were not significantly smaller than controls, *drim2*^{+/-} mitochondria were significantly larger (Fig 3.1.4.2 B) and less dense in body wall muscles (Fig 3.1.4.2 C) than controls.

3.1.5: Mitochondrial Respiration in *drim2* K.O. Larvae

Mitochondrial function was investigated in order to see whether or not abnormal morphology was accompanied by mitochondrial dysfunction. Since mitochondria utilize oxygen to produce ATP, mitochondrial function was analyzed in mutant larvae by measuring the oxygen consumption rate of muscle preparations with a Seahorse XF Bioflux Analyzer (BioScience). After 24 minutes glucose was added to stimulate respiration, and after 48 minutes rotenone and antimycin A were added to inhibit the electron transport chain, thus demonstrating that whatever oxygen consumption was measured previously was mitochondrial in nature (Fig 3.1.5).

**Fig 3.1.5:**

Oxygen consumption rate of *drim2*^{+/+} (square), *white*¹¹¹⁸ (circle) and *drim2* K.O. (triangle) larvae, as measured by a Seahorse XF BioFlux Analyzer. Error bars= S.E.; n=15.

During the first 24 minutes, basal mitochondrial respiration was measured, after which glucose was added to stimulate it. Between 24 and 48 minutes oxygen consumption goes up in *white*¹¹¹⁸ and *drim2*^{+/+} larvae, while mutant oxygen consumption remained constant throughout. At 48 minutes, rotenone and antimycin A were added and oxygen consumption goes down in control tissues, as expected when ETC respiratory complexes are inhibited.

The mitochondrial respiration of *drim2* mutant larvae (Fig 3.1.7, triangle) is severely reduced compared to both *drim2*^{+/+} (Fig 3.1.7, square) and *white*¹¹¹⁸ (Fig 3.1.7, circle) controls. Also, what little oxygen consumption registered for the mutant larvae was not inhibited by rotenone and antimycin as it was for controls, indicating that it was most likely not mitochondrial in nature. These results suggest a severe mitochondrial defect in *drim2* mutant larvae.

3.1.6: Mitochondrial Gene Transcription in *drim2* Mutants

If this gene is a dNTP transporter as it is in yeast, we would expect to observe abnormalities in mitochondrial DNA integrity as well as in mitochondrial function. As a preliminary experiment to test for alterations in mitochondrial DNA, a qRT-PCR analysis was performed on two mitochondrial genes located far from each other on the mitochondrial genome: *16S* and *COXII* (Fig 3.1.6).

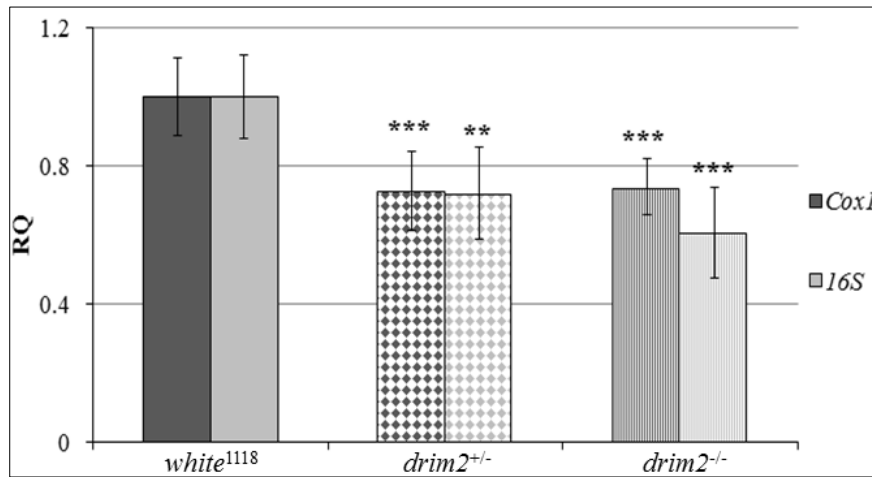


Fig 3.1.6: qRT-PCR of mitochondrial genes *CoxI* (dark gray) and *16S* (light gray) in *white*¹¹¹⁸ (matt), *drim2*^{+/-} (diamond) and *drim2* K.O. (lines) larvae.

Transcription of both genes was reduced by approximately 50% in larvae both heterozygous and homozygous for the *drim2* mutation (Fig 3.1.6), indicating that both have abnormalities in mitochondrial DNA. Since heterozygous larvae do not seem to have an altered mitochondrial phenotype, and since there is no significant difference in mitochondrial gene transcription levels between heterozygous and homozygous mutants, this seems to indicate that the reduced levels of transcription observed are not one of the causes of the mitochondrial phenotype seen in homozygous mutants.

3.1.7: Characterization of the Neuromuscular Junction in *drim2* Mutant Larvae

Muscular movement relies heavily on energy production from mitochondria. However, it also relies on signals from the central nervous system which terminate at the neuromuscular junction, stimulating the muscle fibers to contract. While the mitochondrial dysfunction described in Section 3.1.4 – 3.1.5 could explain the locomotor defects described in Section 3.1.3, neuromuscular junction function was also characterized to verify whether or not there was also a nervous system defect.

To characterize the neuromuscular junction, electrophysiology of the NMJ was conducted by Dr. Michele Scorzeto in the lab of Prof. Aram Megighian in the Department of Human Anatomy and Physiology at the University of Padua, Italy, in order to see whether or not mutant larvae had defects in NMJ function (Fig 3.1.7.1).

NMJ function was evaluated under patch-clamp conditions at the NMJ of muscle 6/7 in third instar larval segment 3. First, spontaneous neurotransmitter release in the unstimulated NMJ was

measured, after which its nerve is stimulated and the evoked release of neurotransmitter was also measured (Fig. 3.1.7.1).

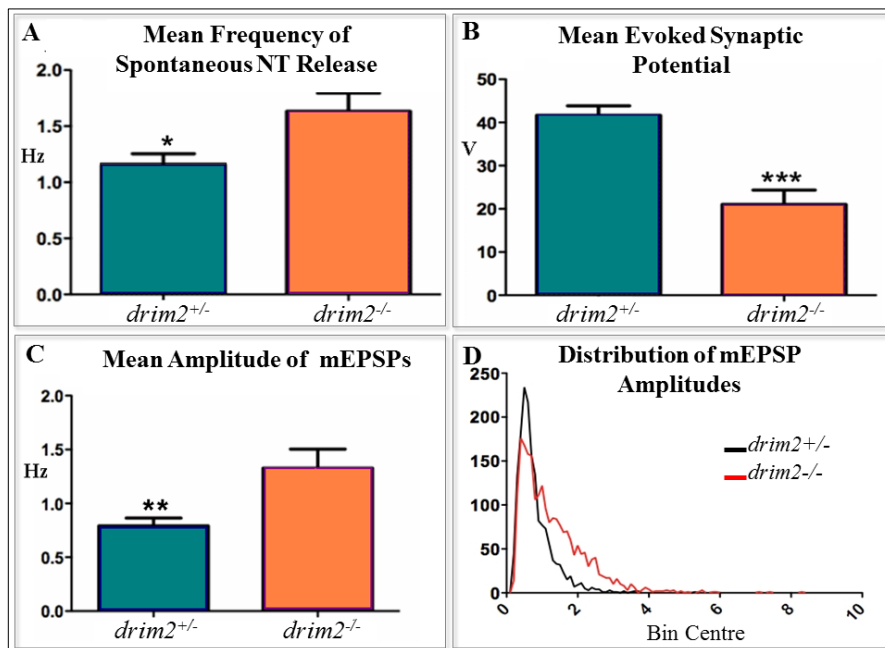


Fig. 3.1.7.1: Electrophysiology of muscle 6/7 of third instar larvae homozygous and heterozygous for the *drim2* mutation. (A) Measure of spontaneous NT release. (B) Measure of NT release after stimulus is applied to the nerve. (C) Mean amplitude of miniature excitatory post-synaptic potentials (mEPSPs). (D) Distribution of amplitudes of mEPSPs. NT= neurotransmitter. Statistical analysis: 2-sample t-test; * $p < 0.05$; ** $p < 0.01$; *** $p < 0.001$; $n = 10$

Drosophila melanogaster NMJs often exhibit spontaneous fusion of single synaptic vesicles to the synaptic membrane, known as miniature excitatory postsynaptic potentials (mEPSPs), colloquially referred to as “minis”, which can be measured postsynaptically (Schwarz, 2006). The nerve which innervates the muscle fiber being studied (in this case, muscle 6/7 of segment 3) can also be stimulated in order to measure the evoked neurotransmitter release.

Mutant larvae had significantly higher levels of mEPSP events, indicating that mutants have more spontaneous neurotransmitter release compared to heterozygous controls (Fig. 3.1.7.1 A). These mEPSPs also have a higher mean amplitude compared to heterozygous controls (Fig. 3.1.7.1 C), which is explained when the distribution of the amplitudes of the mEPSPs is plotted (Fig. 3.1.7.1 D). Since synaptic vesicles contain a relatively constant amount of neurotransmitter, the amplitude of one vesicle fusing to the synaptic membrane is quite constant. Therefore, by plotting the amplitudes of mEPSP events, the number of synaptic vesicles which fuse to the synaptic membrane in each event can be estimated. Usually mEPSP events consist of the fusion of a single synaptic vesicle, which is what we see in the plot of the distribution of the amplitudes of mEPSPs of heterozygous larvae (Fig. 3.1.7.1 D, black line). When we look at the amplitudes of mEPSPs of *drim2* K.O. larvae, on the other hand, we see that fewer mEPSPs consisted of the

fusion of a single vesicle, with far more events consisting of the fusion of multiple synaptic vesicles (Fig. 3.1.7.1 D, red line).

When the muscle 6/7 nerve was stimulated, on the other hand, *drim2* K.O. larvae released significantly lower amounts of neurotransmitter compared to heterozygous mutants (Fig. 3.1.7.1 B). Taken together, these results indicate that mutant larvae have a severe defect in the regulation of neurotransmitter release. From these results, it seems that the *drim2* mutation causes larvae to lose more neurotransmitter at the NMJ than normal, leading to the inability to release normal amounts of NT when a nerve impulse demands it.

A defect in NMJ function can sometimes be caused by an alteration in NMJ morphology. In order to verify if the functional defect measured in mutant larvae was accompanied by a morphological abnormality, the morphology of the NMJ of muscle 6/7 in the third abdominal segment was analyzed by immunohistochemistry. The number of boutons, their size and the level of branching of the neuromuscular junction was measured and quantified. Since mutant larval size is so severely affected by crowded conditions (Section 3.1.2), NMJs of mutant larvae raised in uncrowded conditions were also analyzed, in order to confirm that any abnormalities observed were due to the mutation itself.

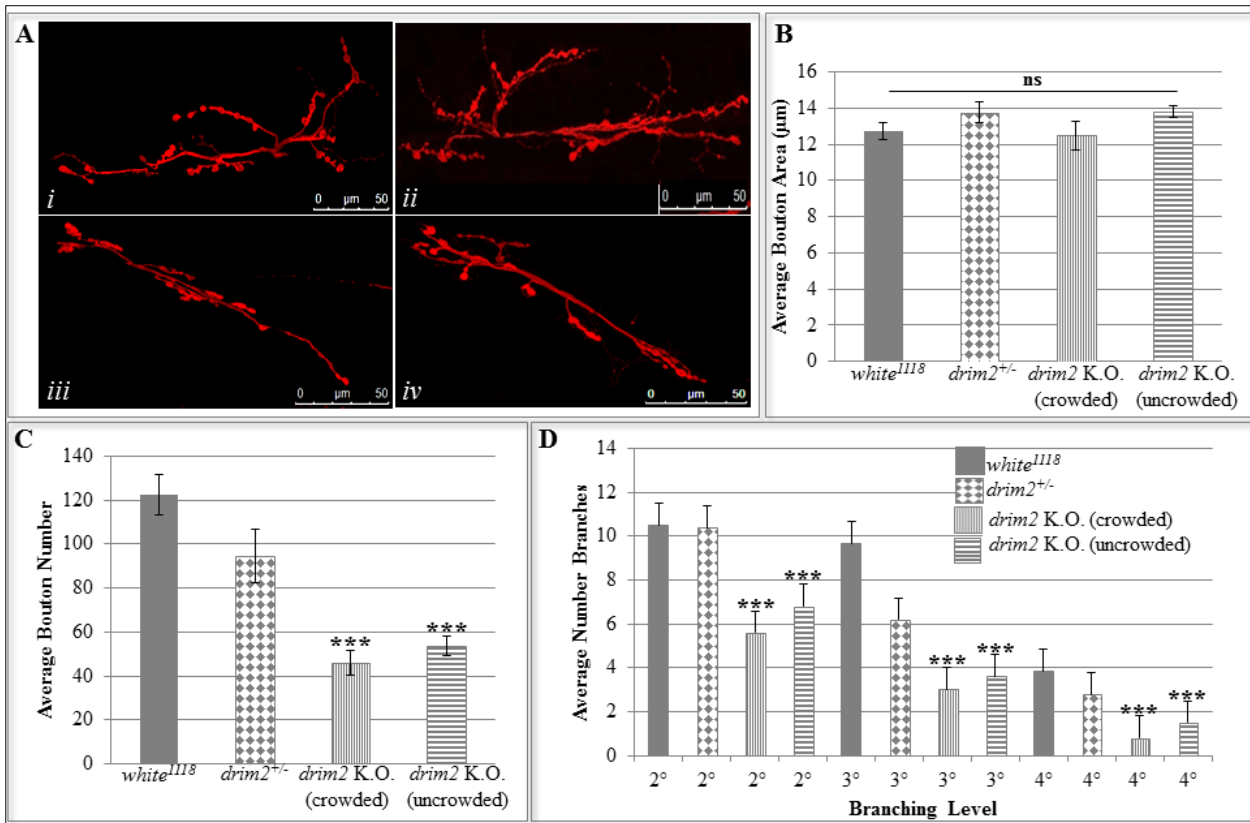


Fig. 3.1.7.2: Characterization of the neuromuscular junction of *white*¹¹¹⁸ (Ai), *drim2*^{+/-} (Aii) and *drim2* mutant, raised both in crowded (Aiii) and uncrowded (Aiv) conditions. (A) Immunohistochemistry staining of the NMJ of muscle 6/7 in segment 3, stained with 1:100 Cy3-conjugated goat α -HRP (Sigma). (B) Average number of boutons in NMJ. Statistical analysis: two-sample t-test, *** $p < 0.001$; $n = 10$. (C) Average bouton size. Statistical analysis: two-sample t-test, $n = 10$, ns = not significant. (D) Average number of branches in NMJ. Statistical analysis: two-sample t-test, *** $p < 0.001$.

Crowded and uncrowded-raised mutant larvae had abnormal muscle 6/7 NMJs (Fig 3.1.7.2 Aiii-iv), both in terms of bouton number (Fig 3.1.7.2 B) and NMJ branching (Fig 3.1.7.2 D). Average bouton size, on the other hand, remained unaffected (Fig 3.1.7.2 C), indicating that the NMJs were not simply smaller in proportion with the smaller mutant larvae. Both the functional and morphological defects seen in mutants thus accompany mitochondrial dysfunction in precipitating the severe locomotor deficit described in Section 3.1.3.

3.1.8: Analysis of Sensory Capabilities in Mutant Larvae

During the locomotor test, the number of times the larvae turned (rather than travelling in a straight line) was also measured, as this is a measure of exploratory tendency. *drim2* K.O. larvae turned significantly less compared to heterozygous larvae and *white*¹¹¹⁸ controls (Fig 3.1.4 A). Since this is also considered an indirect indicator of sensory capability, and since mitochondrial function is also crucial for the correct function of the nervous system, mutant larvae were tested for their ability to perceive visual and gustatory cues in order to analyze whether or not they had any sensory deficiencies.

In order to test for their sensory capabilities, groups of 50 larvae were placed in the center of an arena which was divided into four quadrants, two containing one stimulus (in the form of either illumination or chemically fortified agarose) and two of which containing an opposite one. The proportion of larvae found on each of the stimuli was recorded (Fig 3.1.8 B-D, light gray bars). In order to provide an adequate negative control for this experiment, groups of 50 larvae were allowed to distribute over an arena which was also divided into four quadrants, but whose quadrants all contained neutral agarose with no ulterior stimulus added. This was done to verify that larvae would distribute evenly around this arena if not for the additional stimuli added to the quadrants, and the proportion of larvae found on two of the four were recorded and used as a comparison for each of the sensory behavior tests (Fig 3.1.8 B-D, dark gray bars).

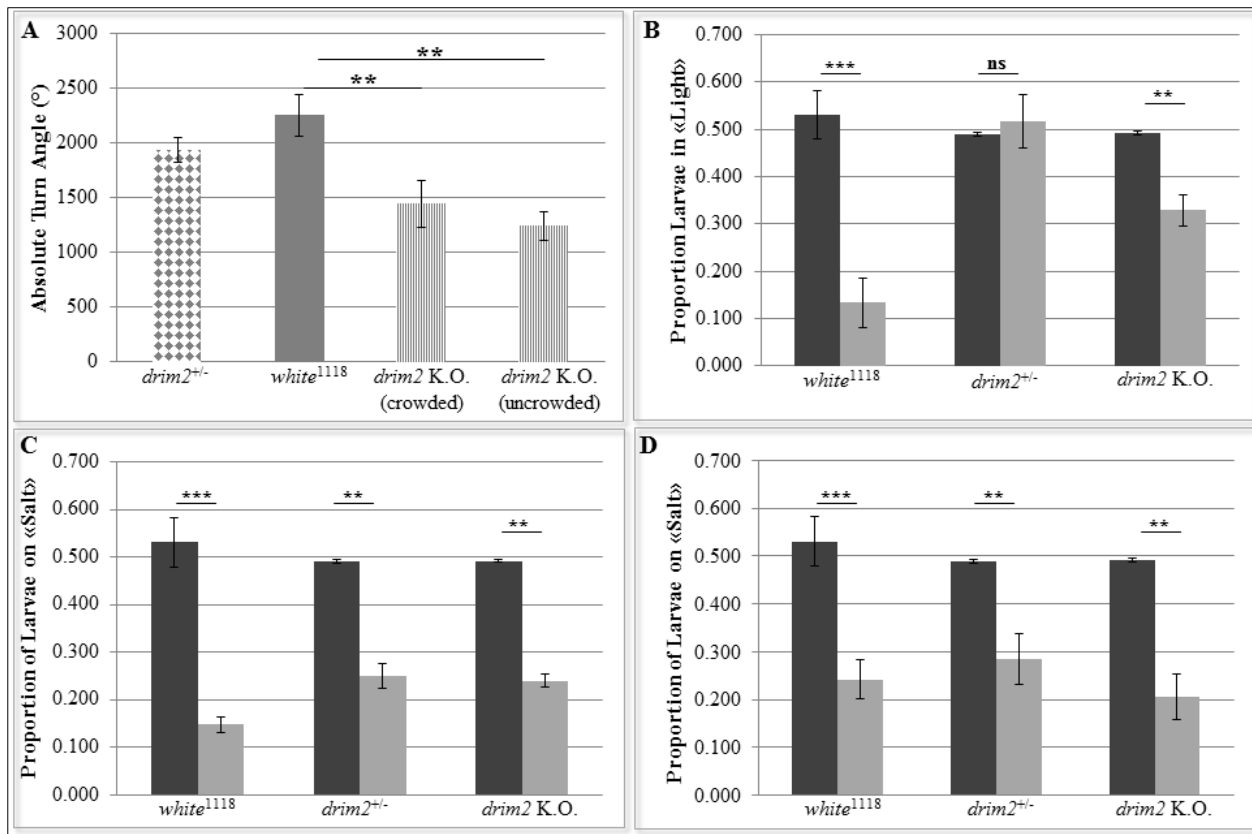


Fig. 3.1.8: Analysis of Larval Behavior. (A) Analysis of exploratory tendency as measured by the absolute turn angle of the larvae over a 2 minute period. Statistical analysis: one-way ANOVA with Sidak correction (n=50) **p<0.01 error bars: S. E. (B) Analysis of visual capabilities as measured by tendency to avoid light. Proportions of larvae in the illuminated quadrants of the arena (light gray) were compared to proportions of larvae found in the corresponding quadrants of an arena which was not differentially illuminated (dark gray). Statistical analysis: chi-square test (n=3); **p<0.01; ***p<0.001 ns= not significant; error bars= S.E. (C-D) Analysis of gustatory capabilities as measured by the ability of larvae to (C) avoid quadrants with 0.5M NaCl or (D) avoid quadrants with 0.5M NaCl and seek quadrants with 1M sucrose (light gray). Proportions of larvae in NaCl-fortified quadrants were compared to the proportion of larvae in corresponding quadrants in an arena containing only neutral agarose (dark gray). Statistical analysis: chi-square test (n=3); **p<0.01; ***p<0.001; error bars= S.E.

Larvae were tested for their visual capacity by placing groups of 50 in the center of an arena divided into 4 quadrants, two of which were illuminated and two of which were not. Larvae were tested for their ability to seek out the dark quadrants over a 5 minute period. If third instar larvae are capable of perceiving light, they will avoid illuminated quadrants of the arena and seek to remain in the dark ones. As expected, *white*¹¹¹⁸ larvae differ significantly in their distribution over the arena compared to when two of the four quadrants are not illuminated (Fig. 3.1.8 B). Surprisingly, while *drim2* K.O. larvae were able to distinguish between light and dark, heterozygous mutants did not significantly seek out the dark quadrants of the arena (Fig 3.1.8 B). Since this defect is only observable in the heterozygous mutants, this could indicate that *drim2*

expression is needed for visual acuity in *Drosophila* larvae, but that another gene may be able to compensate for *drim2* when its transcription is completely absent.

Larvae were tested for their gustatory capacity by placing groups of 50 in the center of an arena divided into 4 quadrants, two of which were fortified with 0.5M NaCl, and two of which were either left as neutral agarose (Fig 3.1.4 C) or were fortified with 1M sucrose (Fig 3.1.4 D). NaCl-fortified agarose are a negative stimulus, and so we expect larvae to avoid remaining on these quadrants. While neutral agarose are a neutral stimulus sucrose-fortified quadrants are a positive one, which should reinforce the tendency of larvae to avoid the salty quadrants by giving them a reason to stay on the sweet ones. Larvae were thus analyzed for their ability to avoid NaCl-fortified quadrants, and/or to seek out sucrose-fortified quadrants. As expected, *white*¹¹¹⁸ larvae differed significantly in their distribution over the arena containing the NaCl stimulus compared to negative controls (Fig. 3.1.8 C-D). In this regard, both *drim2* K.O. and *drim2*^{+/-} larvae were also able to avoid the salt (Fig 3.1.8 C) and seek the sugar (Fig 3.1.8 D), indicating that the *drim2* mutation does not cause gustatory abnormalities.

3.1.9: Evaluating Iron Content in Mutant Larval Proteins

Since *RIM2* was shown to also import iron in yeast mitochondria alongside pyrimidine dNTPs (Froschauer *et. al.*, 2013), we considered the possibility that *drim2* might have the same role in *Drosophila*. Since mitochondria are the sole producers of heme and the primary producers of Fe-S clusters (Richardson *et. al.*, 2010), measuring the iron content of proteins is considered an indirect measurement of the ability of mitochondria to import iron.

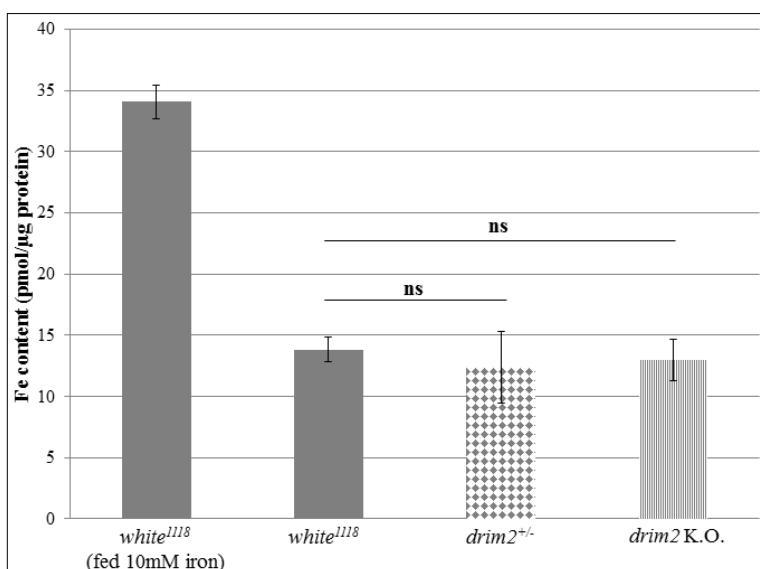


Fig 3.1.9: Iron content of larval proteins as measured by FerroZine assay. Statistical analysis: 2-sample t-test; n= 5; ns= not significant.

The protein iron content of *white*¹¹¹⁸, *drim2*^{+/-} and *drim2*Δ larvae was measured by FerroZine™ assay (Fig 3.1.9). The validity of the protocol was also tested by feeding *white*¹¹¹⁸ larvae with cornmeal-yeast-agar medium fortified with 10mM ferric ammonium citrate (Sigma), which increased the levels of protein iron content as expected (Fig 3.1.9). No significant differences were found in protein iron content between mutant larvae and controls, however, which means that at this time there is no evidence that *drim2* performs this function in *Drosophila*.

3.2: *In vitro* Localization of *drim2* Protein

Despite the fact that *drim2* K.O. larvae present with mitochondrial dysfunction, the subcellular localization of this protein verifies once and for all whether or not this gene transcribes for a mitochondrial protein.

3.2.1: Expression of Tagged *drim2* *in vitro*

Repeated attempts to immunolocalize *drim2* in larval body wall preparations *in vivo* were unsuccessful. Therefore, an HA-tagged *drim2* construct was cloned into a pACT vector and transfected into *Drosophila* S2R+ cells, in order to have cells which constitutively expressed a tagged form of the protein.

Transfected cells were collected 24, 48 and 72 hours after transfection for analysis. Since this was not a stable transfection, therefore only some cells were able to take up the vector, qRT-PCR (Fig 3.2.1 A) and western blot (Fig 3.2.1 B) analysis was performed in order to evaluate both the efficacy of the transfection and the possible effects of toxicity of *drim2* overexpression.

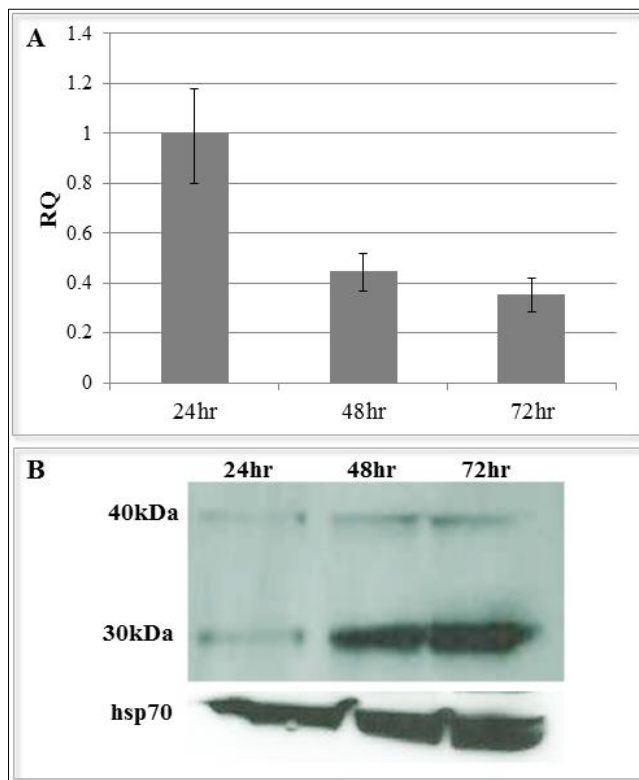


Fig 3.2.1: Analysis of *drim2* expression in cells transfected with pACT-*drim2*-HA. (A) Relative qRT-PCR of *drim2* expression in transfected cells collected 24, 48 and 72 hours after transfection. Error bars= S. E.; n= 4. (B) Western blot of transfected cells collected 24, 48 and 72 hours after transfection. Band at 40kDa is band at predicted molecular weight of *drim2*. Western blot staining conducted with 1:5000 Monoclonal mouse α -HA antibody (Sigma) and 1:5000 goat α -mouse antibody (Sigma) used for cells; 1:5000 monoclonal mouse α -hsp70 (Sigma) and 1:5000 goat α -mouse (Sigma) used as loading control.

Relative qRT-PCR of *drim2* expression over time demonstrates that *drim2* expression dramatically decreased 48 and 72 hours after transfection (Fig 3.2.1 A). This could indicate a toxic effect of *drim2* overexpression, or could simply be an effect of transient expression. However, western blot analysis seems to indicate that protein levels increased 48 and 72 hours after transfection (Fig 3.2.2 B). Also curious are the presence of two distinct bands, one at the predicted molecular weight for *drim2* at 40kDa which remains constant over time, and one at 30kDa which appears to increase in strength over time (Fig 3.1.2 B). One possible explanation for this is that the band seen at 40kDa is the protein that localizes to the mitochondria, which reaches saturation after which the excess *drim2* is cleaved in the cytosol, meaning that the two bands seen in this case are a side effect of strong overexpression. Another possible theory is that *drim2* is cleaved in order to be able to localize to mitochondria, meaning that the band visible at 40kDa is the protein that has been transcribed but which has not yet been cleaved in order to be incorporated into the inner mitochondrial membrane (IMM). However, since there is no obvious cleavage site on the *drim2* protein sequence, and since protein extractions from mutant larvae expressing *drim2* (which do not overexpress the protein) do not result in western blots with two bands (Section 3.3.2), we feel the first hypothesis is the most probable.

3.2.2: Immunolocalization of *drim2* Protein

If this protein exhibits the same function in *Drosophila* as it does in both *Saccharomyces cerevisiae* and humans, it will localize to the inner mitochondrial membrane. Therefore, if it performs the same function we expect the staining of this protein to colocalize with that of mitochondria.

To verify this, cells transfected with HA-tagged *drim2* were stained with MitoTracker[®] Red CMXRos (Life Technologies), then immunohistochemistry staining was performed for the tagged protein, in order to determine the subcellular localization of *drim2* (Fig 3.2.2).

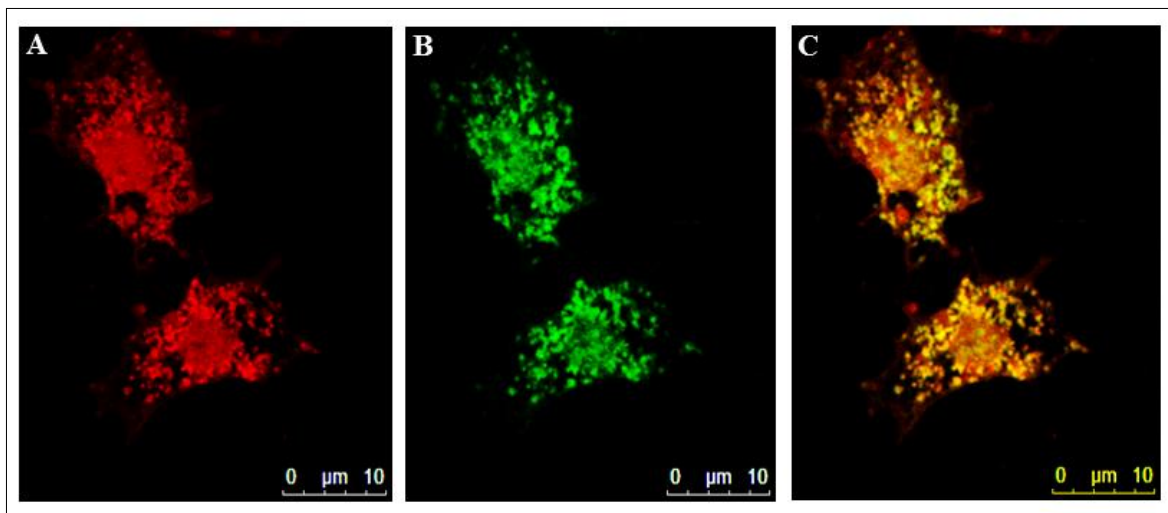


Fig 3.2.2: *Drosophila* S2R+ cells transfected with pACT vector harboring an HA-tagged *drim2* construct. (A) Staining of transfected cells with 100nM MitoTracker[®] Red CMXRos (Life Technologies). (B) Immunohistochemistry of transfected cells with 1:100 monoclonal mouse α -HA antibody (Sigma) and 1:500 FITC-conjugated rabbit α -mouse antibody (Santa Cruz Biotech). (C) Merge of the two scans indicating that the tagged protein colocalizes perfectly with mitochondria.

Confocal scans of the transfected cells indicate that the tagged *drim2* protein colocalizes perfectly with mitochondria (Fig 3.2.2). This demonstrates that in *Drosophila* (as in yeast and humans) this protein, while nuclear-encoded, is a mitochondrial protein.

3.3: Rescuing the *drim2* Mutant Phenotype

In order to investigate whether or not this *Drosophila* model has validity for humans, both human homologs were expressed in a *drim2* mutant background in order to verify functional homology between the *Drosophila* gene and the two human ones. The human homologs were

expressed singly in a *drim2* mutant background in order to see whether or not the human genes were capable of taking the place of the *Drosophila* gene.

3.3.1: Final Crosses and PCR Confirmation of Rescue Lines

drim2, *PNC-1* and *SLC25A36* were cloned into pUAST vectors and microinjected into *Drosophila* embryos previous to the beginning of this project. Fly lines were then crossed with *drim2* K. O. flies in order to be able to express either the *Drosophila* gene or one of the two human homologs in a mutant background. During this project, the final crosses for the generation of these lines were completed. Since the generation of these lines relied on the homologous recombination of the construct on chromosome II, PCR confirmation of the success of the recombination was performed as well.

The M8 fly line, expressing *PNC-1*, and the BF4 line, expressing *SLC25A36*, were also crossed together in order to obtain fly lines which express both human homologs in a *drim2* mutant background. Since initial observations suggested the possibility that the human genes gave an incomplete rescue, this was done in order to see whether or not expressing both human genes in the *drim2* mutant could rescue the mutant phenotype better than the individual genes could. Since these crosses also involved the homologous recombination of both constructs on chromosome II, recombination was confirmed by PCR.

3.3.2: Expressing *drim2*, *PNC-1* and *SLC25A36* in a Mutant Background: Initial Observations

Rescue lines were generated by expressing *drim2*, *PNC-1* or *SLC25A36* in a *drim2* K.O. background, by crossing these “rescue” lines with an *Act5c-GAL4* driver in a mutant background (Fig 3.3.2.1).

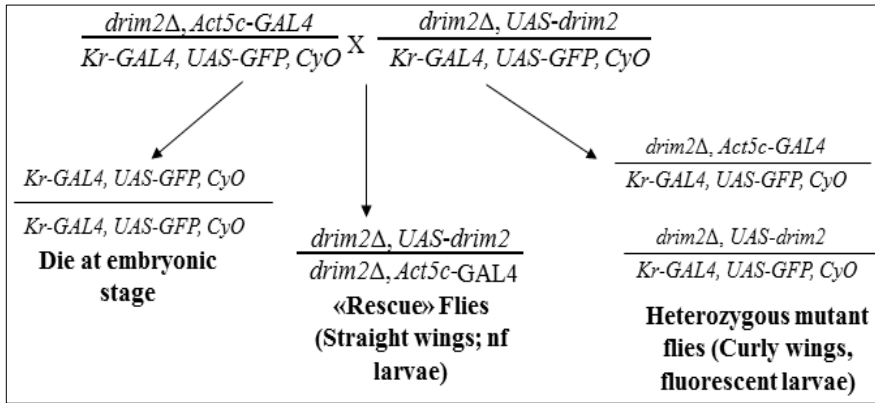


Fig 3.3.2.1: Illustrative diagram of the cross done to generate “rescued” flies using the UAS-GAL4 binary system. Given that flies homozygous for the balancer chromosome die at the embryonic stage, we expect flies born to be 2/3 heterozygous for the mutation and 1/3 “rescue” flies. nf= not fluorescent.

In all cases, flies homozygous for the mutation but expressing one of the three constructs reached the adult stage. Also, “rescued” flies were born in the proportions expected given simple Mendelian genetics (Fig 3.3.2.2), indicating that there is no residual mortality at embryonic or larval stages for “rescue” flies still harboring the homozygous *drim2* mutation.

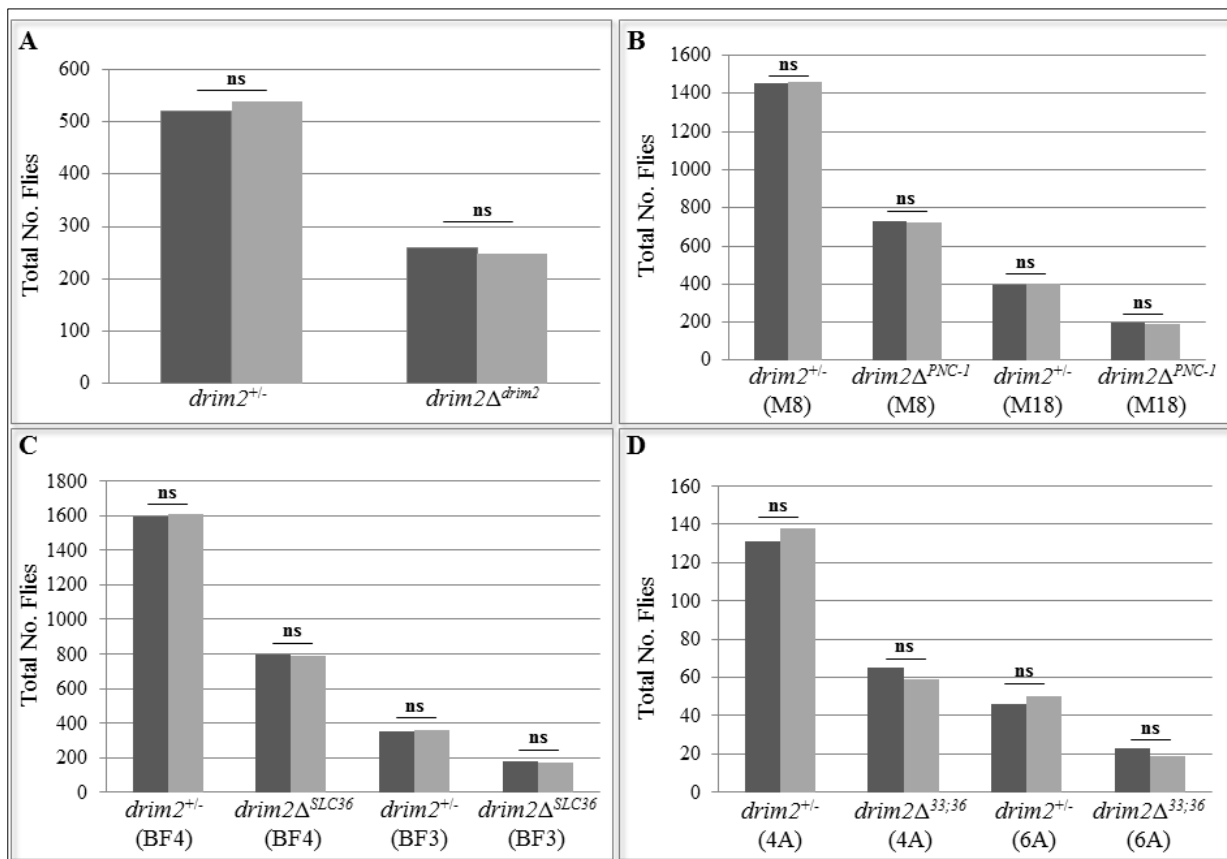


Fig. 3.3.2.2: Total number of heterozygous and homozygous flies born (light gray bars) from the cross described in Fig. 3.3.1.1, compared to the number of heterozygous and homozygous flies expected from such a cross (dark gray bars). Statistical analysis: chi-square test.

There was no statistical difference between the number of heterozygous/homozygous flies “expected” and those born (Chi-square test; $p=0.9997$; $d.f.=1$). While the flies harboring both human homologs also resulted in adult flies, further characterization was done on flies harbouring just one of the two human genes in order to evaluate differences in the ability to rescue the mutant phenotype between them.

3.3.3: Verification of Presence of Construct

The presence of the construct was ultimately verified by western blot analysis (Fig 3.3.3).

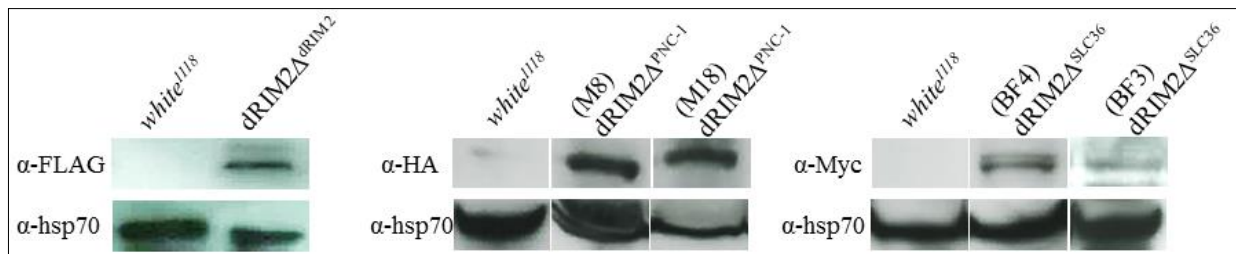


Fig 3.3.3: Western blot analysis of $drim2\Delta^{drim2}$ (1:1000 monoclonal mouse α -FLAG (Sigma); 1:5000 goat α -mouse IgG (Sigma)), $drim2\Delta^{PNC-1}$ (1:2500 monoclonal mouse α -HA (Sigma); 1:5000 goat α -mouse IgG (Sigma)) and $drim2\Delta^{SLC36}$ (1:2500 monoclonal mouse α -Myc (Cell Signaling Technology); 1:5000 goat α -mouse IgG (Sigma)) rescue flies.

The lines coded “M8”, expressing *PNC-1*, and “BF4”, expressing *SLC25A36*, were selected for further characterization.

3.3.4: Vitality Analysis of Rescued Flies

$drim2\Delta^{drim2}$, $drim2\Delta^{PNC-1}$ and $drim2\Delta^{SLC36}$ adults were analyzed to see whether or not they lived as long as $white^{1118}$ controls. Mortality was counted every 2-3 days, and vitality curves were generated to evaluate the longevity of rescued flies (Fig 3.3.4).

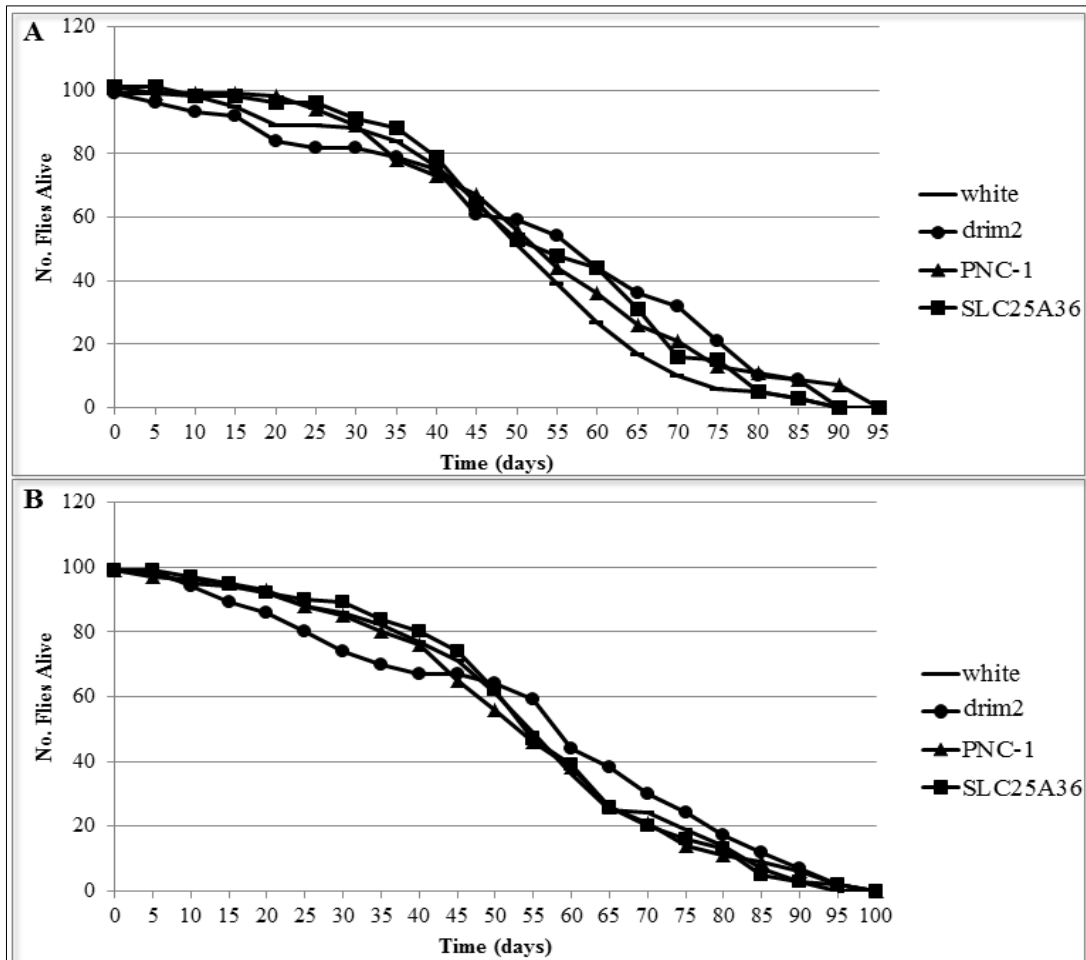


Fig. 3.3.4: Vitality curves for (A) male and (B) female adult $white^{1118}$ (line), $drim2\Delta^{drim2}$ (circle), $drim2\Delta^{PNC-1}$ (triangle) and $drim2\Delta^{SLC36}$ (square) flies; n= 100.

Flies from all three rescue lines lived as long as $white^{1118}$ controls (Fig 3.3.3). This is a further indication that all three genes are capable of fully rescuing the $drim2$ mutant phenotype.

3.3.5: Locomotor Activity of Rescued Larvae

The locomotor activity of third instar $drim2\Delta^{drim2}$, $drim2\Delta^{PNC-1}$ and $drim2\Delta^{SLC36}$ larvae was analyzed and compared to both $white^{1118}$ controls and $drim2$ mutant larvae (Fig 3.3.5).

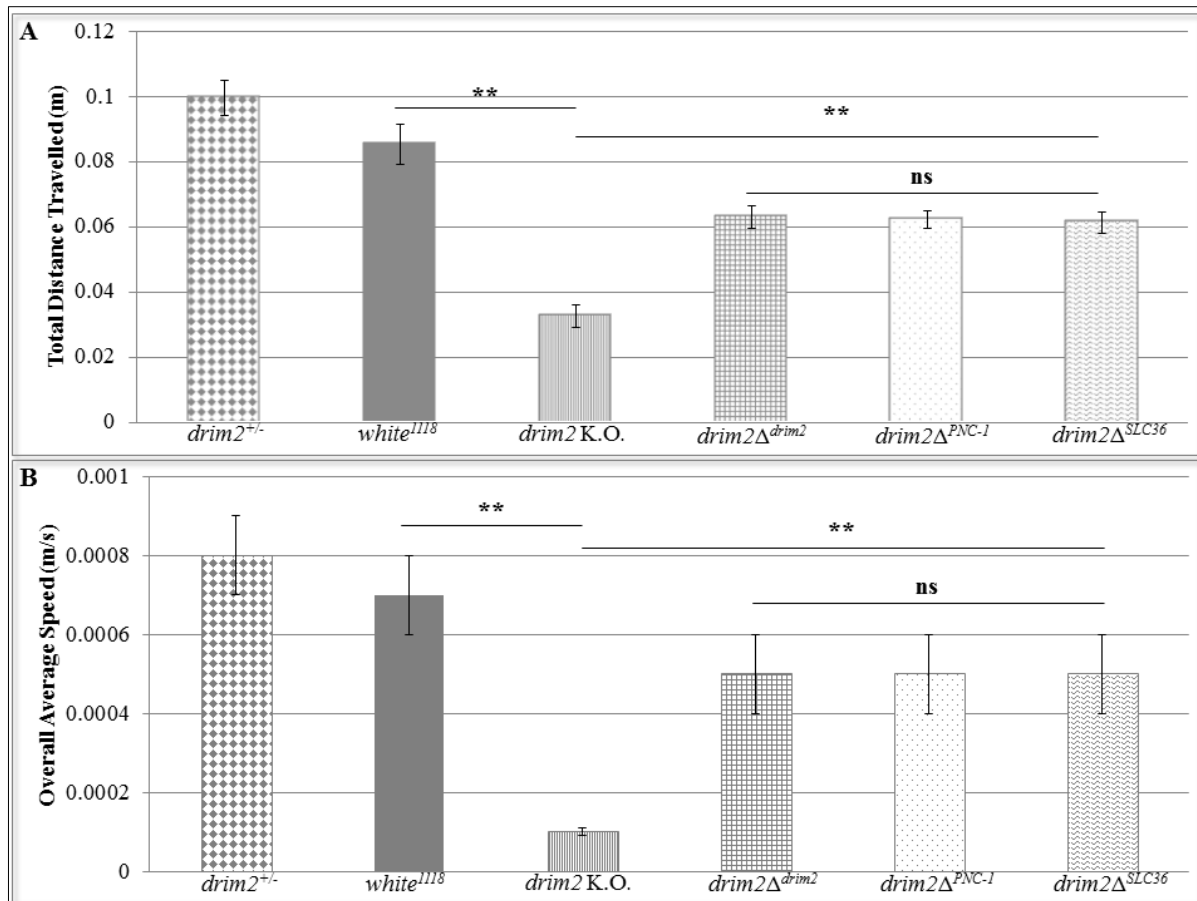


Fig 3.3.5: Locomotor activity of third instar larvae. Statistical analysis: one-way ANOVA with Sidak correction. **p<0.01; n= 50; ns= not significant.

$drim2\Delta^{drim2}$, $drim2\Delta^{PNC-1}$ and $drim2\Delta^{SLC36}$ larvae have a significantly higher locomotor activity than $drim2$ mutants, both in terms of total distance travelled (Fig 3.3.5 A) and overall average speed (Fig 3.3.5 B). While their locomotor activity does not reach control levels, all three rescued lines have the same levels of locomotor activity, indicating that all three of them are capable of rescuing this aspect of the $drim2$ mutant phenotype to the same extent.

3.3.6: Neuromuscular Junction Morphology of Rescued Larvae

The NMJ of muscle 6/7 of *drim2* Δ^{drim2} , *drim2* Δ^{PNC-1} and *drim2* Δ^{SLC36} larvae were characterized in order to determine if these genes could rescue the morphological abnormalities caused by the *drim2* mutation.

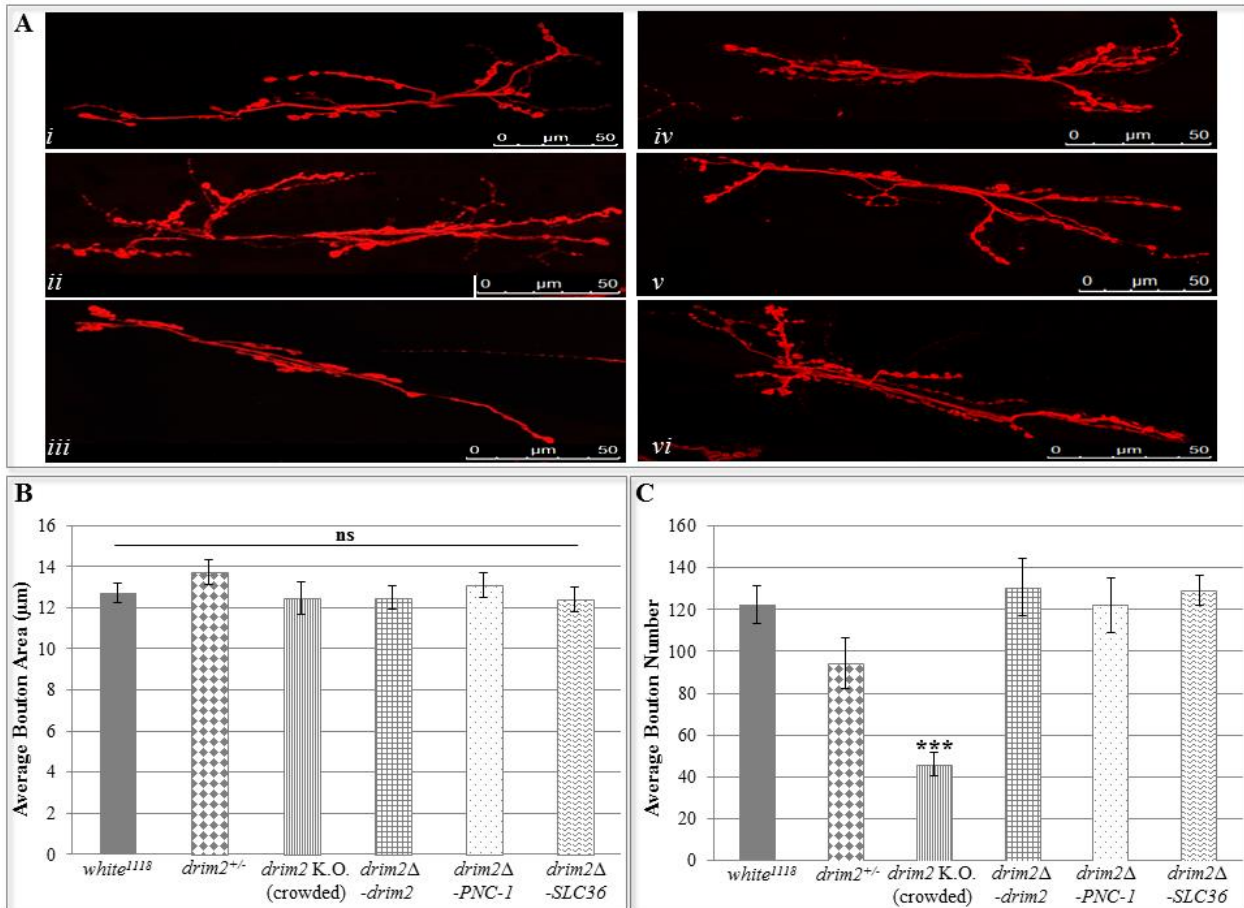


Fig 3.3.6.1: Characterization of the muscle 6/7 NMJ of (Ai) *white¹¹¹⁸* (Aii) *drim2^{+/-}* (Aiii) *drim2* K.O. (Aiv) *drim2* Δ^{drim2} (Av) *drim2* Δ^{PNC-1} and (Avi) *drim2* Δ^{SLC36} larvae. (A) Immunohistochemistry staining of NMJ with 1:100 Cy3-conjugated goat α -HRP. (B) Average bouton area. Statistical analysis: one-way ANOVA; n=10; error bars= S.E.; ns= not significant. (C) Average number of boutons. Statistical analysis: one-way ANOVA; n=10; error bars= S.E.; ***p<0.001.

All three genes (Fig 3.3.6.1 Aiv-vi) were capable of rescuing the *drim2* mutant NMJ phenotype, both in terms of average bouton number (Fig 3.3.6.1 C) and in terms of number of branches (Fig 3.3.6.2).

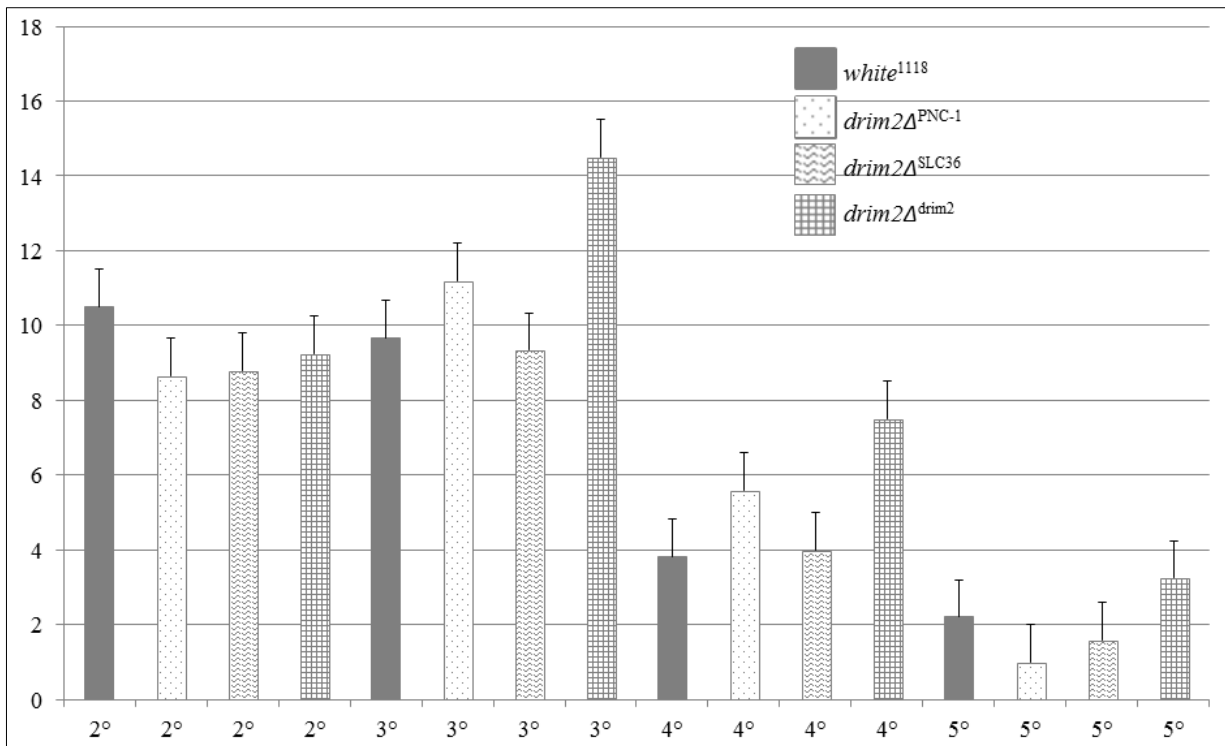


Fig. 3.3.6.2: Number of 2°, 3°, 4° and 5° branches in *white*¹¹¹⁸ (matt); *drim2*Δ^{PNC-1} (dots); *drim2*Δ^{SLC36} (tilde) and *drim2*Δ^{drim2} (square) muscle 6/7 NMJs of third instar larvae. Error bars= positive S. E.

These results indicate that all three genes expressed in a *drim2* mutant background are capable of rescuing the NMJ defects seen in *drim2* K. O. larvae. Furthermore, this indicates that the rescuing of NMJ morphology could have contributed to the rescue of the locomotor defect seen in mutant larvae.

3.3.7: Mitochondrial Respiration of Rescued Larvae

The mitochondrial respiration of third instar $drim2\Delta^{drim2}$, $drim2\Delta^{PNC-1}$ and $drim2\Delta^{SLC36}$ larvae was measured on a Seahorse XF BioFlux Analyzer (Bioscience) and compared to controls and $drim2$ K.O. mutants (Fig. 3.3.7).

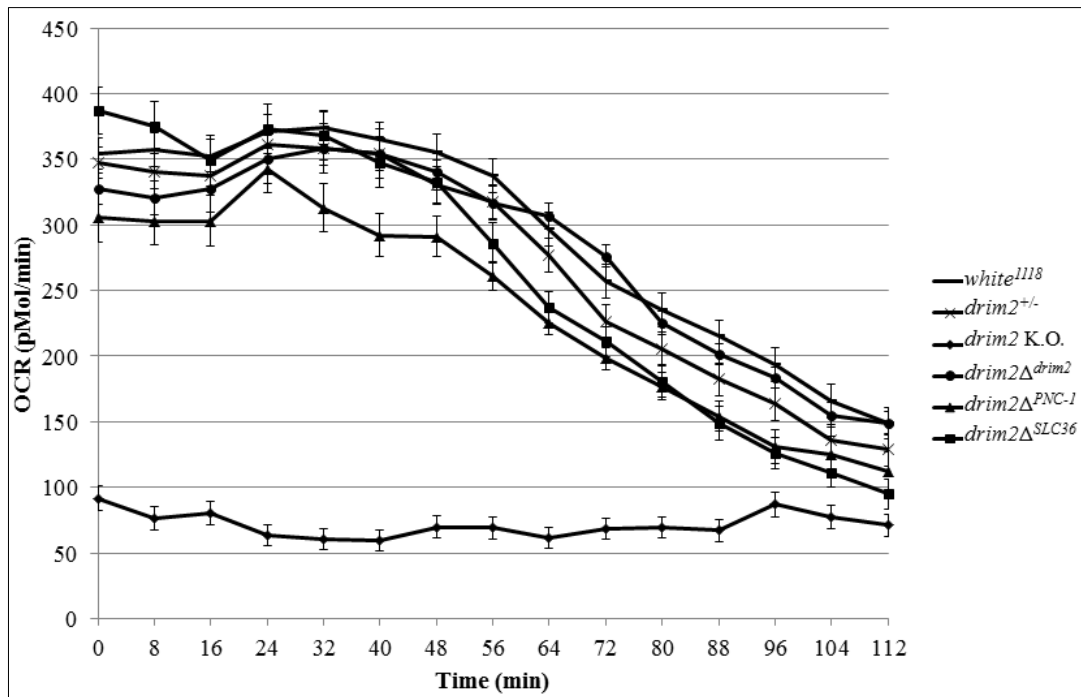


Fig 3.3.7: Mitochondrial respiration of *white*¹¹¹⁸ (line), *drim2*^{+/-} (cross), *drim2*^{-/-} (diamond), *drim2*Δ^{*drim2*} (circle), *drim2*Δ^{*PNC-1*} (triangle) and *drim2*Δ^{*SLC36*} (square) larvae, as measured by a Seahorse XF BioFlux Analyzer (Bioscience). Error bars= S. E., n= 15.

*drim2*Δ^{*drim2*}, *drim2*Δ^{*PNC-1*} and *drim2*Δ^{*SLC36*} larvae respire significantly better than *drim2* mutants (Fig 3.3.7). While *drim2*Δ^{*drim2*} (Fig 3.3.7, circle) and *drim2*Δ^{*SLC36*} (Fig 3.3.7, square) larvae have a mitochondrial respiration comparable to that of controls, *drim2*Δ^{*PNC-1*} larvae (Fig 3.3.7, triangle) have slightly lower levels of mitochondrial respiration than controls.

3.3.8: Transcription of Mitochondrial Genes in Rescued Larvae

Quantitative Real-Time PCR of mitochondrial genes *CoxI* and *16S* was also conducted on *drim2* Δ^{drim2} , *drim2* Δ^{PNC-1} and *drim2* Δ^{SLC36} larvae in order to determine if transcription levels were restored (Fig 3.3.8).

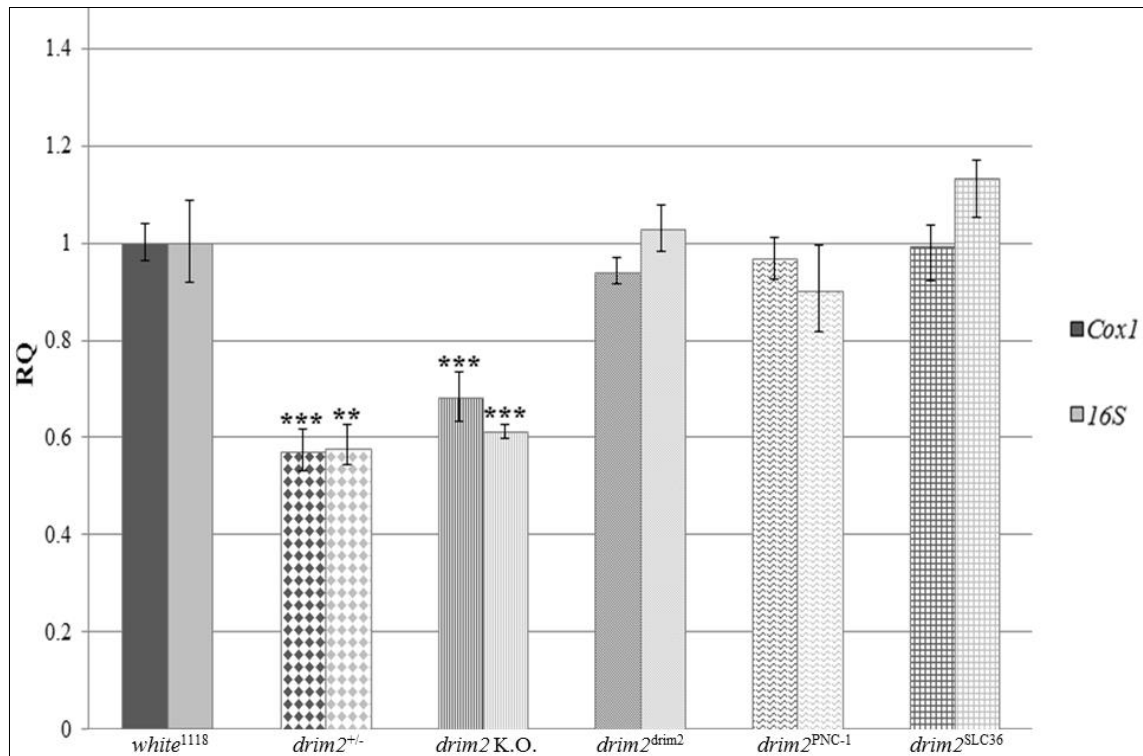


Fig 3.3.8: Quantitative Real-Time PCR analysis of the transcription of mitochondrial genes *CoxI* (dark gray) and *16S* (light gray). Statistical analysis: Student's t-test; n=3; ***p<0.001; error bars= S.E.

Transcription levels of all three mitochondrial genes were completely restored in all three rescue lines, indicating that this aspect of the *drim2* mutant phenotype can also be rescued by both the *Drosophila* and the human homologs of *RIM2*.

3.3.9: Protein Iron Content of Rescued Larvae

Although *drim2* larvae did not have lower levels of iron in their proteins (Section 3.1.9), mutants also had much higher mitochondrial density in muscle fibers than normal larvae (Section 3.1.7). Since little is known about the effect that number of mitochondria can have on protein iron levels, and whether or not more mitochondria can compensate for a deficiency in iron transport,

drim2 Δ^{drim2} , *drim2* Δ^{PNC-1} and *drim2* Δ^{SLC36} larvae were also analyzed for their protein's iron content in order to see whether or not there were differences between rescue lines (Fig. 3.3.9).

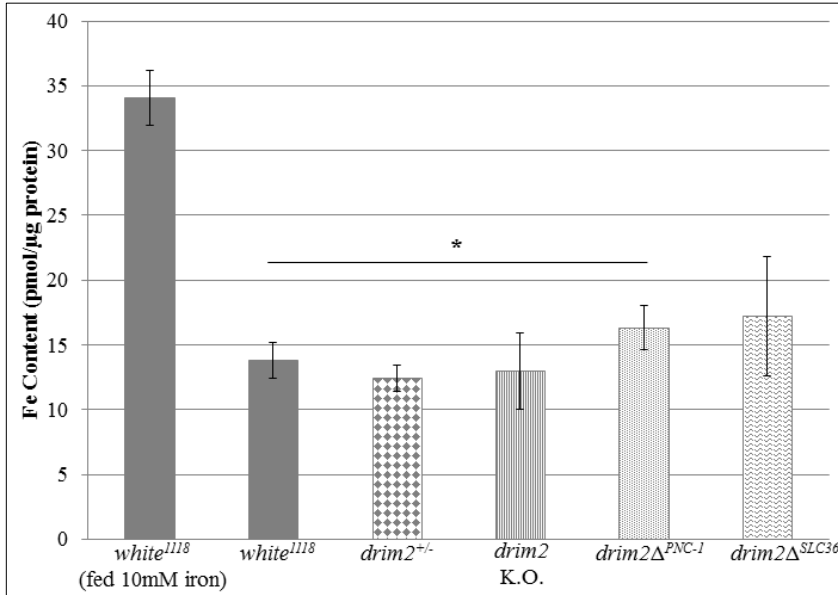


Fig 3.3.9: Larval protein iron content measured by FerroZine™ assay. *white*¹¹¹⁸ controls were fed with Fe-fortified food as a positive control to verify the protocol (First bar). Statistical analysis: 2-sample t-test; n= 5; *p<0.05.

While there was no significant difference in protein iron content between rescue lines, *drim2* Δ^{PNC-1} larvae did have slightly higher iron levels in their proteins compared to *white*¹¹¹⁸ controls (p=0.048; Fig 3.3.9).

3.3.10: Phylogenetic Analysis of *PNC-1* and *SLC25A36*

Phylogenetic analysis conducted on the human SLC25 family has indicated that the two putative human homologs of *RIM2*, *SLC25A33* and *SLC25A36* are more closely related to each other than they are to any other member of the SLC25 family (Palmieri, 2013). A cursory alignment of these two proteins with their yeast and *Drosophila* homolog also support the hypothesis that these human proteins are *RIM2* homologs (Da Re *et. al.*,2014). In order to verify the hypothesis that these two human genes come from a duplication of a *RIM2*-like ancestor, a phylogenetic analysis of *RIM2* homologs was conducted with the use of MrBayes software (Huelsenbeck and Ronquist, 2001) by Prof. Alessandro Grapputo in the Department of Biology at the University of Padua, Italy.

Two phylogenetic trees were generated in this fashion, one using the protein sequences of the *RIM2* homologs (Fig. 3.3.10.1) and one using the nucleotide sequences of the mRNA coding



Fig. 3.3.10.2: Phylogenetic tree from nucleotide sequences with posterior probabilities, generated by Prof. Grapputo using MrBayes software. t.v.= transcript variant

An NCBI search of RIM2 homolog sequences found homologs across metozoa, including plants, fungi, sponges, cnidarians, insects and vertebrates. Furthermore, BLAST searches found two RIM2 homologs in vertebrate species, while only one homolog sequence in invertebrate species. In primates, two transcript variants of *SLC25A36* were also found, except for in the orangutan (*Pongo abelii*), in which were found two transcript variants of *SLC25A33*.

Phylogenetic trees generated using either protein sequences or the nucleotide sequences of the mRNA coding region yielded very similar results, though with some exceptions. For example, the protein tree resulted in the sea urchin *S. purpuratus* and the lancelet *B. floridae* on the same leaf, suggesting that they are sister species. In the codon tree, on the other hand, the sea urchin is placed on a closer branch to the vertebrates, which is not what we would expect given the evolutionary history of the cephalochordate *B. floridae*. There were other minor discrepancies, like the zebrafish *D. rerio* resulting as a sister species of the tilapia *O. niloticus*, with regards to the *SLC25A36* sequence, only in the protein tree. Also, with regards to the sequence of *SLC25A33*, the salmon *S. salar* results as a sister species of *D. rerio* in the protein tree, but instead as a sister species of *O. niloticus* in the codon tree. It is also important to note that the phylogenetic tree generated with the nucleotide sequences of the mRNA coding regions also had overall higher posterior probability values than the one generated from protein sequences.

However, despite these discrepancies, both phylogenetic trees support the hypothesis that *SLC25A33* and *SLC25A36* originated from a duplication event, early in protochordate evolution, of a RIM2-like ancestor, given their appearance early in chordate evolution and their mirrored distribution on either side of this node.

CHAPTER I: **DISCUSSION**

4.1: Characterization of *drim2* in *Drosophila melanogaster*

In this study, a functional characterization of a novel gene, CG18317, in *Drosophila melanogaster* was performed. Due to its significant homology with the mitochondrial pyrimidine nucleotide transporter *RIM2*, it was decided to refer to this gene as *drim2*. *In vitro* and *in vivo* experiments have led to the conclusion that this gene performs a very similar function in *Drosophila* as its yeast homolog does in *Saccharomyces*.

4.1.1: *drim2* is Essential for *Drosophila melanogaster* Survival

When the genomic region encoding for the *drim2* protein was excised by the FRT-FLP system the effects on larval survival were drastic. 100% of larvae homozygous for the mutation died before pupation, thereby rendering them unable to begin metamorphosis. Larvae heterozygous for the mutation, on the other hand, did not seem to be adversely affected by possessing a single copy of the gene. This was not surprising, as previous experiments in the lab involving the conditional knock-down (KD) of *drim2* showed that, although gene expression was knocked-down by approximately 70%, KD flies were able to reach the adult stage and seemed unaffected by the reduced levels of *drim2* (data not shown). The *drim2* mutation, on the other hand, was not able to produce a single escaper fly, indicating that this gene is essential to larval development in *Drosophila melanogaster*, and that no other gene was able to compensate for its absence in this regard.

It is not uncommon that genes important for mitochondrial function to cause death at larval stages. Larvae homozygous for mutations in *dMiro*, a gene necessary for the axonal transport of mitochondria, are recessive lethal in either larval or early pupal stages (Guo *et al.*, 2005). Similarly, ubiquitous silencing of *surf-1*, a gene integral to mitochondrial complex IV activity, also leads to 100% egg-to-adult lethality (Zordan *et al.*, 2006). One possible reason for this is that, given that metamorphosis is a process which requires a significant amount of energy, larvae with defective mitochondria are at a significant disadvantage and die because of their inability to produce the energy necessary. In order to investigate this hypothesis, a characterization of mitochondrial function in mutant larvae was necessary.

4.1.2: *drim2* is a Mitochondrial Protein and is Essential for Correct Mitochondrial Function in *Drosophila melanogaster*

Due to repeated unsuccessful attempts to immunolocalize *drim2* in *in vivo* body wall preparations, a tagged form of the protein was cloned into a pACT vector and transfected into *Drosophila* Schneider S2R+ cells. Immunolocalization experiments with the tagged *drim2* demonstrated a perfect colocalization with MitoTracker[®] stained mitochondria demonstrating that, like its yeast homolog, *drim2* is a nuclear-encoded mitochondrial protein.

Further characterization of *drim2* mutant larvae demonstrated that not only is this protein localized to mitochondria, it is also integral to *Drosophila* mitochondrial function. Indirect evidence to this effect was provided by locomotor activity experiments in *drim2* mutant larvae. Furthermore mitochondria were significantly smaller, more dense and disorganized in mutant larval muscles.

Mitochondrial respiration was also virtually abolished in mutant larvae, which leads to interesting questions as to how these larvae manage to survive without aerobic respiration. Very little is currently known about *Drosophila melanogaster* and their reliance on aerobic respiration at the larval stage. However, it is important to note that *Drosophila* larvae live immersed in the food medium until third instar larvae enter the wandering stage. It is therefore conceivable that they are less reliant on aerobic respiration when they are immersed in this oxygen-poor medium. As metamorphosis requires the complete remodelling of the *Drosophila* body, it is also conceivable that their reliance on aerobic respiration changes over time. This would also explain why so many *Drosophila* mutants with mitochondrial dysfunction survive the larval stages but die before completing metamorphosis.

The presence of small and numerous mitochondria is also not an uncommon phenotype in *Drosophila* mutants for genes involved in mitochondrial DNA replication. This is especially interesting when compared to its putative human homolog *PNC-1* which, when downregulated in human cells results in increased mitochondrial biogenesis (Favre *et. al.*, 2010). The reduction or lack of mitochondrial DNA can potentially lead to a compensation mechanism whereby the organism attempts to produce more mitochondria in an attempt to compensate for the lack of mtDNA. Therefore, further characterization of mtDNA integrity was performed in order to confirm that the mitochondrial dysfunction observed in *drim2* K.O. mutants was due to a reduction in quantity and/or quality of mtDNA.

4.1.3: Mitochondrial DNA Integrity is Compromised in *drim2* Mutants

Quantitative Real-Time PCR of two mitochondrial genes was performed on mutant larvae as a primary indicator of mtDNA content. Expression levels of both *16S* and *CoxI* was found to be significantly reduced in mutant larvae, however they were found to be reduced by approximately the same amounts in larvae heterozygous for the mutation as well. Since there was no locomotor activity or respiratory defects in *drim2*^{+/-} larvae, this reduction in itself does not indicate a mtDNA defect strong enough to precipitate the mitochondrial dysfunction in observed in *drim2* K.O. larvae.

Attempts to further characterize mtDNA integrity proved unsuccessful. Long PCR experiments were performed on mutant larvae, whereby approximately 40% of the mitochondrial genome was amplified by PCR. The theory behind this methodology was that, if the mitochondrial genome contained large-scale deletions, multiple bands would be visible when the PCR product was run on an agarose gel, as opposed to a single band at the predicted molecular weight given the primers used. This method proved unsuccessful, as the same method performed on another *Drosophila* mutant known to have deletions in its mtDNA did not give the expected results (data not shown). Due to these failures to further characterize mtDNA integrity, a collaborator in the lab evaluated mtDNA copy number by Real-Time PCR on mutant DNA extract (Da Re *et. al.*, 2014). These results were then normalized to mitochondrial density, as quantified by electron microscopy experiments. These results conclusively demonstrated that *drim2* mutant larvae had significantly reduced mtDNA copy numbers compared to both their heterozygous counterparts and *white*¹¹¹⁸ controls (Da Re *et. al.*, 2014). This gives credence to the hypothesis that the larvae enter into a compensatory mechanism when mtDNA levels are low, producing larger numbers of mitochondria. It also supports the hypothesis that *drim2* is essential for correct mitochondrial DNA replication.

4.1.4: Evidence That *drim2* is a Mitochondrial dNTP Transporter

To further verify the hypothesis that *drim2* affects mtDNA replication by importing dNTPs, a collaboration with Prof. Vera Bianchi's lab was undertaken to characterize mitochondrial dNTP pools in *Drosophila* Schneider S2R+ cells in which *drim2* was silenced by approximately 80% (Da Re *et. al.*, 2014). These *drim2* K.D. cells had significantly reduced levels of all four dNTPs

in their mitochondria, further supporting the hypothesis that, like its yeast homolog, *drim2* is also a mitochondrial dNTP transporter (Da Re *et. al.*, 2014).

Given that the entire mitochondrial dNTP pool, not just the pyrimidine- dNTP one, were found to be reduced in *drim2* K.D. cells, one might be tempted to conclude that in *Drosophila* *drim2* is capable of transporting all four dNTPs. However, this conclusion cannot be reached at this time, as the removal of a mitochondrial transporter can also have secondary effects on mitochondrial DNA integrity. The knock-out of *RIM2* in yeast, for example, results in a complete lack of mitochondrial DNA (Van Dyck *et. al.*, 1995), despite the fact that it was later demonstrated that *RIM2* only transported pyrimidine dNTPs (Marobbio *et al.*, 2006) and iron (Froschauer *et. al.*, 2013). Because of the possibility of these secondary effects, one cannot rule out the possibility that *drim2* is also a specialized rather than general dNTP transporter without further characterizing the kinetics of the *drim2* protein.

4.1.5: There is No Evidence That *drim2* is an Iron Transporter in *Drosophila melanogaster*

Due to conclusive evidence that *RIM2* co-imports iron as well as pyrimidine dNTPs in *Saccharomyces cerevisiae* (Froschauer *et. al.*, 2013), iron content in mutant larval proteins was analyzed as an indirect measure of their ability to import iron into mitochondria. No differences were found in protein iron content between mutants and controls.

Given these results, there is currently no evidence that *drim2* also imports iron into *Drosophila* mitochondria. However, this does not conclusively prove that it does not import iron. The full mechanics of mitochondrial iron import/export still remains to be fully elucidated, and it is currently unclear if increases in mitochondrial density can potentially compensate for a reduction in the ability of individual mitochondria to import iron. Since the kinetics of the *drim2* protein still remains to be characterized, we propose that iron not be excluded from the list of possible substrates this protein might be capable of transporting.

4.1.6: Knock-out of *drim2* Causes Severe Secondary Effects in *Drosophila melanogaster*

One of the advantages of studying this knock-out *in vivo* is the possibility to study the effects that its removal has on a more complex organism than the single celled *Saccharomyces*

cerevisiae. Since *Drosophila* have organs, a nervous system and a body plan, studying this mutant can give further insight into the organs that are most affected by the absence of *drim2*.

Mutant larvae were characterized for other behavioural and morphological abnormalities, in order to evaluate whether or not the *drim2* mutation had any secondary effects. Since the homolog for this gene has only been fully characterized in yeast thus far, and since its human homologs have not yet been tied to any specific mitochondrial disease, its potential role in a multicellular organism remains completely unknown.

While mutant larvae did not seem to have any sensory abnormalities (Section 3.1.8), they did have abnormal neuromuscular junction morphology, which was also coupled with a significant electrophysiological defect (Section 3.1.7). These morphological defects of the NMJ were present in mutant larvae raised in both crowded and uncrowded conditions, although average bouton size remained unaffected. Taken together, these results strongly suggest that the NMJ abnormalities were caused by the *drim2* mutation itself, rather than being an indirect effect of the reduced larval size observed in mutants.

Little is known about the role of mitochondria in the development of the *Drosophila* NMJ. It is known that mitochondria are integrally involved in neuron function and survival. Mitochondrial dysfunction can cause neural death (Yuan *et al.*, 2003), and the simple lack of mitochondria at the NMJ synapse can cause electrophysiological defects, bouton morphological abnormalities and even postsynaptic muscle deformities (Guo *et al.*, 2005). It is thus conceivable that the NMJ abnormalities observed in the *drim2* mutant could be caused by mitochondrial dysfunction.

Unfortunately it was not possible to further investigate this hypothesis by observing the mitochondria in the NMJ. Staining mitochondria in the NMJ of *drim2* mutants was not possible without fluorescence contamination from background mitochondria present in larval muscles. Expressing mito-GFP under nervous system-specific driver control in a *drim2* K.O. background was not deemed to be worthwhile, given that the *drim2* mutation is present on chromosome II and therefore balanced with *Kr-GAL4,UAS-GFP;CyO*. The presence of GAL4 on the balanced chromosome meant that larvae heterozygous for the mutation would have had GFP expressed in all mitochondria as well as by all *Kruppel*-expressing cells, making the mitochondria in the NMJ impossible to analyse. Therefore, while it is impossible to say whether or not the defects observed in the NMJ are directly linked to defects in synaptic mitochondria, it is still evident that severe NMJ abnormalities are present in *drim2* K.O. larvae.

This could potentially be interesting in the context of utilizing this mutant as a model for mitochondrial diseases. Since it is the first time this gene has been studied in a multicellular organism, this study represents the first indication of what effects the absence of transcription can have at the organismal level. Although the two human homologs of this gene have not yet been tied to mitochondrial diseases, these results could suggest that mutations in these genes in humans could also present with muscular and neuromuscular defects. In order to verify whether or not it is plausible to use this mutant as a model for mutations in the two human homologs of this gene, the functional homology of these genes was investigated in depth.

4.2: Characterization of *drim2*, *PNC-1* and *SLC25A36* Expression in a *drim2* K.O. Background

It is always advisable to conduct “rescue” experiments, whereby the mutated gene is reintroduced into the knock-out line, in order to verify that the mutant phenotype observed was caused by a lack of genetic expression rather than a secondary effect of the genetic manipulation it underwent. To do this, a *drim2* K.O. line harbouring *drim2* under UAS control was generated and crossed with an *Act5c*-GAL4 driver, which was also in a *drim2* K.O. background.

In order to verify functional homology between the *Drosophila* gene and its two human homologs, additional “rescue” lines were generated, harbouring either one of or both of the human *drim2* homologs. This was done in order to see whether or not either of the human genes was capable of rescuing the *drim2* mutant phenotype, with the purpose of validating our model as relevant to human mitochondrial biology and disease.

4.2.1: *drim2* Mutants Expressing Any of the Three Genes Reach Adulthood

One mutant line expressing *drim2*, two expressing *PNC-1*, two expressing *SLC25A36* and two expressing both human homologs were crossed with an *Act5c*-GAL4 driver in order to express the chosen construct ubiquitously in a *drim2* K.O. background. The presence of the construct in the F1 progeny was verified by western blot in order to confirm that the flies studied possessed the transgene of interest.

In all cases, flies reached adulthood and eclosed in the expected heterozygous:homozygous proportions. Of the lines selected for further study (one *drim2*, one *PNC-1* and one *SLC25A36*

line), adult flies did not have reduced longevity compared to *white*¹¹¹⁸ controls. This is the first direct indication that all three genes are capable of rescuing the *drim2* mutant phenotype.

4.2.2: *PNC-1* and *SLC25A36* Can Rescue Mitochondrial Function in the Absence of *drim2*

All three rescue lines selected for study were fully characterized in order to elucidate the totality of the capabilities of the three genes to rescue the *drim2* mutant phenotype. Larval locomotor activity, mitochondrial respiration, mitochondrial gene transcription and NMJ morphology were all rescued in mutant flies expressing any of the three genes. These results not only confirmed that our mutant phenotype was caused by the absence of *drim2* rather than a secondary effect of the genetic manipulation they underwent, but also the relevance of our model for human mitochondrial biology.

These results demonstrate a high degree of functional homology between *Drosophila drim2* and its two human homologs, since they were both able to rescue the *drim2* mutant phenotype in all aspects measured during this project. This is particularly interesting given parallel experiments conducted in Prof. Salviati's lab, which demonstrated that neither *drim2* nor either human homolog, expressed singly or together, were able to rescue the yeast *RIM2* K.O. phenotype (Piazzesi *et. al.*, *In Preparation*). This indicates that the *Drosophila* gene is far more functionally homologous to its human homologs than any of them are to their yeast homolog, making the *Drosophila* model a more relevant one regarding this aspect of mitochondrial biology.

4.2.3: Is There Any Indication of What *SLC25A36* Function Might Be in Human Cells?

Despite the fact that *PNC-1* has been demonstrated to be able to transport dTTP and dUTP in human mitochondria (Floyd *et. al.*, 2007; Franzolin *et. al.*, 2012), the function of *SLC25A36* remains completely unknown. A secondary intention of this work was to possibly uncover a clue as to what the function of *SLC25A36* might be, by evaluating any differences between *PNC-1* and *SLC25A36* rescue lines.

At this time, there is still no evidence as to what the function of *SLC25A36* might be in human cells. There was no difference in the ability to rescue the *drim2* mutant phenotype between these two human genes. While one might argue that the fact that *SLC25A36* can rescue the *drim2* mutant phenotype at all is a good indication that it too is a pyrimidine nucleotide transporter, this

is not necessarily the case. When we look at the predicted structure for *SLC25A36* we see that it has changed very little since its evolutionary split from *PNC-1*. Because of this, it is not wise to rule out the possibility of functional redundancy, whereby *SLC25A36* is capable of reverting to an “ancestral” function in the absence of *PNC-1* (or, in this case, *drim2*) but that it does not perform this function under normal conditions. Until now, knock-down experiments of *SLC25A36* in human cells fail to elicit a mitochondrial mutant phenotype (Franzolin *et. al.*, 2012). Further investigation into the kinetics of this putative transporter is required before any further speculation can be made.

Since the effect of mitochondrial density on the abundance of iron incorporated into proteins has not been fully characterized, mutant larvae expressing *PNC-1* and *SLC25A36* were analysed for larval protein iron content to see if there was any significant differences between these two. The hypothesis was that, if *drim2* was also an iron transporter, but that its effects on iron incorporation into proteins was simply masked by its having a much higher mitochondrial density, and if only one of the two human homologs was capable of transporting iron, then there would be differences in protein iron content between the two rescue lines.

While there was no difference in protein iron content between the two human rescue lines, they did have slightly higher levels of iron in their proteins compared with *white*¹¹¹⁸ controls, with *PNC-1*-expressing lines barely reaching significance (two-sample t-test; p=0.048; df=4). It was unclear whether these differences were due to chance, or whether they indicate the possibility that both human homologs are capable of doubling as iron transporters. Although this possibility cannot be ruled out, the evidence to this effect is, up to this point, too slim to be considered circumstantial, and further studies into the kinetics of these transporters need to be done to verify their ability to transport iron.

4.2.4: Evolutionary History of *PNC-1* and *SLC25A36*

Despite the fact that there is no clear evidence of the function of *SLC25A36* in humans, results from the present study, as well as phylogenetic analysis of the SLC25 family conducted previously (Palmieri, 2013) indicate that *SLC25A36* shares a close homology with *SLC25A33*. This, as well as the fact that both genes could equally rescue the *drim2* K. O. phenotype, led to the hypothesis that these two genes evolved from a single, RIM2-like ancestor. In order to investigate this hypothesis, an NCBI search of *RIM2* homologs was conducted and a

phylogenetic analysis using both protein and nucleotide sequences was generated by Prof. Alessandro Grapputo, from the Department of Biology at the University of Padua, using MrBayes software (Huelsenbeck and Ronquist, 2001).

Both phylogenetic trees generated by Prof. Grapputo during this project gave very similar results. Both support the hypothesis that *SLC25A33* and *SLC25A36* evolved from a duplication event of a *RIM2*-like ancestor early in protochordate evolution.

This hypothesis was further emboldened by an initial phylogenetic tree run on all sequences generated from the NCBI search. Some sequences generated by the search which fell within our inclusion criteria were for *SLC25A32*. The previously published phylogenetic analysis on human SLC25 family members indicates that, while *SLC25A33* and *SLC25A36* are more closely related to each other than they are to any other of the SLC25 family, *SLC25A32* is the next most closely related protein to this pair (Palmieri, 2013). This explains why sequences for *SLC25A32* in some species managed to fall within the criteria of inclusion in our NCBI search. However, when these sequences were included in an initial phylogenetic analysis they were segregated as an outgroup (data not shown). This demonstrates that, while *SLC25A32* might be similar enough to *RIM2* to appear in a cursory NCBI search, it did not evolve from a *RIM2*-like ancestor, therefore the similarities were a result of homoplasy rather than homology. Removing these sequences and running the analysis only using *SLC25A33* and *SLC25A36*, on the other hand, organized both protein sequences and nucleotide sequences in a pattern which is to be expected if these genes evolved from a single common ancestor early in vertebrate evolution. This is as close to confirmation as possible that *SLC25A33* and *SLC25A36* are *RIM2* homologs, as well as paralogs of each other.

4.3: Concluding Remarks

From the results presented in this chapter we can conclude that, like its yeast homolog, *drim2* is also a nuclear-encoded mitochondrial dNTP transporter, essential for mitochondrial function and larval development in *Drosophila melanogaster*. Furthermore, we can conclude that there is a very high degree of functional homology between *drim2* and its two human homologs, *PNC-1* and *SLC25A36*, given their ability to rescue the *drim2* mutant phenotype. Because of this, we argue that the use of *Drosophila melanogaster* as a model for this aspect of mitochondrial biology, and the effects that perturbances of dNTP transport on the organism is of great

relevance to humans. Finally, we propose *PNC-1* and *SLC25A36* as potential candidates in studies with patients with mitochondrial diseases of unknown genetic origin, especially in those who present with defects in mtDNA integrity and, possibly, with neuromuscular defects as well.

*Functional characterization of drim2, the
Drosophila melanogaster
homolog of the yeast mitochondrial
deoxynucleotide transporter*

Functional characterization of drim2, the *Drosophila melanogaster* homolog of the yeast mitochondrial deoxynucleotide transporter

Short Title: **The *Drosophila* deoxynucleotide carrier drim2**

Caterina Da-Rè¹, Elisa Franzolin¹, Alberto Biscontin¹, Antonia Piazzesi¹, Beniamina Pacchioni², Maria Cristina Gagliani³, Gabriella Mazzotta¹, Carlo Tacchetti^{3,6}, Mauro A. Zordan¹, Massimo Zeviani⁴, Paolo Bernardi⁵, Vera Bianchi¹ Cristiano De Pittà^{1,§}, and Rodolfo Costa^{1,§}

¹Department of Biology, University of Padova, Italy

²CRIBI *Biotechnology Centre*, University of Padova, Italy

³MicroScoBio Research Center, Department of Experimental Medicine (DIMES), University of Genova, Italy

⁴MRC Mitochondrial Biology Unit, University of Cambridge, UK

⁵Department of Biomedical Sciences, University of Padova, Italy

⁶Experimental Imaging Center, San Raffaele Scientific Institute, Milano, Italy.

[§]Co-corresponding authors: Rodolfo Costa and Cristiano De Pittà, Dipartimento di Biologia, Università degli Studi di Padova, via U. Bassi 58/B 35131 Padova, Italy; Phone: +39-049-8276217; Fax: +39-049-8276209;

E-mail address: rodolfo.costa@unipd.it, cristiano.depitta@unipd.it

Abstract

The *CG18317* gene (*drim2*) is the *D. melanogaster* homolog of the *S. cerevisiae* *RIM2* gene, which encodes a pyrimidine deoxynucleotide carrier. Here we tested if the *drim2* gene also encodes for a deoxynucleotide transporter in the fruit fly. The protein was localized to mitochondria. *Drosophila* S2R⁺ cells, silenced for *drim2* expression, contained markedly reduced pools of both purine and pyrimidine dNTPs in mitochondria, whereas cytosolic pools were unaffected. In vivo *drim2* homozygous knockout was lethal at the larval stage, preceded by (i) impaired locomotor behavior, (ii) decreased rates of oxygen consumption and (iii) depletion of mtDNA. We conclude that *drim2* is a *Drosophila* deoxynucleotide carrier that transports all DNA precursors and is essential to maintain mitochondrial function.

Author summary

Deoxy-nucleotides are transported across the inner mitochondrial membrane and influx of cytosolic precursors is the main source of dNTPs for the synthesis of the DNA present in mitochondria. The mitochondrial membrane is impermeable to charged molecules thus, carriers in the mitochondrial inner membrane are needed to catalyze the exchange of deoxynucleotides across the membrane. In *Saccharomyces cerevisiae* a *RIM2* protein has been identified as a mitochondrial deoxynucleotide transporter. The fruit-fly represents an ideal system to study the physiological function of dNTP carriers because only one gene, *drim2*, shows significant similarity to the yeast *RIM2*. There is currently no information available concerning the function/s of *drim2* although the putative protein shows domains which are typical of mitochondrial transporters. Our findings show that *drim2* is required to maintain normal deoxynucleotide pools in mitochondria and is essential for normal development of the flies. *drim2* studied here is the first (deoxy)nucleotide transporter ever characterized in *Drosophila melanogaster* and our data provide the first animal model of *RIM2* deficiency.

Introduction

Deoxy- and ribonucleoside triphosphates (dNTPs and rNTPs) are essential for the replication and transcription of the mitochondrial genome. An appropriate supply of these precursors is thus necessary for the maintenance of functional mitochondria throughout the life of cells and organisms [1,2]. The main site of deoxy- and ribonucleotide synthesis is the cytoplasm where they are produced by two *de novo* pathways interconnected through the ribonucleoside diphosphates, which are both the immediate precursors of rNTPs and the substrates for ribonucleotide reductase, the key enzyme in the *de novo* synthesis of dNTPs [3]. In most but not all organisms, NTPs and dNTPs are also synthesized by salvage of (deoxy)nucleosides by dedicated nucleoside- and nucleotide- kinases. Mammals contain two parallel deoxynucleoside salvage pathways, located in the cytosol and, in mitochondria, respectively. The rate-limiting enzymes are two cytosolic and two mitochondrial (mt) deoxynucleoside kinases whose combined substrate specificities permit the salvage of all deoxynucleosides in each of the two subcellular compartments [4]. Ribonucleotide salvage consists primarily in the recycling of ribonucleosides and free purine bases and occurs in the cytoplasm.

The nuclear envelope is freely permeable to nucleotides and the precursors made in the cytoplasm are therefore easily available for nuclear DNA replication and transcription. The mt inner membrane is instead impermeable to nucleotides, and cytosolic nucleotides need membrane carriers to reach the mt matrix where mtDNA transactions take place. At present only a few mt nucleotide carriers are known [5]. In yeast they include the three isoforms of the ATP/ADP exchanger, a GTP/GDP carrier (Ggc1p) [6] and a (deoxy)nucleotide carrier (RIM2p) [7]. Two human genes, *SLC25A33* and *SLC25A36* [5,8], were suggested to code for nucleotide carriers on the basis of their homology to the *S. cerevisiae* *RIM2*. The prediction has been confirmed only in the case of *SLC25A33* [9,10].

The product of *SLC25A33* is a protein 33% identical to RIM2p. It has been named PNC1 [9], to highlight its function as a Pyrimidine Nucleotide Carrier, demonstrated by transport studies with the recombinant protein reconstituted in liposomes [9] and later by isotope-flow experiments in intact cells [10]. The transport properties of yeast RIM2p and human PNC1 are very similar. When reconstituted into liposomes both proteins exchange all pyrimidine ribo- and deoxyribonucleotides and show some activity with guanine nucleotides but not with adenine nucleotides. Thus they appear to be responsible for the import of most nucleic acid precursors into mitochondria. The characterization of RIM2p activity led to the proposal that the carrier imports nucleoside triphosphates in exchange with monophosphates [7].

RIM2p deletion had been found to cause total loss of mtDNA in yeast long before the transport activity of the protein had been identified biochemically [11]. So far there are no data on the *in vivo* effects of PNC1 loss of function in humans or mice. The existing information comes from experiments of PNC1 silencing by siRNA in cultured human cells. Knockdown (KD) of PNC1 led to depletion of mtDNA, reduced transcription of mt genes and impairment of oxidative phosphorylation [9,12]. *In situ* analysis of nucleotide flow in cells with downregulation of PNC1 revealed a slower mitochondrial uptake of uridine triphosphate and a slower release of thymidine nucleotides to the cytoplasm [10]. The same study investigated also the function of the *SLC25A36* gene product. Downregulation of the protein, which is 60% identical to PNC1, had no effect on mitochondrial pools. Therefore, the activity of *SLC25A36* remains unknown [10].

The genome of *Drosophila melanogaster* contains only one gene with significant similarity to yeast *RIM2* and the two human genes. This gene, denominated *CG183173* and here indicated as *drim2*, maps on chromosome 2 (position 22B1), spans 7.503 base pairs and produces three different transcripts, all containing the typical features of mitochondrial carriers [13]. There is currently no information concerning the functions of *drim2*. On account of its homology to RIM2p and PNC1, it may be involved in the mitochondrial transport of nucleotides. We

considered it could be a useful model to investigate how the deletion of a nucleotide carrier affects mitochondrial function in a multicellular animal.

We first silenced *drim2* expression in the *Drosophila* S2R⁺ cell line [14] and found depletion of all mitochondrial dNTP pools, suggesting that the protein is involved in the transport of all four DNA precursors. We then produced *drim2* knockout (KO) flies and found that the homozygous loss of *drim2* is lethal, blocking larval development at the 3rd instar. We analyzed different phenotypic aspects of the *drim2*^{-/-} larvae detecting profound alterations of mitochondrial structure and function, and impairment of larval locomotion that could be related to depletion of mtDNA. Our data suggest that *drim2* codes for a nucleotide transporter essential for the maintenance of functional mitochondria in *Drosophila*.

Results

drim2 is conserved across species and localizes to mitochondria

The RIM2p protein was previously characterized in *Saccharomyces cerevisiae* as a mitochondrial pyrimidine nucleotide transporter [7]. Yeast RIM2p is a member of the mitochondrial carrier protein family distinguished by some typical features: the amino acid sequences include three repeats, each containing two putative trans-membrane sequences (TMSs) and the signature motif [PX(DE)XX(KR)]. Therefore the main structure fold is a six α -helical bundle [9]. To evaluate the degree of conservation of the RIM2p across species, we performed an amino acid alignment of yeast, human and fruit-fly RIM2p sequences and calculated the levels of homology (Fig. 1). The *drim2* gene of *D. melanogaster* codes for three different transcripts, named A, C and D. The corresponding protein isoforms showed comparable degrees of similarity to the yeast sequence ($\approx 40\%$). Interestingly, all *Drosophila* isoforms are closer to human PNC-1 (52-54 % identity) than to yeast RIM2p.

To characterize the subcellular localization of *drim2* we transfected *Drosophila* S2R⁺ cells with a pACT vector expressing HA-tagged *drim2* cDNA under the control of the *Actin 5c* promoter. Mitotracker staining and immunodetection of HA-*drim2* with an α -HA monoclonal antibody clearly indicated that *drim2* localizes to mitochondria (Fig 2a).

Silencing of *drim2* depletes all mitochondrial dNTPs in S2R⁺ cells

Next, we downregulated the expression of endogenous *drim2* in S2R⁺ cells and tested the effects on the size of the mitochondrial deoxynucleoside triphosphate (dNTPs) pools. In cells incubated for 72 h with dsRNA, real-time RT-PCR analysis showed that mRNA was decreased by 80%. If *drim2* is a carrier for pyrimidine nucleotides, its downregulation should affect the dTTP and dCTP pools more than the purine deoxynucleotides dATP and dGTP. To test this prediction, we isolated the mitochondrial and cytosolic dNTP pools from control and silenced S2R⁺ cells by adapting a procedure previously devised for the quantification of mammalian mitochondrial

dNTPs [15]. No data are available on dNTP pool sizes in *Drosophila* cells and we therefore wished to establish the relative abundance of the four dNTPs and the ratios between cytosolic and mitochondrial pools. In mammals dTTP is generally the largest dNTP pool, and dGTP the smallest, with dCTP and dATP occupying intermediate positions. Pool sizes in *Drosophila* are reported in Fig 2b and c. As in mammalian cells [16], mitochondrial pool sizes corresponded to about 3-10% those of the cytosolic pools. The dATP pool was the largest in both cytosol and mitochondria, followed by dTTP, dGTP and dCTP in the cytosol and dTTP, dCTP and dGTP in mitochondria. In both compartments the dCTP pool was particularly small, and comparable in size to the dGTP pool. Since the sizes of dNTP pools are strongly influenced by the position of the cell in the cell-cycle [17] we took care of comparing the concentrations of dNTPs in cultures of *drim2*-silenced and control S2R⁺ cells with similar frequencies of S-phase cells. We observed no difference in the proportion of S-phase cells between silenced and control cultures, with values of about 20-25% depending on the experiment. Therefore, we feel confident that the differences in dNTP pools we measured in the two sets of cultures were not caused by differences in cell-cycle distribution. However, whereas the cytosolic pools were virtually identical in control and silenced cultures (with the exception of the dATP pool that was higher in the latter), all mitochondrial dNTPs were significantly lower in the silenced cells, with levels ranging between 20% (dCTP) and 50% (dATP) of the controls. Thus, downregulation of *drim2* reduced the mitochondrial concentrations of both pyrimidine and purine dNTPs, suggesting that the protein is a general transporter for all four DNA precursors.

Post transcriptional silencing of *drim2* *in vivo*

Next we attempted to knock-down the *drim2* gene *in vivo* by using GAL4/UAS-driven RNAi in living flies [18,19]. Despite high levels of silencing (about 80%) (Fig. S1a), *drim2* KD individuals did reach the adult stage and lived longer than the controls (Fig. S1b). No effects on

egg to adult viability were observed. These results suggest that even a low residual level of *drim2* mRNA is sufficient to maintain the wild-type (wild-type) phenotype.

Characterization of a *Drosophila drim2* knockout strain

Thus we generated a *Drosophila drim2* KO using the technique described in [20] that exploits the specific recombination between FRT sites in the presence of flippase. Heterozygous KO flies (*drim2*^{+/-}) were balanced with a strain expressing GFP [*w*; L2, *Pin1,CyO-GFP*], allowing discrimination between homozygous GFP-negative *drim2*^{-/-}, and heterozygous GFP-positive *drim2*^{+/-} larvae. Real time-PCR showed that *drim2*^{+/-} larvae had about 50% *drim2* mRNA levels compared to a wild-type control (*w*¹¹¹⁸), whereas *drim2*^{-/-} flies were null, as expected (Fig. 3a). The *drim2*^{-/-} third-instar larvae were visibly smaller than their heterozygous counterparts (Fig. 3b). Nevertheless, KO larvae did present mouth hooks, the distinctive character of the third larval stage indicating that their smaller size was not due to a developmental delay (Fig. 3c). The KO heterozygous *drim2*^{+/-} larvae developed into normal adults with no developmental defects. On the contrary, none of *drim2*^{-/-} larvae reached adulthood. Although *drim2*^{-/-} individuals survived through larval development, most of them died at the third larval instar and the survivors failed to progress beyond the pupal stage (Fig. 3d). To further characterize the phenotype, we measured locomotor activities (total distance travelled, overall average speed and inactivity) with the Any Maze software. Wild-type and *drim2*^{+/-} larvae behaved similarly, whereas *drim2*^{-/-} showed marked locomotor defects (Fig. 3e, f, g).

Properties of *drim2*^{+/-} and *drim2*^{-/-} larval mitochondria

Confocal images of body wall preparations stained with Mitotracker Red showed a normal mitochondrial pattern along the z-lines in *w*¹¹¹⁸; however, the *drim2*^{-/-} individuals showed spatially disorganized mitochondria that failed to line up along the z-lines (Fig. 4a). This abnormal pattern was confirmed by transmission electron microscopy (EM) (Fig. 4b). EM carried out in *drim2*^{+/-} and *drim2*^{-/-} larvae (first panel, Fig. 5a) revealed alterations of

mitochondrial number and shape compared to w^{1118} (Fig. 5a). The $\text{drim2}^{+/-}$ mitochondria appeared more elongated, and considerably bigger than those of w^{1118} larvae (Fig. 5a). Morphometric analysis indicated that, on average, the major mitochondrial diameter in $\text{drim2}^{+/-}$ larvae was significantly increased and the minor diameter reduced relative to w^{1118} mitochondria (Fig. 5b-c). In $\text{drim2}^{-/-}$ larvae, mitochondria had a rounder shape (Fig. 5a); the averaged major diameter was unchanged relative to the wild-type whereas the minor diameter was longer than that of mitochondria of both w^{1118} and $\text{drim2}^{+/-}$ (Fig. 5b-c). Accordingly, estimates of the mitochondrial area indicated that $\text{drim2}^{+/-}$ organelles were larger than those from w^{1118} and $\text{drim2}^{-/-}$ flies (Fig. 5d). Furthermore, mitochondrial density, i.e. the number of mitochondria per surface unit, was reduced in $\text{drim2}^{+/-}$ individuals compared to wild-type controls and significantly higher in $\text{drim2}^{-/-}$ larvae (Fig. 5e).

As *RIM2* deletion in yeast and PNC1 downregulation in mammalian cells decreases mtDNA content [11,12], we measured the mtDNA copy number in KO larvae. Unexpectedly, whilst mtDNA was almost 50% depleted in $\text{drim2}^{+/-}$ larvae, $\text{drim2}^{-/-}$ individuals had wild-type levels of mtDNA (Fig. 6a), possibly a consequence of the higher number of mitochondria [21,22]. Normalization of mtDNA content to mitochondrial density did indeed show significant depletion of mtDNA in $\text{drim2}^{-/-}$ larvae (Fig. 6b). The $\text{drim2}^{+/-}$ larvae, (with reduced mitochondrial density), showed also a decrease in mtDNA content but the difference disappeared after normalization (Fig. 6b). The lower relative content of mtDNA in KO individuals is consistent with the reduced concentration of dNTPs detected in drim2 silenced S2R⁺ cells.

A reduced mtDNA copy number might lead to reduced expression of the mtDNA-encoded subunits of the respiratory chain. We measured the levels of mitochondrial transcripts for *Cyclooxygenase-1 (COX1)* and RNA (*16S*) relative to the housekeeping gene *Rpl32* by real time-PCR [23] (Fig. 6c). Mitochondrial transcription was lower in both $\text{drim2}^{-/-}$ and $\text{drim2}^{+/-}$ larvae. In order to establish whether defects in drim2 function also affect mitochondrial respiration we

measured oxygen consumption rates of muscle body-wall preparations of *Drosophila* larvae with the Seahorse technology [24]. Controls and *drim2*^{+/-} larvae maintained a steady respiratory rate which was inhibited by rotenone and antimycin A, demonstrating its mitochondrial origin. On the contrary *drim2*^{-/-} larvae showed severe impairment of oxygen utilization that was insensitive to respiratory inhibitors (Fig. 7a). The same measurements were performed also in S2R⁺ cells silenced for *drim2*. The rate of oxygen consumption was significantly decreased in cells silenced for 96 h, and the cells responded less than the controls to uncoupler (FCCP) and to (oligomycin or rotenone plus antimycin A) (Fig. 7b). No significant differences of respiratory profile were detected between cells undergoing a mock interfering treatment for almost 48 h and the controls. The basal respiration of the two cultures was similar, both being of mitochondrial origin since they were stimulated by FCCP and inhibited by oligomycin or rotenone plus antimycin A (Fig. 7b).

Gene expression profiling in *drim2* knockout *Drosophila* larvae

In order to define the gene expression pattern specifically associated with *drim2* KO, we performed protein-coding microarray analyses (*Drosophila* 1.0 custom platform, Agilent Technologies) on high quality RNA from *drim2*^{-/-} and *drim2*^{+/-}. Using SAM two class analysis we identified 2,964 differentially expressed genes (FDR = 5.10%) of which 1,120 were up-regulated (38%) and 1,844 were downregulated (62%) in *drim2*^{-/-} vs. *drim2*^{+/-} samples (Table S2). A functional annotation web tool (DAVID) was used to identify functional categories occurring in the *drim2*^{-/-} expression signature more frequently than expected by chance. The Group Enrichment Score was used to rank biological significance of deregulated genes. We observed that GO functional categories over-represented in the up-regulated component of the expression signature included oxidative phosphorylation and glycolysis/gluconeogenesis (Fig. S2); in contrast, the downregulated components showed an over-representation of GO categories such as purine and pyrimidine metabolism.

Discussion

Mitochondria contain multiple copies of a small circular DNA coding for essential polypeptide components of the respiratory chain and F-ATP synthase complexes embedded in the inner mitochondrial membrane. Replication and transcription of mtDNA occur during the whole life of the cell, even after it has reached terminal differentiation. Both processes are particularly active during cell proliferation and early development, when mitochondrial biogenesis is induced [25] and thus the request for dNTPs and rNTPs is particularly high. In yeast and mammals the cytoplasm is the main site for nucleotide production, but some synthesis occurs also in mitochondria and in the nucleus. Due to the impermeability of the mitochondrial inner membrane to nucleotides, these are taken up into mitochondria by a partly unknown repertoire of membrane carriers. The nucleotide transporter we have studied here is the *Drosophila* ortholog of yeast RIM2p and human PNC1, two homologous pyrimidine nucleotide transporters [7,9,10]. In yeast, the genetic inactivation of RIM2 causes loss of mtDNA and a petite phenotype [11]. In cultured human cells, downregulation of PNC1 by siRNA can lead to decreased mtDNA copy number [12]. Thus in both yeast and humans the dependence of mitochondria on nucleotides made in the cytosol has been demonstrated.

The study of nucleotide, and especially deoxynucleotide, metabolism has been relatively neglected in *Drosophila*. Most attention has been dedicated to a distinctive multisubstrate deoxynucleoside kinase responsible for the salvage of all deoxynucleosides [26], as opposed to the four separate deoxynucleoside kinases existing in mammals [4]. Given the presence in the genome of the key enzymes for dNTP and rNTP *de novo* synthesis, we assumed that the general picture defined in mammalian cells also applies to *Drosophila* and that also in this species mitochondria obtain their nucleic acid precursors from extra-mitochondrial sources. Thus, after confirming that *drim2* is localized to mitochondria (Fig 2a), we hypothesized that its deletion

may impact the mtDNA content and impair mitochondrial transcription, with negative consequences for oxidative phosphorylation and energy-dependent processes.

We studied the effects of *drim2* ablation on the dNTP pools required for the maintenance of mtDNA. No information was available on the composition of dNTP pools of *Drosophila* cells and we first analysed the total pools of control S2R⁺ cells. They contained relatively more dTTP and dATP than dCTP and dGTP, a pool composition different from that commonly observed in mammalian cells where dTTP and dCTP frequently are the most abundant dNTPs. When we separated mitochondrial and cytosolic pools we found that, as in human cells, in *Drosophila* the dNTP pools of mitochondria amount to no more than 10% of the total dNTPs. In *drim2*-silenced cells, both mitochondrial pyrimidine and purine dNTPs pools were reduced, suggesting that *drim2* acts as a general deoxynucleotide transporter. Cytosolic pools were unaffected, underscoring a specific function of the carrier in the import of nucleotides from the site of their synthesis in the cytoplasm into the mitochondrial matrix where they are consumed for mtDNA synthesis. The possible lack of intramitochondrial dNTP synthesis in *Drosophila* suggested by the genomic data is supported by the appearance of cell toxicity when silencing was prolonged beyond 3 days. Although the treatment did not completely remove *drim2* mRNA, the downregulation was sufficient to impair cell viability *in vitro*. This was not the case when we downregulated the protein *in vivo* using the GAL4/UAS system to ubiquitously activate *drim2*-dsRNAi. A 30% residual level of gene activity was sufficient for the flies to develop normally into adults.

A very different picture appeared after *in vivo* KO of *drim2*. Homozygous *drim2*^{-/-} larvae exhibited a lethal phenotype and died during the third larval stage without reaching adulthood. The homozygous KO produced an overall impairment of larval development associated with reduced dimensions compared to wild-type larvae (Fig. 3b-d). It is known that most *Drosophila* mutants for genes involved in mitochondrial and nucleotide metabolism either do not undergo

metamorphosis, arresting their development at larval stage or manifest developmental defects. This effect is probably related to the particularly high energetic burden of metamorphosis. Larval lethality is frequently associated with neuromuscular and behavioral defects, functions that in *Drosophila* are particularly sensitive to OXPHOS-dependent energy drop [27-29]. Here, *drim2*^{-/-} larvae showed severe defects in their locomotor activity (Fig. 3 e-g).

From the morphological point of view, mitochondria of both *drim2*^{-/-} KO and heterozygous *drim2*^{+/-} larvae displayed evident anomalies (Fig. 5). EM analysis in *drim2*^{-/-} larvae revealed a higher number of mitochondria (Fig. 5), possibly a physiological response compensating for the progressive loss of mitochondrial function. However, expression profiling did not demonstrate activation of mitochondrial biogenesis. Genes such as *PGC-1α*, *NRF-1*, *NRF-2* and *TFAM* were not up-regulated in *drim2*^{-/-} larvae. An alternative explanation for the increased number of mitochondria may be reduced mitochondrial turnover rather than increased biogenesis.

Interestingly, among the genes involved in nucleotide metabolism that are differentially expressed in homozygous KO larvae only nucleoside diphosphate kinase (NDK) was clearly upregulated, while all others were downregulated. Since NDK catalyzes the final step in the synthesis of dNTPs and rNTPs, this result suggests a homeostatic response to reduced availability of nucleoside triphosphates in mitochondria. The downregulated genes encode both for synthetic and catabolic enzymes and participate in the regulation of different pool components in combination with other enzymes. Changes detected in individual members of a complex enzyme network are difficult to interpret and may reflect general unspecific stress rather than a concerted metabolic adjustment related to the lack of mitochondrial nucleotides.

Despite the severity of the KO phenotype, direct quantitation of mtDNA in the homozygous larvae did not show the expected depletion. However, after correction for the increased mitochondrial density a significant mtDNA depletion was found in *drim2*^{-/-} larvae in agreement with the decrease of mitochondrial transcripts (Fig. 6) and previous observations in human cells

with silenced PNC1 [12]. These results indicate that *drim2* and *PNC1* are necessary for mtDNA transcription and replication in flies and humans, respectively.

Mitochondrial disorders are characterized by impaired oxygen consumption, and homozygous KO larvae and *drim2*-silenced cells are no exception (Fig. 7), as expected on the basis of the reduced mtDNA copy number and transcription.

Yeast *RIM2* was identified in screens for suppressors of high iron toxicity in strains deleted for the two yeast mitochondrial iron transporters *Mrs3* and *Mrs4* or for the vacuolar iron transporter *CCC1* [30,31]. Thus the protein was proposed to play a dual role as pyrimidine nucleotide and iron transporter. However, recent data show that in wild-type yeast deletion of *RIM2* alone is irrelevant for mitochondrial iron supply [32]. The *Drosophila* genome contains *mfrn*, the gene for mitoferrin that is the homologue of the yeast iron carriers *Mrs 3* and *4*. Therefore, we assume that the effects of *drim2* KO detected here depend primarily on the lack of nucleotide transport into mitochondria.

Our findings strongly suggest that the *D. melanogaster* *CG18317* (*drim2*) gene is essential to maintain mitochondrial function by providing deoxynucleotides for mtDNA transactions. *drim2* is the first (deoxy)nucleotide carrier characterized in *Drosophila* and our KO larvae are the first animal model of *RIM2* deficiency. The data presented here may offer a key to understand the functional role of *RIM2* in a multicellular animal, and further support its general function in deoxynucleotide transport in mitochondria.

Materials and methods

Cell cultures

The *Drosophila* S2R⁺ cell line derived from a primary culture of late stage (20-24 h old) *D. melanogaster* embryos [14]. It was obtained from *Drosophila* Genomics Resource Center (DGRC) (<http://dgrc.cgb.indiana.edu/>). S2R⁺ cells grow at 25°C without CO₂ in Schneider's

medium (Life Technologies) with 10% heat-inactivated fetal bovine serum (FBS) (Sigma-Aldrich) as a loose, semi-adherent monolayer, showing a doubling time of about 48 h.

dsRNA production and RNAi procedures

dsRNAi synthesis was performed employing the T7 Megascript kit (Life Technologies) [19,33]. The oligonucleotides primers used to synthesize dsRNA starting from cDNA were drim2_T7 forward (F) and reverse (R) (primer sequences are reported in Table S1). These primers give two complementary 700 bp RNA products that anneal as temperature decrease, forming a final 700 bp dsRNA. About 2×10^6 cells suspended in 1 ml of serum-free medium were mixed with 2 $\mu\text{g/ml}$ dsRNA, plated in a 24 wells plate and incubated at room temperature (RT) for 1 h. Subsequently, one volume of complete medium 2X was added and cells were grown in the presence of dsRNA for 2 days at 25°C.

dNTP pool extraction and analysis

At the end of the treatment with dsRNA, about 10×10^6 S2R⁺ cells were centrifuged in 15 ml tubes for 10 min at $400 \times g$ and the pellet washed twice with ice-cold PBS. The cells were then resuspended in 200 μl of extraction buffer (0.21 M mannitol, 0.07 M sucrose, 0.2 M EGTA, 10 mM TrisHCl pH 7.5, 0.5% BSA) and a suspension of glass beads (0.1 mm diameter) corresponding to about $\frac{1}{2}$ the volume of the cellular pellet was added. The cell-bead suspension was introduced in a Bullet Blender Storm homogenizer (Next Advance) and shaken for 2 min at speed 8, then 400 μl of extraction buffer were added and the glass beads were removed by a short centrifugation. Mitochondrial and cytosolic nucleotide pools were isolated from the whole cell homogenate by differential centrifugation and methanol extraction as described [15]. All manipulations took place in a cold room. The pellet remaining after mitochondrial pool extraction was dissolved in 1 ml of 0.3 M NaOH. The A_{260} nm of the NaOH fraction containing the cellular macromolecules left after soluble pool extraction was used as an index of cell mass in different samples [34]. The sizes of the dNTP pools were determined with a DNA

polymerase-based assay[35] with the modifications reported in [16]. Two different aliquots of each pool extract were analysed and pool sizes were normalized by the A_{260} nm of the NaOH lysates.

Immunolocalization of drim2

HA-tagged drim2 cDNA was cloned in a pACT vector under the control of *Actin 5c* promoter [36]. 500,000 cells were seeded on round coverslips and grown for 16 h, then they were transfected with 20 μ l CellFectin II Reagent and 2.5 μ g vector and incubated for 8 h. The medium was removed and replaced with complete Schneider medium (containing 10% heat-inactivated FBS). After 48h from transfection cells were washed once with 1x PBS and incubated with 100 nM MitoTracker Red CMXRos and 1 μ g/ml Cyclosporin H in Schneider's Medium for 20 min [36]. Then the cells were washed in 1X PBS and fixed in 4% paraformaldehyde for 20min. After a second wash in PBS cells were permeabilized for 5 min with 50 mM NH₄Cl in PBS + 0.1% Triton, then blocked for 1h in 3% goat serum in PBS, washed again and incubated with 1:100 monoclonal mouse α -HA antibody (Sigma-Aldrich) at 4°C O.N. Cells were washed again with PBS then incubated with 1:500 FITC-conjugated α -mouse IgG (Sigma-Aldrich) with 2% goat serum for 45min. After a final wash in PBS the slides were mounted with Vectashield mounting medium. Images were taken with a Leica SP5 confocal microscope at 63X magnification.

Flies stocks and breeding conditions

Flies were raised on standard cornmeal medium and were maintained at 23° C, 70% relative humidity, on a 12h light: 12h dark cycle. The UAS fly strains (Transformant ID #44203 and #44202) used to perform post-transcriptional silencing were from the VDRC (Vienna *Drosophila* RNAi Center). Other *D. melanogaster* strains were obtained from the Bloomington Stock Center.

Egg-to-adult viability

For each of the transgenic lines around 300 fertilized eggs were collected on standard yeast–glucose–agar medium in a Petri dish (60 \times 15 mm). The fertilized eggs were incubated at 23°C,

and for each experimental condition, the number of individuals reaching the third instar larva, pupa, or adult, and the relative percentages were calculated [37].

Genomic DNA extraction

Single individuals (flies or larvae) were homogenized in separate vials in 50 µl of extraction buffer containing 10mM Tris-HCl (pH 8.2), 1mM EDTA and 25 mM NaCl. Proteinase K was added to a final concentration of 200 µg/ml and the homogenate incubated for 45 min at 37° C followed by heat inactivation of the enzyme at 95° C for 5 min. Genomic DNA used to quantify the mtDNA copy number was extracted starting from 10 larvae using the phenol/chloroform precipitation.

Primers

All oligonucleotides used in this work were reported in the Table S1. They were designed using the on-line tool Primer-BLAST [38].

Generation of knockout strain

We obtained from Exelixis *Drosophila* Stock Center available stocks bearing PiggyBac insertions (PBac[RB] CG18317^{e01575} and PBac[RB] CG18317^{e00041}) at the boundaries of the *drim2* locus. In order to obtain the gene deletion we exploited the specific recombination between the FRT element within the PBac elements catalyzed by FLP recombinase [20,39]. The obtained KO lines were checked for the presence of the deletion. To this purpose the following couples of primers were used upstream deletion (*drim2*KO^{e01575} F and R), giving a product size of 150 nt, and downstream deletion (*drim2*KO^{e00041} F and R), giving a product size of 240 nt.

RNA isolation and qRT-PCR experiments

Total RNA was extracted from approximately 10 larvae or 2X10⁶ cells using Trizol (Life Technologies) and further purified by precipitation with LiCl 8M. RNA samples were checked for integrity by capillary electrophoresis (RNA 6000Nano LabChip, Agilent Technologies). For each sample, 1 µg of RNA was used for first-strand cDNA synthesis, employing 10 mM

deoxynucleotides, 10 μ M oligo-dT and SuperScript II (Life Technologies). qRT-PCRs were performed in triplicate in a 7500 Real-Time PCR System (Life Technologies) using SYBER Green chemistry (Promega). The $2^{-\Delta\Delta C_t}$ (RQ, relative quantification) method implemented in the 7500 Real Time PCR System software was used to calculate the relative expression ratio [40]. The drim2 oligonucleotides primer used were drim2 F and R. Specific primers were designed for *CoxI* (*CoxI* F and R). The *16S* primers used were *16S* F and R [41]. *Rp49* was used as endogenous control and the oligonucleotides employed were *Rp49* F and R.

Body wall preparations

A small portion of the tail was cut from third instar larvae, internal organs were removed by gently squeezing from head to tail, and the preparation was turned inside-out by rolling the cuticula along a holding tweezer.

Mitochondrial pattern in muscle fibers

Body wall preparations of larvae were stained with 500 nM MitoTracker Red CMXRos (Life Technologies) for 45 min. Tissues were then washed in 1X PBS and fixed in 4% PFA for 20 minutes. After a brief wash they were mounted in 80% glycerol. Scans of muscle 6 were taken with a Leica SP5 Confocal Microscope at 63X magnification.

Measurements of oxygen consumption

Oxygen measurements were made using the XF24 Extracellular Flux Analyzer (Seahorse Bioscience). Measurements were performed both in whole tissues of *Drosophila* larvae (body wall preparations) and in *S2R⁺* *Drosophila* cells, using different Seahorse technologies. The instrument was maintained on a temperature of 25°C. In the case of tissues, each dissected larvae was placed into a well of an islet capture 24-well microplate. Islet capture screens were used to keep the larvae in place. Basal oxygen consumption rates (OCR), reported in the unit of picomoles per minute, was measured several times before injecting the first drug to be tested. Chemicals were sequentially added in each well as described in figure legends. Cells were

seeded onto XF-24 well-plates at 20,000 cells/well and cultured for 48 h. The following day the culture medium was replaced with serum-free Schneider medium (Life Technologies). Basal OCR were measured three times, loaded compounds were then sequentially injected.

Analysis of larval locomotor behavior

The locomotor activity of a single third stage larva inside an arena was recorded for a 120 seconds period using a video tracking system. The arena consisted in a Petri dish (5 cm in diameter) covered by a thin layer of agar gel 1%. The Petri dish was placed inside a box, the internal walls of which were painted black, containing a ring of ultrabright white LEDs to generate a uniform illumination. After closing the box, the movement of the larva inside the arena was video recorded using a Canon digital video camera (10 frames per second). A specific software (AnyMaze) was utilized to track the path covered by the moving animal during the recording time period of 120''. The software calculated the total length of the path, the average speed and the maximum speed of the larvae. A total number of 50 larvae were analyzed for each genotype. The tests were performed at the same time of the day for all strains.

Electron Microscopy

Third stage larvae were dissected in Ca^{2+} -free haemolymph-like saline-3 (HL3) and transferred into a fixation solution containing 3% glutaraldehyde, 2% paraformaldehyde, 100 mM sucrose, and 2 mM EGTA, in 0.1 mM sodium phosphate buffer, pH 7.2. Samples were fixed for 2 h and washed overnight at 4°C in 0.1 mM phosphate buffer, pH 7.2. Samples were then post-fixed for 2 h with cold 1% OsO_4 , in 0.1 mM sodium cacodylate buffer, pH 7.2, rinsed 3-4 times (5 min each) in 0.1 mM sodium phosphate buffer pH 7.2. Subsequently larvae were dehydrated through an ethanol gradient, followed by a propylene oxide-resin gradient. Finally samples were embedded in Epon resin (Sigma-Aldrich) and polymerized at 60°C for 3 days. The analysis was performed on 60 nm ultrathin sections of larval body-wall muscles, stained for 20 min with uranyl acetate, and examined with a Philips CM10 electron microscope (FEI Company). For the

statistical analyses the shortest and the longest diameter of mitochondria, were measured using ImageJ software (<http://rsb.info.nih.gov/ij/>). In addition we measured the area and the density of mitochondria in the same larvae [42]. We analyzed 30 cell profiles for each phenotype considered measuring the entire area of the cell, the area occupied by mitochondria over the entire cell profile, and the total number of mitochondria. The average size of mitochondria was expressed in square micron, as the ratio between the area occupied by mitochondria in 20 cell profiles, and their number.

Determination of mtDNA levels

Total DNA from larvae was extracted using phenol/chloroform precipitation. The amount of mtDNA was assessed by the ratio of mtDNA to nuclear DNA (nDNA) copy number determined by quantitative real time amplification of the mitochondrial *16S* gene and the nuclear *Rpl32* gene. Primers used in this work (*16S* F and R; *Rpl32* F and R) were those previously reported by [41]. We generated two gene-specific calibration curves with six 10-fold serial dilutions (100-10,000,000 copies) of plasmids containing the cloned target sequences (Life Technologies). Concentration of plasmid stock solutions was assessed with a NanoDrop ND-1000 spectrophotometer (Nanodrop), and the plasmid copy number of dilutions was calculated using Avogadro's number. Reactions were performed in triplicate using the SYBR Green chemistry according to the manufacturer's recommendations (GoTaq qPCR Master Mix, Promega) in a 7500 Real Time PCR System instrument (Life Technologies). Data were normalized to the ratio of mtDNA/nDNA copy number in controls (arbitrary set to 100%) [43,44].

DNA microarray design

Probes were designed using the Agilent eArray Custom Microarray Design Service (<https://earray.chem.agilent.com/earray/index.jsp>), which applies proprietary prediction algorithms to design 60 mer oligo-probes. Microarrays were synthesized *in situ* using the Agilent ink-jet technology with 8 x 60 K format. A total of 32,162 probes representing *D. melanogaster*

transcripts were successfully obtained. A custom microarray platform, named “*Drosophila* 1.0” (eArray Design ID: 035757), showed 30,814 duplicate probes and 1,348 single probes. Each array included default positive (1,011 probes) and negative (308 probes) controls. Probe sequences and other details on the microarray platform can be found in the Gene Expression Omnibus (GEO) database (<http://www.ncbi.nlm.nih.gov/geo/>) under accession number: GPL17290.

Microarray labeling and hybridization

Gene expression profiling was carried out on *drim2*^{-/-} and *drim2*^{+/-} *Drosophila* larvae using the *Drosophila* 1.0 custom platform (Agilent Technologies). Total RNA was obtained from the whole body of 3rd instar larvae for each genotype. Four and three biological replicates were analyzed for *drim2*^{-/-} and *drim2*^{+/-} samples respectively for a total of 7 microarray experiments. 800 ng of total RNA was labeled with “Agilent One-Color Microarray-Based Gene Expression protocol” according to the manufacturer’s instructions. The synthesized cDNA was transcribed into cRNA and labeled with Cy3-dCTP. Labeled cRNA was purified with RNeasy Mini columns (Qiagen). The quality of each cRNA sample was verified by total yield and specificity calculated with NanoDrop ND-1000 spectrophotometer measurements. 1.65 µg of labeled cRNA was used in each reaction and hybridization was carried out at 65°C for 17 h in a hybridization oven rotator (Agilent). The arrays were washed using Agilent Gene expression washing buffers and Stabilization and Drying Solution, as suggested by the supplier. Slides were scanned on an Agilent microarray scanner (model G2565CA) and Agilent Feature Extraction software version 10.5.1.1 was used for image analysis. Gene expression data are available in the GEO database with the accession number: GSE48012.

Statistical analysis of gene expression data

Inter-array normalization of expression levels was performed with quantile method [45] to correct possible experimental distortions. A normalization function was applied to the expression

data of all the experiments and the values of within-arrays replicate spots were then averaged. Feature Extraction Software which provided spot quality measures was used to evaluate the quality and reliability of the hybridization. In particular, the flag "glsFound" (set to 1 if the spot had an intensity value significantly different from the local background and to 0 when otherwise) was used to filter out unreliable probes: the flag equal to 0 was to be noted as "not available (NA)." Probes with a high proportion of NA values were removed from the dataset in order to carry out a more solid, unbiased, statistical analysis. Forty percent of NA was used as the threshold in the filtering process, and a total of 25,350 *Drosophila* transcripts were obtained. Principal Component Analysis (PCA), cluster analysis, and profile similarity searches were performed with Multi Experiment Viewer version 4.8.1 (tMev) of the TM4 Microarray Software Suite. The identification of differentially expressed mRNAs was performed with two class Significance Analysis of Microarray (SAM) program with default settings [46]. The normalized expression values of the biological replicates for each genotype were log₂ transformed and mediated. Gene Ontology (GO) analysis of differentially expressed genes was performed using the DAVID tool [47].

Acknowledgements

This work was funded by grants from the University of Padova (Progetto Strategico di Ateneo – 2008: “Models of mitochondrial diseases”) (to P.B., V.B., R.C.); Fondazione CARIPLO – Scientific Research in Biomedicine 2011 (“MITGEN: Definition and characterization of disease genes in mitochondrial disorders”) (to M.Z. and R.C.); Telethon Project N. GGP11011 (“MitMed: a multicenter consortium for the identification and characterization of nuclear genes responsible for human mitochondrial disorders”) (to M.Z. and R.C.); Italian Telethon Grant GGP09019 (to V.B.); Italian Association for Cancer Research Grant 1091 (to V.B.); Italian Association for Cancer Research Grant 12035 (to C.T.), Fondazione Compagnia di San Paolo (to

C.T.) and Telethon Program Project N. GPP10005 "Therapeutic strategies to combat mitochondrial disorders" (to M.Z and P.B.).

Author Contributions

R.C., V.B., C.D.P. and C.D.R. conceived the study. C.D.R., E.F., A.B., A.P., B.P. G.M. and C.G. performed the experiments. C.D.R, R.C., V.B. and C.D.P. compiled and analyzed the data. C.T. designed electron microscopic experiments. P.B., M.A.Z. and M.Z. provided critical advice and suggested experiments. V.B., R.C. and C.D.R. wrote the manuscript.

References

1. Magnusson J, Orth M, Lestienne P, Taanman JW. (2003) Replication of mitochondrial DNA occurs throughout the mitochondria of cultured human cells. *Exp Cell Res* 289: 133-142.
2. Pontarin G, Ferraro P, Bee L, Reichard P, Bianchi V. (2012) Mammalian ribonucleotide reductase subunit p53R2 is required for mitochondrial DNA replication and DNA repair in quiescent cells. *Proc Natl Acad Sci U S A* 109: 13302-13307.
3. Nordlund P, Reichard P. (2006) Ribonucleotide reductases. *Annu Rev Biochem* 75: 681-706.
4. Eriksson S, Munch-Petersen B, Johansson K, Eklund H. (2002) Structure and function of cellular deoxyribonucleoside kinases. *Cell Mol Life Sci* 59: 1327-1346.
5. Arco AD, Satrustegui J. (2005) New mitochondrial carriers: An overview. *Cell Mol Life Sci* 62: 2204-2227.
6. Vozza A, Blanco E, Palmieri L, Palmieri F. (2004) Identification of the mitochondrial GTP/GDP transporter in *saccharomyces cerevisiae*. *J Biol Chem* 279: 20850-20857.
7. Marobbio CM, Di Noia MA, Palmieri F. (2006) Identification of a mitochondrial transporter for pyrimidine nucleotides in *saccharomyces cerevisiae*: Bacterial expression, reconstitution and functional characterization. *Biochem J* 393: 441-446.
8. Haitina T, Lindblom J, Renstrom T, Fredriksson R. (2006) Fourteen novel human members of mitochondrial solute carrier family 25 (SLC25) widely expressed in the central nervous system. *Genomics* 88: 779-790.
9. Floyd S, Favre C, Lasorsa FM, Leahy M, Trigiante G, et al. (2007) The insulin-like growth factor-I-mTOR signaling pathway induces the mitochondrial pyrimidine nucleotide carrier to promote cell growth. *Mol Biol Cell* 18: 3545-3555.

10. Franzolin E, Miazzi C, Frangini M, Palumbo E, Rampazzo C, et al. (2012) The pyrimidine nucleotide carrier PNC1 and mitochondrial trafficking of thymidine phosphates in cultured human cells. *Exp Cell Res* 318: 2226-2236.
11. Van Dyck E, Jank B, Ragnini A, Schweyen RJ, Duyckaerts C, et al. (1995) Overexpression of a novel member of the mitochondrial carrier family rescues defects in both DNA and RNA metabolism in yeast mitochondria. *Mol Gen Genet* 246: 426-436.
12. Favre C, Zhdanov A, Leahy M, Papkovsky D, O'Connor R. (2010) Mitochondrial pyrimidine nucleotide carrier (PNC1) regulates mitochondrial biogenesis and the invasive phenotype of cancer cells. *Oncogene* 29: 3964-3976.
13. Kunji ER. (2004) The role and structure of mitochondrial carriers. *FEBS Lett* 564: 239-244.
14. Schneider I. (1972) Cell lines derived from late embryonic stages of *Drosophila melanogaster*. *J Embryol Exp Morphol* 27: 353-365.
15. Pontarin G, Gallinaro L, Ferraro P, Reichard P, Bianchi V. (2003) Origins of mitochondrial thymidine triphosphate: Dynamic relations to cytosolic pools. *Proc Natl Acad Sci U S A* 100: 12159-12164.
16. Ferraro P, Franzolin E, Pontarin G, Reichard P, Bianchi V. (2010) Quantitation of cellular deoxynucleoside triphosphates. *Nucleic Acids Res* 38: e85.
17. Ferraro P, Pontarin G, Crocco L, Fabris S, Reichard P, et al. (2005) Mitochondrial deoxynucleotide pools in quiescent fibroblasts: A possible model for mitochondrial neurogastrointestinal encephalomyopathy (MNGIE). *J Biol Chem* 280: 24472-24480.
18. Brand AH, Perrimon N. (1993) Targeted gene expression as a means of altering cell fates and generating dominant phenotypes. *Development* 118: 401-415.
19. Ni JQ, Liu LP, Binari R, Hardy R, Shim HS, et al. (2009) A *Drosophila* resource of transgenic RNAi lines for neurogenetics. *Genetics* 182: 1089-1100.
20. Parks AL, Cook KR, Belvin M, Dompe NA, Fawcett R, et al. (2004) Systematic generation of high-resolution deletion coverage of the *Drosophila melanogaster* genome. *Nat Genet* 36: 288-292.
21. Clay Montier LL, Deng JJ, Bai Y. (2009) Number matters: Control of mammalian mitochondrial DNA copy number. *J Genet Genomics* 36: 125-131.
22. Medeiros DM. (2008) Assessing mitochondria biogenesis. *Methods* 46: 288-294.
23. Ponton F, Chapuis MP, Pernice M, Sword GA, Simpson SJ. (2011) Evaluation of potential reference genes for reverse transcription-qPCR studies of physiological responses in *Drosophila melanogaster*. *J Insect Physiol* 57: 840-850.
24. Wu M, Neilson A, Swift AL, Moran R, Tamagnine J, et al. (2007) Multiparameter metabolic analysis reveals a close link between attenuated mitochondrial bioenergetic function and enhanced glycolysis dependency in human tumor cells. *Am J Physiol Cell Physiol* 292: C125-36.
25. Wenz T. (2013) Regulation of mitochondrial biogenesis and PGC-1 α under cellular stress. *Mitochondrion* 13: 134-142.

26. Munch-Petersen B, Piskur J, Sondergaard L. (1998) The single deoxynucleoside kinase in *Drosophila melanogaster*, dm-dNK, is multifunctional and differs from the mammalian deoxynucleoside kinases. *Adv Exp Med Biol* 431: 465-469.
27. Hayward DC, Delaney SJ, Campbell HD, Ghysen A, Benzer S, et al. (1993) The sluggish-A gene of *Drosophila melanogaster* is expressed in the nervous system and encodes proline oxidase, a mitochondrial enzyme involved in glutamate biosynthesis. *Proc Natl Acad Sci U S A* 90: 2979-2983.
28. Ghezzi D, Arzuffi P, Zordan M, Da Re C, Lamperti C, et al. (2011) Mutations in TTC19 cause mitochondrial complex III deficiency and neurological impairment in humans and flies. *Nat Genet* 43: 259-263.
29. Iyengar B, Roote J, Campos AR. (1999) The *tamas* gene, identified as a mutation that disrupts larval behavior in *Drosophila melanogaster*, codes for the mitochondrial DNA polymerase catalytic subunit (DNApol-gamma125). *Genetics* 153: 1809-1824.
30. Yoon H, Zhang Y, Pain J, Lyver ER, Lesuisse E, et al. (2011) RIM2, a pyrimidine nucleotide exchanger, is needed for iron utilization in mitochondria. *Biochem J* 440: 137-146.
31. Lin H, Li L, Jia X, Ward DM, Kaplan J. (2011) Genetic and biochemical analysis of high iron toxicity in yeast: Iron toxicity is due to the accumulation of cytosolic iron and occurs under both aerobic and anaerobic conditions. *J Biol Chem* 286: 3851-3862.
32. Froschauer EM, Rietzschel N, Hassler MR, Binder M, Schweyen RJ, et al. (2013) The mitochondrial carrier RIM2 co-imports pyrimidine nucleotides and iron. *Biochem J* 455: 57-65.
33. Flockhart IT, Booker M, Hu Y, McElvany B, Gilly Q, et al. (2012) FlyRNAi.org--the database of the *Drosophila* RNAi screening center: 2012 update. *Nucleic Acids Res* 40: D715-9.
34. Bianchi V, Fortunati E. (1990) Cellular effects of an anionic surfactant detected in V79 fibroblasts by different cytotoxicity tests. *Toxicol In Vitro* 4: 9-16.
35. Sherman PA, Fyfe JA. (1989) Enzymatic assay for deoxyribonucleoside triphosphates using synthetic oligonucleotides as template primers. *Anal Biochem* 180: 222-226.
36. von Stockum S, Basso E, Petronilli V, Sabatelli P, Forte MA, et al. (2011) Properties of Ca²⁺ transport in mitochondria of *Drosophila melanogaster*. *J Biol Chem* 286: 41163-41170.
37. Zordan MA, Cisotto P, Benna C, Agostino A, Rizzo G, et al. (2006) Post-transcriptional silencing and functional characterization of the *Drosophila melanogaster* homolog of human *Surf1*. *Genetics* 172: 229-241.
38. Ye J, Coulouris G, Zaretskaya I, Cutcutache I, Rozen S, et al. (2012) Primer-BLAST: A tool to design target-specific primers for polymerase chain reaction. *BMC Bioinformatics* 13: 134-2105-13-134.
39. Thibault ST, Singer MA, Miyazaki WY, Milash B, Dompe NA, et al. (2004) A complementary transposon tool kit for *Drosophila melanogaster* using P and piggyBac. *Nat Genet* 36: 283-287.
40. Livak KJ, Schmittgen TD. (2001) Analysis of relative gene expression data using real-time quantitative PCR and the 2^{-ΔΔC(T)} method. *Methods* 25: 402-408.
41. Oliveira MT, Kaguni LS. (2011) Reduced stimulation of recombinant DNA polymerase gamma and mitochondrial DNA (mtDNA) helicase by variants of mitochondrial single-stranded DNA-binding

protein (mtSSB) correlates with defects in mtDNA replication in animal cells. J Biol Chem 286: 40649-40658.

42. Rabouille C. (1999) Quantitative aspects of immunogold labeling in embedded and nonembedded sections. Methods Mol Biol 117: 125-144.
43. Andreu AL, Martinez R, Marti R, Garcia-Arumi E. (2009) Quantification of mitochondrial DNA copy number: Pre-analytical factors. Mitochondrion 9: 242-246.
44. Chabi B, Mousson de Camaret B, Duborjal H, Issartel JP, Stepien G. (2003) Quantification of mitochondrial DNA deletion, depletion, and overreplication: Application to diagnosis. Clin Chem 49: 1309-1317.
45. Bolstad BM, Irizarry RA, Astrand M, Speed TP. (2003) A comparison of normalization methods for high density oligonucleotide array data based on variance and bias. Bioinformatics 19: 185-193.
46. Saeed AI, Bhagabati NK, Braisted JC, Liang W, Sharov V, et al. (2006) TM4 microarray software suite. Methods Enzymol 411: 134-193.
47. Huang da W, Sherman BT, Lempicki RA. (2009) Systematic and integrative analysis of large gene lists using DAVID bioinformatics resources. Nat Protoc 4: 44-57.

FIGURE LEGENDS

Figure 1. Sequence alignment of RIM2 proteins s from different species. Sequences included in the alignment, performed with Multiple Sequence Alignment T-Coffee, are those of *Saccharomyces cerevisiae*, *Homo sapiens* (SLC25A33) and *Drosophila melanogaster* (drim2 isoforms A, C and D). The alignment highlights identical residues (*) and similar ones (. and :), the positions of the six transmembrane α -helices (red lines) and the three signature motifs (blue boxes).

Figure 2. Mitochondrial localization of drim2 and effects of drim2 silencing on the deoxynucleotides pool contents of S2R⁺. a. *Drosophila* cells were transiently transfected with pACT-drim2 HA tagged, incubated with Mitotracker dye (red) and then immunolabeled with the anti-HA antibody (green). Overlay of images confirms the mitochondrial localization of drim2. Pyrimidine and purine dNTP pool sizes in cytosol (b) and mitochondria (c) of drim2 silenced S2R⁺ cells and in controls. Pool sizes are expressed as pmol dNTP/A_{260 nm} of the alkali lysates obtained after pool extraction as indicated in Materials and Methods. Values are means \pm

standard deviation (s.d.) from four experiments for control and five experiments for RNAi (Student's *t*-test * $p < 0.05$, ** $p < 0.01$, *** $p < 0.005$).

Figure 3. Morphological, developmental and behavioral effects of *drim2* KO *in vivo*. All experiments were carried out in parallel in *w¹¹¹⁸* (closed column), *drim2^{+/-}* (grey column) and *drim2^{-/-}* (open column) third-stage larvae. a, *drim2* mRNA levels, expressed as relative quantity of template in the sample (RQ), were determined by qRT-PCR. b, Third-stage KO larvae. Heterozygous *drim2^{+/-}* larva (right) and homozygous *drim2^{-/-}* larva (left). Notice the smaller size of the latter. c, Both hetero- and homozygous KO larvae present mouth hooks, the distinctive characters of the third larval stage. d, Relative percentage of egg to adult viability calculated at three developmental stages, *i.e.*, third-stage larvae, pupae and adults. (e-g) Larval locomotor activity characterized by the three parameters, each calculated in a total recording time period of 120 seconds: (e) total distance travelled (*i.e.* as millimeters covered), (f) overall average speed (millimeters over 120 seconds) and (g) inactivity (seconds over 120 seconds). Data plotted are means \pm s.d. (Student's *t*-test *** $p < 0.005$).

Figure 4. Mitochondria disposition around z-lines. Confocal images (a) and electromicroscopy (b) of body wall preparations of *w¹¹¹⁸* and *drim2^{-/-}* larvae. Arrows indicate the z-lines.

Figure 5. Electron microscopic analysis on third-stage larval body-wall sections. Characterization was carried out on *w¹¹¹⁸*, *drim2^{+/-}* and *drim2^{-/-}* larvae. a, Cross sectional ultrastructure of larval muscles, illustrating the distribution and morphology of mitochondria. (b and c) Morphometric analyses of mitochondrial dimensions in terms of minor (b) and major diameter (c), both expressed in nanometers and presented as box plots. d, Mean \pm standard error of the total area occupied by mitochondria (expressed in square microns). e, Mitochondria density \pm standard error was plotted as the number of mitochondria per square micron of cell

profile area. Data were obtained by analyzing all the mitochondria present in 20 cell profiles for each of the strain considered. (Student's *t*-test * $p < 0.05$, ** $p < 0.01$, *** $p < 0.005$).

Figure 6. Mitochondrial DNA content and analysis of mitochondrial transcription in larvae. All experiments were carried out on w^{1118} , $drim2^{+/-}$ and $drim2^{-/-}$ larvae. a, mtDNA content was measured by quantitative real time-PCR. Data are ratios of mtDNA to genomic DNA relative to the control ratio in w^{1118} larvae. Values are expressed as a mean of three independent experiments and error bars represent the s.d. of the mtDNA/nDNA ratio among the replicates. b, mtDNA content was normalized to mitochondria frequency, shown in the previous figure. c, Analysis of mitochondria transcription. Transcripts of the mitochondrial genes *Cyclooxygenase-1 (COX1)* and *(16S)* were measured by real time-PCR and related to the level of transcripts of the nuclear gene *Rpl32*. For each conditions data are presented as the mean of relative quantity of template in the sample (RQ) \pm s.d. from three individual experiments. (Student's *t*-test * $p < 0.05$, ** $p < 0.01$, *** $p < 0.005$).

Figure 7. Oxygen consumption rates in larvae and in S2R+ cells. a, Oxygen consumption was measured in w^{1118} (black vehicles), $drim2^{+/-}$ (grey vehicles) and $drim2^{-/-}$ (empty vehicles) third-stage larvae. The addition of 5 μ M rotenone plus 5 μ M antimycin A is indicated by the arrow. b, Respiratory profile of control and $drim2$ -silenced S2R+cells. We analyzed untreated cells (black vehicles), cells silenced for 48 hours with dsRNA (grey vehicles) and cells silenced for 96 hours (empty vehicles). Ten mM glucose, 1 μ M FCCP and 5 μ M rotenone plus 5 μ M antimycin A were added at the times marked by arrows.

Figure 8. Altered gene pathways in $drim2$ KO *Drosophila*. Heat map representing a selection of deregulated transcripts in $drim2^{-/-}$ vs. $drim2^{+/-}$ involved in purine (22 transcripts) and pyrimidine (13 transcripts) metabolism which were provided by DAVID tool. A color-coded scale for the normalized expression values is used: yellow and blue represent high and low expression levels in $drim2^{-/-}$ with respect to $drim2^{+/-}$, respectively. The expression level of each

transcript was calculated as the $\text{Log}_2 [\text{drim}2^{-/-} / \text{drim}2^{+/+}]$ and the complete list of differentially expressed genes identified by SAM algorithm is provided in the Supplementary Information (Table S2).

Figure 2

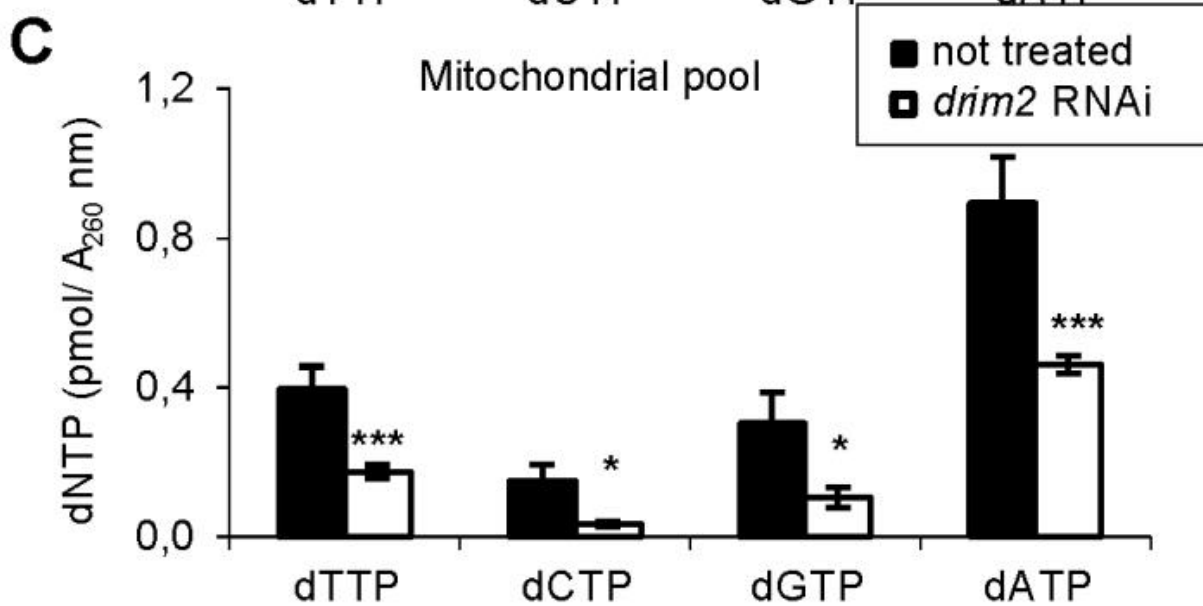
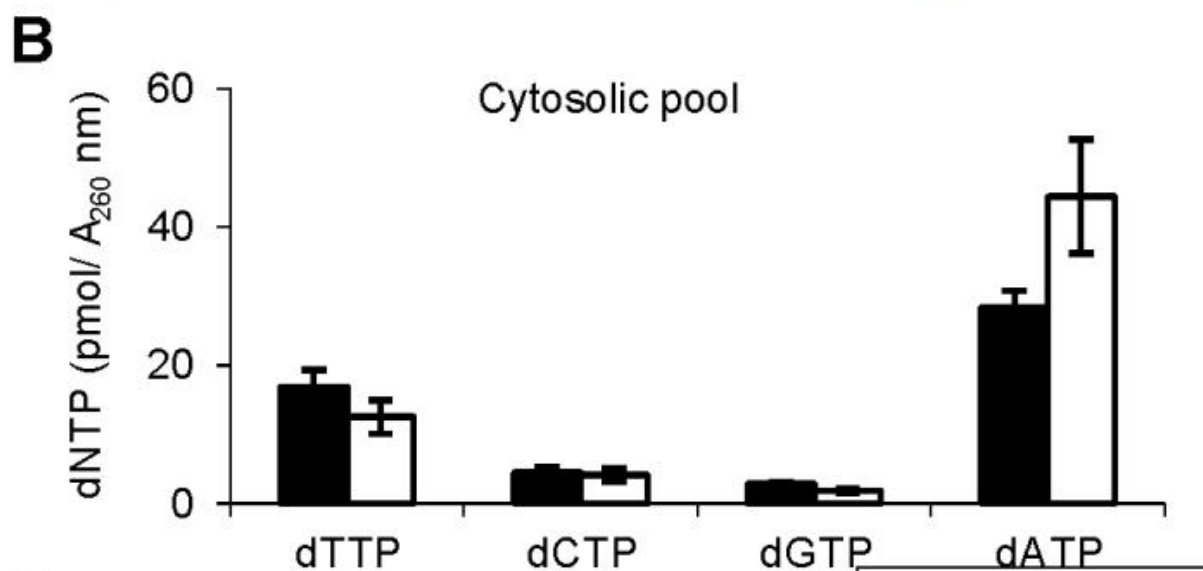
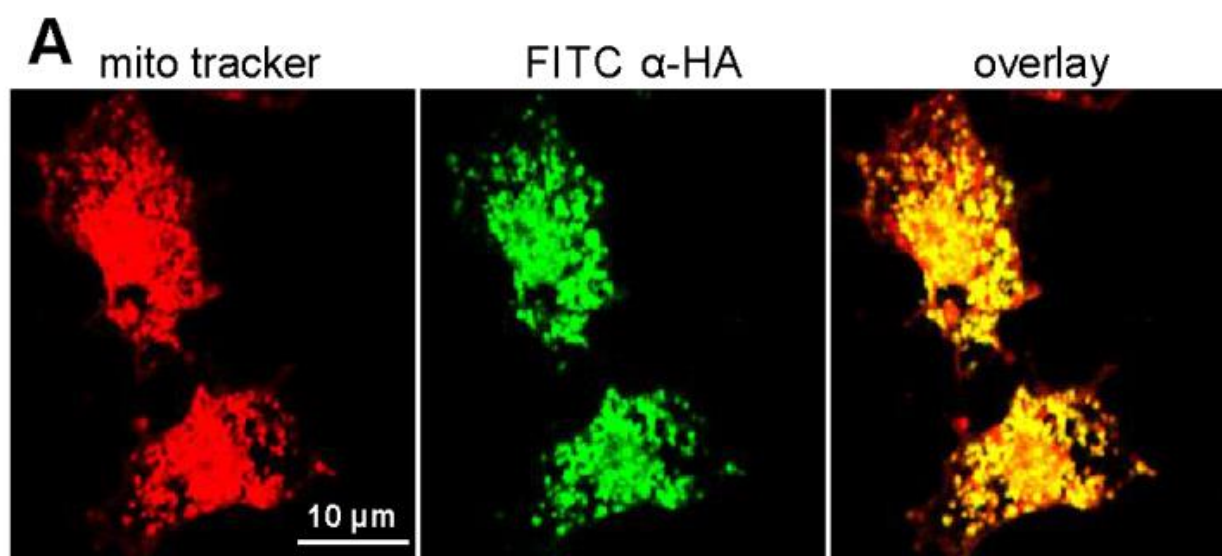


Figure 3

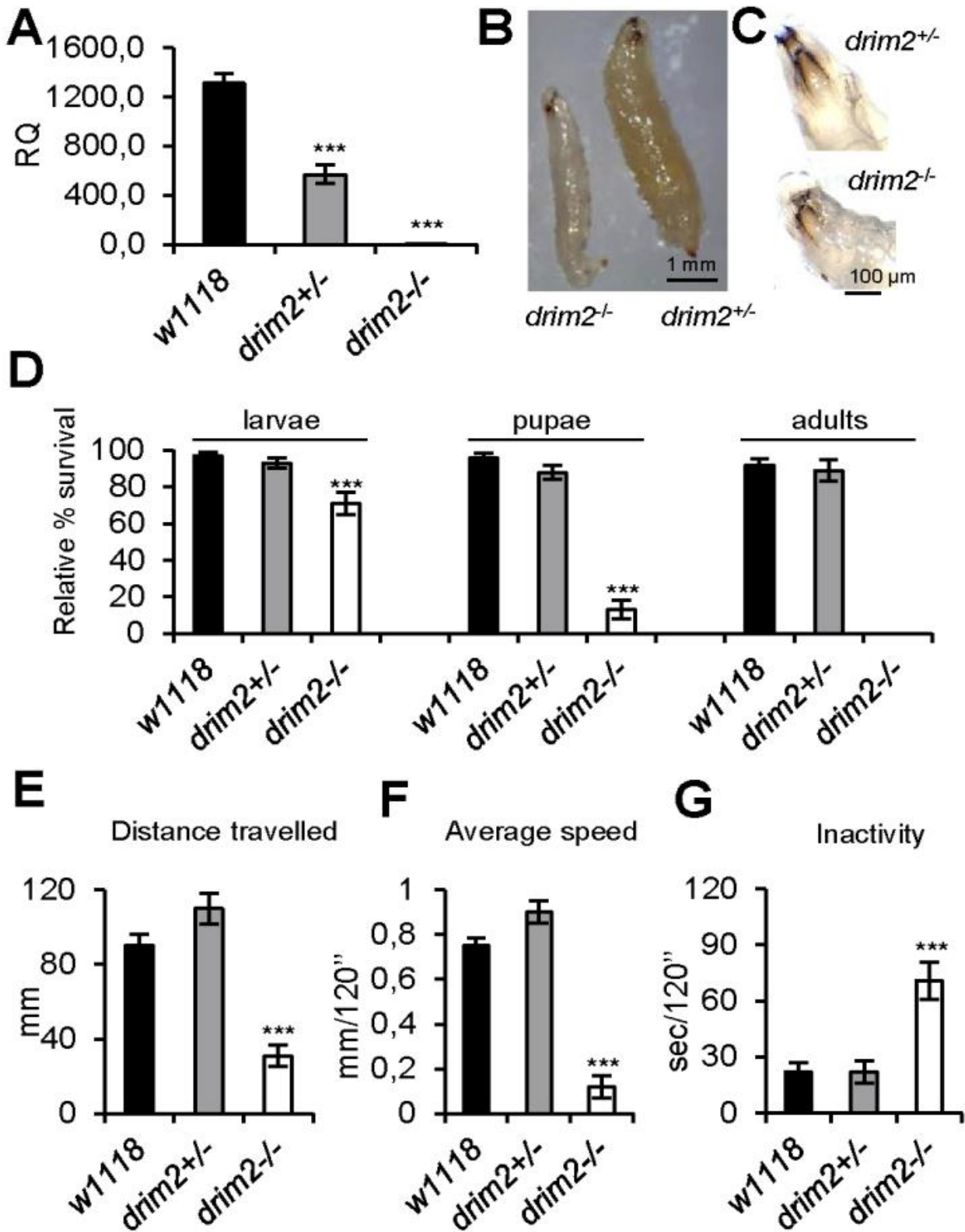


Figure 4

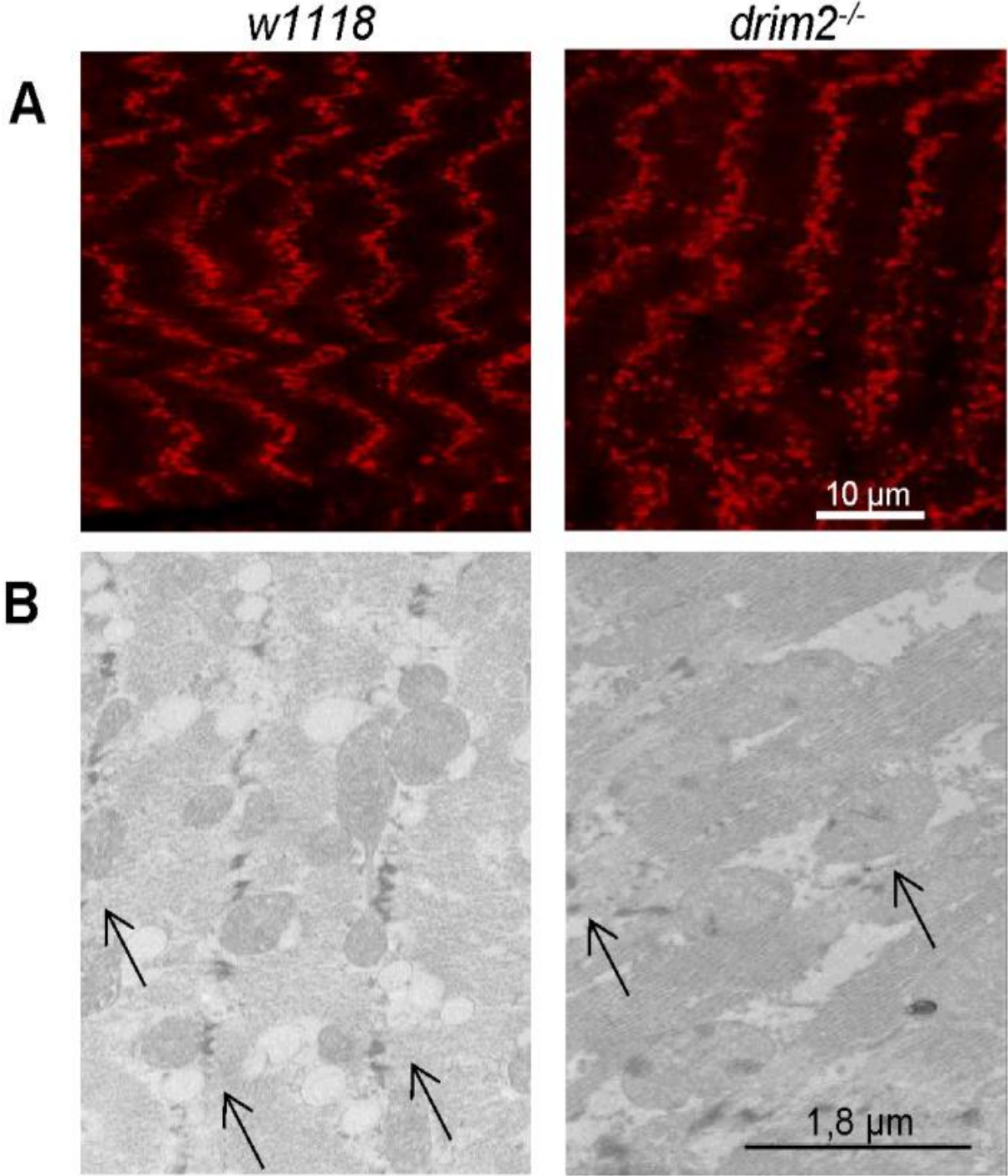


Figure 5

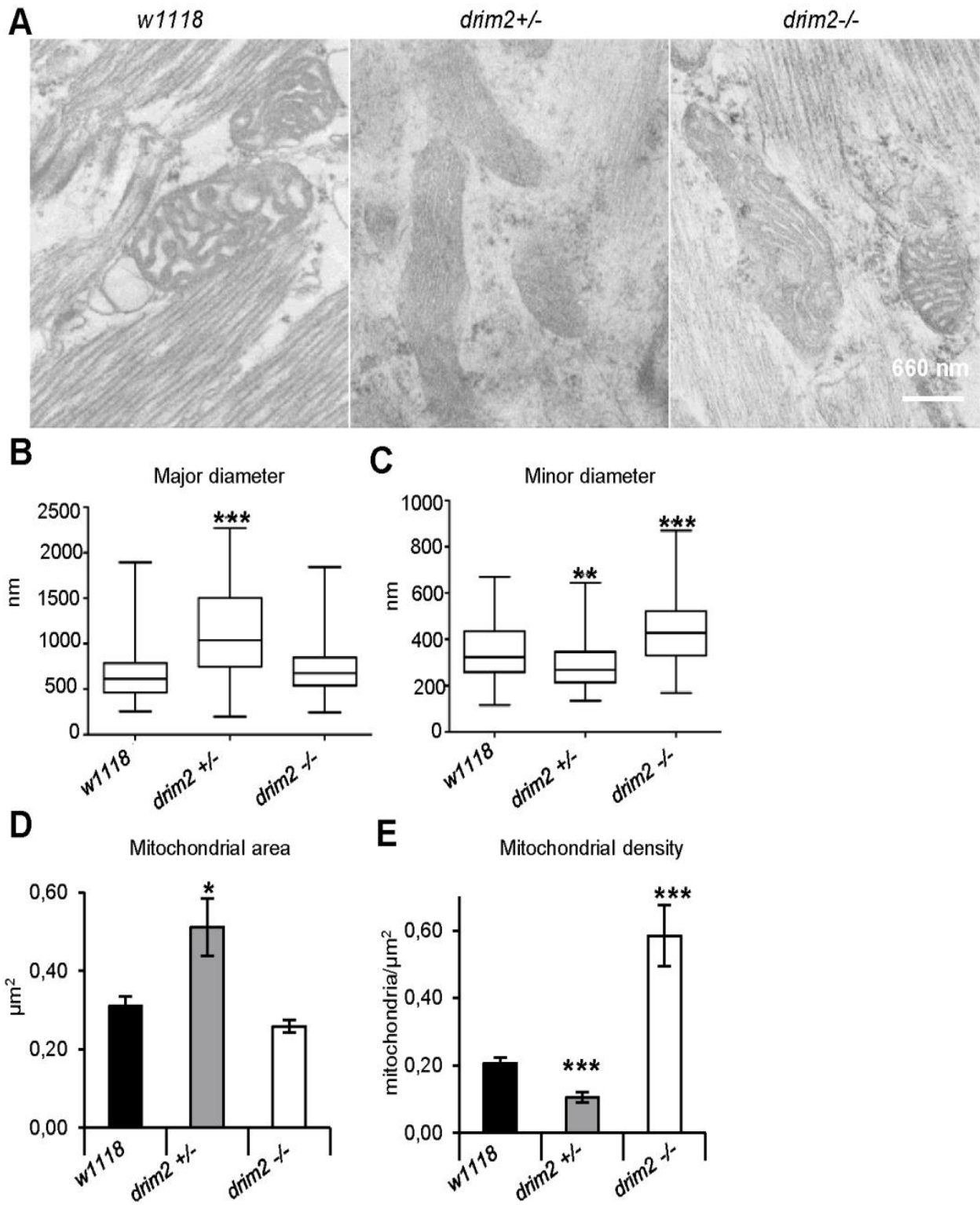


Figure 6

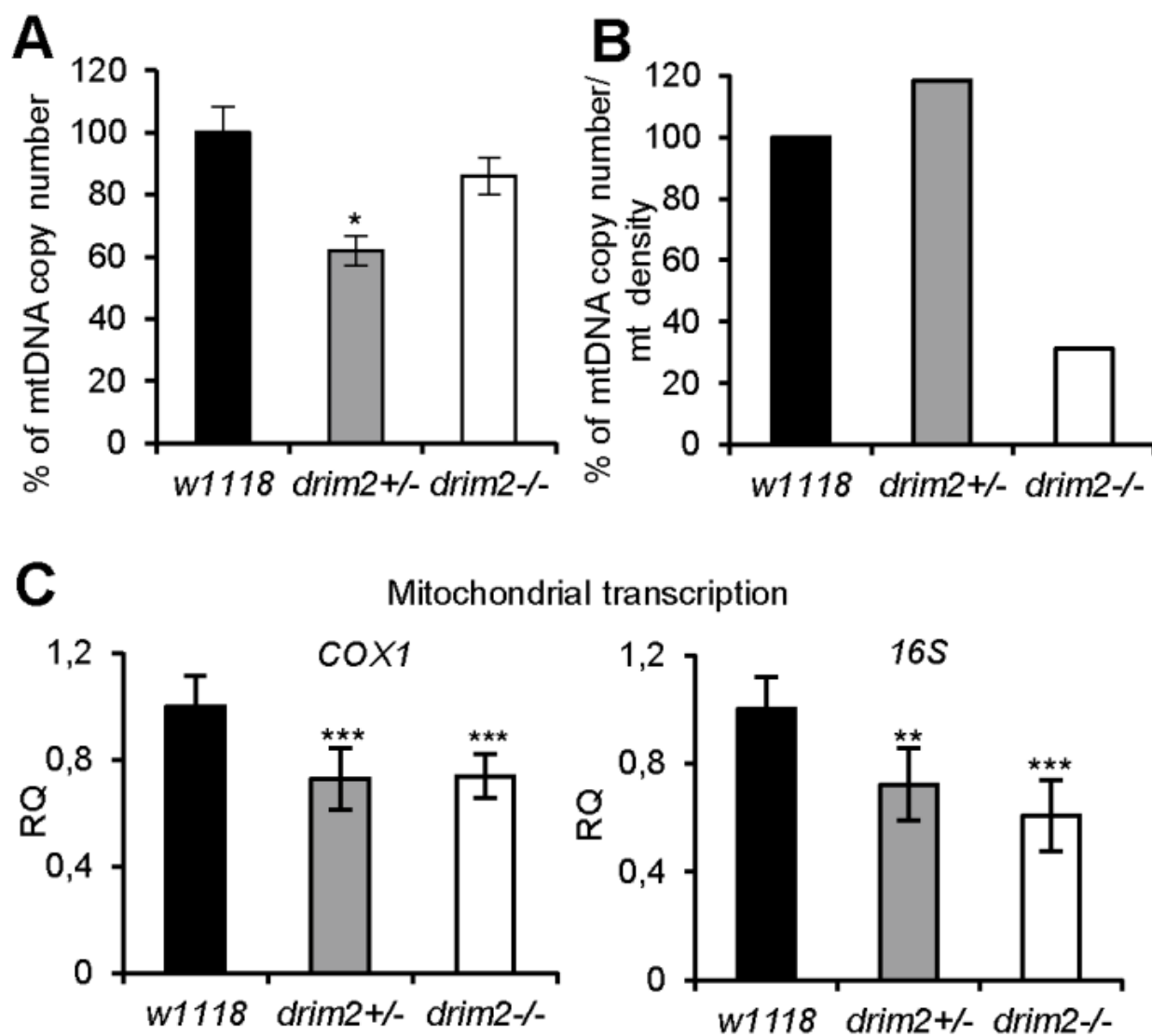


Figure 7

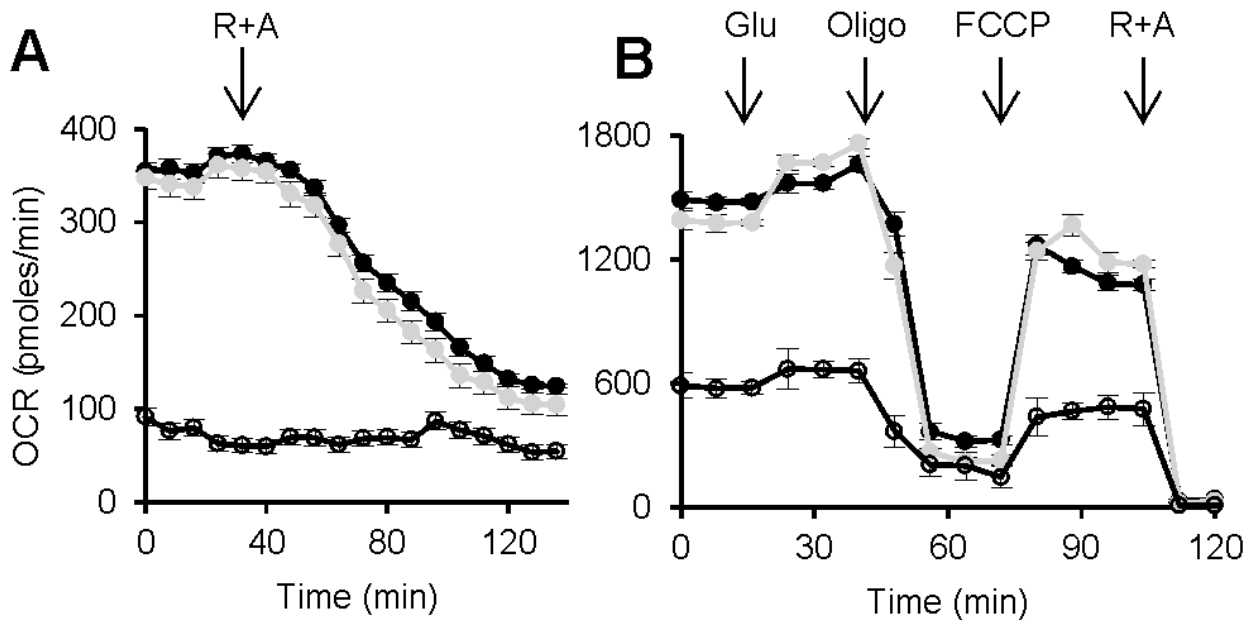
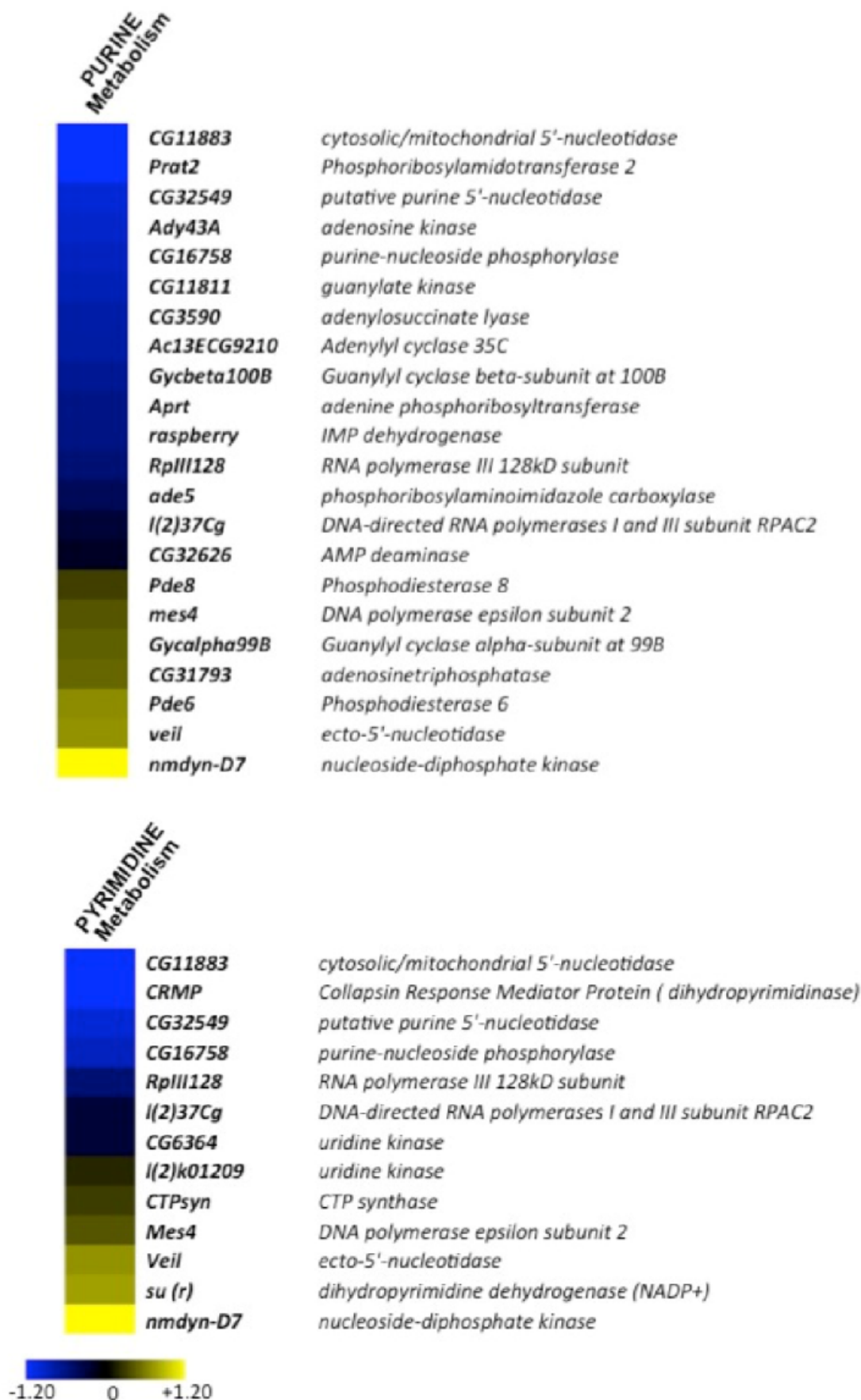


Figure 8



SUPPORTING INFORMATION

Table S1. Sequences of oligonucleotides used in this study. Primer sequences are indicated as 5'-3' direction.

Table S2. List of differentially expressed genes in *drim2*^{+/-} vs. *drim2*^{-/-} larvae detected by SAM two class analysis (FDR = 5.10%). The expression level of each transcript was calculated as the Log2 [expression value].

Figure S1. Developmental effects of *drim2* KD *in vivo*. All experiments were carried out in *w*¹¹¹⁸ (closed column) as well as in specific controls *w*; *UAS-drim2* (grey column) and in KD *w*; *UAS-drim2/Act5C-Gal4* (open column) third-stage larvae. a, *drim2* mRNA levels in each strain measured by qRT-PCR. b, Relative percentage of egg to adult viability calculated at three developmental stages, *i.e.*, third-stage larvae, pupae and adults. Data plotted are means \pm s.d. (Student's *t*-test *** $p < 0.005$).

Figure S2. Functional classification of genes altered in *drim2* KO *Drosophila*. Heat map representing a selection of deregulated transcripts in *drim2*^{-/-} vs. *drim2*^{+/-} involved in Oxidative phosphorylation (10 transcripts) and Glycolysis/gluconeogenesis (6 transcripts) which were provided by DAVID tool. A color-coded scale for the normalized expression values is used: yellow and blue represent high and low expression levels in *drim2*^{-/-} with respect to *drim2*^{+/-} respectively. The expression level of each transcript was calculated as the Log2 [*drim2*^{-/-} / *drim2*^{+/-}]. The complete list of differentially expressed genes identified by SAM algorithm is provided in the Table S2.

Figure S1

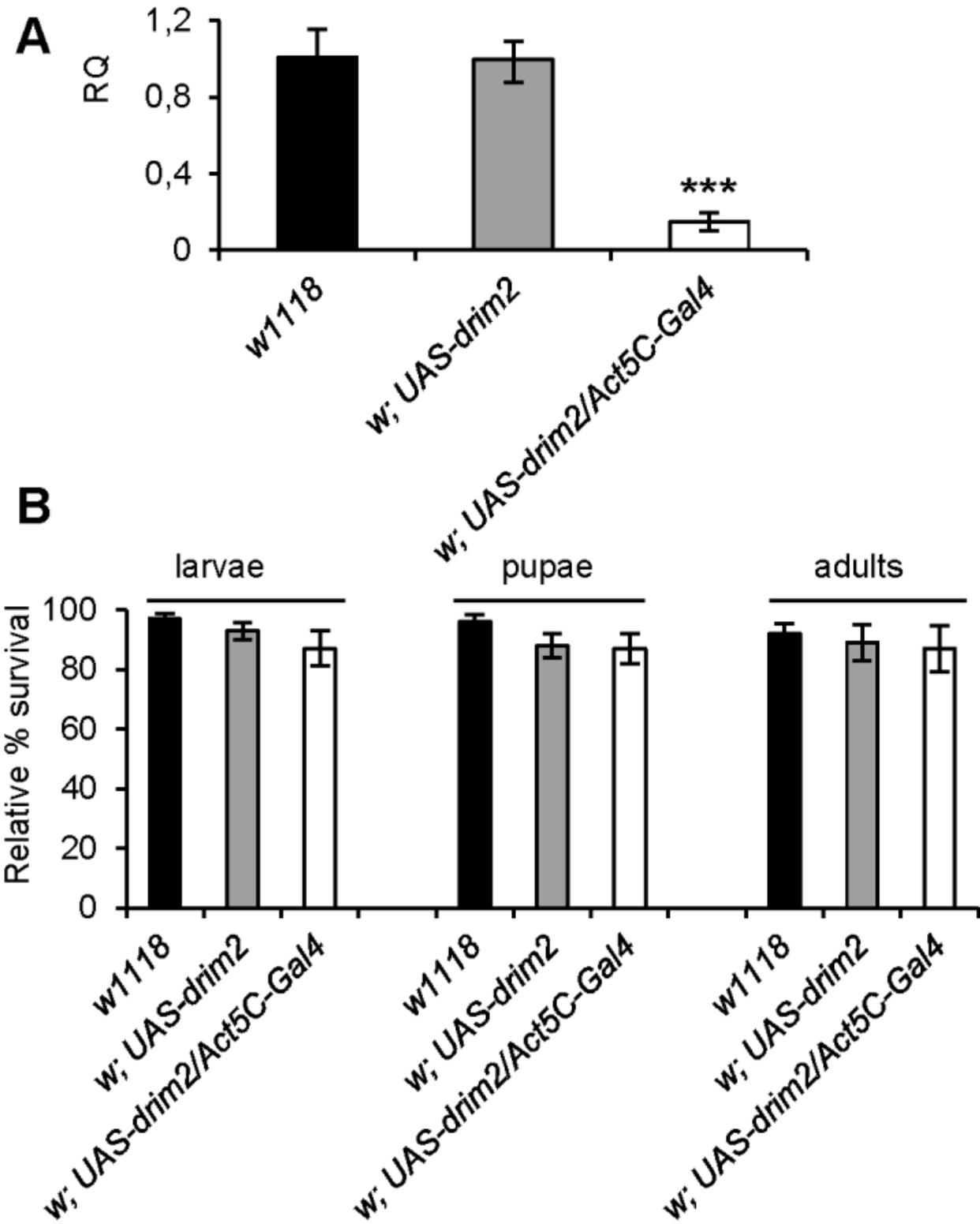
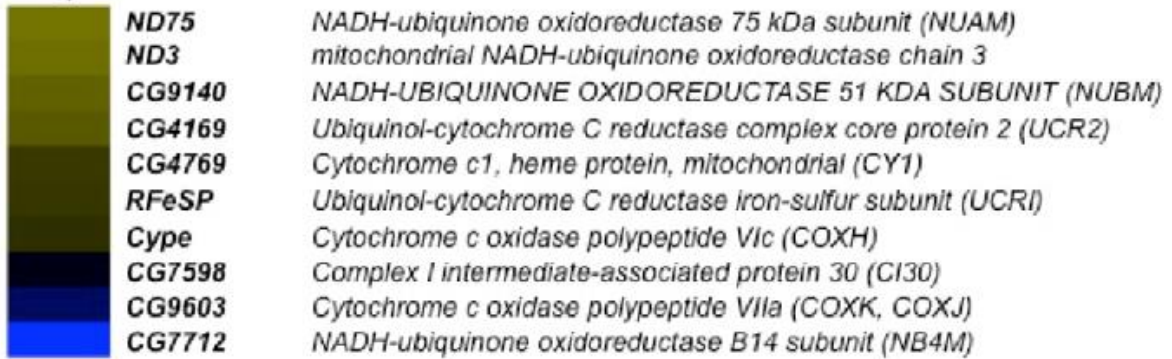
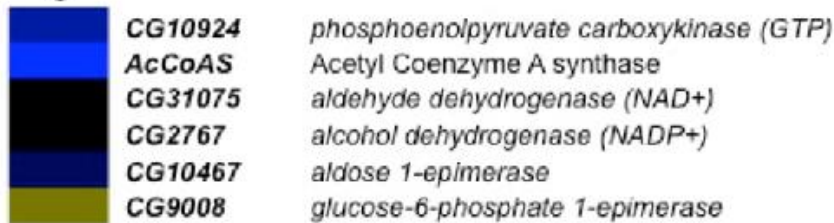


Figure S2

Oxidative
phosphorylation



Glycolysis-
Gluconeogenesis



-1.0 0.0 +1.0

Table S1

Primer name	Sequence 5' -3'
<i>drim2_T7</i> F	taatacgactcactatagggagatgtatgcgtttgccaaagttaa
<i>drim2_T7</i> R	taatacgactcactatagggagaatggtacaccctctcgatgcactg
<i>drim2KO</i> ^{e01575} F	atttcgcctcacagcttg
<i>drim2KO</i> ^{e01575} R	gatgacaaagtgcaccatcg
<i>drim2KO</i> ^{e00041} F	ctcttcgattctgggcattc
<i>drim2KO</i> ^{e00041} R	tactattccttcactcgcacttattg
<i>drim2</i> F	tcggttacggatcgaacaa
<i>drim2</i> R	tcggttacggatcgaacaa
<i>CoxI</i> F	tgctcctgatatagcattcccacga
<i>CoxI</i> R	tccacatgagcaattccagcgg
<i>16S</i> F	aaaaagattgcgacctcgat
<i>16S</i> R	aaaccaacctggcttacacc
<i>Rp49</i> F	tcggttacggatcgaacaa
<i>Rp49</i> R	gacaatctccttgcgcttct
<i>Rpl32</i> F	aggcccaagatcgtgaagaa
<i>Rpl32</i> R	tgtgcaccaggaacttctgaa

C **HAPTER II:**

dTTC19

Further characterization of the *Drosophila dTTC19* mutant, a model for mitochondrial disease of the ETC

Human diseases caused by dysfunctional mitochondria affect approximately 1:8500 individuals (Sánchez-Martínez *et. al.*, 2006). Since the mitochondrial genome only encodes for 13 proteins, a large proportion of mitochondrial proteins are encoded for by nuclear genes, meaning that mutations which cause mitochondrial diseases can be either nuclear or mitochondrial in nature. Unfortunately this, combined with the fact that mitochondrial diseases are multifactorial in nature makes their genetic source a very difficult and important area of study. Many mutant lines of *Drosophila melanogaster* have long been used as models for human mitochondrial diseases (Sánchez-Martínez *et. al.*, 2006), including the *dTTC19* mutant.

TTC19 is a protein involved in the assembly of Complex III of the electron transport chain (ETC), mutations in which have been tied to late-onset mitochondrial encephalopathy (Ghezzi *et. al.*, 2011) and psychosis (Nogueira *et. al.*, 2013) in humans. In *Drosophila*, lack of transcription of the *TTC19* homolog results in adult flies with a severely reduced Complex III activity, locomotor deficits and bang sensitivity (Ghezzi *et. al.*, 2011). Mutant larvae, on the other hand, had normal levels of Complex III activity, consistent with the late-onset mitochondrial disease seen in humans (Ghezzi *et. al.*, 2011). In this study, the *dTTC19* mutant line was characterized further, and mutant lines expressing *dTTC19* under UAS-GAL4 control in order to confirm that the mutant phenotype observed was due to a lack of *dTTC19* transcription.

Further characterization of the *dTTC19* mutant demonstrated that they have sensory abnormalities, consistent with the fact that humans with *TTC19* mutations exhibit adverse symptoms in the brain. Interestingly, sensory abnormalities were found in *dTTC19* Δ larvae, indicating that these mutants do present with a (albeit less pronounced) mutant phenotype at the larval stage as well. It also emphasises the fact that the nervous system is that most strongly affected by the *dTTC19* mutation, once again mirroring what is seen in humans.

CHAPTER II: **INTRODUCTION**

1.1 The Electron Transport Chain

Eukaryotic organisms rely on aerobic cellular respiration in order to produce chemical energy. In eukaryotic cells this process occurs in mitochondria terminating in the electron transport chain, involving five protein complexes embedded in the inner mitochondrial membrane. Energy is produced by the oxidation of NADH and FADH₂, passing these electrons through the electron transport chain using molecular oxygen as the final acceptor, and capturing the energy released during this process to produce ATP (Fig 1.1.1).

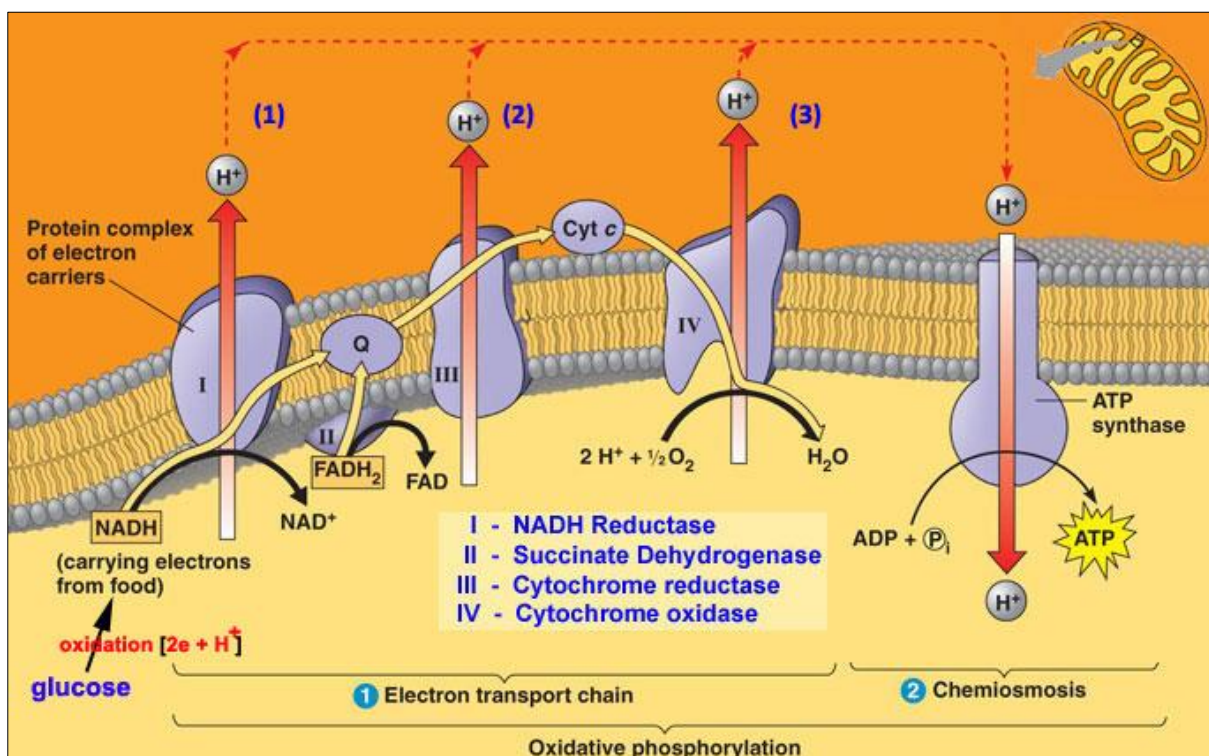


Fig. 1.1.1: Electron Transport Chain in eukaryotic cells. Source: Brace *et. al.*, 2012

Despite the fact that mitochondria possess their own genome, it only encodes for a total of 13 proteins, and therefore all of the respiratory chain complexes are encoded for, at least in part, by nuclear genes. Thus the correct assembly and function of the respiratory chain complexes rely on the coordination of nuclear- and mitochondrially-encoded proteins, the malfunction of which can lead to serious diseases. In this study, particular attention was given to the assembly of and diseases associated with Complex III, as the gene of interest is a putative metazoan Complex III assembly factor.

1.1.1: Complex III Structure and Function

Complex III, also referred to as the bc_1 complex or ubiquinol cytochrome c reductase, is a dimeric complex composed of 11 subunits, three of which are catalytic (Fig. 1.1.1 A; Iwata *et al.*, 1998). Electrons are transported through this complex to complex IV and four H^+ protons are exported to the intermembrane space in a process known as the “Q cycle” (Fig. 1.1.1 B).

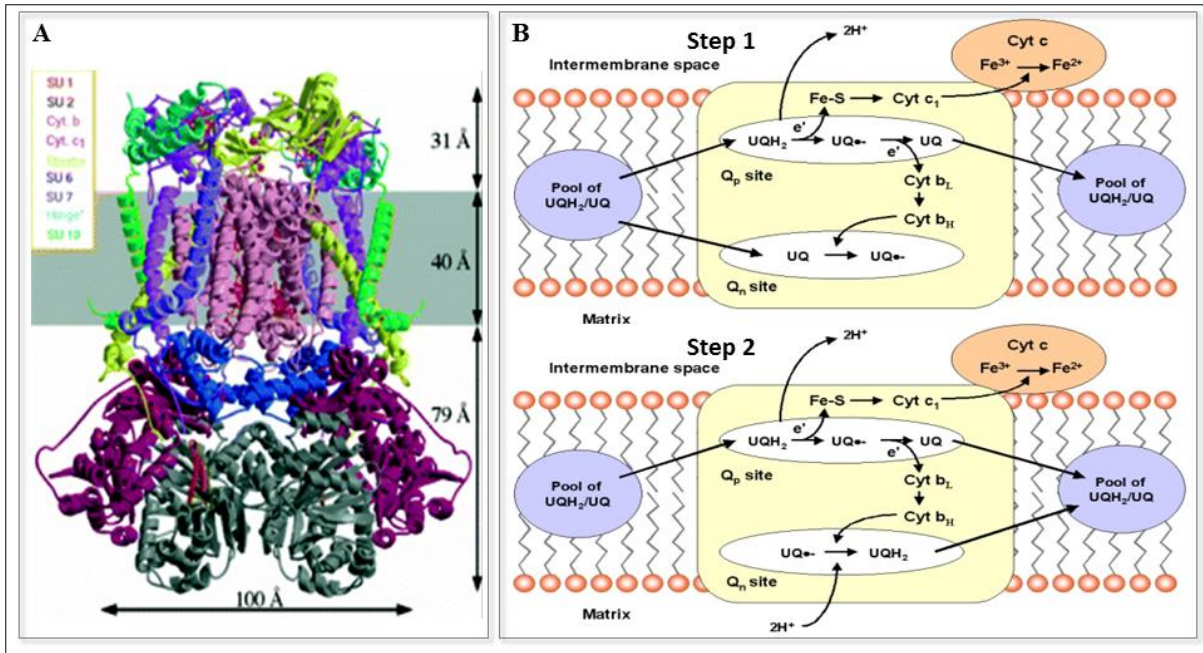


Fig. 1.1.1: (A) Structure of Complex III. Source: Zhang *et al.*, 1998. (B) Q-cycle in Complex III. Source: Balber, 2001.

During the first step of the Q cycle, ubiquinol (UQH₂) diffuses to the Q_P site on Complex III and is oxidized in a 2-step process, during which one electron is transferred to the Rieske protein then to cytochrome c , one to the b_L heme protein, and two H^+ protons are pumped into the intermembrane space (Balber, 2001). During the second step of the Q cycle, a second UQH₂ molecule binds to the Q_P site for oxidation, during which another two H^+ protons are pumped into the intermembrane space, UQ•⁻ is reduced to UQH₂ and returned to the membrane pool (Balber, 2001).

1.1.2: Complex III Assembly

While the assembly process for Complex III still remains to be fully elucidated, it is clear that multiple assembly factors are involved, primary studies of which have been conducted in *Saccharomyces cerevisiae* because of the convenient ability of this model organism to survive with a complete lack of Complex III activity on a fermentable source (Fig. 1.1.2).

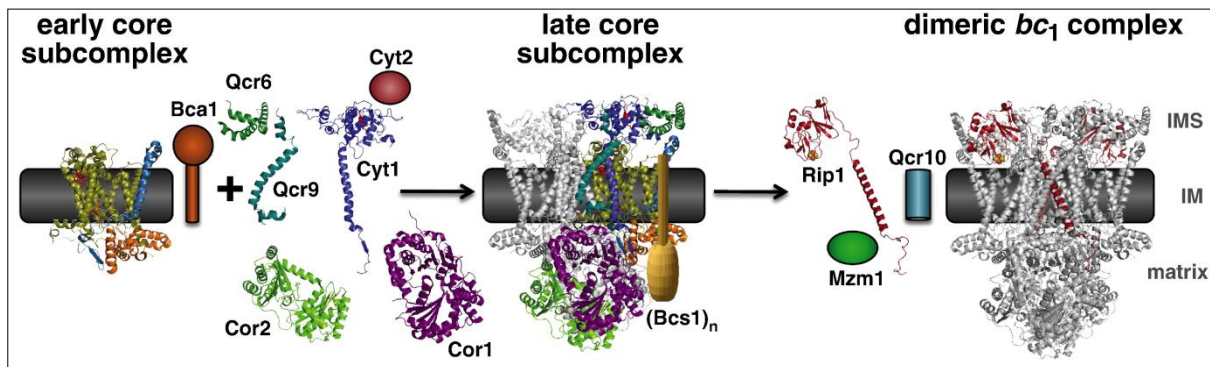


Fig. 1.1.2: Diagram of current knowledge of the assembly of Complex III in *Saccharomyces cerevisiae*. Source: Smith *et. al.*, 2012.

In yeast, assembly factors Bcs1 and Cyt2 interact with supernumerary subunits to form the late core complex (Fig 1.1.2). The assembly factors Bcs1 and Mzm1 then interact with this late core complex and help incorporate the catalytic Rip1 subunit (Smith *et. al.*, 2012).

Homologs for these assembly factors have been found in mammals. LYRM7 is the mammalian homolog of Mzm1 and has been shown to be a UQCRFS1 chaperone and Complex III assembly factor in human cells (Sánchez *et. al.*, 2013). BCS1L is the human homolog for Bcs1 and has also been shown to be a Complex III assembly factor (Smith *et. al.*, 2012). However, it is clear that there exist other assembly factors which have yet to be identified in yeast or in mammalian cells. This study focuses on another (albeit currently still putative) Complex III assembly factor, TTC19.

1.2 Complex III Dysfunction and Disease

Complex III deficiencies are found in various tissues in a wide variety of human diseases. These deficiencies have been tied to a variety of different mutations, in both nuclear and mitochondrial DNA, but many Complex III deficiencies are of unknown genetic origin (Ghezzi *et. al.*, 2011).

For example, Complex III activity was found to be reduced by 20% in platelets of untreated Parkinson's patients (Haas *et. al.*, 1995) and by 50-60% in the colonic mucosal of patients with ulcerative colitis (Sifroni *et. al.*, 2010). However, while Complex III deficiencies are often coupled with numerous disorders, there are also many mitochondrial diseases which are specifically characterized by a severe reduction in Complex III activity.

1.2.1: Mitochondrial Diseases Tied to Mutations in Complex III-encoding Genes

Complex III subunits are in most part encoded for by nuclear genes, with one subunit being encoded for by a mitochondrial gene. Therefore, mitochondrial diseases involving defective Complex III activity can be associated with either nuclear or mitochondrial genes.

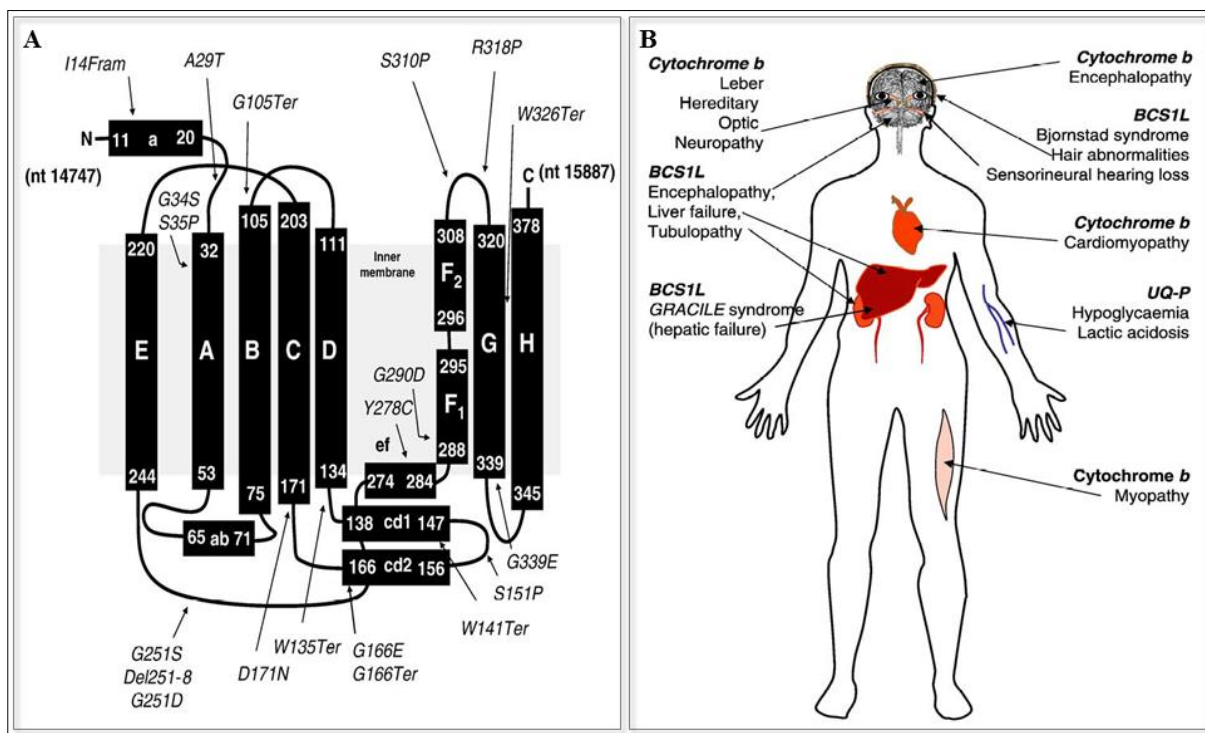


Fig 1.2.1.: (A) Mutations in the mitochondrial cytochrome *b* gene which have been associated with mitochondrial diseases. (B) Diagram of various Complex III-related mitochondrial diseases, including the various organs affected and the genes associated with them. Source: Bénit *et. al.*, 2009.

Cytochrome *b* is the only mitochondrially-encoded component of Complex III, and many different mutations in this gene have been found to be associated with mitochondrial diseases (Fig 1.2.1 A). Various mutations in this gene have been found in patients with exercise intolerance, a progressive myopathy characterized by extreme fatigue and cramps after moderate exercise and

lactic acidosis (Dumoulin *et. al.*, 1996; Lamantea *et. al.*, 2001; Mancuso *et. al.*, 2003). Mutations in cytochrome *b* have also been tied to mitochondrial encephalomyopathy involving both skeletal muscle and the brain (Keightley *et. al.*, 2000), encephalopathy and Leber Hereditary Optic Neuropathy (LHON) (Fig. 1.2.1 B), characterized by progressive degeneration of retinal ganglion cells (Bénil *et. al.*, 2009).

Although no mutations in nuclear-encoded Complex III genes have been currently connected to mitochondrial diseases, alterations in these genes have been identified as potential genes of interest in other kinds of disease. For example, Complex III activity was found to be very different between normal and invasive cancer cell lines, and knocking down *UQCRC1*, the gene which encodes for the Rieske Iron-Sulphur Complex III subunit, decreased metastatic potential in these cells (Owens *et. al.*, 2011).

1.2.2: Complex III Assembly Factors and Disease

Of particular interest to this study are mutations in genes encoding for Complex III assembly factors which are also tied to mitochondrial diseases characterized by Complex III deficiency. *BCS1L* is a nuclear gene which encodes for a member of the AAA ATPase family which facilitates the insertion of the Rieske catalytic subunit into Complex III (Morà *et. al.*, 2010). Mutations in *BCS1L* have been found in patients with encephalopathy and liver failure (de Lonlay *et. al.*, 2001), and GRACILE syndrome, a fatal metabolic disorder characterized by fetal growth retardation, lactic acidosis, aminoaciduria and defective iron metabolism (Vispaa *et. al.*, 2002).

1.3: Tetratricopeptide 19

Tetratricopeptide 19 (TTC19) is a gene found in all metazoa but not found in plants or fungi (Ghezzi *et. al.*, 2011), therefore it does not have a previously studied homolog in yeast. However, indirect evidence in humans and *Drosophila* suggests that it too is a metazoan Complex III assembly factor.

1.3.1: Human TTC19

In humans, the *TTC19* gene encodes for a mitochondrial protein and is located on chromosome 17p12 with highest levels of expression in the heart, bone tissue, ovaries and kidneys (TiGER Database). This gene encodes for two known transcript variants. Transcript variant 1 is a 3,505bp mRNA which is translated into a 380 amino acid (NM_017775.3). Transcript variant 2 is a 3,642bp mRNA which is translated into a 273 amino acid (NM_001271420.1).

This nuclear gene encodes for a protein which is embedded in the inner mitochondrial membrane as part of Complex III, and is a putative Complex III assembly factor (Ghezzi *et al.*, 2011).

1.3.2: TTC19 and Mitochondrial Disease

TTC19 mutations have been found in four patients with progressive encephalopathy, meaning they presented with a neurodegenerative disorder which presented later in life and worsened over time. In two patients symptoms appeared in late infancy, while in another clinical symptoms did not present until 42 years of age (Ghezzi *et al.*, 2011). Despite mitochondrial dysfunction presenting as a severe lack of Complex III in patients, muscle biopsies were morphologically normal, indicating that the disease caused by *TTC19* mutations was particularly affecting the brain.

The hypothesis that *TTC19* is a Complex III assembly factor is further supported by the fact that this progressive encephalopathy was couple with severe Complex III deficiencies and an accumulation of Complex III assembly intermediates, indicating that Complex III cannot be properly formed in these individuals (Ghezzi *et al.*, 2011). Recently, mutations in *TTC19* have even been found in a family with progressive psychosis, including severe mood disorders, violent behaviour and hallucinations (Nogueira *et al.*, 2013), further indicating that *TTC19* mutations primarily affect brain function in humans.

1.3.3: *dTTC19* in *Drosophila*

In *Drosophila*, the *dTTC19* gene (CG15173) is located on chromosome 2L and encodes for a protein which is 369 amino acids in length (flybase.org). This protein also co-localizes with mitochondria (Ghezzi *et al.*, 2011), so it was attempted to see whether or not it was possible to create a *dTTC19* knock-out model for mitochondrial disease in flies.

A fly line harbouring a *PiggyBac* element within the open reading frame of the first exon of *dTTC19* is available from Bloomington Stock Centre at Indiana University (Fig. 1.3.3).

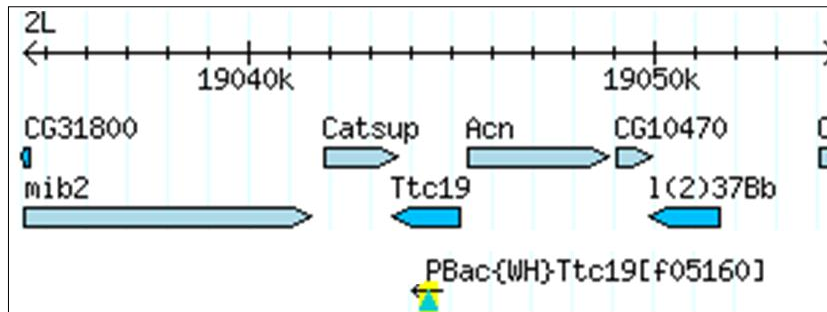


Fig 1.3.3: Map of *dTTC19* and the location of the *PiggyBac* element. Source: flybase.org

These flies, in which *dTTC19* transcription was abolished by the presence of the transposon, were characterized. While no overt larval mutant phenotype was reported, adult *dTTC19* mutant flies did present with impaired locomotor activity, bang sensitivity and reduced fertility in females (Ghezzi *et al.*, 2011). These adults also had severely reduced Complex III activity, while activity of this complex was not impaired in larvae (Ghezzi *et al.*, 2011). This is particularly interesting with respect to the human patients with *TTC19* mutations, as mitochondrial disease in these individuals also presented later in life, with onset from late infancy in two siblings to age 42 in another patient (Ghezzi *et al.*, 2011).

In this project, the *dTTC19* mutant was characterized further, and an attempt was made to rescue this mutant phenotype in *Drosophila*.

C **HAPTER II:** **MATERIALS AND METHODS**

2.1: Generating “Rescue” Lines for the *dTTC19* Mutant

Previous work has been done in this lab to characterize a fly line harboring a p-element in the coding region of the *dTTC19* gene, thereby rendering that gene unexpressed. During this project, flies expressing *dTTC19* under UAS control were generated in order to confirm that the effects seen in the mutant were in effect caused by the lack of the gene itself, and not a side effect of the presence of the p-element.

2.1.1: Cloning the *dTTC19* Gene

RNA was extracted and retrotranscribed from *white*¹¹¹⁸ larvae as described in Chapter I Section 2.3.1. Primers were designed by adding an HA tag to the 3' end of the gene, and including restriction sites for enzymes which were found to not cleave the gene. The coding region of the gene was cloned using the primers listed in Table 2.1.1 using the same method described in Chapter I Section 2.3.2.

Name	Sequence	Description
dTTC F	5'-GCGCGGCCGCATCTTAGTGAGAAATATTTGCAAGT-3'	Forward Primer Red: NotI Restriction Site
dTTC R	5'-GGCTCGAGTTAAGCGTAATCTGGAACATCGTATGGGTA CTGGCGCTTCTCTCCATTTCAGG-3'	Long Reverse Primer Red: XhoI Restriction Site Blue: HA Tag
HA R	5'-GGCTCGAGTTAAGCGTAATCTGGAACATCG-3'	Short Reverse Primer Red: XhoI Restriction Site Blue: HA Tag

Table 2.4.1: Primers used to clone *dTTC19* gene

2.1.2: Cloning *dTTC19* into pUAST Vector

In order to have the expression of our construct under the control of the UAS-GAL4 system, the gene was cloned into a pUAST vector containing the Upstream Activating Sequence (UAS) as a promoter.

In order to ensure maximum cloning efficiency, the construct was first cloned into a pGEM vector and screened as described in Chapter I Section 2.3.3. Once the sequence was verified, the pGEM vector and the empty pUAST vector were digested as described in Table 2.1.2.

Reagent	pUAST Digestion	pGEM Digestion	Source
Buffer D 10X	1X	1X	Promega
BSA 10mg/μl	0.1mg/μl	0.1mg/μl	NEB
NotI 10U/μl	0.5U/μl	0.5U/μl	NEB
XhoI 10U/μl	0.5U/μl	0.5U/μl	Promega
pUAST 2μg/μl	1μg	-	-
pGEM(dTTC19) 305ng/μl	-	1μg	-
DNase Free H ₂ O	Tot vol: 80μl	Tot vol: 80μl	Life Technologies

Table 2.1.2: Digestion Mix used to clone *dTTC19* into pUAST vector

Digestions were run on a 0.8% UltraPure™ Agarose gel and DNA was purified as described in Section 2.3.4.

2.1.3: Screening for Positive pUAST Colonies

Colonies which grew on LB Agar plates with Ampicillin were then screened by PCR in order to verify the presence of the construct as described in Chapter I Section 2.3.3 with the primers listed in Table 2.1.3. Colonies resulting positive for the construct were sent to BMR Genomics for sequencing using the same primers used for screening.

Name	Sequence
pUAST F	5'- AGTACTGTCCTCCGAGCG -3'
pUAST R	5'- GATGAGTTTGGACAAACCAC -3'

Table 2.1.3: Primers used for screening PCR and sequencing

One colony was stocked at -80°C in 20% glycerol and the pUAST vector was purified with a PureLink™ HiPure Plasmid Midi Prep Kit as per the manufacturer's instructions (Invitrogen). 10μg of DNA were sent to BestGene Inc. for microinjection.

2.1.4: Creating Rescue Lines in a *dTTC19* K.O. Background

Once the flies were microinjected with our construct, balanced and sent back to us, they needed to be crossed with our *dTTC19* mutants in order to get the construct in a K.O. background. A driver in a *dTTC19* K.O. background was also generated.

Three fly lines with the construct on chromosome III were chosen and the following crosses illustrated in Figure 2.1.4 were done. For simplicity $w^{1118};dTTC19\Delta / dTTC19\Delta;UAS-$

$dTTC19/TM6b, Tb$ flies and $w^{1118}; dTTC19\Delta/dTTC19\Delta; Act5c-GAL4/TM6b, Tb$ are referred to as $dTTC19\Delta^{dTTC19}$ and $dTTC19\Delta^{Act5c-GAL4}$, respectively.

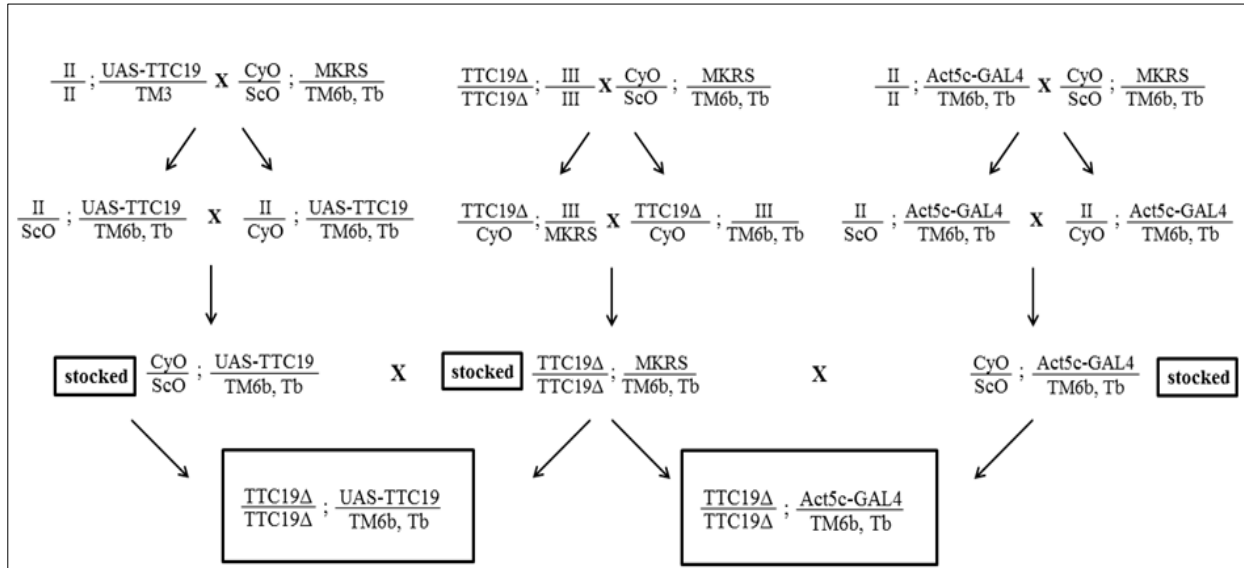


Figure 2.1.4: Crosses done to generate the Act5c-GAL4 driver and UAS-dTTC19 construct in a TTC19 K.O. background.

Flies were screened for the presence of the p-element causing the $dTTC19$ mutation and the presence of the construct were confirmed by PCR with the primers listed in Table 2.1.4 to verify that the procedure was done correctly.

Name	Sequence	Description
TTC19 F	5'- GCAAGTTTACGCAAGTTATGG -3'	Primer designed on TTC19 gene
WH 5'	5'- TCCAAGCGGCGACTGAGATG -3'	Primer designed on p-element in TTC19 gene
UAS F	5'- AGTACTGTCTCCGAGCG -3'	Primer designed on UAS promoter
TTC19 R	5'- CGGCGATTTTCTCCAGTAGC -3'	Primer designed on TTC19 gene

Table 2.1.4: Primers used to screen $dTTC19\Delta^{dTTC19}$ and $dTTC19\Delta^{Act5c-GAL4}$ lines.

2.2: Locomotor Activity of $dTTC19$ Mutant Larvae and Adults

Locomotor activity of adult *Drosophila* is usually measured by Trikinetics, whereby adults are placed in small glass vials containing a small food source and the number of times they pass through a laser intersecting the middle of the vial is recorded on a computer. This kind of experiment is commonly used to determine circadian rhythms, and it was previously shown in

this lab that *TTC19* mutant flies have lower levels of locomotor activity by using this method (Ghezzi *et. al.*, 2011).

Here, we perfected another method for measuring locomotor activity with the use of AnyMaze™ software, which allows us to obtain a more in depth analysis of the locomotor behavior of the flies.

Circular Plexiglas arenas measuring 10cm in diameter were built for this purpose, each containing 4 circular chambers measuring 3cm in diameter and 4mm in height. 3 day-old flies were collected under brief CO₂ anesthesia and placed in vials containing only a water source. Flies were thus starved for 16 hours (\pm 1hour) to induce exploratory behavior. Flies were then placed singly in each chamber, placed in a light box illuminated underneath by a single LED light source and filmed from above for 10 minutes. Their movements were tracked and their speed, distance travelled, time spent mobile/immobile and turning angle were calculated by AnyMaze™ software.

2.3: Visual Capacity of *dTTC19* Mutant Flies

In order to test for visual acuity, flies were anaesthetized with brief CO₂ exposure, placed in same sex groups of 20-25 in a tube with a water source and wrapped in aluminum foil. These flies were thus deprived of food and light for 16 hours to induce both exploratory and light-seeking behaviour, after which they were placed in a starting chamber under red light. This starting chamber was attached to a light maze, which consisted of a Plexiglas maze with a 4mm-wide series of binary paths, ending in 9 exit points capped with collection tubes. This maze was placed in a light box and illuminated in the top left-hand corner with an LED light source. After 1 hour the flies were collected and scored: 9 points for exiting into the tube closest to the light source, 8 for exiting in the second closest tube to the light source (etc.), and 0 for not completing the maze. The scores were summed and normalized to the total possible score for each line (9 x total no. flies). Mazes were washed with 50% dish soap and water after each use.

2.4: Sensory Capabilities of *dTTC19A* Larvae

In order to test for a possible, previously undetected larval mutant phenotype, mutant larvae were tested for their sensory capabilities as described in Chapter I, Section 2.2.4. Briefly, groups of 50

larvae were placed in the center of an agarose plate subdivided into quarters, each containing either two salty sections, two salty and two sweet sections, or two well illuminated and two dark sections. Larvae were thus placed in a light box and filmed for 10 minutes, after which the number of larvae in each quadrant was counted to see whether or not they could distinguish between visual or gustatory cues. A chi-square test was then performed comparing these data to those collected from groups of 50 larvae which had crawled over an agarose plate similarly divided into quadrants, but whose quadrants did not contain any visual or gustatory cues.

CHAPTER II: **RESULTS**

3.1: Characterization of *dTTC19* Larvae

Previous studies in flies with the *dTTC19* mutation found that the aberrant mitochondrial phenotype caused by the mutation only presented after eclosion (Ghezzi *et. al.*, 2011). These adults had a severe Complex III deficiency, while third instar larvae had normal levels of Complex III activity (Ghezzi *et. al.*, 2011). In order to confirm that *dTTC19* K.O. larvae do not present with any overt mutant phenotype, mutant larval behaviour was characterized in more depth.

3.1.1: Larval Locomotor Activity

The locomotor activity of *dTTC19* mutant larvae was tested by tracking the movements of wandering third instar larvae on an agarose plate over a two minute time period (Fig 3.1.1). Mutant flies were also outcrossed with their *white*¹¹¹⁸ genetic background to obtain larvae heterozygous for the mutation, in order to see whether or not flies with a single copy of the *dTTC19* gene also exhibit a mutant phenotype.

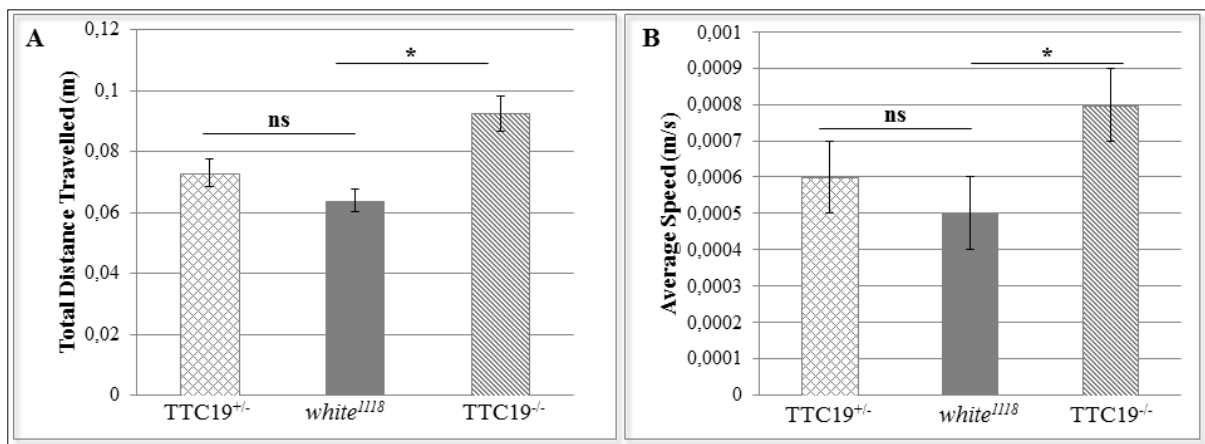


Fig 3.1.1: Locomotor Activity of larvae heterozygous for the *dTTC19* mutation (lattice), homozygous for the *dTTC19* mutation (diagonal lines) and *white*¹¹¹⁸ (matt), as measured by (A) total distance travelled and (B) overall average speed over a 2 minute period. Statistical analysis: one-way ANOVA with Sidak correction; n=50; *p<0.05; error bars= S. E.; ns= not significant.

No locomotor deficiencies were observed in larvae either heterozygous or homozygous for the *dTTC19* mutation, consistent with previous reports that this mutation does not produce an aberrant phenotype in larval stages. In fact, *dTTC19* mutant larvae even moved for longer distances (Fig. 3.1.1 A) and faster (Fig. 3.1.1 B) than *white*¹¹¹⁸ controls. This, combined with normal Complex III activity which was previously reported in larvae (Ghezzi *et. al.*, 2011), led

to the conclusion that these mutants do not present with an altered mitochondrial phenotype at the larval stage.

3.1.2: Larval Behaviour

In humans, mutations in the *TTC19* gene cause diseases which affect primarily the brain (Ghezzi *et. al.*, 2011; Nogueira *et. al.*, 2013). For this reason larvae were analysed for sensory abnormalities by testing for their ability to distinguish between different sensory cues.

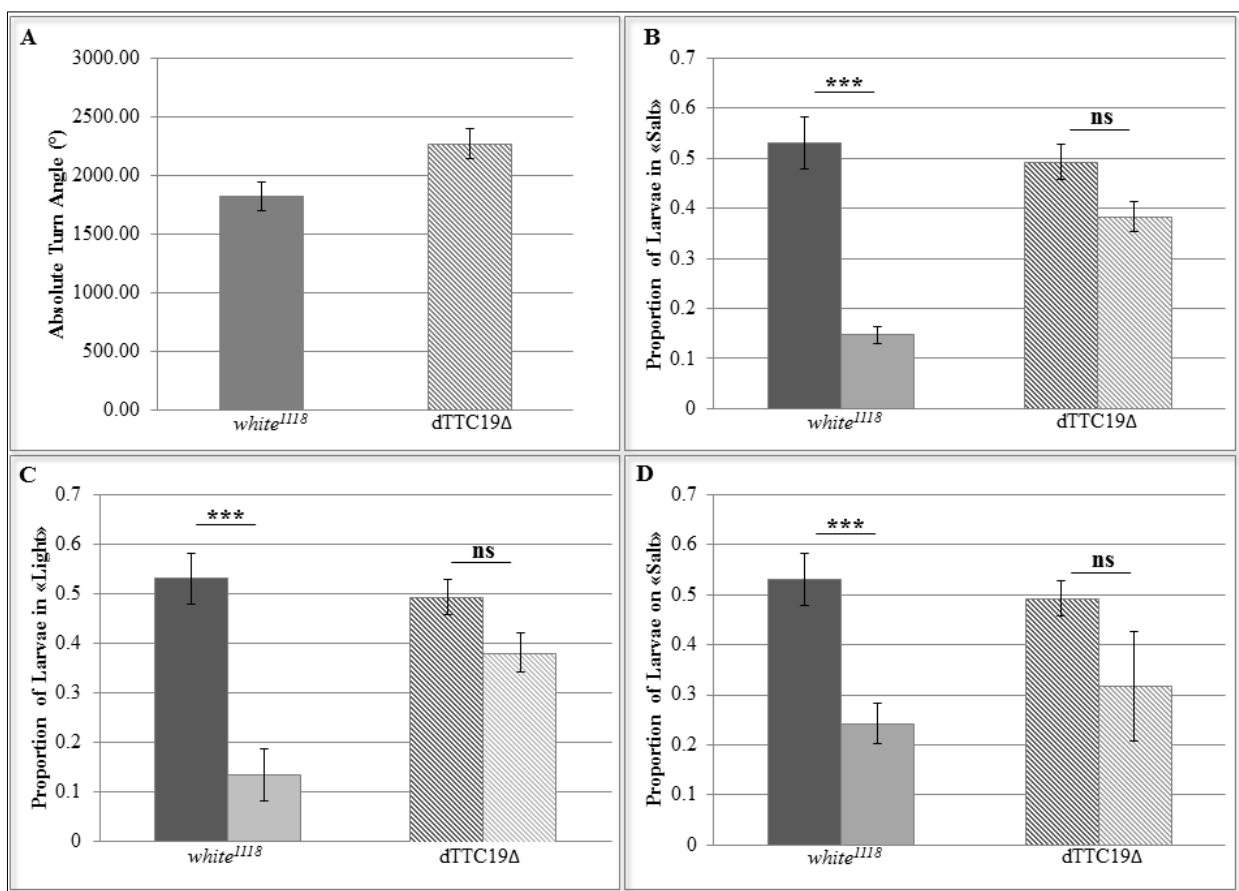


Fig. 3.1.2: (A) Exploratory tendency of *white*¹¹¹⁸ and *dTTC19* mutant larvae over a 2 minute period as measured by their absolute turn angle (n=50). (B-D) Ability of *white*¹¹¹⁸ and *dTTC19* K.O. larvae to distinguish visual (B) and gustatory cues, when presented with an arena containing quadrants either fortified with 0.5M NaCl (C) or with alternating quadrants fortified with 0.5M NaCl and 1M sucrose (D). Statistical analysis: chi-square; n=3; ***p<0.001; error bars= S.E; ns= not significant.

When tested for locomotor activity, larvae were also measured for their turning angle, which is considered an indirect measure of exploratory tendency (Fig 3.1.2 A). The tendency of third instar larvae to turn over a 2 minute period was measured by AnyMazeTM software. *dTTC19*

mutant larvae did not have lower absolute turn angle values compared to *white*¹¹¹⁸ controls (Fig 3.1.2 A), meaning they explored their arenas as much as controls did. Despite this, sensory abnormalities in mutant larvae were discovered upon further investigation.

To test visual acuity, groups of 50 larvae were placed in the centre of an arena divided into four quadrants, two illuminated from beneath and two not, in order to see whether or not the larvae were able to seek out the dark quadrants and avoid the illuminated ones over the course of 5 minutes. To test for gustatory abnormalities, groups of 50 larvae were placed in a similar arena, with two quadrants fortified with 0.5M NaCl and two either with plain agarose or fortified with 1M sucrose. The number of larvae found in either the neutral or the sweet quadrants were recorded after 5 minutes of exploration. The proportions of larvae found in either the illuminated or the salty quadrants were compared with negative controls, performed with larvae allowed to explore a similarly divided agarose arena, but one which did not contain any additional cues in its quadrants.

Dark grey bars in Fig. 3.1.2 B-D represent the proportion of larvae found in two out of four quadrants of an arena which contained only neutral agarose. These negative controls served to both demonstrate that the larvae did not prefer certain parts of the arena for reasons other than those later added in the form visual and gustatory cues, and as an “expected” value for the chi-square test. Light grey bars indicate the proportion of larvae found on either the two illuminated quadrants (Fig. 3.1.2 B), or the two quadrants fortified with 0.5M NaCl (Fig 3.1.2 C-D).

Exploratory tendency in larvae is often measured by absolute turn angle, which can be used as an indirect measure of sensory capabilities. Despite the fact that mutant larvae did not explore their arenas less than *white*¹¹¹⁸ larvae (Fig 3.1.2 A), *dTTC19* mutant larvae presented with both visual (Fig 3.1.2 B) and gustatory (Fig 3.1.2 C-D) abnormalities, as evident by their lack of ability to avoid quadrants with negative cues. In all three cases, the proportion of larvae found in quadrants containing negative cues did not differ significantly from negative controls (Fig 3.1.2 B-D). This is the first indication that this mutation does in fact produce abnormalities in larvae as well as in adults.

3.2 Characterization of *dTTC19* Mutant Adults

3.2.1: In Depth Analysis of Locomotor Activity

Adults harbouring the *dTTC19* mutation were previously tested for locomotor defects with a standard TriKinetics protocol (Ghezzi *et al.*, 2011). While this protocol is ideal for observing the circadian rhythms in flies, as it is possible to track their movements over several days, it lacks the ability to tease out the details as to what aspects of locomotor activity is affected in flies.

In order to investigate these locomotor defects more thoroughly, starved adults were placed in circular PlexiGlas arenas and their movements were tracked over a 10 minute period with AnyMaze™ software. This software was then able to calculate the total distance travelled (Fig 3.2.1.1 A), overall average speed (Fig 3.2.1.1 B) and the total time the flies spent mobile (Fig 3.2.1.1 C) and immobile (Fig 3.2.1.1 D).

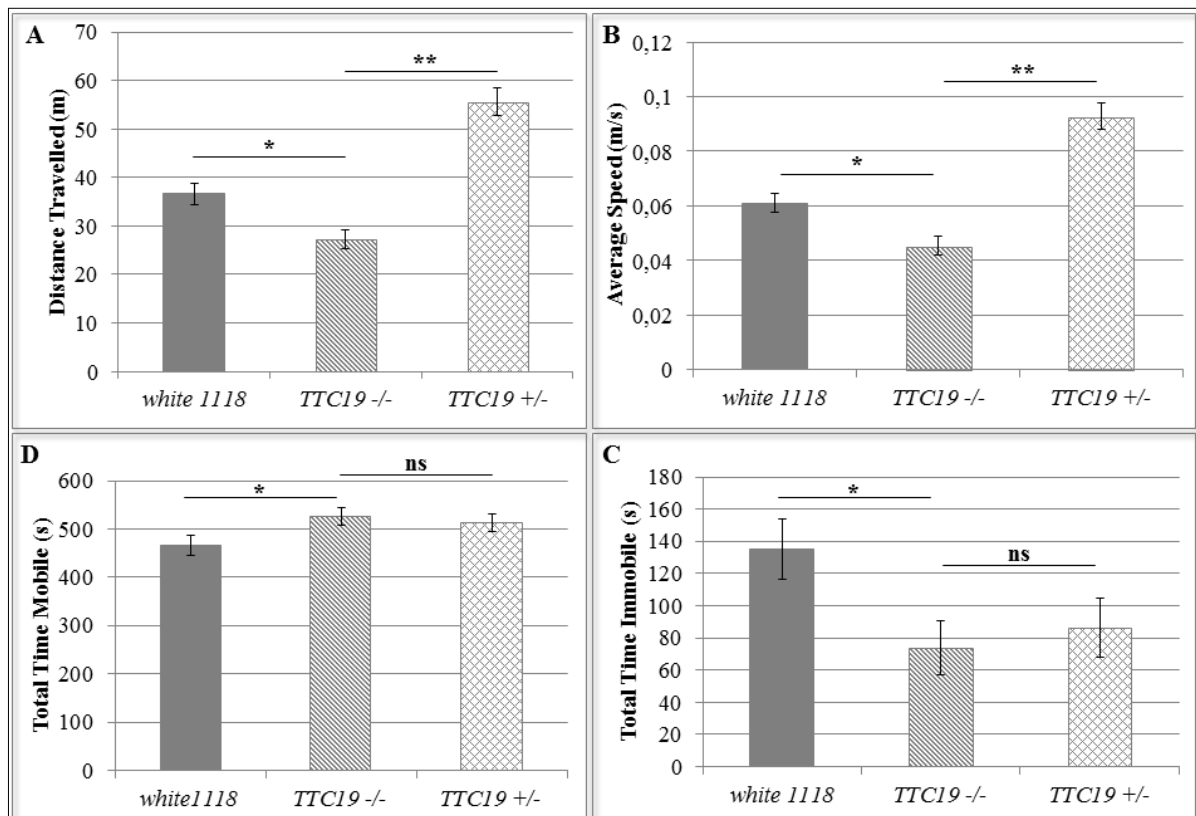


Fig. 3.2.1.1: Locomotor activity of adult males over a 10 minute period, as measured by (A) total distance travelled (B) overall average speed, (C) total time mobile and (D) total time immobile. Statistical analysis: one-way ANOVA with Sidak correction; n=50; *p<0.05; **p<0.01; error bars= S.E.; ns= not significant.

Adults homozygous for the *dTTC19* mutation moved significantly less compared to both *white*¹¹¹⁸ and heterozygous controls, both in terms of total distance travelled (Fig 3.2.1.1 A) and their overall average speed (Fig 3.2.1.1 B). However, mutant flies do not spend less time moving than controls; in fact they spend slightly more time moving than *white*¹¹¹⁸ flies, although they did not significantly differ from heterozygous flies (Fig 3.2.1.1 C-D). This leads to the conclusion that the locomotor deficits seen in mutant flies are not due to a lack of a drive to explore the arena, which is often seen in flies with severe visual deficits (Fig. 3.2.1.2).

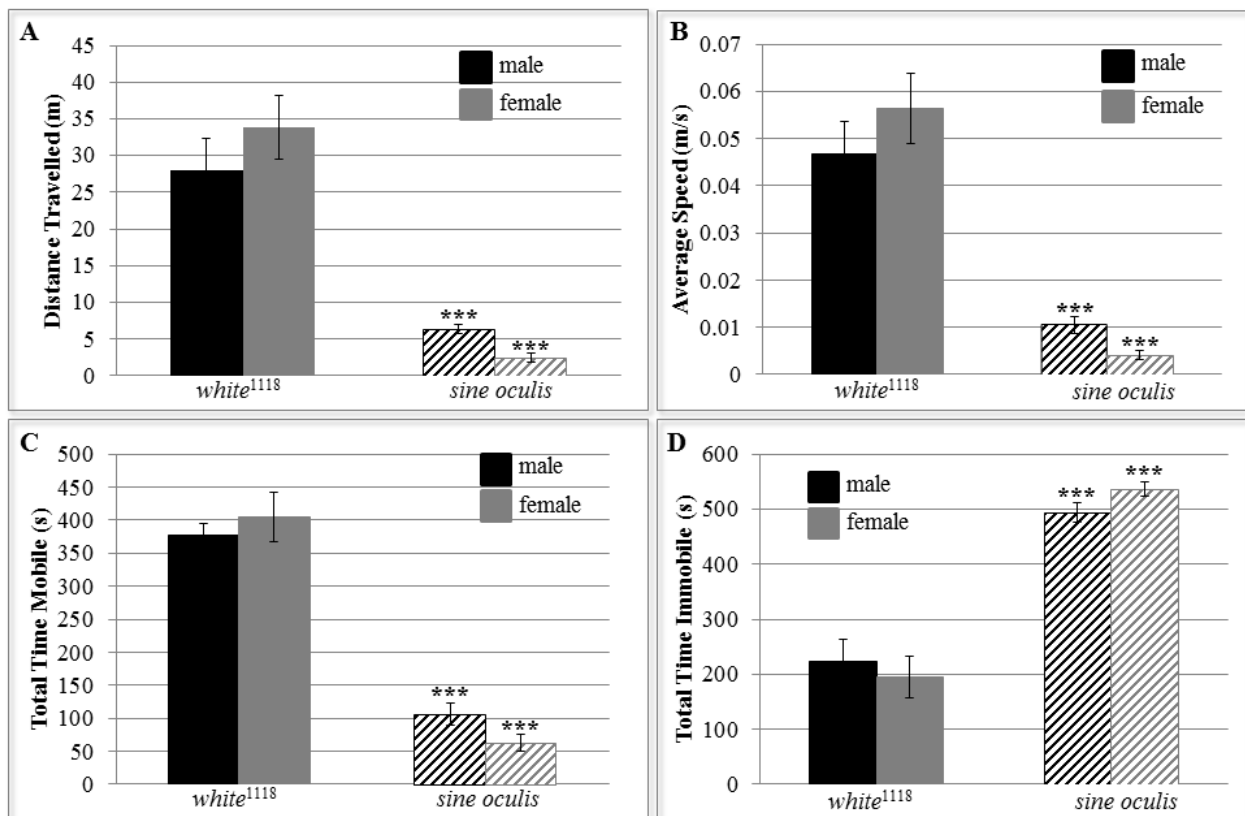


Fig. 3.2.1.2: Locomotor activity of *white*¹¹¹⁸ (matt) and eyeless *sine oculis* (stripes) flies, as measured by their (A) Total distance travelled, (B) Overall average speed and total time spent (C) mobile and (D) immobile over a 10 minute period. Statistical analysis: one-way ANOVA with Sidak correction; ***p < 0.001; n = 20; error bars = S. E.

When *sine oculis* flies, which harbour a mutation which causes them to be born eyeless, are measured for locomotor activity in the same way, we see that they too move significantly shorter distances (Fig. 3.2.1.2 A) at a significantly slower average speed (Fig. 3.2.1.2 B) compared to controls, despite the fact that their mutation does not cause a mitochondrial defect. However, this method for the measurement of locomotor activity brings to light that *sine oculis* flies move for far shorter periods of time with respect to controls (Fig. 3.2.1.2 C-D), indicating that the

locomotor deficit measured is most likely due to a lack of drive to explore the arena, rather than an inability to move as quickly as controls. The fact that *dTTC19* mutant flies are not able to cover the same distance as controls over the same time is stronger evidence that these mutants have energy deficits as a manifestation of their severe Complex III deficiencies, rather than as a result of visual deficits or a general lack of will to explore their arena.

3.2.2: Visual Acuity in *dTTC19* Mutant Adults

Since *dTTC19* mutant larvae showed signs of visual defects, and since the *dTTC19* mutant phenotype was far more severe in adults than in larvae, *dTTC19* Δ adults were tested for visual acuity (Fig. 3.2.2). Same-sex groups of 20-25 adult mutant flies were placed in a PlexiGlas light maze, in a light box illuminated in the top left-hand corner. Food and light starved flies were allowed to explore the maze for one hour, after which flies were scored based on how close to the light source they exited the maze.

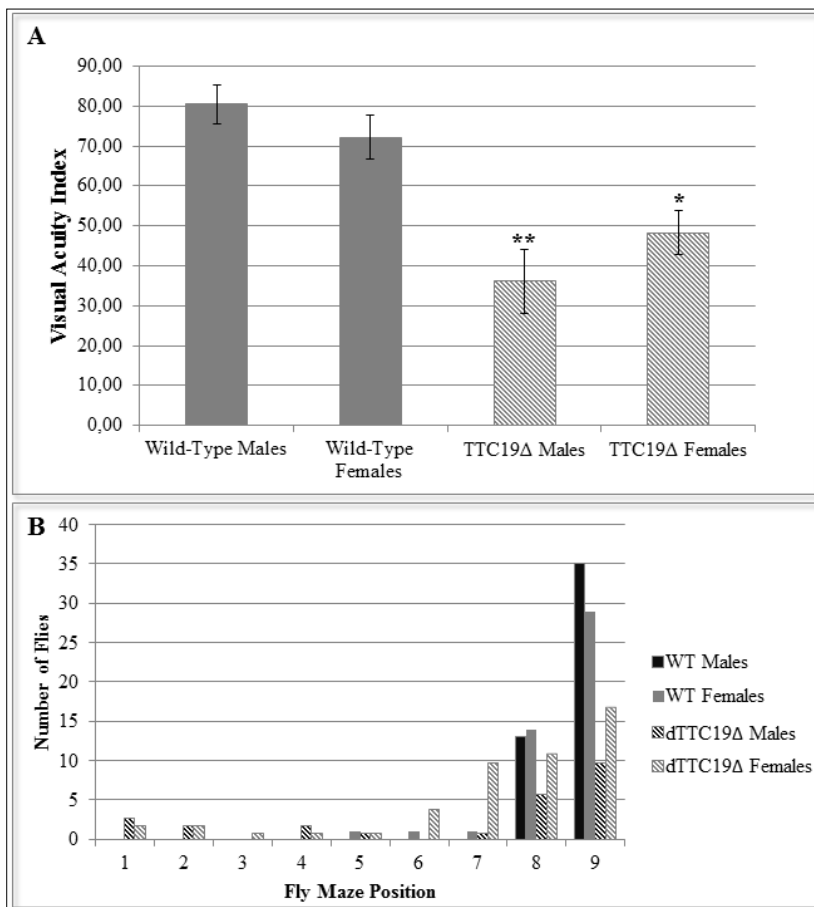


Fig 3.2.2: Visual Acuity of *dTTC19* Δ flies compared with wild-type controls. (A) Bar chart of visual acuity index of wild-type (mat) and *dTTC19* Δ (diagonal lines) adults, as measured by total visual score of flies/total possible score \times 100. Statistical analysis: two-sample t-test; $n=3$; * $p<0.05$; ** $p<0.01$; error bars= S.E. (B) Histogram of number of flies which exited at each of the 9 maze exit points, with position 9 being the closest to the light source and 1 the farthest.

Visual acuity scores were determined based on the position of the light maze at which the flies exited over the course of one hour. Flies which exited the maze closest to the light source received a score of 9; the ones which exited at the second closest point received a score of 8 etc., while flies which did not complete the maze received 0. The scores for all the flies in each replica were summed, normalized to the total possible score for that replica (9xno. flies) and multiplied by 100 (Fig 3.2.2.1 A). Histograms of the distribution of the exit points of the flies were generated by summing the total number of flies in all three replicas which exited at each of the 9 points of the light maze (Fig 3.2.2.1 B).

Both male and female *dTTC19Δ* adults showed significant problems in visual acuity compared to wild-type controls (Fig 3.2.2.1 A). Fewer mutant flies completed the maze than wild-type controls and, of those who did, a larger proportion of them exited the maze farther from the light source (Fig 3.2.2.1 B). However, despite the fact that they were less adept at exiting the maze close to the light source, mutant flies still exited the maze with a non-normal distribution, indicating that they can still perceive light to a certain extent. This is particularly evident when their distribution is compared to that of other mutants with impaired visual acuity (Fig 3.2.2.2).

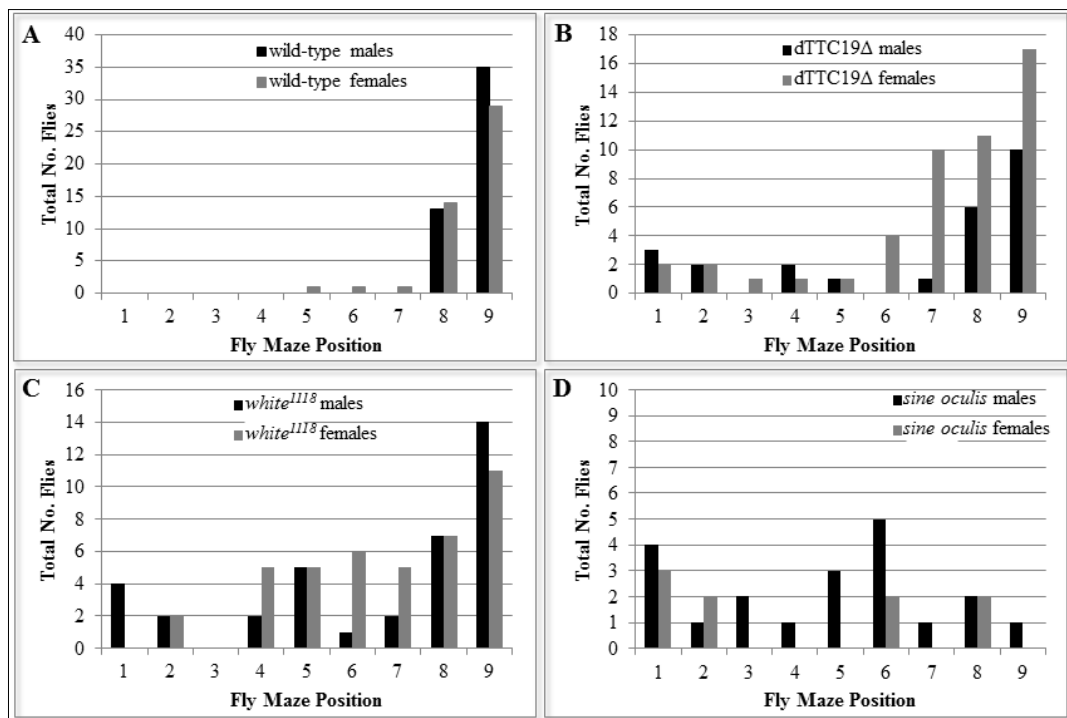


Fig 3.2.2.2: Histograms of distributions of total number of (A) wild-type, (B) *dTTC19Δ*, (C) *white¹¹¹⁸* and (D) *sine oculis* flies exiting the visual acuity maze (n=3) at all 9 exit points, with “9” being the exit closest to the light source.

*white*¹¹¹⁸ flies lack an ATP-binding cassette (ABC) transporter, which is responsible for transporting the eye pigment precursors to the eye, resulting in flies with white eyes (Mackenzie *et. al.*, 1999). Because of this, *white*¹¹¹⁸ flies have a reduced visual capacity compared to red-eyed wild-type controls. *sine oculis* mutants, on the other hand, harbour a mutation which causes apoptosis in the larval eye imaginal disc, resulting in flies without eyes. Because of this, *sine oculis* mutants lack the ability to see at all.

When we plot the total number of flies which completed the maze over an hour and the positions at which they exit, we can see if their distribution is normal, as one would expect if there was no external stimulus, or not. A comparison of the distribution of *dTTC19*Δ flies (Fig 3.2.2.2 B) to that of *white*¹¹¹⁸ (Fig 3.2.2.2 C) and *sine oculis* (Fig 3.2.2.2 D) flies, shows that it resembles the distribution of *white*¹¹¹⁸ flies, in that the distribution is skewed towards the light source. It is clear that, while fewer flies completed the maze in all mutant cases, a larger proportion of *white*¹¹¹⁸ and *dTTC19*Δ adult flies exited closer to the light source, rather than farther. The eyeless *sine oculis* flies, on the other hand, have a distribution closer resembling a normal distribution, as well as an even smaller number of flies which managed to complete the maze (Fig 3.2.2.2 D). From this we can conclude that *dTTC19* mutant flies have visual defects, though they are still able to perceive the light stimulus to a certain extent.

3.3: Generation of *dTTC19* Rescue Line

The *dTTC19* mutant line was generated by the insertion of a transposon in one of the gene's introns, thus blocking transcription. Therefore, in order to conclusively demonstrate that the mutant phenotype observed is due to a lack of the dTTC19 protein rather than an after-effect of the presence of the transposon, three *Drosophila* lines capable of expressing wild-type *dTTC19* in a *dTTC19* K.O. background were generated.

To do this, *dTTC19* was cloned into a pUAST vector and sent to Best Gene Inc. for microinjection into *Drosophila* embryos. Flies in whose genomes the constructs had successfully recombined were balanced and sent back to us. For the generation of these rescue lines, three lines which harboured the construct on chromosome III were selected and crossed so as to obtain them in a *dTTC19* K.O. background.

Unfortunately, due to a delay in microinjection, the fly lines did not arrive in time to be fully characterized. The expression of the construct must first be confirmed by qRT-PCR and western

blot analysis. If at least two of the three lines generated express the construct, they will undergo the same characterization that the mutant did.

C **HAPTER II:** **DISCUSSION**

4.1: Characterization of *dTTC19* Mutant Larvae

4.1.1: *dTTC19* Mutant Larvae have a Previously Unnoticed Mutant Phenotype

Previous studies in the *dTTC19* mutant did not report any larval mutant phenotype (Ghezzi *et al.*, 2011). This was likely due to the fact that prime focus was placed on Complex III deficiency-related phenotypes, and Complex III activity was found to be normal in the *dTTC19* mutant larvae (Ghezzi *et al.*, 2011). This study reports the first evidence of a mutant phenotype in *dTTC19* mutant larvae as well.

Mutant larvae were unable to distinguish between positive and negative visual and gustatory cues (Section 3.1.2). This indicates that mutant larvae, as well as adults, have sensory abnormalities, something which is not unusual in mitochondrial disease. Mitochondrial dysfunction has been identified as the causal factor in a number of optic neuropathies, such as Leber's Hereditary Optic Neuropathy (LHON), as mitochondrial function is often crucial for neuronal survival (Carelli *et al.*, 2004). It is therefore not surprising that sensorial abnormalities manifest in a mitochondrial mutant. Also, it is important to note that *TTC19* mutations in humans have been tied to diseases primarily affecting brain function, meaning that these results are in keeping with that.

The fact that an albeit light mutant phenotype is evident in *dTTC19* K. O. larvae leads to interesting speculation as to the reasons for the late onset of the more severe mutant phenotype seen in this model.

4.1.2: Possible Effect of Heteroplasmy in *dTTC19* Mutants?

Mitochondrial heteroplasmy is usually associated with defects in mitochondrial DNA, whereby the number of defective mtDNA copies reaches a certain threshold which precipitates a mutant phenotype. While *dTTC19* is not known to be involved in mitochondrial DNA integrity or replication it is involved in mitochondrial respiration, and thus it is not inconceivable that a similar effect may be happening in these mutants. It was hypothesized that, due to a lack of *dTTC19*, far less Complex III was being assembled and therefore fewer mitochondria were able to respire properly. As the life cycle continues mitochondria replicate and, proceeding on the assumption that a lack of Complex III activity does not affect a mitochondrion's fission abilities, more and more mitochondria lacking Complex III activity are produced. This, combined with the progression of the life cycle and the increased reliance on mitochondrial ATP production during

the energy-costly period of metamorphosis, finally precipitates the severe mutant phenotype seen in adulthood. This could also explain the discrepancies seen in Complex III activity between larvae and adults, as it was conducted on a large pool of individuals and therefore slight variances between individual mitochondria would have been masked. In order to evaluate the validity of this hypothesis, an attempt was made to investigate the function of individual mitochondria in larval body walls.

Unfortunately, attempts to characterize mitochondrial function proved to be unsuccessful. A characterization of mitochondrial membrane potential was attempted, first indirectly via MitoTracker[®] staining. Since MitoTracker[®] dyes take advantage of mitochondrial membrane potential in order to stain them, it was reasoned that differential staining between different mitochondria might indicate a differential in membrane potentials between individual organelles. While preliminary staining seemed to indicate that portions of muscle fibres were stained differentially from others, the method was deemed too unreliable. Larval muscle tissue is not the ideal medium for MitoTracker[®] staining, which occasionally presented poor penetrance of the tissue or high background staining. Also, since it is a dye which requires live tissue, this method was far too susceptible to error, as parts of the tissue could die or be compromised during the relatively lengthy dissection and staining process.

Because of these limitations, attempts were made to evaluate mitochondrial membrane potential more directly via TMRM staining. This methodology has been performed on larval body walls successfully and, similarly to MitoTracker[®] staining, it involves using a live fluorescent dye which uses membrane potential to stain mitochondria. However, TMRM is not a fixable dye, and therefore the larvae are first stained and then filmed under a confocal microscope over a period of time. FCCP, an uncoupler, is then added to the medium, whereby one can see the disappearance of the fluorescence due to a disappearance of mitochondrial membrane potential, thus confirming that all fluorescence previously recorded was not due to background staining of other organelles. The intensity of this fluorescence can then be measured over time. It was reasoned that this method could be adapted to see whether or not different muscle fibres, or even different portions of the same muscle fibre, showed differential levels of fluorescence.

Unfortunately this method too proved to be unsuccessful. The methodology was designed to be used at a higher magnification, and when it was attempted to repeat it at a lower one in order to be able to visualize entire muscle fibres in one field of vision, it was clear that it was impossible to keep the entire field of vision in focus, and therefore differences in fluorescence were not

distinguishable. This means that, to this date, our hypothesis of functional differences between mitochondria remains unconfirmed.

4.2: Characterization of *dTTC19* Mutant Adults

The behaviour of adult flies harbouring the *dTTC19* mutation was also further characterized in this study.

4.2.1: *dTTC19* Mutant Adults Exhibit Visual Defects Similar to *white*¹¹¹⁸ Flies

Flies lacking *dTTC19* expression were tested for visual acuity by placing same-sex groups of 20-25 in a light maze which was illuminated in one corner. Light-seeking exploratory behaviour was induced by previously starving the flies of light and food for 16 hours. Flies were allowed one hour to complete the maze, and flies exiting each of the 9 exit points were counted and scored accordingly: 9 for exiting closest to the light source, 8 for exiting the second closest point to the light source etc., and 0 for not completing the maze. The distribution of the number of flies exiting each point was also taken into account (Section 3.2.2).

Mutant flies showed significant visual defects compared to wild-type controls, both in terms of their overall visual acuity score and the number of flies which exited the maze far from the light source (Section 3.2.2). However, a larger proportion of mutant flies still exited the maze at positions 9 and 8, meaning their distribution was still skewed towards the light source. This indicates that, while they have some visual defects, they are still able to see to a certain extent. The distribution of the number of mutant flies exiting the maze is comparable to that of *white*¹¹¹⁸ flies, which lack the protein necessary to transport pigment precursors to the eye. In fact, the visual acuity score of *dTTC19* mutant flies does not differ significantly from that of *white*¹¹¹⁸ flies (two-sample t-test; $p=0.469$; $d.f.=2$), while it does differ significantly from *sine oculis* mutants which completely lack eyes (two-sample t-test; $p=0.0278$; $d.f.=2$). Unlike *white*¹¹¹⁸ mutants, however, *dTTC19* mutants do not lack eye pigment, indicating that the mutation itself causes visual defects.

A further investigation into the cause of these visual defects could be very interesting. A look into the levels of apoptosis in the retina, as well as staining of mitochondria in these cells could provide a clearer picture of why these visual deficits are present in these mutants.

Since vision is one of the senses which *Drosophila* require for exploratory behaviour, reduction in locomotor activity can sometimes be attributed to a decreased visual capacity. Because of this, the locomotor activity of *dTTC19* mutant flies was investigated more thoroughly.

4.2.2: *dTTC19* Mutant Adults have Defects in Locomotor Activity Independent of Exploratory Tendencies

In order to elucidate whether or not *dTTC19* mutant flies had locomotor deficits due to a lack of energy production rather than a decreased tendency to explore their arena, locomotor activity was measured over 10 minutes and tracked with AnyMazeTM software. These flies were previously starved for 16 hours in order to induce exploratory behaviour.

Flies homozygous for the *dTTC19* mutation travelled shorter distances and had a lower average speed than both *white*¹¹¹⁸ and heterozygous flies (Section 3.2.1). However, this was not due to a tendency to remain immobile for longer periods of time. Mutant flies actually spent longer periods of time moving compared to *white*¹¹¹⁸ flies, but were simply unable to cover as much distance as these controls. Since *dTTC19* mutant flies showed no lack of exploratory tendency, this is stronger evidence that their locomotor deficits are caused by a mitochondrial defect, rather than the visual acuity defect they presented with.

4.3: Future Prospects for *dTTC19* Rescue Lines

In order to confirm that the entirety of the mutant phenotype observed in the *dTTC19* mutant were due to a lack of *dTTC19* expression, rather than a side effect of the presence of the *PiggyBac* element, rescue lines were generated in order to express wild-type *dTTC19* in a knock-out background. Also, in order to validate the relevance of this model for human Complex III deficiencies caused by *TTC19* mutations, an attempt was made to generate rescue lines expressing human *TTC19* in a *Drosophila* mutant background.

4.3.1: Generation of *Drosophila* Rescue Lines

Three lines harbouring *dTTC19* under UAS control on chromosome III were crossed with *dTTC19* mutants in order to obtain the construct in a knock-out background. Unfortunately,

unforeseen delays during microinjection meant that these lines were not characterized in time for presentation here. Quantitative Real-Time PCR primers were designed for *dTTC19* and verified as described in Chapter I Section 2.4.6. The first step in the characterization of these lines involves the verification of the expression of the gene of interest. When the construct is microinjected into *Drosophila* embryos and it recombines into the genome it can recombine anywhere, meaning that sometimes it recombines in a place which inhibits its transcription. Because of this, expression has to be verified first by qRT-PCR, then by western blot analysis. Once expression is confirmed, the lines will be fully characterized to see whether or not the mutant phenotype is rescued when *dTTC19* is re-expressed in a knock-out background.

4.3.2: Generation of Human TTC19 Rescue Lines was Unsuccessful

Attempts were made to generate *Drosophila* knock-out lines expressing human *TTC19* in order to further validate this model as relevant for human mitochondrial diseases tied to Complex III. Unfortunately, numerous attempts to clone the human gene were unsuccessful. RNA extractions and subsequent retrotranscription were performed on samples from numerous human tissues, including heart tissue, muscle cells and blood, all of which have high levels of *TTC19* expression (information from TiGER Database). Extractions were also performed on HeLa cells, with the same negative result at the first step of the cloning process. Attempts were also made to use shorter primers lacking the FLAG tag when cloning, with the intention of subcloning the tag into the construct at a later time. The integrity of the cDNA was confirmed in all cases by PCR of a housekeeping gene. Future studies will include ordering a vector containing the CDS of human *TTC19* and creating the rescue lines from there.

CHAPTER III:
**A NEW PROTOCOL FOR
STUDYING SOCIAL
BEHAVIOUR IN DROSOPHILA**

A new protocol for using social behaviour in *Drosophila melanogaster* as a model for neurological disorders with antisocial behaviour

Drosophila melanogaster is already a well-established model for human neurodegenerative diseases, including Parkinson's (Feany and Bender, 2000), Alzheimer's (Crowther *et. al.*, 2005) and Huntington's disease (Lee *et. al.*, 2004). *Drosophila* has also been used as a model for many behavioural disorders, including alcoholism (Kaun *et. al.*, 2011) and drug use (McClung and Hirsh, 1998). In this study, we utilized the opensource software "Ctrax", developed by Caltech to track social behaviour in *Drosophila melanogaster*, both to confirm that *Drosophila* exhibit social behaviour and to propose that they can be used as a model for yet another subset of neurological disorders: those which present with antisocial behaviour.

Same-sex groups of 20 flies were placed in an arena, where they were restricted to a monolayer, and their behaviour was recorded over a one-hour period between ZT5 and ZT9. These films were then tracked with Ctrax software and the data were analysed with an R statistical package especially designed for this study, which used the flies' coordinates to measure locomotor activity, average speed, the proportion of time spent in certain areas of the arena and the proportion of time spent within five body-lengths of each other. Both *white*¹¹¹⁸ and *sine oculis* mutants were tested in order to verify whether or not visual acuity was necessary for social behaviour, and mutants either under- or over-expressing dopamine were tested to see whether or not dysregulation of this protein, tied to many neurological disorders, had an effect on sociality. Flies overexpressing a mutated form of SNAP-25, a protein critical in synaptic vesicle docking and thus neurotransmitter release, were also tested in this regard. Wild-type flies raised in isolation were also tested for social abnormalities, in order to see whether or not *Drosophila* social behaviour requires previous social contact, and to see if they could also be used as a model for socioemotional deprivation in humans.

This study demonstrates that social behaviour in *Drosophila* requires flies to be able to see each other, as is clear from the complete asociality observed in *sine oculis* mutants. It is also clear that both under- and over-expression of dopamine, both tied to behaviour disorders in humans, have a strong effect on social behaviour in *Drosophila*. While the overexpression of SNAP-25 did not cause social problems in flies, rearing individuals in isolation prior to testing did. This is strong evidence that subtle changes in brain chemistry can translate into a strong defect in sociality in *Drosophila melanogaster*, and is therefore proposed as a new model for the study of the genetic basis for human antisocial behaviour.

C **HAPTER III:** **INTRODUCTION**

1.1: Neurotransmission

1.1.1: Neurotransmission: An Overview

Across the animal kingdom, neurons are used to transmit information across relatively long distances, a process known as neurotransmission. A signal from the central nervous system is transmitted as an electrical impulse across neurons, terminating in the mobilization of synaptic vesicles and the release of neurotransmitters, resulting in a multitude of responses like muscle contractions, gland secretions and organ function (Purves *et. al.*, 2001).

Neurotransmitters are synthesized in the cell body and transported along the axon to the synapse, where they are packaged into synaptic vesicles. Upon receiving a signal, the vesicles fuse to the presynaptic membrane, releasing the neurotransmitter, where it can bind to postsynaptic receptors and elicit a response from the receiving cell. Neurotransmitter which does not fuse to the postsynaptic receptors diffuses out of the synapse, where it can be transported back into the neuron and either degraded or repackaged into synaptic vesicles for reuse (Fig 1.1.1).

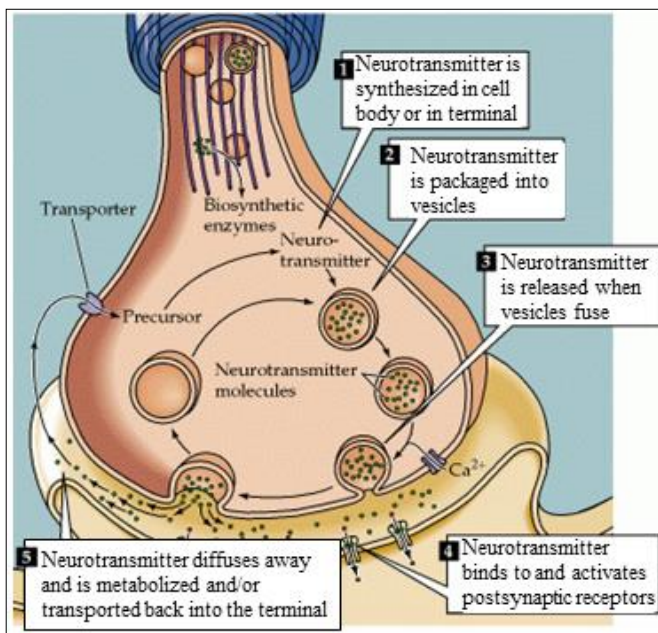


Fig 1.1.1: Diagram of neurotransmitter life cycle. (1) Neurotransmitter is synthesized in the cell body and transported to the synapse (2) neurotransmitter is packaged into vesicles which (3) fuse to the synaptic membrane to release neurotransmitter, which either (4) binds to the postsynaptic receptors or (5) diffuses away and is transported back into the neuron, where it is either enzymatically degraded or recycled for reuse. Source: Purves *et. al.*, 2001

There are many different kinds of neurons which use different neurotransmitters in order to carry these signals. In this project, special attention will be given to dopamine, a critical neurotransmitter whose dysregulation has been tied to a wide range of disorders. The synaptic protein SNAP-25, a critical component of the vesicle docking machinery required for the fusion

of the synaptic vesicles to the membrane and the release of neurotransmitters, was also investigated.

1.1.2: Dopamine

3,4-dihydroxyphenethylamine, or dopamine (DA) is a catecholamine neurotransmitter, crucial in the nervous systems of species ranging from *C. elegans* (Kindt *et. al.*, 2007), the bivalve mollusc *Spisula solida* and the starfish *Asteria rubens* (Cottrell, 1967), to *Drosophila* (Friggi-Grelin *et. al.*, 2003) and humans (Björklund and Dunnett, 2007). As this suggests, dopamine and the function of dopaminergic neurons are highly conserved across the animal kingdom (Riemensperger *et. al.*, 2005).

Dopamine is synthesized from the non-essential amino acid tyrosine (Fig 1.1.2.1). Tyrosine Hydroxylase (TH) catalyses the conversion of tyrosine to L-DOPA, which is then decarboxylated to produce dopamine. Dopamine can then be further hydroxylated to produce norepinephrine, the precursor for the important hormone adrenaline (Fig 1.1.2.1).

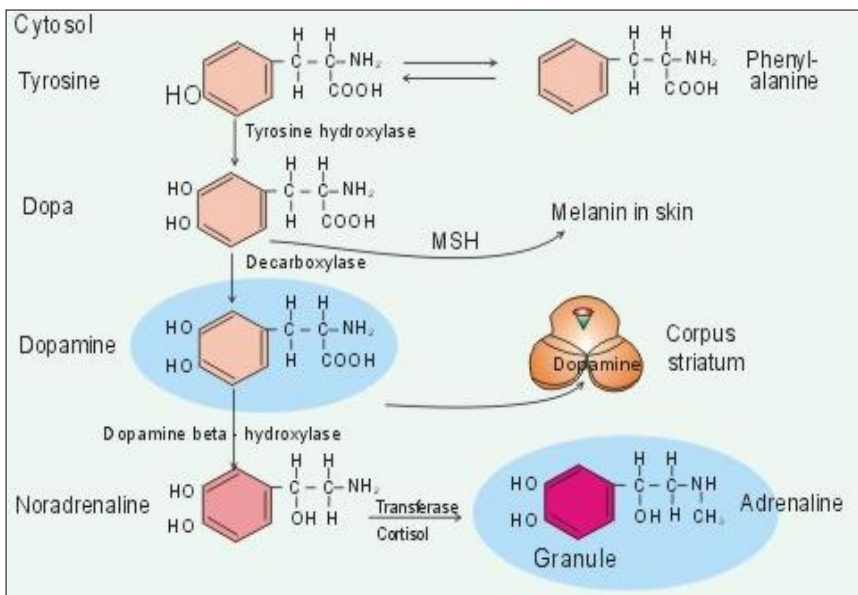


Fig 1.1.2.1: Synthesis of catecholamines, including dopamine, in humans (Zubieta-Calleja and Paulev, 2004)

In both *Drosophila* and mammals, dopamine is necessary for olfactory memory and conditioning, whereby a positive or negative value is assigned by the animal to an otherwise neutral stimulus (Riemensperger *et. al.*, 2005). Dopamine has also been found to influence

sexual behaviour and arousal, both in mammals (Hull *et. al.*, 2004) and in *Drosophila* (Kume *et. al.*, 2005). Some studies even associate the dopaminergic system and humour (Cannon and Bseikri, 2004). Most famously, however, dopamine is involved in the neurobiology of reward, which also makes it integrally involved in addiction (Cannon and Bseikri, 2004).

In *Drosophila*, dopamine is also required for cuticle pigmentation (Wright, 1984). Dopamine produced in the cuticle during development is then processed by phenol oxidases to form melanin (Fig 1.1.2.2) (Wittkopp *et. al.*, 2002).

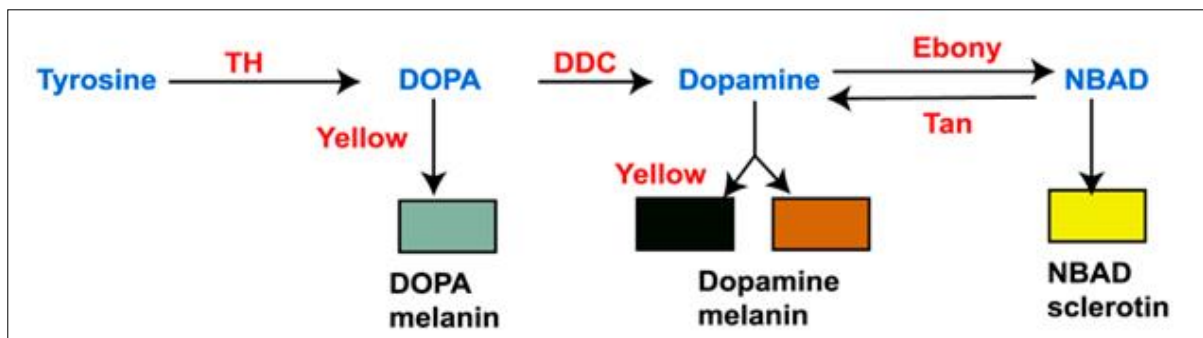


Fig 1.1.2.2: Cuticle pigmentation pathway in *Drosophila* (Gibert *et. al.*, 2007).

Like all neurotransmitters, dopamine is packaged into synaptic vesicles, small phospholipid membrane spheres which contain a relatively fixed amount of neurotransmitter. These vesicles need to be transported to the synapse and docked onto the presynaptic membrane for the neurotransmitter to be released into the synapse and elicit the response it needs to. One of the critical components of this docking machinery is SNAP-25.

1.1.3: SNAP-25

Synaptosomal-associated protein 25 (SNAP-25) was one of the first pre-synaptic target membrane-SNARE (t-SNARE) proteins to be discovered (Oyler *et. al.*, 1989), essential for presynaptic vesicle docking and membrane fusion (Fig 1.1.3) (reviewed in Rizo and Südhof, 2002). It is also highly conserved across many species due to its integral role in neurotransmission.

Since it does not contain a transmembrane domain, SNAP-25 is attached to the plasma membrane by palmitoylation of four cysteine residues located in the central region of the protein

(Chen and Scheller, 2001). Two coils of SNAP-25, one of syntaxin and one of VAMP intertwine to form a coiled-coil structure necessary for correct vesicle docking and exocytosis (Chen and Scheller, 2001).

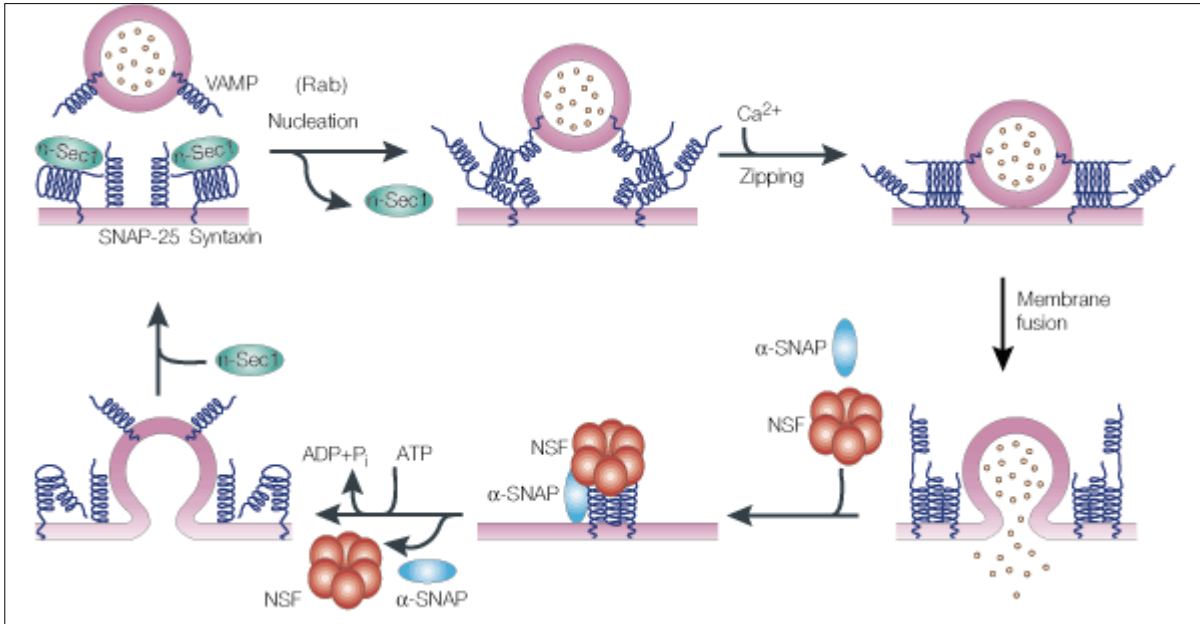


Fig 1.1.3: The SNARE complex and its role vesicle docking and membrane fusion (Chen and Scheller, 2001).

In humans there are two isoforms, SNAP-25a and SNAP25b, both involved in vesicle exocytosis but differing in their ability to stabilize vesicles in the primed state (Cai *et al.*, 2008), and in their expression pattern at different times of development (Puffer *et al.*, 2001).

1.2: Neurological Disorders Involving Sociality Problems

It is becoming increasingly evident that mental illnesses are in fact extremely prevalent. In 2010, it was estimated that 38.2% of the EU population suffers from at least one mental illness (Wittchen *et al.*, 2011). Unfortunately, despite this prevalence mental illness remains grossly under treated, with less than one third of affected people receiving treatment (Wittchen *et al.*, 2011). While part of the cause for this lack of treatment is undoubtedly attributed to social stigma surrounding mental illness (Mojtabai, 2010), part of it is due to the gaps that still exist in our current understanding of its multifactorial causes. This is why the genetic sources, environmental sources and brain pathways involved in mental illness are an extremely important field in medical research.

1.2.1: Dopamine and Disease

Abnormal functioning of the dopaminergic system has long been associated with many kinds of mood disorders, such as ADHD, depression and schizophrenia.

Attention-Deficit/Hyperactivity Disorder (ADHD) is a very common mood disorder in children, and many studies indicate a strong genetic basis for it (reviewed in Faraone *et. al.*, 2005). While the comorbidity of ADHD with other mental illnesses of approximately 65% complicates the identification of its causative genetic sources (Madras *et. al.*, 2005), genes involved in the dopaminergic system have been considered strong candidates for years (Swanson *et. al.*, 2000). The monoamine dopamine transporter DAT, which is responsible for sequestering dopamine into neurons, was found to be elevated by anywhere from 17% (Dresel *et. al.*, 2000) to 70% (Dougherty *et. al.*, 1999) in the brains of adult patients with ADHD, leading to an oversequestration of dopamine and thus a decrease in extracellular dopamine levels. Many anti-ADHD medications target this transporter in order to modulate brain dopamine levels (Madras *et. al.*, 2005).

Parkinson's Disease (PD) is the most common neurodegenerative movement disorder in the world, affecting approximately 1% of people over 60 (Samii *et. al.*, 2004) and precipitated by the loss of dopaminergic neurons projecting from the substantia nigra pars compacta (SNc) to the striatum (Venda *et. al.*, 2010). While the most famous presentations of PD are the motor symptoms such as rigidity and tremors, PD also exhibits many under-reported, under-treated non-motor symptoms including depression, apathy and sleep disorders (Chaudhuri and Schapira, 2009). These non-motor symptoms can precede motor-symptoms by over a decade, often leading to misdiagnosis and delayed treatment (Chaudhuri and Schapira, 2009). Evidence for an important contribution of dopamine dysfunction to the progression of non-motor symptoms of PD has also been reported by imaging of the hypothalamus (Politis *et. al.*, 2008) and the limbic system (Remy *et. al.*, 2005) in PD patients, particularly in cases of depression.

The "Dopamine Hypothesis", suggesting that hyperactivity of dopaminergic transmission is associated with schizophrenia, was proposed decades ago when research into dopaminergic mechanisms indicated they may have a causative role in the disease (Carlsson, 1988). In the '90s, *in vivo* imaging demonstrated that unmedicated schizophrenic patients had higher levels of extracellular dopamine than healthy controls (Laruelle *et. al.*, 1996; Breier *et. al.*, 1997). A more recent study also found a significant difference in dopamine storage capacity in the striatum and the amygdala of schizophrenia patients compared to healthy controls (Kumakura *et. al.*, 2007).

Also, imaging of brain regions innervated by dopaminergic neurons, such as the amygdala, indicate that these regions are highly relevant in the formation of delusions (Heinz and Schlagenhaut, 2010).

Taken together, there is overwhelming evidence that dopamine is a key factor in a variety of mood disorders in humans, making it an extremely attractive candidate for study in animal models.

1.2.2: SNAP-25 and Disease

Given its crucial role in vesicle formation, defects in SNAP-25 activity have also been associated with a variety of mental illnesses and neurodegenerative diseases.

Attention-Deficit/Hyperactivity Disorder, or ADHD, is a mood disorder affecting 3-5% of children in the USA (Dougherty *et al.*, 1999) and 5% of young people in the EU (Wittchen *et al.*, 2011) characterized by impulsivity, inattention and motor restlessness (Madras *et al.*, 2005). Adoption and twin studies have indicated a strong genetic basis for ADHD, accounting for up to 70% of the prevalence (Biederman and Faraone, 2002). Many genes are implicated in this undoubtedly multifactorial disease, one of which is SNAP-25.

The colomba mouse model is a mouse harbouring a deletion of a portion of chromosome 2q, including the gene encoding for the mouse SNAP-25 homolog. These mice present with spontaneous hyperactivity, motor ability delays, learning deficiencies and Ca²⁺-dependant dopamine release deficits (Wilson, 2000). Reintroduction of SNAP-25 into this mouse model leads to a reduction in hyperactivity (Faraone et al 2005). Genome-wide association studies, on the other hand, have led to conflicting results regarding the association between SNPs in the SNAP-25 gene and ADHD (reviewed in Faraone *et al.*, 2005).

Schizophrenia is a mental illness commonly characterized by visual and/or auditory hallucinations, delusions and paranoia, affecting 0.3-0.66% of the global population (van Os and Kapur, 2009), and causing those afflicted to die approximately 12-15 years prior to the average population (Saha *et al.*, 2007). While there are a variety of factors that have been associated with schizophrenia, including maternal and environmental (van Os and Kapur, 2009), there is a plethora of evidence to also suggest a strong genetic component, including the involvement of

SNAP-25. Altered levels of SNAP-25 have been reported in post-mortem brains of schizophrenic patients, both in the inferior temporal cortex, the prefrontal association cortex (Thompson *et. al.*, 1998) and in the hippocampus (Young *et. al.*, 1998). Three polymorphisms in SNAP-25 were also found to be significantly associated with antipsychotic-induced weight gain in schizophrenia patients (Musil *et. al.*, 2008). Taken together, these studies indicate that defects in SNAP-25 are linked to many neurological disorders in humans, also making its role in behavioural disorders another attractive point of investigation.

1.2.3: Neurological Disorders of Childhood Deprivation

There is compelling evidence to suggest that a lack of social contact during human postnatal development can lead to serious cognitive and social problems in later life. There is also evidence that these problems do not necessarily stem from an educational point of view, but that a lack of social contact in infancy can actually lead to a defect in brain development which can cause these social problems in adolescence and adulthood. One example of an important case study to this effect is one conducted in postinstitutionalized Romanian orphans after the Communist era.

During the 1980s, Romanian President Nicolai Ceausescu was responsible for implementing a series of social policies which resulted in tens of thousands of children being placed in orphanages, where their sheer numbers resulted in them receiving little to no adult social contact during childhood (Carlson and Earls, 1997). Children raised in these institutions reportedly had significant behavioural problems: one study conducted in children adopted by British Columbian families reported that these children scored significantly higher on the Child Behavioural Checklist compared to both Canadian-born children and children adopted from Romania before the age of 4 months (Fisher *et. al.*, 1997). These children exhibited internalizing behavioural problems, and the researchers were able to demonstrate a positive correlation between the severity of behavioural defects and length of institutionalization (Fisher *et. al.*, 1997). A positive correlation between institutionalization and salivary cortisol levels in Romanian orphans was also reported, although at the time researchers were unable to determine whether this was due to brain dysfunction caused by deprivation suffered during childhood (Gunnar *et. al.*, 2001). It was later demonstrated that Romanian postinstitutionalized children had significantly reduced glucose metabolism in regions of the brain associated with the limbic system (Chugani *et. al.*, 2001) and significantly less white matter in the left uncinate fasciculus (Eluvathingal *et. al.*,

2006), indicating the physiological effects socioemotional deprivation can have on brain development.

Studies in nonhuman primates have also shown that social deprivation during early development can result in behavioural problems in these animals (Suomi, 1997). Similar studies in rodents have also demonstrated the importance of postnatal handling for normal brain function later in life (Meaney *et. al.*, 1985). In this study, social deprivation will also be investigated in *Drosophila melanogaster*, in order to see whether or not rearing flies in isolation can alter their social behaviour.

1.3: Social Behaviour in *Drosophila*

To date, there have been very few studies published attempting to describe whether or not *Drosophila* exhibit sociality, and what factors can have an effect on this behaviour. In 2012, Simon and colleagues developed a protocol to investigate whether or not flies tend to aggregate, randomly distribute themselves or avoid each other when placed in an arena together, by measuring the distance between pairs of flies in a same-sex group of 40 individuals (Simon *et. al.*, 2012). Flies were placed in a vertical triangular arena and still images of their distribution were taken and analysed over a 1 hour period. Researchers tested wild-type flies and compared their distribution to *white*¹¹¹⁸ flies and *para*^{sbl} mutants, which lack pigmentation in the eye (therefore leading to some visual impairment) and have broad olfaction defects, respectively. While *white*¹¹¹⁸ mutants did show a decrease in their social space index *para*^{sbl} flies did not, leading the researchers to the conclusion that flies rely on visual rather than olfactory cues when forming social groups (Simon *et. al.*, 2012). However, this study relied on still images of groups of flies, thereby lacking a more continuous observational approach. Also, being vertical arenas, the natural tendency of flies to move towards negative geotaxis could have obscured more subtle differences in the tendency to socialize between different fly strains.

In 2009, The California Institute for Technology (Caltech) developed open-source software capable of processing video footage of flies in a planar arena and tracking their movements and orientation, called The Caltech Multiple Walking Fly Tracker, or Ctrax (Branson *et. al.*, 2009). Restricting flies to a monolayer was shown to greatly improve the efficiency of this kind of software in tracking the flies' movements and behaviour (Simon and Dickinson, 2010). These data can then be exported and analysed accordingly. While this software has been used

extensively to investigate the locomotor activity of multiple flies at the same time (White *et. al.*, 2010; Humphrey *et. al.*, 2012; Diaper *et. al.*, 2013), one 2012 study did utilize this software to investigate social behaviour in *Drosophila*. Instead of utilizing the flies' relative position to each other, however, this study used the number of frontal approaches, rear approaches and social preening events to define social interaction, and compared these data to randomly moving vectors (Schneider *et. al.*, 2012). This study reported very different results compared to the one previously described, with olfactory mutants having drastic social defects, while flies were still able to form normal social networks under dim red light (Schneider *et. al.*, 2012). Furthermore, this study reported significant differences in socialization between different wild-type lines, and that raising flies in isolation does not affect social behaviour, though they did not specify the method by which flies were raised in isolation (Schneider *et. al.*, 2012).

Given the fact that this behaviour still represents a relatively new field of study, the mechanisms of social behaviour in *Drosophila* still remain to be fully elucidated. This study attempts to do this using entirely open source software. Also, this is the first time the sociality of flies harbouring mutations in genes known to cause depression and/or mental illness in humans has been investigated.

1.3.1: SNAP-25 and *Drosophila*

The SNAP-25 protein has been highly conserved throughout evolution, the *Drosophila* one having 81% amino acid identity with the mouse protein (Risinger *et. al.*, 1993). In flies, SNAP-25 is also highly expressed in synaptic regions of the nervous system, including in the neuromuscular junction (Rao *et. al.*, 2001). While SNAP-25 null mutant larvae have almost normal neurotransmission, SNAP-25 null adults have blocked neurotransmission and die at the pharate adult stage (Vilinsky *et. al.*, 2001). Adult flies homozygous for a point mutation in SNAP-25 exhibited paralysis at 38°C, while larvae showed reduced neurotransmitter release at 37°C but greatly increased evoked release at 22°C (Rao *et. al.*, 2001). This mutant phenotype was rescued by the introduction of wild-type SNAP-25, consistent with the conclusion that these defects were caused by the point mutation in SNAP-25 (Rao *et. al.*, 2001).

1.3.1.1: The *Drosophila* SNAP-25 Mutant

Null mutants for SNAP-25 have almost normal neurotransmitter release at the larval stages, most likely due to a redundancy effect of SNAP-24, which normally is not involved in neurotransmission (Vilinsky *et. al.*, 2002). Because of this functional overlap, the overexpression of a mutated version of SNAP-25, which still becomes incorporated into the SNARE complex but due to its altered shape cannot function normally, could cause more severe defects than a null mutation can.

A *Drosophila* line harbouring a mutated version of SNAP-25 under UAS-GAL4 control was previously generated in the lab of Prof. Aram Megighian (Department of Anatomy and Physiology, University of Padua, Italy). This SNAP-25 was point mutated at position 206, a highly conserved residue, and thus this line is referred to as SNAP-25^{R206D}. These flies were crossed with an *elav*-GAL4 driver so as to direct the overexpression of mutated SNAP-25 in the nervous system.

Flies overexpressing this point-mutated form on SNAP-25 in the nervous system had a far more severe larval mutant phenotype compared to SNAP-25 K. O. mutants. SNAP-25^{R206D} larvae had abnormal electrophysiological recordings at the NMJ, which was shown to not be due to an increased calcium sensitivity (Megighian *et. al.*, 2013). In this study, the effect of the overexpression of this point mutation on *Drosophila* adult behaviour was investigated.

1.3.2: Dopamine Dysfunction and *Drosophila* Behaviour

Abnormal dopamine levels have also been shown to significantly affect *Drosophila* behaviour. Inhibition of tyrosine hydroxylase, the enzyme involved in the rate-limiting step of dopamine synthesis, by 3-iodo-tyrosine (3IY) resulted in a significant increase in sleep during the day (Andretic *et. al.*, 2005) and in a reduction in cocaine-induced behaviour (Bainton *et. al.*, 2000). Pharmacological inhibition of DTH also results in a decrease in locomotor activity (Pendleton *et. al.*, 2000) and a preference for temperatures that are colder than normal (Bang *et. al.*, 2011). Flies with mutations in *Ddc*, the gene encoding the enzyme dopa decarboxylase which catalyses the production of dopamine from L-DOPA, show defects in learning ability (Tempel *et. al.*, 1984).

Dopamine dysregulation can also significantly affect courtship behaviour. Female dopamine-depleted flies show increased resistance to copulation (Neckameyer *et. al.*, 1999).

Overexpression of tyrosine hydroxylase, on the other hand, resulting in an overproduction of dopamine, was reported to lead to a dramatic increase in male-male courtship (Liu *et. al.*, 2008). Given these clear indications that dopamine levels can influence *Drosophila* behaviour, and given dopamine's role in many mental illnesses in humans, it is an ideal candidate for a study in its role in social behaviour in *Drosophila*.

1.3.2.1: The *Pale*⁴ Mutant

In *Drosophila*, the *pale* locus encodes for the *Drosophila Tyrosine Hydroxylase* (DTH) gene, homozygous null mutations in which lead to embryonic lethality and an unpigmented cuticle (Neckameyer and White, 1993). Flies heterozygous for the *pale* mutation, on the other hand, are viable, and are reported to have normal locomotor activity (Pendleton *et. al.*, 2002) although they are reported to have reduced levels of tyrosine hydroxylase activity (Neckameyer and White, 1993). This mutant was thus selected for analysis, in order to see whether or not they exhibit defects in sociality due to their altered dopamine levels, despite the lack of an overt mutant phenotype. Since the mutation is homozygous lethal and the gene is present on the third chromosome, it was balanced with TM3 and generated in an *ebony*¹ mutant background (Source: Bloomington Stock Centre, Indiana University).

1.3.2.2: The *ebony*¹ Mutant

In *Drosophila*, the *ebony* gene encodes for the enzyme N-β-alanyl dopamine synthetase, which converts dopamine to NBAD in the cuticle, which is later converted to a tan pigment (Wittkopp *et. al.*, 2002). Due to its role in the conversion of dopamine to pigment, *ebony* mutants have much higher levels of dopamine than wild-type controls, even in decuticularized brains (Ramadan *et. al.*, 1993). *ebony* mutants have been reported to have abnormal circadian rhythms (Newby and Jackson, 1991), and an increase in male-male courtship (Liu *et. al.*, 2008). As the *pale*⁴ mutant is in an *ebony*¹ mutant background, and since mutations in the *ebony* gene can lead to significant behavioural defects, this mutant was also chosen for social behaviour analysis, both as a control for the *pale*⁴ mutant and to see if elevated dopamine levels in the brain could also have an effect on social behaviour in *Drosophila*.

C **HAPTER III:** **MATERIALS AND METHODS**

2.1: Maintaining Fly Stocks

All fly lines used in this Chapter were raised as described in the Materials and Methods of Chapter I, with the exception of WT-ALA wild-type flies.

WT-ALA wild-type flies were collected in 2004 from Bolzano, Naturno, Foresta and Postal in Alto Adige, Italy. Isofemale lines of *Drosophila melanogaster* were created from these flies and raised in standard fly vials on cornmeal-yeast-agar medium. Lines from all four areas were pooled together to create the wild-type line and raised in 250mL vials on 50mL cornmeal-yeast-agar medium. Every month, a part of this pool is added to other isofemale lines. The F1 is then mixed again with the previous wild-type pool to generate our WT-ALA wild-type line.

2.1.1: SNAP-25 Mutants

When SNAP-25 is knocked out completely in *Drosophila*, SNAP-24 can compensate for its absence, even though it is not normally involved in neurotransmission in wild-type larvae (Vilinsky *et. al.*, 2002). Because of this, a mutated form of SNAP-25, thus leading to the incorporation of a defective SNAP-25 protein into the SNARE complex, can often elicit a more severe phenotype than a clean knock-out mutant can.

A *Drosophila* line capable of expressing a mutated form of SNAP-25 under UAS-GAL4 control was previously generated in the lab of Prof. Aram Megighian from the Department of Human Anatomy and Physiology at the University of Padua, Italy (Megighian *et al.*, 2013). This mutated SNAP-25 construct harbors a point-mutation at position 206, producing an aspartic acid instead of an arginine. This SNAP-25^{R206D} line was crossed with an *elav-GAL4* driver in order to overexpress the mutated *SNAP-25* in the entire nervous system.

2.1.2: e¹;pale⁴/TM3 Mutant Line

In order to investigate the effects of the levels of dopamine in the brain, the e¹;pale⁴/TM3 mutant line was ordered from Bloomington Stock Center at Indiana University. In order to tease out the effects of the various mutations, these flies were crossed with wild-type flies to obtain heterozygous pale⁴/+ and TM3/+ flies. *ebony*¹ mutants were also ordered in order to investigate the effects of an overexpression of dopamine in the nervous system on social behavior.

2.2: Adult Locomotor Activity

Traditional methods of analyzing locomotor activity involve recording the number of times a fly crosses a laser point in a small tube over the course of several days. While this is an excellent method for investigating the time of day during which flies are most active, therefore being far more useful in the characterization of circadian mutants, it cannot provide the researcher with more detailed information such as speed, time spent exploring, turning angle etc. In order to investigate these various parameters, a protocol was developed taking advantage of AnyMaze™ software.

Circular Plexiglas arenas 10cm in diameter were built for this purpose, each containing four circular chambers measuring 2cm across and 4mm high. 3 day old flies were anaesthetized with CO₂ 16 hours prior to testing and placed in individual plastic cylindrical tubes measuring 1.5cm in diameter and 6cm in length, with only a water source. This starvation method induces exploratory behavior in flies, pushing them to move around as much as they are able. Variability in time spent in starvation was minimized to one hour in order to avoid problems in locomotor activity being due to problems caused by the lack of food itself. Flies were also always tested between ZT0 and ZT2 in order to eliminate variability due to circadian rhythms.

A single fly was placed in each chamber of the arena and placed on a raised pedestal in a light box. This box was illuminated from one LED light from beneath the pedestal and four strip LED lights placed around the four edges of the box, in order to not have any directionality of light thereby not influencing the direction the flies might move in. The flies were filmed from above with a Canon 2.0 megapixel camera and tracked with AnyMaze™ software over the course of 10 minutes. Arenas were washed with dish soap between uses, in order to minimize the effect of the smell of the previous fly influencing the behavior of the fly preceding it.

The AnyMaze™ software then calculates the fly's movements based on a number of parameters including speed, time spent mobile, time spent immobile, total distance travelled, absolute turn angle, number of mobile or immobile episodes etc. This permits a more detailed analysis of the fly's movements, as well as a statistical analysis of each parameter tested.

2.3: Testing Visual Acuity in *Drosophila*

Many behaviours in *Drosophila* depend on their ability to see each other. It is therefore important to test their visual capacity when conducting new behaviour experiments, in order to verify whether or not differences between genotypes could not be due to differences in visual acuity.

To test this, a triangular Plexiglas light maze was built. This maze possesses a single 3mm wide entry point. The maze consists of 4mm-wide binary paths, ending in a total of 9 exit points. These exit points are closed off with 1.5ml Eppendorf tubes to collect the flies that reach the end of the maze. This is then placed in a light box which can be illuminated in the top left hand corner with an LED light.

3-4 day old flies were anaesthetized with CO₂ and placed in same-sex groups of 10 in plastic cylindrical tubes measuring 1.5cm in diameter and 6cm in length with only a source of water. These tubes were then wrapped in aluminum foil and flies were thus kept for 16 hours. This starvation method was done to induce both exploratory and light seeking behavior, pushing the flies to move through the maze towards the light source.

The flies were then brought to a dark room where 20 individuals were placed in a starting chamber by gentle aspiration. The starting chamber was then attached to the maze, the light box was closed and the LED light source was turned on, after which the flies were allowed to proceed through the maze for one hour. The maze was washed with dish soap between tests, in order to not have the path decisions of the flies influenced by the smell of the fly that travelled through the maze before them.

After testing was completed, flies which arrived at the end of the maze were collected and given a score: 9 points for entering the tube closest to the light source, 8 points for entering the second closest to the light source etc. Flies which did not complete the maze received a score of 0. The score was then represented as a proportion of the total score possible for that group of flies.

2.4: Analyzing Social Behavior in Flies

In order to understand whether or not there are differences in sociality between flies of different genotypes, a new protocol was developed in order to investigate the social groups that different flies form.

Circular Plexiglas arenas were built measuring 12cm in diameter, containing a single chamber measuring 8cm in diameter and 3mm in height. The edges of the chamber were sloped in order to avoid aberrant light reflections influencing the behavior of the flies.

For group-raised flies, they were kept in standard size culture tubes in mixed-sex groups in a thermostat at 23°C under a 12hr:12hr light:dark cycle. These flies were removed from this thermostat 2 hours prior to testing to acclimatize them to room temperature (approx. 25°C). 3-5 day old flies were tested at the same time each day in order to minimize the influence of circadian rhythms on social behavior. In this case, flies were chosen to be analyzed between ZT5 and ZT9. Same sex groups of 20 flies were placed in the chamber by gentle aspiration, after which the arena was placed in the light box and filmed by the camera described in Section 2.1 for one hour. The flies were then anaesthetized with CO₂ and the sex of the flies was double checked in order to confirm that only same sex groups were analyzed.

For isolated flies, dark pupae were detached from culture tubes with a moist paintbrush and attached to the side of small cylindrical plastic tubes measuring 1cm in diameter and 7.5cm in length, containing standard fly culture medium in the bottom. Flies that were born in these isolated conditions were raised at 23°C under 12hr:12hr light:dark cycle and tested under the same conditions as described for group-raised flies.

These films were then transferred to another computer and imported into VirtualDub software. The frame rate was converted from 30 frames per second (fps) to 20fps and 45 minutes of film was decompressed for analysis. This decompressed film was then imported into Ctrax: The Caltech Multiple Fly Tracker. The behaviour and movements of the flies was then tracked over the 45 minute period and the frame-by-frame results were exported as a .csv file.

In order to analyze these results, an R statistical package was purposely written for these data and run with R x64 2.15.2. This package was designed to analyze multiple aspects of the behavior of these groups of flies. First, tracks with less than 60 frames were eliminated, and data were reduced to 1fps for further analysis. Density plots of the flies' distribution in the arena were generated, in order to determine whether or not they tended to spend more time close together or away from each other. Also, using the coordinates of each fly generated by Ctrax, a clustering analysis based on Ripley's K function was done by comparing the distribution of the coordinates with a distribution of randomly generated points within an arena of the same size. A social index was then generated by measuring how far the distribution of coordinates deviated from randomness. These social indices for each frame were then plotted in order to see whether or not

the flies tend to change their level of interaction with each other over time. Flies were also analysed for their locomotor activity and for the frequency of “close encounters”, defined as the number of times that pairs of flies were within 5 body lengths of each other.

C **HAPTER III:** **RESULTS**

3.1: Social Behaviour in *Drosophila melanogaster*

While there is some indication that *Drosophila melanogaster* exhibit social behaviour, few studies have been conducted to study this. One study placed same-sex groups of flies in vertical and triangular arenas, still images were taken of their distribution over a one-hour period and the distance between each of the flies was measured as an indication of social interaction (Simon *et. al.*, 2012). Since the development of the Caltech Multiple Walking Fly Tracker (Ctrax), which tracks fly movement and orientation of multiple flies over time, another study on social interactions in *Drosophila* compared the number of times flies approach each other from the front, from the rear and the number of times they preened each other compared to the number of times that randomly moving vectors intersected (Schneider *et. al.*, 2012). These two studies had very different methodologies, and they also presented conflicting results. The study which defined social behaviour as the tendency of flies to remain within two body lengths of each other indicated that flies use visual rather than olfactory cues, since white-eyed flies formed less compact social groups, while olfactory mutants formed groups indistinguishable from those formed by wild-type flies (Simon *et. al.*, 2012). The study that used front approach, rear approach and social preening as a measure of sociality, on the other hand, suggested that flies rely on chemosensory rather than visual cues to socially interact, as chemosensory mutants were indistinguishable from randomly intersecting trajectories, while flies were still capable of interacting when placed under dim far-red light (850nm) (Schneider *et. al.*, 2012). Due to these diverging methodologies and contradicting results, a definitive methodology for investigating social behaviour in *Drosophila* still remains to be standardized.

In this study, elements from both previously published studies were incorporated to develop this new protocol. As in the first study the position of the flies in the arena was used as a measure of social interaction, and their distribution in the arena over time was compared to the distribution of 20 randomly placed or evenly spaced objects in the given arena size. As in the second study, flies were placed in horizontal circular arenas so as to avoid flies' natural tendency to travel towards negative geotaxis, thus obscuring subtle differences between social groups. Also, Ctrax software was used to track the flies' movements continuously over time. The new component of this protocol involves the writing of an R statistical package to analyse the data gathered by Ctrax, meaning that this is the first time the analysis of social behaviour in *Drosophila* will be possible using entirely open-source software. Furthermore, this is the first study which indicates that social interactions in *Drosophila* could be used as a model for the genetic basis of antisocial behaviour in humans.

3.1.1: Social Behaviour in wild-type flies

In order to confirm that the new protocol is adequate for the analysis of social behaviour in *Drosophila melanogaster*, 3 replicas for each sex of wild-type flies were tested. Same-sex groups of 20 flies were placed in a circular arena and filmed over 1 hour, 45 minutes of which were tracked with Ctrax Software. An R statistical package especially designed during this project for analysing social interactions was then employed to investigate various aspects of the data exported by Ctrax (Fig. 3.1.1).

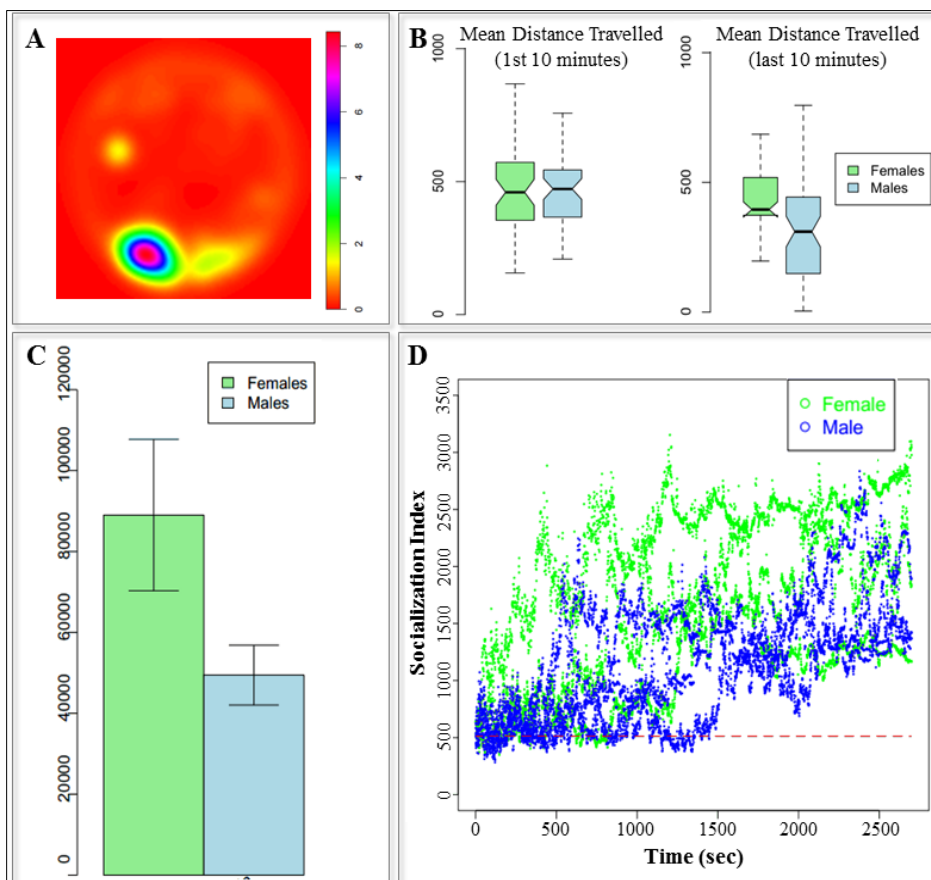


Fig 3.1.1: Analysis of social behaviour in wild-type flies, as analysed by new R stats package. (A) Example of a density plot for one replica of female wild-type flies, representing the proportion of time spent in areas of the arena. (B) Locomotor activity during the first and last 10 minutes of the 45 minute track. (C) Frequency that pairs of flies spent within five body lengths of each other. (D) Plot of social index of each replica over 45 minute period, compared to the social index of 20 randomly distributed points in an area the size of the arena (red line).

The data exported by Ctrax were analysed in a number of different ways. Locomotor activity behaviour of flies was calculated, in order to see whether or not any differences seen between genotypes in social behaviour could be due to differences in locomotor activity (Fig. 3.1.1 B). Density plots were also generated, in order to see which parts of the arena were more frequently occupied by the flies (Fig. 3.1.1 A). To evaluate social interactions, two kinds of analyses were performed. First, a package was designed to calculate the distance between pairs of flies in each frame of a 1fps data frame. The mean number of distances which were within 20 pixels,

corresponding to approximately 5 fly body lengths, can then be plotted (Fig. 3.1.1 C). While female wild-type flies appeared to be more social than males in this regard, the differences between the two were not statistically significant (t-test with Bonferroni adjustment; $p=0.151$; d.f.=2).

Finally, in order to visualize socialization over time, social indices were generated and plotted on a frame-by-frame basis (Fig. 3.1.1 D). Social indices were generated for each frame of a 1fps dataset with the use of a clustering analysis based on Ripley's K function. This analysis the distribution of the position of each of the flies in the frame, and compares it to the distribution of 20 randomly distributed points in an area the size of the arena. The social indices were then generated by calculating how far the distribution of these flies deviates from randomness. A social index above the random line indicates clustering, or flies that tend to seek each other out. A social index below randomness, on the other hand, indicates repulsion, or flies which are actively avoiding each other. A social index for each frame was thus calculated and the indices for all replicas were plotted on the same graph in order to see the flies' tendency to cluster, remain random or avoid each other over time (Fig. 3.1.1 D). This socialization index plot for wild-type flies indicates that socialization increases over time. Social indices over the first few minutes hover around the line which indicates randomness (Fig. 3.1.1 D; red line), consistent with the classic *Drosophila* exploratory behaviour exhibited when they are placed in a new environment. Once the arena is sufficiently explored, flies tend to cluster together over time.

3.1.2: Social Behaviour in *white*¹¹¹⁸ and *sine oculis* Flies

In order to test the claim made by Simon and colleagues that *Drosophila* rely on visual cues for social behaviour, two visual mutants were tested for social behaviour with the protocol described in Section 3.1.1. White-eyed *white*¹¹¹⁸ flies and completely eyeless *sine oculis* flies were tested for their social behaviour and compared to wild-type flies. As described in Section 3.1.1 flies were tested for locomotor activity (3.1.2.1 A), frequency of "close encounters", defined as the frequency of times pairs of flies were within 5 body lengths of each other (Fig. 3.1.2.1 B), and for their socialization over time (Fig. 3.1.2.2).

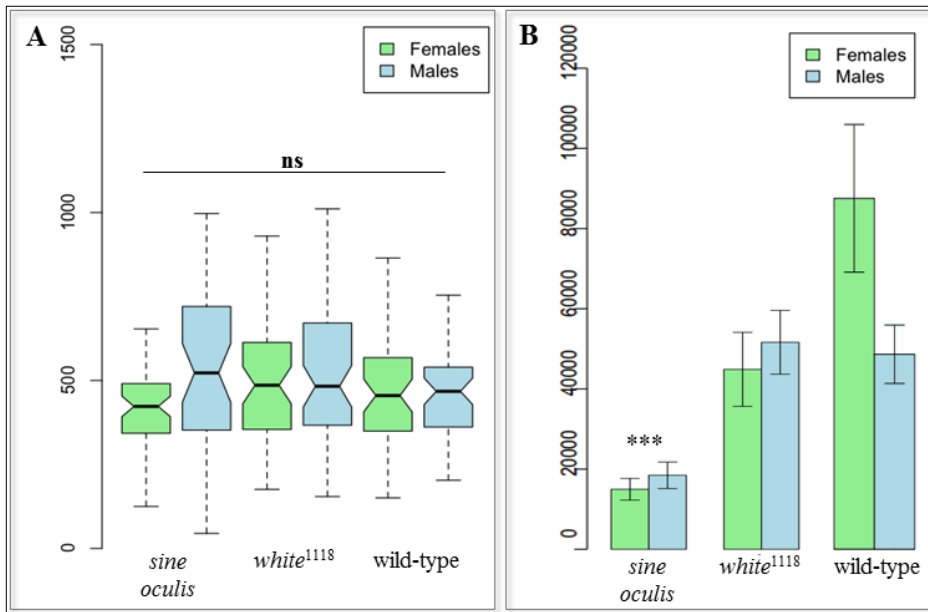


Fig 3.1.2.1: (A) Total distance travelled by flies in the first 10 minutes ($n=3$). (B) Frequency of pairs of flies being within 5 fly body lengths of each other ($n=3$). Statistical analysis: t-test with Bonferroni correction; $n=3$; *** $p<0.001$; ns=not significant; error bars= S. E.

The two visual mutant genotypes tested did not have significant differences in locomotor activity between them (Fig. 3.1.2.1). However, they did differ significantly in their social behaviour. While *white¹¹¹⁸* flies had slightly (though not significantly) lower frequencies of “close encounters” than wild-type flies, *sine oculis* eyeless flies had significantly fewer close encounters than both *white¹¹¹⁸* and wild-type controls (Fig. 3.1.2.1 B). Density and socialization plots shine an even brighter spotlight on the differences between these three genotypes (Fig. 3.1.2.2)

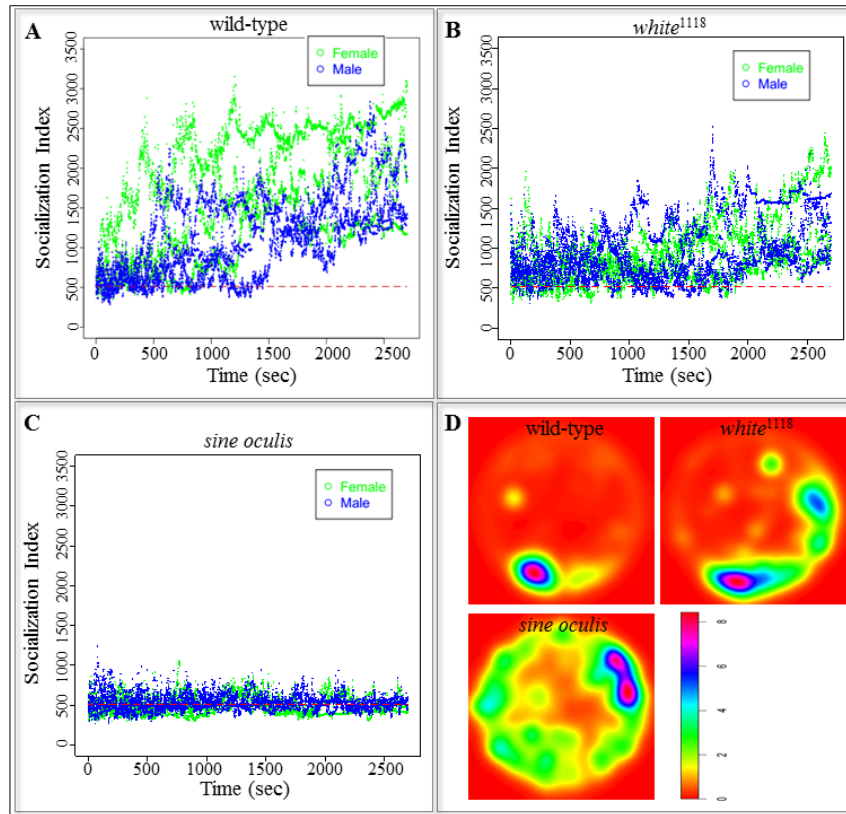


Fig. 3.1.2.2: (A-C) Socialization plots of all replicas of (A) wild-type, (B) *white*¹¹¹⁸ and (C) eyeless *sine oculis* flies. (n=3). (D) Density plots for one replica of wild-type, *white*¹¹¹⁸ and eyeless *sine oculis* females.

As described in Section 3.1.1, the socialization plot of wild-type flies indicates that when the flies are first placed in the arena their distribution is random, consistent with the exploratory behaviour flies exhibit when placed in a new arena. As time passes, flies tend to cluster and remain in groups (Fig. 3.1.2.2 A). Distribution of *white*¹¹¹⁸ flies remains close to random for a longer time, and while they do tend to cluster as time goes on, they do not reach as high a social index (meaning they do not cluster as closely) as wild-type flies do (Fig. 3.1.2.2 B). Eyeless *sine oculis* flies, on the other hand, have a socialization index which remains flat-lined, always close to the randomness line (Fig. 3.1.2.2 C). Density plots of these three genotypes also support these observations (Fig. 3.1.2.2 D). The density heat map for wild-type females shows a small part of the arena which is occupied for the majority of the time analysed. *white*¹¹¹⁸ flies have a density plot which shows a slightly wider heat spot, yet it still demonstrates clustering to one side of the arena, while eyeless *sine oculis* flies were far more evenly distributed around the arena (Fig. 3.1.2.2 D). This indicates that *Drosophila* rely on visual cues in order to socialize with each other. Also, since *sine oculis* flies do not have impaired olfaction or gustation, and since they did not cluster at all over time, it is unlikely that *Drosophila* can compensate for a lack of visual acuity with either of these senses in this regard.

3.1.3: The Effect of Isolation on Social Behaviour

Isolation after birth has been known to affect brain chemistry and behaviour in rodents (Meaney, *et. al.*, 1985), primates (Suomi, 1997) and humans (Gunnar *et. al.*, 2001). Despite this, some social behaviour experiments in animals are conducted on individuals raised in isolation, including one study investigating the tendency of single fragile X mutant flies to seek out social interaction (Bolduc *et. al.*, 2010). For these reasons, the effect of raising flies in isolation on their social behaviour was investigated by placing dark pupae in individual tubes and raising the eclosed flies for 3-5 days before testing. Both wild-type and *white*¹¹¹⁸ flies were isolated and tested for behavioural abnormalities.

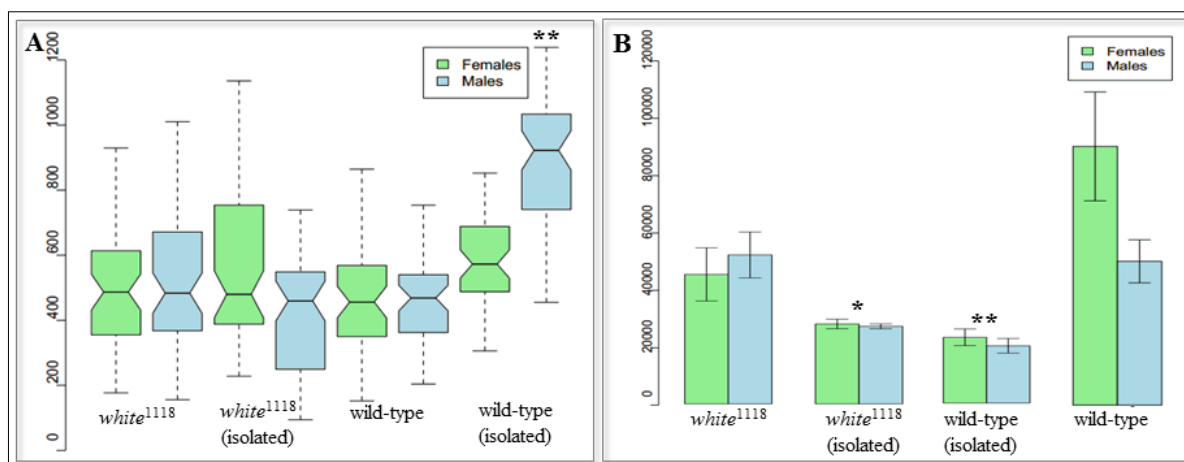


Fig. 3.1.3.1: (A) Locomotor activity in isolated and group-raised wild-type and *white*¹¹¹⁸ flies. Statistical analysis; ANOVA with Tukey's post-hoc test; n=3; **p<0.01. (B) Frequency at which pairs of flies are within five body lengths of each other (close encounters). Statistical analysis: t-test with Bonferroni correction; *p<0.05 **p<0.01; n=3; error bars= S. E.

Both wild-type and *white*¹¹¹⁸ flies had significantly altered behaviour when they were raised in isolation. Isolation caused wild-type flies to move significantly more than group-raised flies, while *white*¹¹¹⁸ isolated flies did not have altered locomotor activity compared with group-raised controls (Fig. 3.1.3.1 A). However, both wild-type and *white*¹¹¹⁸ isolated flies had significantly reduced frequencies of close encounters compared to group-raised controls (Fig. 3.1.3.1 B). This indicates that flies rely on previous social contact to form social groups, which should be kept in consideration when designing future social behaviour experiments in *Drosophila*. Furthermore, it suggests that this could be potentially used as a model for the effects of social deprivation on brain development.

3.1.4: Differences between wild-type lines

WT-ALA wild-type lines were maintained in a fashion which minimized inbreeding as much as possible by adding fresh wild-type lines to the pool every month, thus representing real wild *Drosophila* flies as much as possible. However, there are other wild-type lines utilized in the lab, though they are raised in laboratory conditions like other genetically mutated flies, leading to significant inbreeding the longer they are kept in the lab. In this case the Oregon-R fly line was selected for study, which was ordered from Bloomington Stock Center in 2002, and has been lab-bred since well before then. In order to see whether or not these inbred wild-type flies behaved in the same way as WT-ALA flies did, they were analysed in the same way.

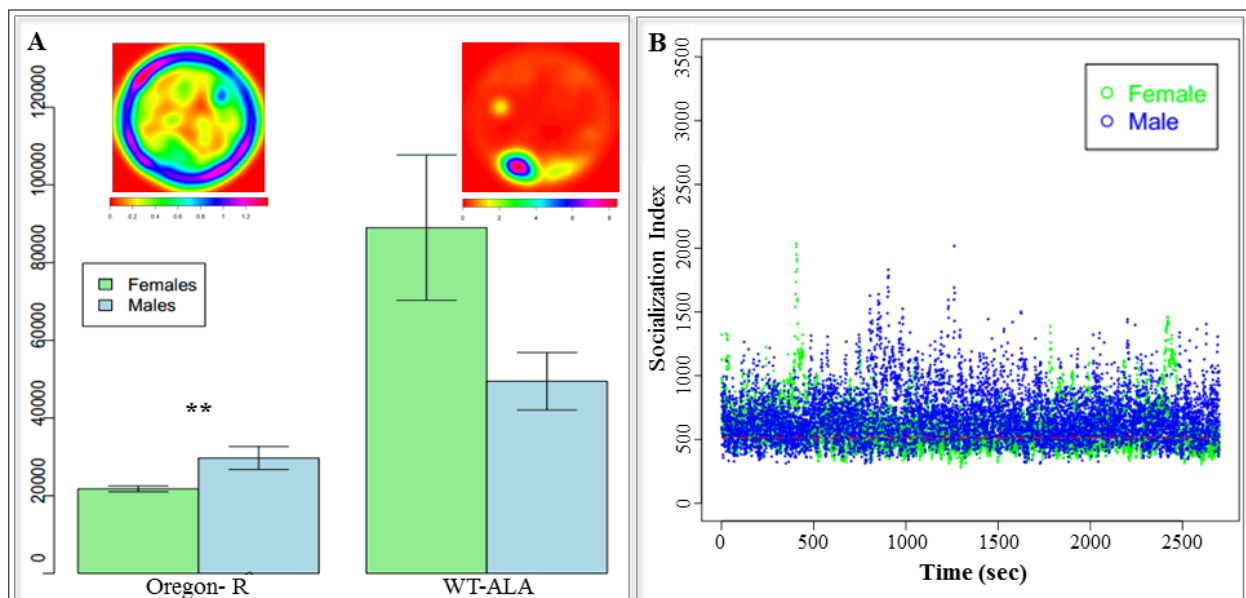


Fig. 3.1.4: Social behaviour of Oregon-R flies as compared to the WT-ALA wild-type line. (A) Frequency of close encounters, as measured by number of times flies were within 5 body lengths of each other, with a density plot for a single female replica for Oregon-R and WT-ALA. Statistical analysis: t-test with Bonferroni correction; ** $p < 0.01$; $n = 3$; error bars = S. E. (B) Socialization plot for Oregon-R flies.

Not only were there significant differences between the two wild-type lines tested, inbred Oregon-R flies had drastic defects at the social level compared to WT-ALA controls. Despite the fact that Oregon-R flies do not have visual defects, they have socialization plots which are only marginally better than *sine oculis* flies (Fig. 3.1.4 B), and significantly fewer close encounters than WT-ALA lines (Fig. 3.1.4 A). This drastic difference needs to be investigated further, in order to understand the reason for these differences. However, since WT-ALA flies most closely resemble genuine wild *Drosophila* populations, they were used as the wild-type controls for the duration of this study.

3.2: Dopamine Dysregulation and Social Behaviour

Once the protocol for investigating social behaviour in *Drosophila* was established, and once it was established that flies rely on visual acuity to form social groups, a fly line harbouring a mutation for the tyrosine hydroxylase enzyme, responsible for the synthesis of dopamine was analysed in order to see whether or not having lower levels of dopamine could affect social behaviour. Since the mutation in the *pale* locus encoding for tyrosine hydroxylase is embryonic lethal in the homozygous state, the fly line $e^1;pale^4/TM3$, with the mutation in the *pale* locus balanced with TM3 in an *ebony* background, was tested as previously described.

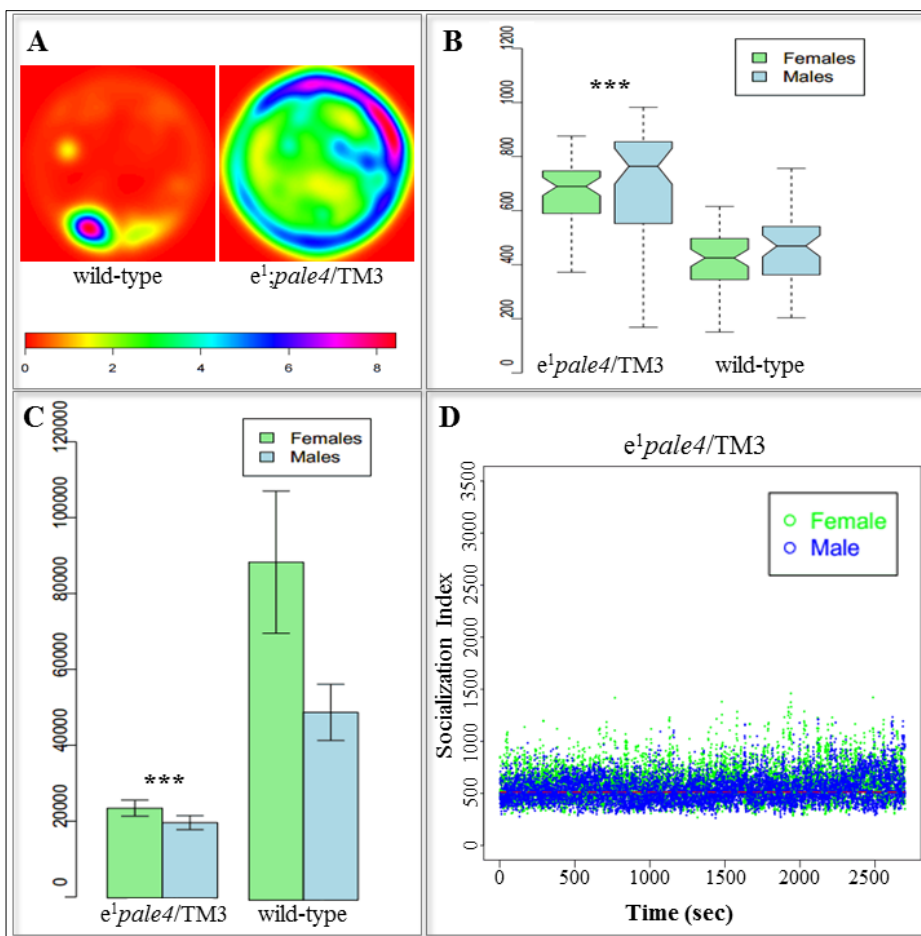


Fig. 3.2: (A) Density plot for one replica of wild-type and $e^1;pale^4/TM3$ females. (B) Locomotor activity as measure by distance travelled in first 10 minutes (n=3). (C) Frequency of pairs of flies being within 5 body lengths of each other. Statistical analysis: t-test with pooled SD; n=3; ***p<0.001; error bars= S. E. (D) Socialization plot of $e^1;pale^4/TM3$ flies (n=3).

Flies heterozygous for the *pale* mutation had severely altered social behaviour when compared to wild-type controls (Fig. 3.2). Heterozygous mutant flies had significantly fewer close encounters than wild-type controls (Fig. 432 C). Density plots for these mutants show that they occupy almost the entire arena (Fig. 3.2 A), and their socialization plot indicates that they too, as eyeless *sine oculis* mutants, have a social index which does not change over time and remains close to randomness (Fig. 3.2 D).

After this initial indication that alterations in dopamine levels could severely affect social behaviour, this needed to be confirmed. First of all, since the $e^1;pale^4/TM3$ fly line contains not just the $pale^4$ mutation but the TM3 and $ebony$ ones as well, flies were outcrossed with wild-type flies in order to obtain $pale^4/+$ and TM3/+ flies in order to obtain each of the mutations singly. $ebony$ mutant flies were also tested for social behaviour defects, as they have been reported to have other social abnormalities in the past, such as increased male-male courtship behaviour (Liu *et al.*, 2008). Also, since we have demonstrated that visual acuity is required for social behaviour, all genotypes tested were also tested for visual deficits.

3.2.1: Visual Acuity in Dopamine Mutants

All genotypes analysed for social behaviour were also tested for visual deficits. Flies were induced to light-seeking and exploratory behaviour by starving flies and keeping them in the dark for 16 hours. Same-sex groups of 20-25 flies were then placed in a light maze, which consisted of binary path decisions ending in a total of 9 exit points capped with collection tubes. This maze was then placed in a light box which was illuminated in the top left-hand corner with an LED light, the flies were allowed to explore the maze for one hour and the flies which exited the maze were collected and counted based on where they exited. Flies were thus scored: 9 points for exiting the maze closest to the light source, 8 points for exiting the second closest point to the light source etc., and 0 for not completing the maze. This score was then normalized to the total possible score for each replica (Fig. 3.2.1).

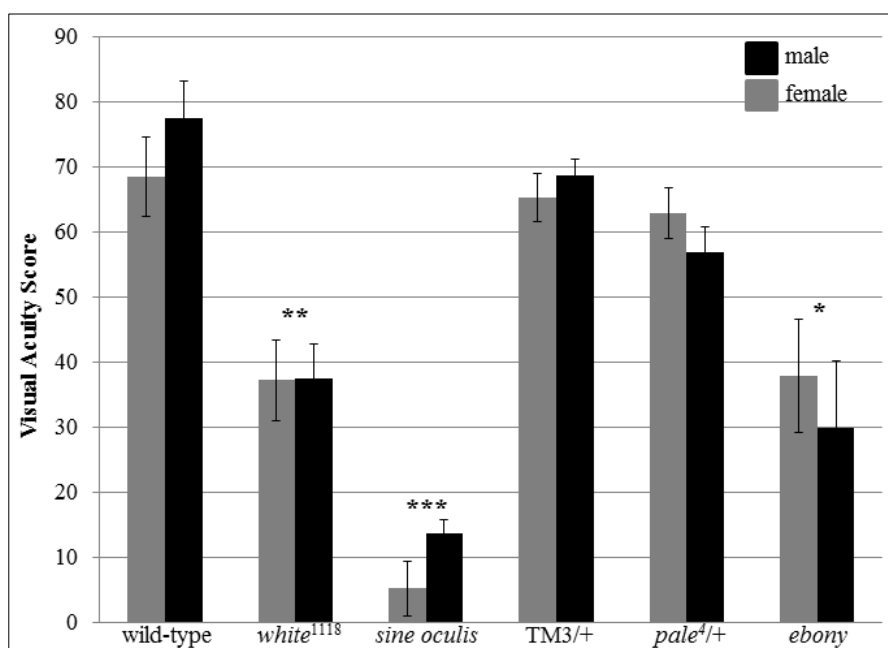


Fig. 3.2.1: Visual Acuity of fly lines used in social behaviour analysis, as measured by visual acuity score taken from how same-sex groups of 20-25 flies navigates a light maze. Statistical test: two-sample t-test; * $p < 0.05$; ** $p < 0.01$; *** $p < 0.001$; $n = 3$; Error bars = S. E.

Flies heterozygous for the TM3 balancer and the *pale*⁴ mutation did not present with any visual deficits (Fig. 3.2.1) when compared to wild type controls. Flies homozygous for the *ebony* mutation, on the other hand do presents with significantly lower visual acuity scores compared to wild-type controls (Student's t-test; $p=0.015$; d.f.=2), in keeping with previous studies reporting visual deficits in *ebony* mutants (Hotta and Benzer, 1969). When compared to *white*¹¹¹⁸ flies, on the other hand, differences in visual acuity scores were not statistically significant (Student's t-test; $p=0.32$; d.f.=2).

3.2.2: Social Behaviour in Dopamine Mutants

Once visual acuity was established, social behaviour was investigated in *pale*⁴/+, TM3/+ and *ebony*¹ mutants, in order to confirm which mutations in the *e*¹;*pale*⁴/TM3 may have precipitated the behavioural abnormalities seen in Section 3.2.

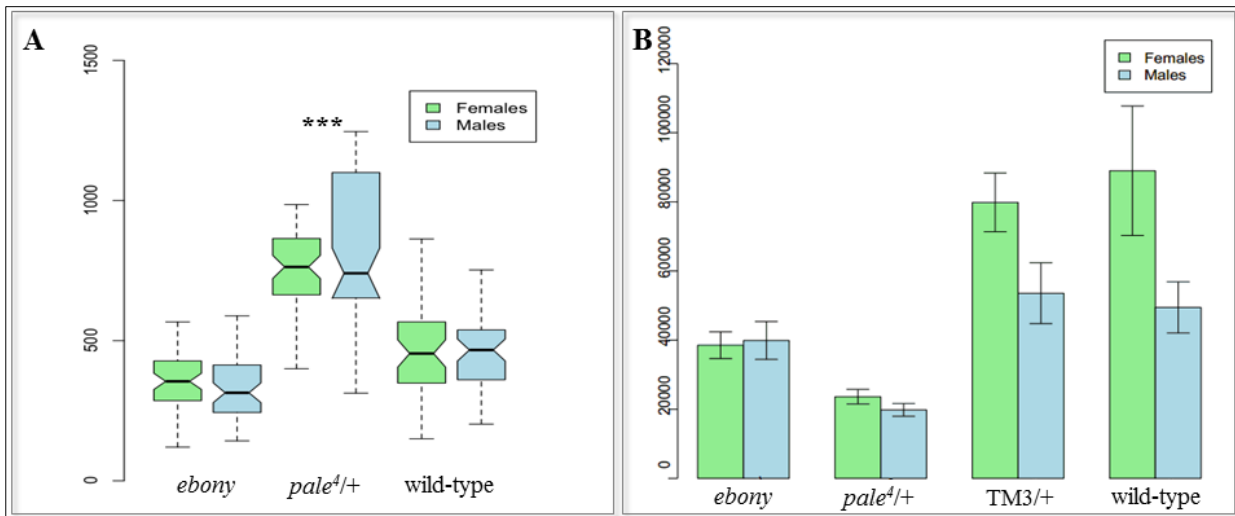


Fig. 3.2.2.1: (A) Locomotor activity of genotypes tested for social behaviour. Statistical analysis: t-test with Bonferroni correction; $n=3$; *** $p<0.001$. (B) Frequency of close encounters, defined by pairs of flies being within 5 body lengths of each other. Statistical analysis: t-test with Bonferroni correction; $n=3$; *** $p<0.001$, error bars= S. E.

While *ebony* and TM3/+ flies did not differ significantly in their locomotor activity with respect to wild-type controls, *pale*⁴/+ flies moved significantly more than controls (Fig. 3.2.2.1 A). This increased locomotor activity is mirrored by a significant decrease in the frequency of close encounters in *pale*⁴/+ flies (Fig. 3.2.2.1 B). Interestingly, *ebony*¹ flies, which overexpress dopamine in their brains, also have significantly altered social behaviour. Along with

significantly fewer close encounters observed in *ebony* flies, they also had a flat social index over time compared to wild-type controls (Fig. 3.2.2.2 D)

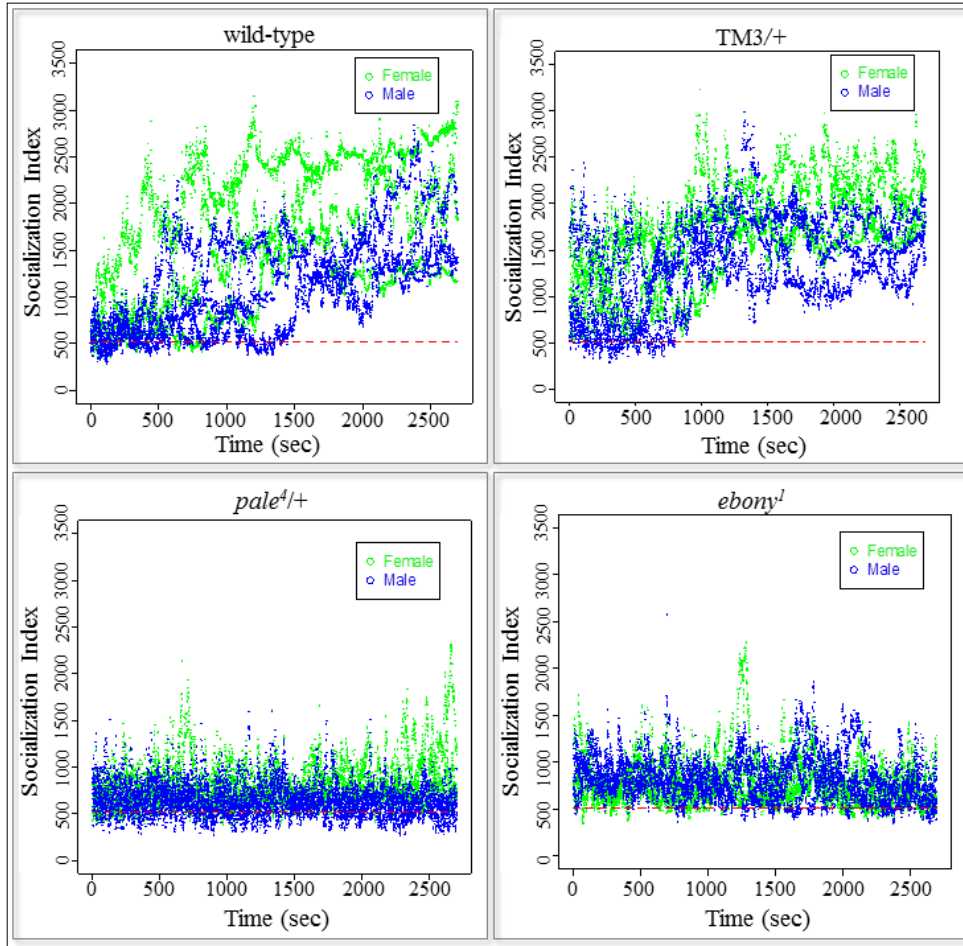


Fig. 3.2.2.2: Socialization plots for (A) wild-type, (B) TM3/+, (C) *pale*⁴/+ and (D) *ebony*¹ flies. (n= 3)

When *e*¹;*pale*⁴/TM3 flies are outcrossed with wild-type flies, we see that only flies with mutations involving dopamine regulation lead to abnormalities in social behaviour, while flies heterozygous for the TM3 balancer, which has a short-bristle phenotype, have socialization plots similar to wild-type flies (Fig. 3.2.2.2 B) and a frequency of close encounters which did not differ significantly from controls (Fig. 3.2.2.1 B; t-test with Bonferroni correction; p=1.00; d.f.= 2). This confirms that the socialization problems initially observed in *e*¹;*pale*⁴/TM3 flies was due to dysregulation of dopamine, rather than a side effect of other mutations present in the mutant line.

3.3: Characterization of SNAP-25^{R206D} Mutants

Correct neurotransmission relies not only on correct levels of neurotransmitter, but also on the correct functioning of the release of that neurotransmitter at the synapse. This NT release relies on the coordination of a number of different proteins required for mobilizing and docking the synaptic vesicles containing the NT protein, in order for them to be able to fuse to the synaptic membrane and release the protein into the synapse. One protein necessary for the docking of these vesicles is SNAP-25, a core member of the SNARE complex bound to the synaptic membrane responsible for recruiting vesicles to the synapse for fusion. In this study, a mutated version of SNAP-25 was overexpressed in the nervous system of *Drosophila melanogaster* (referred to as SNAP-25^{R206D}), so that a defective protein is incorporated into the SNARE complex thus leading to defective neurotransmission (Megighian *et. al.*, 2013).

3.3.1: Locomotor Activity of SNAP-25 Mutants

Since SNAP-25 is a protein involved in the release of neurotransmitter at the synapse, flies overexpressing a mutated version of SNAP-25 were tested for their locomotor activity when starved for 16 hours. When flies are starved this induces exploratory behaviour, during which time *Drosophila melanogaster* are compelled to explore their arena more than usual in order to seek out food. The distance they travel and the speed at which they travel is thus taken as an indirect measure of their muscular capacity, as it is assumed that they are moving at maximum capacity. Since SNAP-25 is also a necessary protein for the neuromuscular junction, adult flies expressing mutated SNAP-25 were tested in this regard.

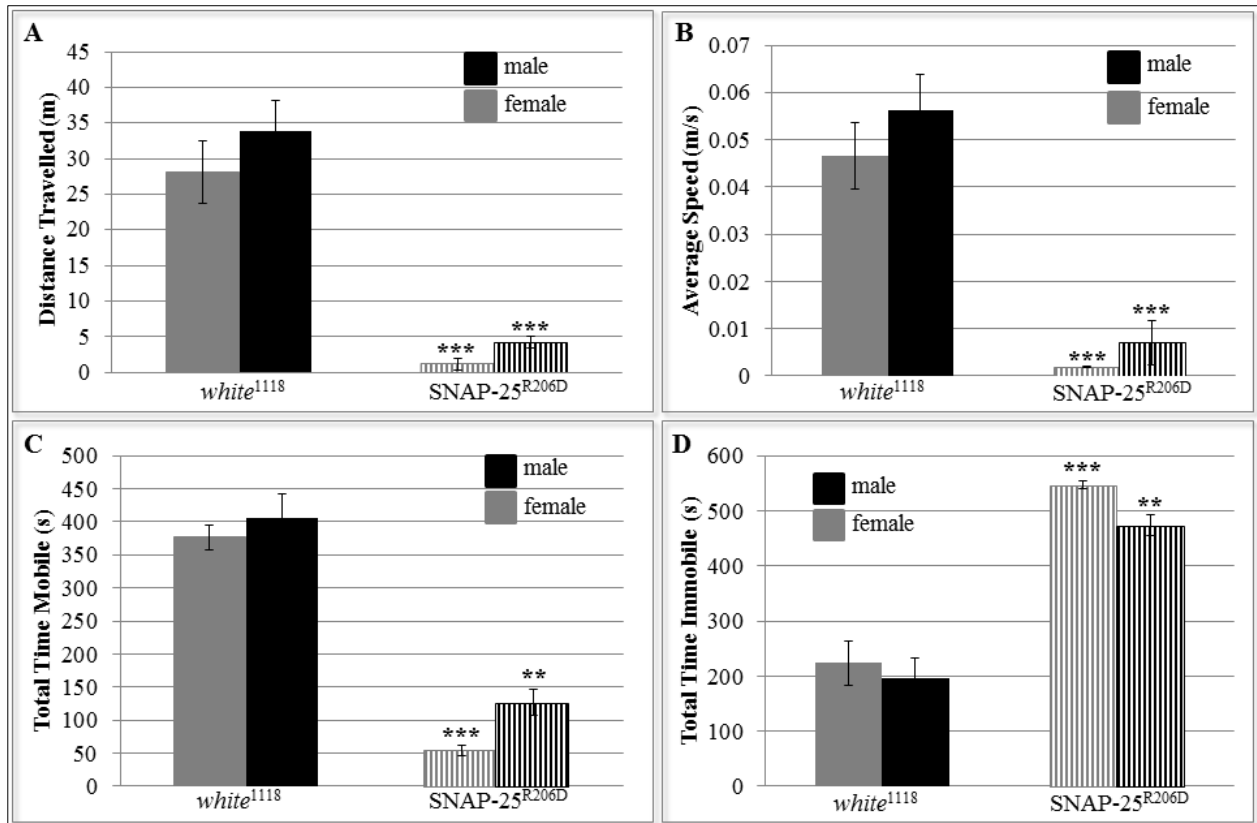


Fig. 3.3.1: Locomotor activity of *white*¹¹¹⁸ and SNAP-25^{R206D} flies, as measured by (A) Total distance travelled in 10 minutes, (B) Overall average speed and the total time spent (C) mobile and (D) immobile in the 10 minute period. Statistical analysis: one-way ANOVA with Sidak post-hoc correction; n=20; **p<0.01; ***p<0.001; error bars= S. E.

Flies overexpressing the point-mutated SNAP-25 in the nervous system had significant locomotor defects. Mutant flies covered significantly less distance (Fig. 3.3.1 A), significantly slower (Fig. 3.3.1 B) and for a significantly smaller proportion of time (Fig. 3.3.1 C-D) compared to *white*¹¹¹⁸ controls. This indicates that mutating SNAP-25, leading to a defective SNARE complex, can lead to severe locomotor defects in *Drosophila melanogaster*.

3.3.2: Social Behaviour in SNAP-25 Mutants

The social behaviour of flies overexpressing a point-mutated version of SNAP-25 in the nervous system was analysed and compared to both *white*¹¹¹⁸ flies, the genetic background of the SNAP-25 mutant, and WT-ALA controls.

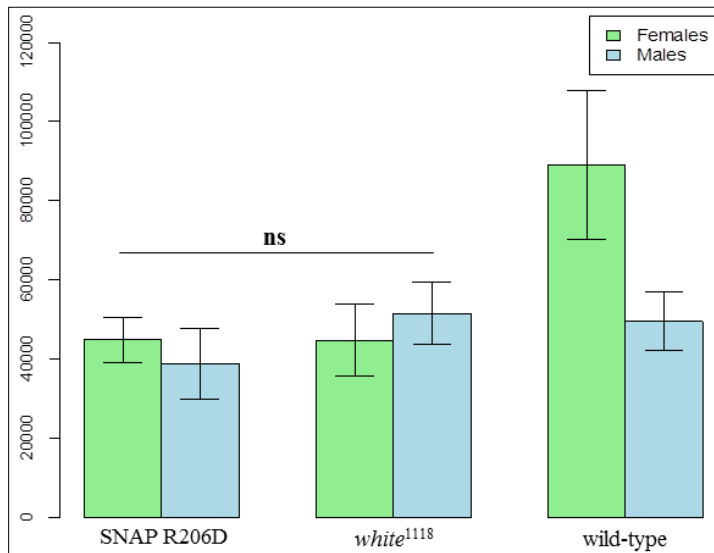


Fig. 3.3.2.1: Frequency of close encounters, as defined by the number of times flies were within 5 body lengths of each other, in flies overexpressing a point-mutated version of SNAP-25 (SNAP-25^{R206D}), *white*¹¹¹⁸ and wild-type controls. Statistical analysis: t-test with pooled SD and Bonferroni correction; n= 3; ns= not significant; error bars= S. E.

Unlike dopamine mutants, flies overexpressing a mutated form of SNAP-25 did not have fewer close encounters compared to *white*¹¹¹⁸ flies, the genetic background of the mutant line, or wild-type controls (Fig. 3.232.1). Also, flies overexpressing mutated SNAP-25 did not have altered locomotor activity compared to controls (Fig. 3.3.2.2 A), and their socialization plots indicate that they do form groups over time (Fig. 3.3.2.2 B), similar to *white*¹¹¹⁸ controls (Fig. 3.3.2.2 C).

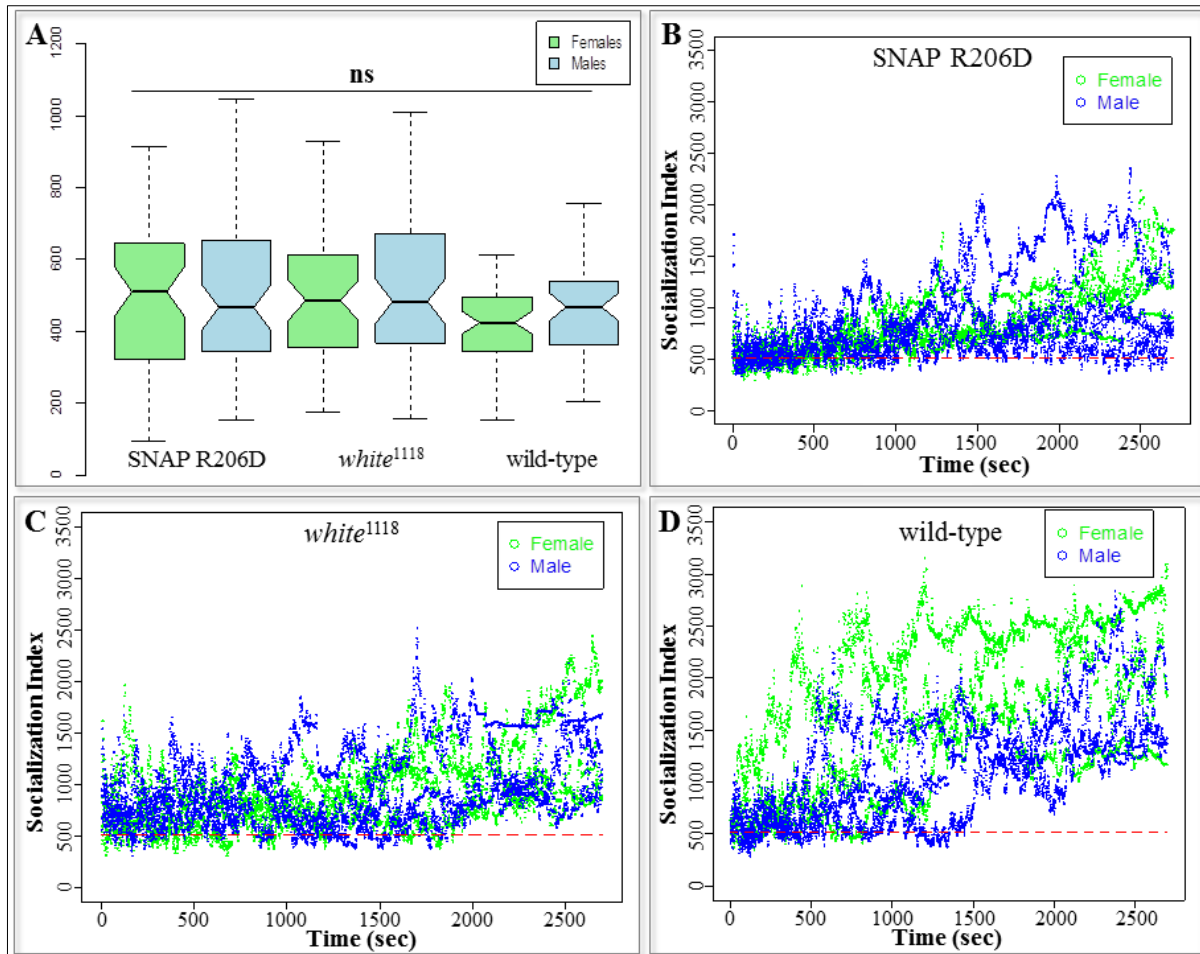


Fig. 3.3.2.2: (A) Locomotor activity, as measured by total distance travelled in the first 10 minutes of tracking, of SNAP-25 R206D, *white*¹¹¹⁸ and wild-type flies. Statistical analysis: t-test with pooled SD and Bonferroni correction; n= 3; ns= not significant. (B-D) Socialization plots for (B) Flies overexpressing mutated SNAP-25, (C) *white*¹¹¹⁸ and (D) wild-type flies (n= 3).

These results indicate that the overexpression of a mutated form of SNAP-25, thus the possession of a defective SNARE complex, does not significantly impact social behaviour in *Drosophila melanogaster* the way that dopamine dysregulation does. Also, when compared to their genetic background *white*¹¹¹⁸, they did not have altered socialization at all.

3.3.3: Marking Flies for Mixed Social Groups

While flies overexpressing a mutated form of SNAP-25 did not seem to have altered social behaviour compared to their *white*¹¹¹⁸ counterparts, the same may not be the case when mutant flies are mixed with *white*¹¹¹⁸ ones. In order to see whether or not flies segregate themselves based on genotype, another interesting possibility with regards to modelling antisocial behaviour in humans, a statistical package is currently being developed to analyse social behaviour in groups containing more than one genotype. Before this is done, however, a method for marking the flies so that the researcher is capable of distinguishing between the genotypes analysed needed to be developed.

Since the fly lines harbouring the mutated SNAP-25 construct under UAS control was on chromosome II, the construct was balanced with CyO in order to be able to distinguish flies overexpressing SNAP-25, with curly wings, from *white*¹¹¹⁸ flies, which had straight wings. However, if this method for studying mixed social groups is to be fully exploited, other methods for distinguishing between genotypes during behaviour films needed to be developed. In order to do this, experiments investigating the effects of marking flies were conducted.

Water-based enamel paint was used to mark flies, in order to avoid volatile chemicals present in the paint from emitting adverse olfactory cues. Flies were anaesthetized with brief CO₂ exposure, after which they were either marked on the scutellum or the abdomen with a small drop of paint. Flies were kept under anaesthesia until the paint dried, after which they were placed in standard fly tubes on cornmeal-yeast-agar medium. 100% of marked flies were alive after being kept this way for 7 days, which is a first indication that this method of marking does not harm them or cause them to be unable to perform their natural functions, all things that could also adversely affect their behaviour (data not shown). Flies thus raised for three days were initially tested for locomotor activity.

Locomotor activity for marked *white*¹¹¹⁸ flies was investigated under exploratory conditions as described in Section 2.2 (Fig. 3.3.4).

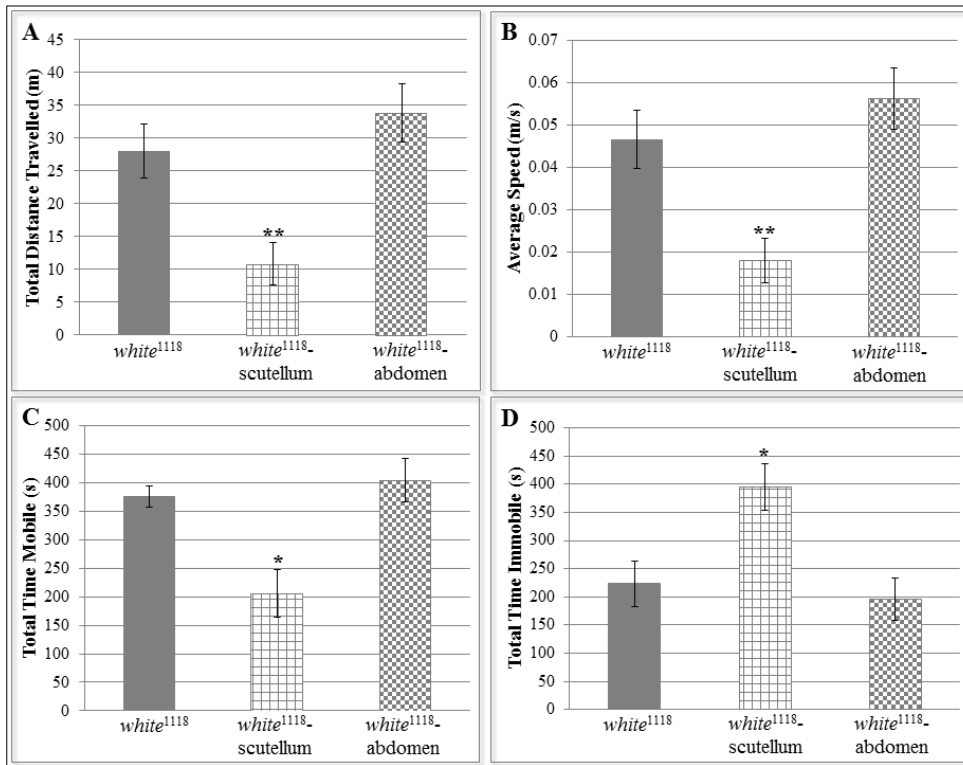


Fig. 3.3.3: Locomotor activity of *white*¹¹¹⁸ adult flies that were either painted on the scutellum, on the abdomen or left unmarked, as measured by (A) total distance travelled over 10 minutes, (B) their overall average speed, and the amount of time (out of 10 minutes) they spent (C) mobile and (D) immobile. Statistical Analysis: one-way ANOVA with Sidak post-hoc correction; n=20; *p<0.05; **p<0.001; error bars= S. E.

Flies marked on the scutellum, which is covered in sensory bristles, had severely reduced locomotor activity compared to controls. Flies marked on the abdomen, on the other hand, did not have locomotor deficits, indicating that the problems observed in the scutellum-marked flies were probably due to the placement of the paint rather than the weight of it. This also suggests that over stimulating the sensory bristles on the scutellum affects *Drosophila* behaviour.

C **HAPTER III:** **DISCUSSION**

4.1: Social Behaviour in *Drosophila melanogaster*

This is one of the few studies conducted to date investigating social behaviour in *Drosophila melanogaster*. A new protocol was developed during this study, incorporating elements from two previous studies and developing a new R statistical package in order to be able to investigate social behaviour in *Drosophila* using entirely open-source software. This new protocol was then used to see whether or not flies with subtle defects in neurotransmission had altered social behaviour, rendering them useful as a model for antisocial behaviour in humans.

4.1.1: *Drosophila melanogaster* Exhibit Social Behaviour

It has been demonstrated that this new protocol works well for studying social behaviour in *Drosophila*. With the use of this protocol we have confirmed that, when flies are placed in an arena in same-sex groups, *Drosophila melanogaster* tend to cluster together over time. When we analyse the distribution of wild-type flies in the arena with Ripley's K function, we see that initially they distribute randomly, indicating that they tend to explore their arena singly and without forming small groups or following each other to do so. After a few minutes, on the other hand, their distribution begins to deviate from randomness, indicating a clustered distribution which demonstrates that the flies seek each other out after exploring their new environment. Once it was established that *Drosophila* exhibit social behaviour which can be measured and quantified in this way, the sensory cues necessary for the formation of these groups were investigated.

4.1.2: *Drosophila* Social Behaviour Relies on Visual Acuity

Once it was confirmed that the protocol developed during this study was acceptable for studying social behaviour in *Drosophila melanogaster*, the visual mutants *white*¹¹¹⁸ and *sine oculis* were tested in order to verify the claim that *Drosophila melanogaster* relies on visual cues to form social groups.

White-eyed *white*¹¹¹⁸ flies exhibit slightly lower levels of social behaviour as measured by their distribution over time and their frequency of close encounters, defined by the number of times that pairs of flies were within five body lengths of each other. Eyeless *sine oculis* flies, on the other hand, had a far more drastic social behaviour phenotype, with significantly fewer close

encounters and a flat distribution over time which never departs from randomness. This indicates that *Drosophila melanogaster* rely on visual cues to form groups, as there seems to be a correlation between visual acuity and social behaviour (Fig. 4.1.2). Furthermore, it indicates that visual cues are the primary ones which *Drosophila* rely on, as eyeless flies were not able to use another sense to compensate for their lack of vision to form social groups.

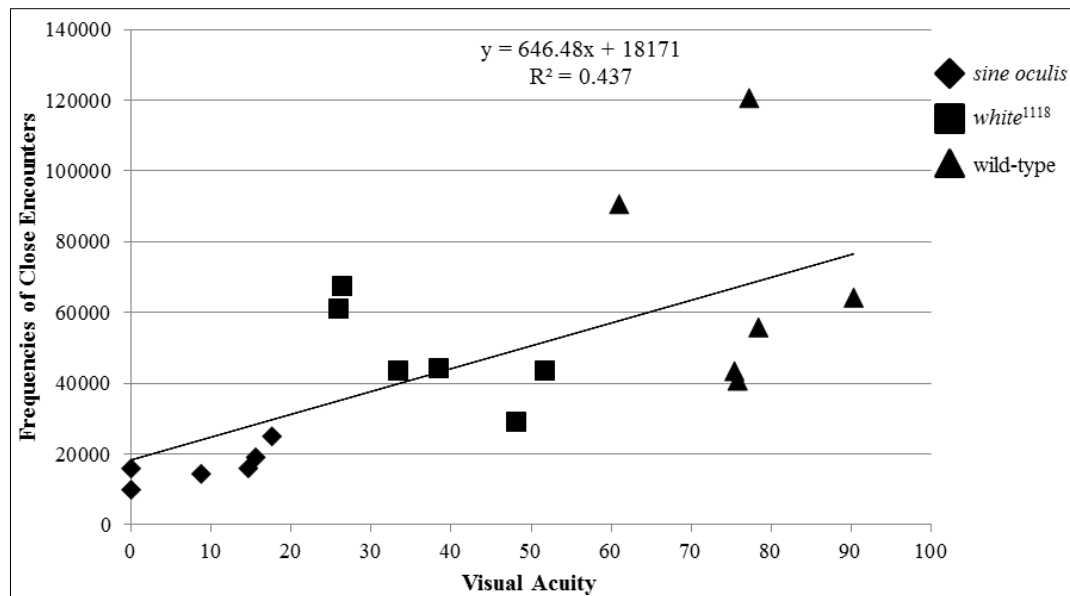


Fig. 4.1.2: Correlation plot of visual acuity score and frequency of close encounters. R^2 = coefficient of determination; error bars = S. E.

When we plot visual acuity, as measured by visual index calculated from groups of flies navigating a light maze, against the frequency of close encounters, we see that there is a strong, statistically significant correlation between visual acuity and sociality (Fig. 4.1.2; Pearson's Correlation; $p = 0.00282$; d.f. = 16). This is clear evidence that *Drosophila* rely primarily on visual cues to form social groups over time.

Once social behaviour was confirmed and the sensory cues necessary for that behaviour were established, we proceeded to investigate whether or not subtle changes in brain chemistry or social contact could affect sociality in *Drosophila*.

4.1.3: Previous Social Contact can Affect Social Behaviour in *Drosophila*

Although there have been few studies investigating social behaviour in *Drosophila*, one study attempted to investigate whether or not the *Drosophila* model for Fragile X Syndrome had

altered social behaviour with respect to controls (Bolduc *et. al.*, 2010). In order to do this, flies which had been isolated within three hours of eclosion were placed in chambers and monitored for the time they spent close to the mesh which separated them from another fly in a second chamber. This led us to question the reason behind using isolated flies for this protocol, and whether or not the absence of previous social contact could influence social behaviour. To do this, dark pupae were placed in individual tubes and eclosed flies were thus raised in isolation for 3-5 days. These flies were then placed in same-sex groups of 20 in circular arenas and their behaviour was filmed and tracked as previously described. Both WT-ALA and *white*¹¹¹⁸ flies were tested for the effects of isolation on social behaviour.

Flies raised in isolation had significantly altered social behaviour in both wild-type and *white*¹¹¹⁸ flies (Section 3.1.3). Isolated flies had significantly fewer close encounters compared to group-raised flies, and their socialization plots indicate they do not form clusters over time.

These results indicate that the absence of social contact in adults can have dramatic effects on social interactions later in life. This leads us to the conclusion that flies should not be raised in isolation prior to behavioural analyses, as it could influence the results. Furthermore, it could prove to be an interesting model for early social deprivation. Many animals, including humans, have been shown to have severely altered brain structure and chemistry if they are deprived of social contact in early infancy, yet the biological reason for this, and the potential genetic predisposition for this could also be investigated in this model.

4.1.4: Circadian Rhythms Probably Affect Social Behaviour

This study was conducted in the afternoon between ZT5 and ZT9 in order to minimize the possible effects of circadian rhythms on social behaviour. This time frame corresponds with the typical afternoon lull in locomotor activity in wild-type flies (Fig. 4.1.4).

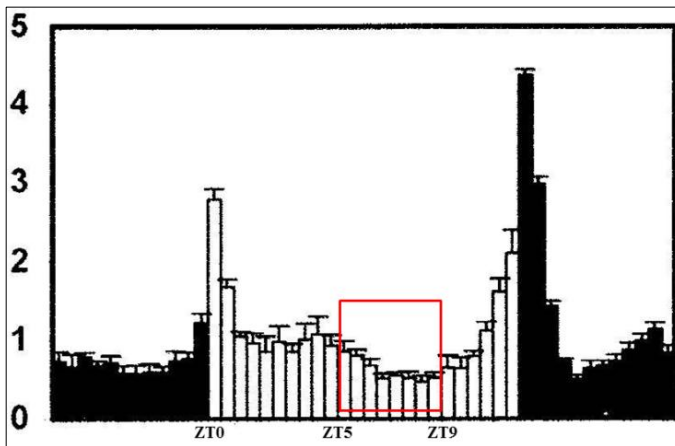


Fig. 4.1.1: χ -square periodogram of wild-type flies raised in 12hr:12hr light:dark conditions, indicating the relative locomotor activity of flies over a 24 hour period. Source: Allada *et. al.*, 2003, with slight modifications indicating the zeitgeber time (ZT) of interest, and red square indicating the period of time social behaviour was investigated within.

While the effects of circadian rhythms was not fully investigated during this project, some observations made in the lab during this study leads us to believe that clustering behaviour can be significantly altered if flies are tested at different times of the day (data not shown). This could mean that, if flies harbour a mutation which affects their circadian rhythms, they might appear to have significantly altered social behaviour, when in reality they simply form social groups at a different time of day. The effects of circadian rhythms on sociality should be more thoroughly investigated not only to rule them out as a potential contributing factor for social abnormalities seen in our mutants, but also as such a study could shine a light on the biological reason why *Drosophila* form these social groups in the first place.

4.1.5: Why are there Differences Between wild-type Lines?

In order to study social behaviour in *Drosophila melanogaster*, a WT-ALA wild-type line was used which most closely resembled genuine wild flies, which maintain genetic diversity as much as possible by adding a fresh isofemale line to the pool every month and raising them in large bottles. However, another wild-type line was also tested for social behaviour. Oregon-R flies, wild-type flies which have been lab inbred for well over a decade, behaved very differently compared to WT-ALA flies. Oregon-R had socialization plots similar to eyeless flies and dopamine mutants, and they had significantly fewer close encounters compared to WT-ALA flies as well.

While differences between wild-type lines have been previously reported (Schneider *et. al.*, 2012), differences this extreme are unprecedented. Further investigation into these lines is

needed in order to evaluate the reason for these discrepancies. One possible explanation is that lab-bred flies lose social behaviour, which might mean that *Drosophila melanogaster* exhibit social behaviour as a form of protection from predators, something which is no longer needed in the lab. One way to investigate this is to look at a few different wild-type lines which have been inbred for a varying number of years, and to see whether or not there is a correlation between sociality and number of years of lab-breeding. Another possibility is that our Oregon-R line accumulated a mutation while they were being inbred which resulted in antisocial behaviour. This could be investigated by studying outcrossed Oregon-R flies with both WT-ALA and a different, inbred wild-type line. If this turns out to be the case, our Oregon-R flies could prove to be very useful in dissecting the genetic basis for social behaviour in *Drosophila*. Either way, this discrepancy promises to provide an interesting point of study for the future.

4.2 *Drosophila melanogaster* as a Model for Antisocial Behaviour

Once a protocol for investigating social behaviour in *Drosophila* was developed and confirmed, the purpose of this study was to establish whether or not *Drosophila melanogaster* could be useful as a model for human neurological disorders which present with social defects. To investigate this we selected two proteins involved in neurotransmission which have been tied to behavioural neurological disorders in humans: the neurotransmitter dopamine and the SNARE complex component SNAP-25. Fly lines which had altered levels of dopamine, or which expressed a defective copy of SNAP-25 were tested for social behaviour and compared to WT-ALA wild-type flies.

4.2.1: Mutants Heterozygous for *pale*⁴ Mutation are Antisocial

In order to investigate whether or not altered dopamine levels have an effect on social behaviour, the *e*¹;*pale*⁴/TM3 line was initially studied. This fly line is heterozygous for a mutation at the *pale* locus, the enzyme which encodes for tyrosine hydroxylase, responsible for dopamine synthesis in the nervous system. While homozygous mutants are embryonic lethal, flies heterozygous for the mutation are not reported to have any overt problems. Despite the lack of an obvious mutant phenotype, *e*¹;*pale*⁴/TM3 flies presented with severe social defects, both in terms of their socialization plots, the frequency of close encounters and even their locomotor activity. These were the first indications that altered dopamine levels could alter social behaviour.

However, we had to confirm whether or not the presence of other mutations in the $e^1;pale^4/TM3$ line could have confounded these results. The TM3 balancer used for the $pale^4$ mutation exhibits a short-bristle, or “stubble” phenotype. *Drosophila*’s bristles are an important sensory part of the fly, and so it is not inconceivable that an altered tactile sense could influence social behaviour. The mutant line also contains the *ebony*¹ mutation, which causes an increase in dopamine levels, so the presence of both $pale^4$ and *ebony*¹ mutations in the same line make the actual dopamine levels in these flies unclear. Because of this, the flies were outcrossed with wild-type flies in order to obtain $pale^4/+$ and $TM3/+$ flies for study. Flies harbouring the *ebony*¹ mutation were also tested, in order to investigate the effects of an overproduction of dopamine in the brain on social behaviour.

4.2.2: Decreased Dopamine has an Effect on Social Behaviour

In order to confirm that decreases in dopamine affect social behaviour, $e^1;pale^4/TM3$ flies were outcrossed with WT-ALA wild-type flies in order to obtain flies heterozygous for the $pale^4$ mutation without the presence of other potentially confounding factors.

Flies heterozygous for the $pale^4$ mutation in a wild-type background also had altered social behaviour, similar to that observed in $e^1;pale^4/TM3$ flies. These flies had higher levels of locomotor activity, occupied a larger proportion of the arena and had a significantly lower frequency of staying within 5 body lengths of each other compared to wild-type controls. As these flies did not possess any other mutations that could have caused the alterations in social behaviour, this is strong evidence indicating that decreased levels of dopamine affect social behaviour in *Drosophila melanogaster*.

4.2.3: Stubble Phenotype has No Effect on Social Behaviour

Drosophila melanogaster possess bristles on their scutellum which are important tactile organs for them. Since one study suggested that *Drosophila melanogaster* use a tactile sense during social behaviour (Schneider *et. al.*, 2012), and since the TM3 balancer in the $e^1;pale^4/TM3$ line exhibit a “stubble” or short-bristle phenotype, $TM3/+$ flies which resulted from the $e^1;pale^4/TM3$ x WT-ALA cross were also tested for their social behaviour.

Flies possessing the “stubble” phenotype did not present with an altered social behaviour compared to wild-type controls. This suggests that the stubble phenotype did not contribute to the altered social behaviour seen in $e^1;pale^4/TM3$ flies.

While this indicates that short bristles are not enough to alter *Drosophila* social behaviour, it does not rule out the possibility that touch is a sense used in social behaviour. Other mutants with a more drastic phenotype should be tested in order to investigate this possibility further.

4.2.4: Both $pale^4/+$ and $TM3/+$ Flies have Normal Visual Acuity

Since it was previously determined that visual acuity is necessary for social behaviour, $pale^4/+$ and $TM3/+$ flies were tested for visual acuity in order to ensure that the mutation did not cause any visual deficits which may have influenced sociality.

Both $pale^4/+$ and $TM3/+$ flies did not score differently from wild-type controls. Although $TM3/+$ flies had normal socialization levels, $pale^4/+$ flies had severe social defects compared to wild-type controls, indicating that these behavioural deficits were not due to a lack of visual acuity.

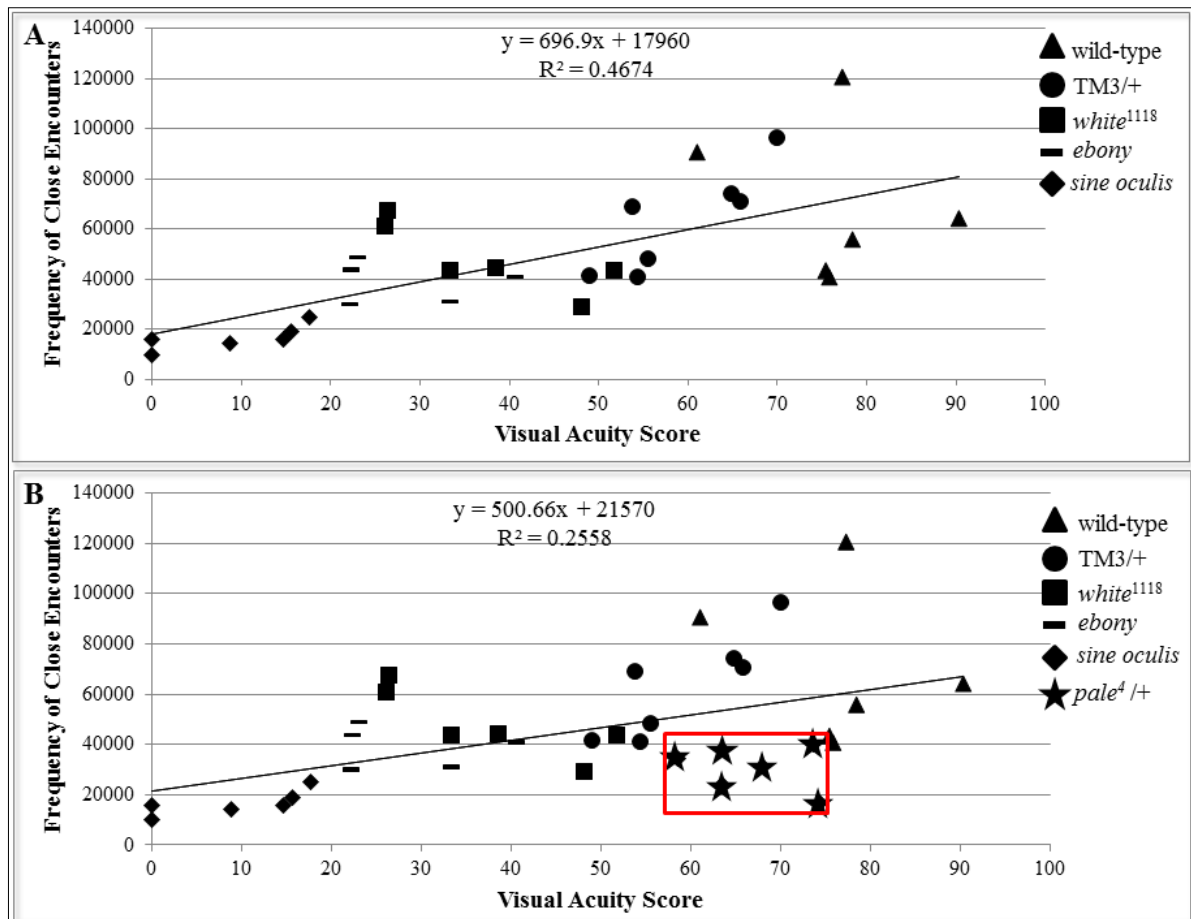


Fig. 4.2.4: Correlation between visual acuity score, as measured by a light maze, and the frequency of close encounters, defined by the number of times pairs of flies were within 5 body-lengths of each other. R^2 = coefficient of determination. Red box indicating data for *pale*⁴/+ flies, clear outliers in the correlation.

A further indication of this is the previously described correlation between visual acuity and close encounters. Adding the data for *TM3/+* flies to this correlation actually increases the significance of the correlation between visual acuity and frequency of close encounters (Pearson's correlation; $p = 0.00044$; d.f. = 22). Adding the data for the *ebony* mutants also does not alter the trendline, the coefficient of determination or the significance of the correlation very much compared to the correlation which only included the visual mutants (Fig. 4.2.4 A; Pearson's correlation; $p = 0.000031$; d.f. = 28). However, when we also add the data obtained from the *pale*⁴/+ flies, we can see that the trendline and the coefficient of determination are very different with respect to the previous correlation (Fig. 4.2.4 B). Also, the significance of this correlation is dramatically decreased (Pearson's correlation; $p = 0.026$; d.f. = 34). This is clear evidence that, while visual acuity is not affected in *pale*⁴/+ flies, they have significantly altered social behaviour, most likely due to lower levels of dopamine in their brains.

These data present the first evidence that dysregulation of dopamine in *Drosophila* can alter their social behaviour. We therefore suggest that this model can be used as a model for behaviour disorders in humans.

4.2.5: *ebony*^l Mutants have Social Defects

Since both overexpression and under-expression of dopamine is tied to behaviour disorders, and since the *e*¹;*pale*⁴/TM3 also contained the *ebony* mutation, *ebony*^l mutant flies, which overexpress dopamine in their brains, were also tested for social behaviour. These flies also exhibited significantly fewer close encounters and abnormal socialization plots compared to wild-type controls, although they did not have increased locomotor activity as was seen in *pale*⁴/+ flies.

However, it is also important to note that *ebony* mutants also had impaired visual acuity, which is consistent with previously reported retinograms from these flies (Hotta and Benzer, 1969). Because of this, an argument could be made that their social deficits are as a result of their visual deficits. However, it is important to note that *ebony*^l mutants scored similarly to *white*¹¹¹⁸ mutants in the light maze. While *ebony*^l mutants did not have significantly fewer close encounters compared to *white*¹¹¹⁸ flies (t-test with Bonferroni correction; p= 1.00; d.f.= 2), they did have different socialization plots compared to *white*¹¹¹⁸ flies. While *white*¹¹¹⁸ flies tend to cluster over time, despite the fact that they take longer to do so than wild-type flies, *ebony*^l mutants show no such clustering tendency over time, and their social indices do not reach those of *white*¹¹¹⁸ flies. This indicates that, while part of the social defects could be due to the visual defects they present with, these defects probably do not explain the entirety of them. Because of this, it was concluded that overexpression of dopamine in the *Drosophila* nervous system can also lead to social behaviour abnormalities, though not to the extent that reduced levels of dopamine can.

4.3: The Effect of the SNAP-25^{R206D} point-mutation on *Drosophila* Behaviour

Along with the investigation into the effect of the dysregulation of dopamine in the nervous system on social behaviour, we also investigated the potential role of the SNARE complex member SNAP-25 on social behaviour. This protein is integrally involved in the exocytosis of

neurotransmitters, but when it is knocked-out its function can be replaced by SNAP-24 (Vilinsky *et. al.*, 2002). Because of this, overexpressing a mutated version of SNAP-25 leads to the incorporation of a defective protein into the SNARE complex, often leading to more severe problems due to the malfunctioning exocytosis (Megighian *et. al.*, 2013). Since mutations in SNAP-25 have also been tied to behavioural disorders in humans, flies overexpressing a mutated form of SNAP-25 in the nervous system were tested for social behaviour.

4.3.1: SNAP-25 Mutants Socialize as *white*¹¹¹⁸ Flies Do

Flies expressing a mutated form of SNAP-25 in the nervous system did not have altered social behaviour compared to *white*¹¹¹⁸ flies. They did not have significantly fewer close encounters, altered locomotor activity or socialization plots compared to *white*¹¹¹⁸ controls.

*white*¹¹¹⁸ controls were used because of the fact that the overexpression of a mutated form of SNAP-25 was conducted in a *white*¹¹¹⁸ background. However, it is important to note that, as per usual when creating flies harbouring a genetic construct, a *white*⁺ marker was used in order to ensure successful recombination of the construct. Because of this, flies overexpressing mutated SNAP-25 actually had red eyes, and therefore should have been more similar in their social behaviour to wild-type rather than *white*¹¹¹⁸ controls.

Despite this, due to the integral role of SNAP-25 in the nervous system, it cannot be excluded that expressing mutated SNAP-25 in *Drosophila melanogaster* could lead to visual defects. Unfortunately, due to time constraints, SNAP-25^{R206D} mutant flies could not be tested for visual acuity. Although they have red eyes, a visual defect caused by the mutation could explain why their social behaviour is more similar to *white*¹¹¹⁸ rather than wild-type controls.

From these results, we can conclude that overexpressing a mutated form of SNAP-25 in the *Drosophila melanogaster* nervous system certainly does not alter their social behaviour to the extent that dopamine dysregulation does. Furthermore, if SNAP-25^{R206D} mutants present with visual defects in future studies, we will be able to conclude that this mutation does not affect social behaviour in *Drosophila melanogaster* at all.

4.3.2: SNAP-25 Mutants have Locomotor Activity Defects

Although flies expressing a mutated form of SNAP-25 in the nervous system did not present with significant social behaviour abnormalities, they did present with significantly reduced locomotor activity compared to *white*¹¹¹⁸ controls. SNAP-25^{R206D} mutants moved significantly slower and covered significantly less distance than *white*¹¹¹⁸ controls. However, an interesting point to note is that these flies also moved for significantly less time compared to *white*¹¹¹⁸ controls. In this, they were far more similar in their locomotor behaviour to eyeless *sine oculis* mutants, rather than to the *dTTC19* mutants analysed in Chapter II. This could indicate that their locomotor defect may not necessarily be due to a lack of energy production, as one would expect from mitochondrial dysfunction as seen in the *TTC19* mutant, but rather due to a lack of drive to explore their arena.

In sum, the locomotor defects measured in SNAP-25^{R206D} flies could be indicative of a neuromuscular defect, a visual defect, or both. Both the NMJ activity and the visual acuity of these flies should be investigated in future studies in order to explain these defects more thoroughly.

4.3.3: Flies can be Marked on the Abdomen but not on the Scutellum

A second statistical package to study social behaviour in *Drosophila* is in the process of being developed which is capable of indentifying each fly. This methodology has great potential for the study of the capabilities of flies to discriminate between each other, and whether or not flies segregate themselves into separate social groups based on their genotypes. However, to be able to take full advantage of this method for this purpose, a method of marking the flies in order for the researcher to be able to distinguish between genotypes which does not affect their behaviour needed to be developed.

To do this, non-volatile water-based enamel was chosen to mark the flies, in order to avoid volatile chemicals influencing the flies' behaviour by smell. Flies were marked either on the scutellum or on the abdomen under brief CO₂ anaesthesia, and their locomotor activity was analysed after exploratory behaviour was induced by starvation.

Flies marked on the abdomen did not have impaired locomotor activity compared to unmarked controls. However, when flies were marked on the scutellum they moved significantly less and

more slowly than unmarked controls (Section 3.3.3). This indicates that their impaired locomotor activity is most likely not due to the weight of the paint, as the size of the paint drop was similar between abdomen- and scutellum-marked flies. Instead, the locomotor impairment was most likely due to its placement. *Drosophila* have sensory bristles which cover the scutellum, although their use remains to be fully elucidated. It is possible that painting flies on the scutellum impregnates the bristles and thus overstimulates them, which somehow signals the flies to alter their locomotor behaviour. Whatever the reason, it is clear that these results should be kept in mind when marking flies for any behavioural analysis, and that marking them on the scutellum can alter their behaviour and thus should be avoided.

4.4: Concluding Remarks

From this study, a new and successful protocol was developed to study social behaviour in *Drosophila* using only open source software. This methodology confirms that *Drosophila melanogaster* form social groups between ZT5 and ZT9, and that they rely on visual cues to do so. Furthermore, this study indicates that dysregulation of dopamine, though not SNAP-25, and social isolation can cause social abnormalities in *Drosophila*. This is also true for flies heterozygous for the *pale*⁴ mutation, which do not have any other reported mutant phenotype, indicating that this method is capable of teasing out subtle defects in dopamine mutants. Because of this, we propose that social behaviour in *Drosophila melanogaster* can be used as a model for the genetic basis of neurological disorders which present with behavioural defects in humans (Piazzesi *et. al.*, *In Preparation*). This model also, at the very least, demonstrates that future studies into *Drosophila* behaviour should avoid using socially isolated flies, and at best may be useful as a model for the effects of social deprivation during infancy. In sum, we propose that the genetic basis for sociality be added to the long list of uses of *Drosophila melanogaster* as a model organism.

BIBLIOGRAPHY

- Allada, R., Kadener, S., Nandakumar, N., Rosbash, M. (2003). A recessive mutant of *Drosophila Clock* reveals a role in circadian rhythm amplitude. *EMBO Journal* 22(13): 3367-3375
- Allen, G. E. (1975). The Introduction of *Drosophila* into the Study of Heredity and Evolution: 1900-1910. *Isis* 66(3): 322-333
- Anderson, S., Bankier, A. T., Barrell, B. G., de-Brujin, M. H. L., Coulson, A. R., Drouin, J., Eperon, I. C., Nierlich, D. P., Roe, B. A., Sanger, F., Schreier, H. P., Smith, A. J. H., Stader, R., Young, I. G. (1981). Sequence and organization of the human mitochondrial genome. *Nature* 290: 427-465
- Andretic, R., van Swinderen, B., Greenspan, R. J. (2005). Dopaminergic Modulation of Arousal in *Drosophila*. *Current Biology* 15: 1165-1175
- Bainton, R. J., Tsai, L. T-Y., Singh, C. M., Moore, M. S., Neckameyer, W. S., Heberlein, U. (2000). Dopamine modulates acute responses to cocaine, nicotine and ethanol in *Drosophila*. *Current Biology* 15: 187-194
- Bang, S., Hyun, S., Hong, S.-T., Kang, J., Jeong, K., Park, J.-J., Choe, J., Cung, J. (2011). Dopamine Signalling in Mushroom Bodies Regulates Temperature-Preference Behaviour in *Drosophila*. *PLoS Genetics* 7(3): 1-12
- Baranzini, S. E., Wang, J., Gibson, R. A., Galwey, N., Naegelin, Y., Barkhof, F., Radue, E.-W., Lindberg, R. L. P., Uitdehaag, B. M. G., Johnson, M. R., Angelakopoulou, A., Hall, L., Richiardon, J. C., Prinjha, R. K., Gass, A., Geurts, J. J. G., Kragt, J., Sombekke, M., Vrenken, H., Qualley, P., Lincoln, R. R., Gomez, R., Caillier, S. J., George, M. F., Mousavi, H., Guerrero, R., Okuda, D. T., Cree, B. A. C., Green, A. J., Waubant, E., Goodin, D. S., Pelletier, D., Matthews, P. M., Hauser, S. L., Kappos, L., Polman, C. H., Oksenberg, J. R. (2009). Genome-wide association analysis of susceptibility and clinical phenotype in multiple sclerosis. *Human Molecular Genetics* 18(4): 767-778
- Beal, M. F. (2005). Less stress, longer life. *Nature Medicine* (11): 598-599
- Behrend, L., Henderson, G., Zwacka, R. M. (2003). Reactive oxygen species in oncogenic transformation. *Molecular Mechanisms of Signalling* 31(6): 1441-1444
- Bénil, P., Lebon, S., Rustin, P. (2009). Respiratory-chain diseases related to complex III deficiency. *Biochimica et Biophysica Acta* 1793: 181-185
- Biederman, J., Faraone, S. V. (2002). Current concepts on the neurobiology of Attention-Deficit/Hyperactivity Disorder. *Journal of Attention Disorders* 6(supp1): S7-S16
- Björklund, A., Dunnett, S. B. (2007). Dopamine neuron systems in the brain: an update. *Trends in Neurosciences* 30(5): 194-202
- Blaber, M. (2001). *Lecture 3: Electron Transport*. BCH 4053 Biochemistry I. Available at: <http://www.mikeblaber.org/oldwine/BCH4053/Lecture38/Lecture38.htm>

- Bolduc, F. V., Valente, D., Nguyen, A. T., Mitra, P. P., Tully, T. (2010). An assay for social interaction in *Drosophila fragile X* mutants. *Landes Bioscience* 4(3): 216-225
- Bottomley, S. S. (2006). Congenital sideroblastic anemias. *Current Hematology Reports* 5(1): 41-49
- Branson, K., Robie, A. A., Bender, J., Perona, P., Dickinson, M. H. (2009). High-throughput ethomics in large groups of *Drosophila*. *Nature Methods* 6: 451-457
- Breier, A., Su, T.-P., Saunders, R., Carson, R. E., Kolachana, B. S., de Bartolomeis, A., Weinberger, D. R., Weisenfeld, N., Malhotra, A. K., Eckelman, W. C., Pickar, D. (1997). Schizophrenia is associated with elevated amphetamine-induced synaptic dopamine concentrations: Evidence from a novel positron emission tomography method. *PNAS* 94(6): 2569-2574
- Bridges, C. B., Anderson, E. G. (1925). Crossing Over in the X Chromosomes of Triploid Females of *Drosophila melanogaster*. *Genetics* 10: 418-441
- Brown, T. A., Cecconi, C., Tkachuk, A. N., Bustamante, C., Clayton, D. A. (2005). Replication of mitochondrial DNA occurs by strand displacement with alternative light-strand origins, not via a strand-coupled mechanism. *Genes and Development* 19: 2466-2476
- Byrne, P. G., Rice, W. R. (2006). Evidence for adaptive male mate choice in the fruit fly *Drosophila melanogaster*. *Proceedings of the Royal Society of Biological Sciences*. 273(1589): 917-922
- Cai, F., Chen, B., Zhou, W., Zis, O., Liu, S., Holt, R. A., Honer, W. G., Song, W. (2008). SP1 regulates a human *SNAP-25* gene expression. *Journal of Neurochemistry* 105: 512-523
- Cannon, C. M., Bseikri, M. R. (2004). Is dopamine required for natural reward? *Physiology & Behavior* 81: 741-748
- Carelli, V., Ross-Cisneros, F. N., Sadun, A. A. (2004). Mitochondrial dysfunction as a cause of optic neuropathies. *Progress in Retinal and Eye Research* 23(1): 53-89
- Carlson, M., Earls, F. (1997). Psychological and Neuroendocrinological Sequelae of Early Social Deprivation in Institutionalized Children in Romania. *Annals of the New York Academy of Sciences* 807: 419-428
- Carlsson, A. (1988). The current status of the dopamine hypothesis of schizophrenia. *Neuropsychopharmacology* 1(3): 179-186
- Cavanillas, M. L., Fernández, O., Comabella, M., Alcina, A., Fedetz, M., Izquierdo, G., Lucas, M., Cénit, M. C., Arroyo, R., Vandenbroeck, K., Alloza, I., García-Barcina, M., Antigüedad, A., Leyva, L., Gómez, C. L., Olascoaga, J., Otaegui, D., Blanco, Y., Saiz, A., Montalbán, X., Matesanz, F., Urcelay, E. (2011). Replication of top markers of a genome-wide association study in multiple sclerosis in Spain. *Genes and Immunity* 12: 110-115

- Chaudhuri, K. R., Schapira, A. H. V. (2009). Non-motor symptoms of Parkinson's disease: dopaminergic pathophysiology and treatment. *Lancet Neurology* 8: 464-474
- Chugani, H. T., Behen, M. E., Muzik, O., Juhász, C., Nagy, F., Chugani, D. C. (2001). Local Brain Functional Activity Following Early Deprivation: A Study of Postinstitutionalized Romanian Orphans. *NeuroImage* 14: 1290-1301
- Chen, Y. A., Scheller, R. H. (2001). SNARE-mediated membrane fusion. *Nature Reviews Molecular Cell Biology* 2: 98-106
- Collins, C. A., DiAntonio, A. (2007). Synaptic development: insights from *Drosophila*. *Current Opinion in Neurobiology* 17: 35-42
- Copeland, W. C. (2008). Inherited Mitochondrial Diseases of DNA Replication. *Annual Review of Medicine* 59: 131-146
- Cottrell, G. A. (1967). Occurrence of Dopamine and Noradrenaline in the Nervous Tissue of Some Invertebrate Species. *British Journal of Pharmacology and Chemotherapy* 29(1): 63-69
- Crowther, D. C., Kinghorn, K. J., Miranda, E., Page, R., Curry, J. A., Duthie, F. A. I., Gubb, D. C., Lomas, D. A. (2005). Intraneuronal A β , non-amyloid aggregates and neurodegeneration in a *Drosophila* model of Alzheimer's disease. *Neuroscience* 132(1): 123-136
- Da Re, C., Franzolin, E., Biscontin, A., Piazzesi, A., Pacchioni, B., Gagliani, M. C., Mazzotta, G., Tacchetti, C., Zordan, M. A., Zeviani, M., Bernardi, P., Bianchi, V., De Pittà, C., Costa, R. (2013). Functional characterization of drim2, the *Drosophila melanogaster* homolog of the yeast mitochondrial deoxynucleotide transporter. *Accepted for Publication by The Journal of Cell Biology*
- de Lonlay, P., Valnot, I., Barrientos, A., Gorbatyuk, M., Tzagoloff, A., Taanman, J. W., Benayoun, E., Chretien, D., Kadhom, N., Lombes, A., de Baulny, H. O., Niaudet, P., Munnich, A., Rustin, P., Rotig, A. (2001). A mutant mitochondrial respiratory chain assembly protein causes complex III deficiency in patients with tubulopathy, encephalopathy and liver failure. *Nature Genetics* 29: 57-60
- Démolis, N., Mallet, L., Bussereau, F., Jacquet, M. (1993). *RIM2*, *MSII* and *PGII* and located within an 8 kb segment of *Saccharomyces cerevisiae* chromosome II, which also contains the putative essential gene with a leucine zipper motif. *Yeast Sequencing Report* 9(6): 645-659
- Diaper, D. C., Adachi, Y., Sutcliffe, B., Humphrey, D. M., Elliot, C. J. H., Stepto, A., Ludlow, Z. N., Vanden Broeck, L., Callaerts, P., Dermaut, B., Al-Chalabi, A., Shaw C. E., Robinson, I. M., Hirth, F. (2013). Loss and gain of *Drosophila* TDP-43 impair synaptic efficacy and motor control leading to age-related neurodegeneration by loss-of-function phenotypes. *Human Molecular Genetics* 22(8): 1539-1557
- Dolce, V., Fiermonte, G., Runswick, M. J., Palmieri, F. (2001). The human mitochondrial deoxynucleotide carrier and its role in the toxicity of nucleoside antivirals. *PNAS* 98(5): 2284-2288

- Dougherty, D. D., Bonab, A. A., Spencer, T. J., Raunch, S. L., Madras, B. K., Fischman, A. J. (1999). Dopamine transporter density in patients with attention deficit hyperactivity disorder. *The Lancet* 354: 2132-2133
- Dresel, S., Krause, J., Krause, K. H., LaFougere, C., Brinkbaumer, K., Kung, H. F., Hahn, K., Tatsch, K. (2000). Attention deficit hyperactivity disorder: binding of [^{99m}Tc]TRODAT-1 to the dopamine transporter before and after methylphenidate treatment. *European Journal of Nuclear Medicine* 27(10): 1518-1524
- Duffy, J. B. (2002). GAL4 System in *Drosophila*: A Fly Geneticist's Swiss Army Knife. *Genesis* 34(1-2): 1-15
- Dumoulin, R., Sagnol, I., Ferlin, T., Bozon, D., Stepien, G., Mousson, B. (1996). A novel gly290asp mitochondrial cytochrome *b* mutation linked to a complex III deficiency in progressive exercise intolerance. *Molecular and Cellular Probes* 10: 389-391
- Egli, D., Selvaraj, A., Yepiskoposyan, H., Zhang, B., Hafen, E., Georgiev, O., Schaffner, W. (2003). Knockout of "metal-responsive transcription factor" MTF-1 in *Drosophila* by homologous recombination reveals its central role in heavy metal homeostasis. *EMBO Journal* 22(1): 100-108
- Eluvathingal, T. J., Chugani, H. T., Behen, M. E., Juhász, C., Muzik, O., Maqbool, M., Chugani, D. C., Makki, M. (2006). Abnormal Brain Connectivity in Children After Early Severe Socioemotional Deprivation: A Diffusion Tensor Imaging Study. *Pediatrics* 117(6): 2093-2100
- Ernster, L. and Schatz, G. (1981). Mitochondria: A Historical Review. *The Journal of Cell Biology* 91(3): 227s-255s
- Faraone, S. V., Perlis, R. H., Doyle, A. E., Smoller, J. W., Gorlanick, J. J., Holmgren, M. A., Sklar, P. (2005). Molecular Genetics of Attention-Deficit/Hyperactivity Disorder. *Biological Psychiatry* 57: 1313-1323
- Favre, C., Zhdanov, A., Leahy, M., Papkovsky, D., O'Connor, R. (2010). Mitochondrial pyrimidine nucleotide carrier (PNC1) regulates mitochondrial biogenesis and the invasive phenotype of cancer cells. *Oncogene* 29: 3964-3976
- Feany, M. B., Bender, W. W. (2000). A *Drosophila* model of Parkinson's disease. *Nature* 404: 394-398
- Ferraro, P., Nicolosi, L., Bernardi, P., Reichard, P., Bianchi, V. (2006). Mitochondrial deoxynucleotide pool sizes in mouse liver and evidence for a transport mechanism for thymidine monophosphate. *PNAS* 103(49): 18586-18591
- Fisher, L., Ames, E. W., Chisholm, K., Savoie, L. (1997). Problems Reported by Parents of Romanian Orphans Adopted to British Columbia. *International Journal of Behavioral Development*. 20(1): 67-82

- Floyd, S., Favre, C., Lasorsa, F. M., Leahy, M., Trigiantè, G., Stroebel, P., Marx, A., Loughran, G., O'Callaghan, K., Marobbio, C. M. T., Slotboom, D. J., Kunji, E. R. S., Palmieri, F., O'Connor, R. (2007). The Insulin-like Growth Factor-I-mTOR Signaling Pathway Induces the Mitochondrial Pyrimidine Nucleotide Carrier to Promote Cell Growth. *Molecular Biology of the Cell* 18(9): 3545-3555
- Franzolin, E., Miazzi, C., Frangini, M., Palumbo, E., Rampazzo, C., Bianchi, V. (2012). The pyrimidine nucleotide carrier PNC1 and mitochondrial trafficking of thymidine phosphates in cultured human cells. *Experimental Cell Research* 318(17): 2226-2236
- Freisinger, P., Futterer, N., Lankes, E., Gempel, K., Berger, T. M., Spalinger, J., Hoerbe, A., Schwantes, C., Linder, M., Santer, R., Burdelski, M., Schaefer, H., Setzer, B., Walker, U. A., Horvath, R. (2006). Hepatocerebral mitochondrial DNA depletion syndrome caused by deoxyguanosine kinase (DGUOK) mutations. *Archives of Neurology* 63(8):1129–1134.
- Friggi-Grelin, F., Iché, M., Birman, S. (2003). Tissue-Specific Developmental Requirements of *Drosophila* Tyrosine Hydroxylase Isoforms. *Genesis* 35: 260-269
- Froschauer, E. M., Rietzchel, N., Hassler, M. R., Binder, M., Schweyen, R. J., Lill, R., Mühlhoff, U., Wiesenberger, G. (2013). The mitochondrial carrier RIM2 co-imports pyrimidine nucleotides and iron. *Biochemical Journal* 455: 57-65
- Garesse, R., Kaguni, L. S. (2005). A *Drosophila* Model of Mitochondrial DNA Replication: Proteins, Genes and Regulation. *IUBMB Life* 57(8): 555-561
- Gateff, E., Scheiderman, H. (1967). Developmental studies of a new mutant of *Drosophila melanogaster*: Lethal malignant brain tumor (l(2)gl 4). *American Zoologist* 7: 760.
- Ghezzi, D., Arzuffi, P., Zordan, M., Da Re, C., Lamperti, C., Benna, C., D'Adamo, P., Diodato, D., Costa, R., Mariotti, C., Uziel, G., Smiderle, C., Zeviani, M. (2011). Mutations in *TTC19* cause mitochondrial complex III deficiency and neurological impairment in humans and flies. *Nature Genetics* 43: 259-263
- Gibert, J.-M., Peronnet, F., Schlötter, C. (2007). Phenotypic Plasticity in *Drosophila* Pigmentation Caused by Temperature Sensitivity of a Chromatin Regulator Network. *PLoS Genetics* 3(2): e30
- González-Vioque, E., Torres-Torronteras, J., Andreu, A. L., Martí, R. (2011). Limited dCTP Availability Accounts for Mitochondrial DNA Depletion in Mitochondrial Neurogastrointestinal Encephalomyopathy (MNGIE). *PLoS Genetics* 7(3): e1002035
- Guernsey, D. L., Jiang, H., Campagna, D. R., Evans, S. C., Ferguson, M., Kellogg, M. D., Lachance, M., Matsuoka, M., Nightingale, M., Rideout, A., Saint-Amant, L., Schmidt, P. J., Orr, A., Bottomley, S. S., Fleming, M. D., Ludman, M., Dyack, S., Fernandez, C. V., Samuels, M. E. (2009). Mutations in mitochondrial carrier family gene *SLC25A38* cause nonsyndromic autosomal recessive congenital sideroblastic anemia. *Nature Genetics* 41: 651-653

- Gunnar, M. R., Morison, S. J., Chisholm, K., Schuder, M. (2001). Salivary cortisol levels in children adopted from Romanian orphanages. *Development and Psychopathology* 3: 611-628
- Guo, X., Macleod, G. T., Wellington, A., Hu, F., Panchumarthi, S., Schoenfield, M., Marin, L., Charlton, M. P., Atwood, H. L., Zinsmaier, K. E. (2005). The GTPase dMiro Is Required for Axonal Transport of Mitochondria to *Drosophila* Synapses. *Neuron* 47(3): 379-393
- Haas, R. H., Nasirian, F., Nakano, K., Ward, D., Pay, M., Hill, R., Shults, C. W. (1995). Low platelet mitochondrial complex I and complex II/III activity in early untreated parkinson's disease. *Annals of Neurology* 37(6): 714-722
- Haitina, T., Lindblom, J., Renström, T., Fredriksson, R. (2006). Fourteen novel human members of mitochondrial solute carrier family 25 (SLC25) widely expressed in the central nervous system. *Genomics* 88(6): 779-790
- Heinz, A., Schlagenhaut, F. (2010). Dopaminergic Dysfunction in Schizophrenia: Salience Attribution Revisited. *Schizophrenia Bulletin* 36(3): 472-485
- Holt, I. J., Lorimer, H. E., Jacobs, H. T. (2000). Coupled Leading- and Lagging-Strand Synthesis of Mammalian Mitochondrial DNA. *Cell* 100(5): 515-524
- Hotta, Y., Benzer, S. (1969). Abnormal Electroretinograms in Visual Mutants of *Drosophila*. *Nature* 222(5191): 354-356
- Huelsenbeck, J. P., Ronquist, F. (2001). MRBAYES: Bayesian inference of phylogenetic trees. *Bioinformatics* 17: 754-755.
- Hull, E. M., Muschamp, J. W., Sato, S. (2004). Dopamine and serotonin: influences on male sexual behavior. *Physiology & Behaviour* 83: 291-307
- Humphrey, D. M., Parsons, R. B., Ludlow, Z. N., Riemensperger, T., Esposito, G., Verstreken, P., Jacobs, H. T., Birman, S., Hirth, F. (2012). *Alternative oxidase* rescues mitochondria-mediated dopaminergic cell loss in *Drosophila*. *Human Molecular Genetics* 21(12): 2698-2712
- Iwata, S., Lee, J. W., Okada, K., Lee, J. K., Iwata, M., Rasmussen, B., Link, T. A., Ramaswamy, S., Jap, B. K. (1996). Complete Structure of the 11-Subunit Bovine Mitochondrial Cytochrome bc₁ Complex. *Science* 281(5373): 64-71
- Kaun, K. R., Azanchi, R., Maung, Z., Hirsh, J., Heberlein, U. (2011). A *Drosophila* model for alcohol reward. *Nature Neuroscience* 14: 612-619
- Keightley, J. A., Anitori, R., Burton, M. D., Quan, F., Buist, N. R. M., Kennaway, N. G. (2000). Mitochondrial Encephalomyopathy and Complex III Deficiency Associated with a Stop-Codon Mutation in the Cytochrome *b* Gene. *American Journal of Human Genetics* 67: 1400-1410
- Kelley, R. I., Robinson, D., Puffenberger, E. G., Strauss, K. A., Morton, D. H. (2002). Amish lethal microcephaly: a new metabolic disorder with severe congenital microcephaly and 2-ketoglutaric aciduria. *American Journal of Medical Genetics* 112(4):318-326.

- Kindt, K. S., Quast, K. B., Giles, A. C., De, S., Hendrey, D., Nicastro, I., Rankin, C. H., Schafer, W. R. (2007). Dopamine Mediates Context-Dependent Modulation of Sensory Plasticity in *C. elegans*. *Neuron* 55(4): 662-676
- Koide, K., Slonim, D. K., Johnson, K. L., Tantravahi, U., Cowan, J. M., Bianchi, D. W. (2011). Transcriptomic analysis of cell-free fetal RNA suggests a specific molecular phenotype in trisomy 18
- Kramer, J. M., Staveley, B. E. (2003). GAL4 causes developmental defects and apoptosis when expressed in the developing eye of *Drosophila melanogaster*. *Genetics and Molecular Research* 2(1): 43-47
- Kumakura, Y., Cumming, P., Vernaleken, I., Buchholz, H.-G., Siessmeier, T., Heinz, A., Kienast, T., Bartenstein, P., Gründer, G. (2007). Elevated [¹⁸F]Fluorodopamine Turnover in Brain of Patients with Schizophrenia: An [¹⁸F]Fluorodopa/Positron Emission Tomography Study. *The Journal of Neuroscience* 27(30): 8080-8087
- Kume, K., Kume, S., Park, S. K., Hirsh, J., Jackson, F. R. (2005) Dopamine Is a Regulator of Arousal in the Fruit Fly. *The Journal of Neuroscience* 25(32): 7377-7384
- Kunji, E. R. S., Robinson, A. J. (2006). The conserved substrate binding site of mitochondrial carriers. *Biochimica et Biophysica Acta – Bioenergetics* 1757(9-10): 1237-1248
- Lamantea, E., Carrara, F., Mariotti, C., Morandi, L., Tiranti, V., Zeviani, M. (2001). A novel mutation (Q352X) in the mitochondrial cytochrome *b* gene associated with a combined deficiency of complexes I and III. *Neuromuscular Disorders* 12: 49-52
- Laruelle, M., Abi-Dargham, A., Van Dyck, C. H., Gil, R., D'Souza, C. D., Erdos, J., McCance, E., Rosenblatt, W., Fingado, C., Zoghbi, S. S., Baldwin, R. M., Seibyl, J. P., Krystal, J. H., Charney, D. S., Innis, R. B. (1996). Single photon emission computerized tomography imaging of amphetamine-induced dopamine release in drug-free schizophrenic patients. *PNAS* 93: 9235-9240
- Lee, W.-C. M., Yoshihara, M., Littleton, J. T. (2004). Cytoplasmic aggregates trap polyglutamine-containing proteins and block axonal transport in a *Drosophila* model of Huntington's disease. *PNAS* 101(9): 3224-3229
- Lightowers, R. N., Chrzanowska-Lightowers, Z. M. A. (2012). Exploring our origins – the importance of OriL in mtDNA maintenance and replication. *EMBO reports* 13: 1038-1039
- Lill, R., Kispal, G. (2000). Maturation of cellular Fe-S proteins: an essential function of mitochondria. *Trends in Biochemical Sciences* 8(1): 352-356
- Lin, H., Li, L., Jia, X., Ward, D. M., Kaplan, J. (2011). Genetic and Biochemical Analysis of High Iron Toxicity in Yeast: Iron Toxicity is Due to the Accumulation of Cytosolic Iron and Occurs Under Both Aerobic and Anaerobic Conditions. *The Journal of Biological Chemistry* 286: 3851-3862

- Liu, T., Dartevelle, L., Yuan, C., Wei, H., Wang, Y., Ferveur, J.-F., Guo, A. (2008). Increased Dopamine Level Enhances Male-Male Courtship in *Drosophila*. *The Journal of Neuroscience* 28(21): 5539-5546
- Lodish, H., Berk, A., Kaiser, C. A., Krieger, M., Scott, M. P., Bretscher, A., Ploegh, H., Matsudaria, P. (2007). *Molecular Cell Biology*, Sixth Edition. W. H. Freeman Inc. ISBN-13: 978-0716776017
- Loya, C. M., Lu, C. S., Van Vactor, D., Fulga, T. A. (2009). Transgenic microRNA inhibition with spatiotemporal specificity in intact organisms. *Nature Methods* 6: 897-903
- Mackenzie, S. M., Brooker, M. R., Gill, T. R., Cox, G. B., Howells, A. J., Ewart, G. D. (1999). Mutations in the *white* gene of *Drosophila melanogaster* affecting ABC transporters that determine eye colouration. *Biochimica et Biophysica Acta – Biomembranes*. 1419(2): 173-185
- Madras, B. K., Miller, G. M., Fischman, A. J. (2005). The Dopamine Transporter and Attention-Deficit/Hyperactivity Disorder. *Biological Psychiatry* 57(11): 1397-1409
- Magnusson, J., Orth, M., Lestienne, P., Taanman, J.-W. (2003). Replication of mitochondrial DNA occurs throughout the mitochondria of cultured human cells. *Experimental Cell Research* 289(1): 133-142
- Mancuso, M., Filosto, M., Stevens, J. C., Patterson, M., Shanske, S., Krishna, S., DiMauro, S. (2003). Mitochondrial myopathy and complex III deficiency in a patient with a new stop-codon mutation (G339X) in the cytochrome *b* gene. *Journal of Neurological Sciences* 209: 61-63
- Marobbio, C. M., Di Noia, M. A., Palmieri, F. (2006). Identification of a mitochondrial transporter for pyrimidine nucleotides in *Saccharomyces cerevisiae*: bacterial expression, reconstitution and functional characterization. *Biochemical Journal* 393: 441-446
- Mathews, C. K., Song, S. (2007). Maintaining precursor pools for mitochondrial DNA replication. *The FASEB Journal* 21(10): 2294-2303
- McClung, C., Hirsh, J. (1998). Stereotypic behavioural responses to free-base cocaine and the development of behavioral sensitization in *Drosophila*. *Current Biology* 8(2): 109-112
- McGuire, S. E., Mao, Z., Davis, R. L. (2004). Spatiotemporal Gene Expression Targeting with the TARGET and Gene-Switch Systems in *Drosophila*. *Science* 2004(220): p16
- Meaney, M. J., Aitken, D. H., Bodnoff, S. R., Iny, L. J., Sapolsky, R. M. (1985). The effects of postnatal handling on the development of the glucocorticoid receptor systems and stress recovery in the rat. *Progress in Neuro-Psychopharmacology & Biological Psychiatry* 9(5-6): 731-734
- Megighian, A., Zordan, M., Pantano, S., Scorzeto, M., Rigoni, M., Zanini, D., Rossetto, O., Montecucco, C. (2013). Evidence for a radial SNARE super-complex mediating neurotransmitter release at the *Drosophila* neuromuscular junction. *Journal of Cell Science* 127(2): 1-22

- Missirlis, F., Holmberg, S., Georgieva, T., Dunkov, B. C., Rouault, T. A., Law, J. H. (2006). Characterization of mitochondrial ferritin in *Drosophila*. *PNAS* 103(15): 5893-5898
- Mojtabai, R. (2010). Mental illness stigma and willingness to seek mental health care in the European Union. *Social Psychiatry and Psychiatric Epidemiology* 45(7): 705-712
- Molinari, F., Raas-Rothschild, A., Rio, M., Fiermonte, G., Encha-Razavi, F., Palmieri, L., Palmieri, F., Ben-Neriah, Z., Kadhom, N., Vekemans, M., Attié-Bitach, T., Munnich, A., Rustin, P., Colleaux, L. (2005). Impaired Mitochondrial Glutamate Transport in Autosomal Recessive Neonatal Myoclonic Epilepsy. *AJHG* 76(2): 334-339
- Montoya, J., Lòpez-Pèrez, M. J., Ruiz-Pesini, E. (2006). Mitochondrial DNA transcription and diseases: Past, present and future. *Biochimica et Biophysica Acta – Bioenergetics* 1757(9-10): 1179-1189
- Mòran, M., Marin-Buera, L., Gil-Borlado, M. C., Rivera, H., Blàzquez, A., Seneca, S., Vázquez-Lòpez, M., Arenas, J., Martìn, M. A., Ugalde, C. (2010). Cellular pathophysiological consequences of *BCS1L* mutations in mitochondrial complex III enzyme deficiency. *Human Mutation* 31(8): 930-941
- Morgan, T. H. (1910). Sex-limited inheritance in *Drosophila*. *Science* 32:120-122.
- Morgan, T. H. (1911). Random segregation versus coupling in Mendelian inheritance. *Science* 34: 384
- Mùhlenhoff, U., Stadler, J. A., Richhardt, N., Seubert, A., Eickhorst, T., Schweyen, R. J., Lill, R., Wiesenberger, G. (2003). A Specific Role of the Yeast Mitochondrial Carriers Mrs3/4p under Iron Limiting Conditions. *The Journal of Biological Chemistry* 278: 40612-40620
- Muller, H. J. (1928). The Production of Mutations by X-Rays. *PNAS* 14(9): 714-726
- Musil, R., Spellmann, I., Riedel, M., Dehning, S., Douhet, A., Maino, K., Zill, P., Müller, N., Möller, H.-J., Bondy, B. (2008). SNAP-25 gene polymorphisms and weight gain in schizophrenic patients. *Journal of Psychiatric Research* 42(12): 963-970
- Nantes, I. L., Mugnol, K. C. U. (2008). Incorporation of Respiratory Cytochromes in Liposomes: An Efficient Strategy to Study the Respiratory Chain. *Journal of Liposome Research* 18(3): 175-194
- National Research Council (2000). *Scientific Frontiers in Developmental Toxicology and Risk Assessment*. Washington, DC: The National Academies Press.
- Neckameyer, W. S., White, K. (1993). *Drosophila* Tyrosine Hydroxylase is Encoded by the *Pale* Locus. *Journal of Neurogenetics* 8(4): 189-199
- Neckameyer, W. S., Woodrome, S., Holt, B., Mayer, A. (1999). Dopamine and senescence in *Drosophila melanogaster*. *Neurobiology of Aging* 21: 145-152

- Newby, L. M., Jackson, F. R. (1991). *Drosophila Ebony* Mutants Have Altered Circadian Activity Rhythms but Normal Eclosion Rhythms. *Journal of Neurogenetics* 7(2-3): 85-101
- Nie, G., Sheftel, A. D., Kim, S. F., Ponka, P. (2004). Overexpression of mitochondrial ferritin causes cytosolic iron depletion and changes iron homeostasis. *Blood* 105(5): 2161-2167
- Nogueira, C., Barros, J., Sà, M. J., Azevedo, L., Taipa, R., Torracó, A., Meschini, M. C., Verrigni, D., Nesti, C., Rizza, T., Teixeira, J., Carrozzo, R., Pires, M. M., Vilarinho, L., Santorelli, F. M. (2013). Novel *TTC19* mutation in a family with severe psychiatric manifestations and complex III deficiency. *Neurogenetics* 14: 153-160
- Owens, K. M., Kulawiec, M., Desouki, M. M., Vanniarajan, A., Singh, K. K. (2011). Impaired OXPHOS Complex III in Breast Cancer. *PLoS One* 6(8): e23846
- Oyler, G. A., Higgins, G. A., Hart, R. A., Battenberg, E., Billingsley, M., Bloom, F. E., Wilson, M. C. (1989). The identification of a novel synaptosomal-associated protein, SNAP-25, differentially expressed by neuronal subpopulations. *JCB* 109(6): 3039-3052
- Palmieri, F. (2004). The mitochondrial transporter family (SLC25): physiological and pathological implications. *European Journal of Physiology* 447: 689-709
- Palmieri, F. (2008). Diseases caused by defects of mitochondrial carriers: A review. *Biochimica et Biophysica Acta* 1777: 564-578
- Palmieri, F. (2013). The mitochondrial transporter family SLC25: Identification, properties and physiopathology. *Molecular Aspects of Medicine* 34(2-3): 465-484
- Parks, A. L., Cook, K. R., Belvin, M., Dompe, N. A., Fawcett, R., Huppert, K., Tan, L. R., Winter, C. G., Bogart, K. P., Deal, J. E., Deal-Herr, M. E., Grant, D., Marcinko, M., Miyazaki, W. Y., Robertson, S., Shaw, K. J., Tabios, M., Vysotskaia, V., Zhao, L., Andrade, R. S., Edgar, K. A., Howie, E., Killpack, K., Milash, B., Norton, A., Thao, D., Whittaker, K., Winner, M. A., Friedman, L., Margolis, J., Singer, M. A., Kopczynski, C., Curtis, D., Kaufman, T. C., Plowman, G. D., Duyk, G., Francis-Lang, H. L. (2004). Systematic generation of high-resolution deletion coverage of the *Drosophila melanogaster* genome. *Nature genetics* 36(3): 288-293
- Pendleton, R. G., Rasheed, A., Hillman, R. (2000). Catecholamine effects upon behavior and development in *Drosophila*. *Drug Development Research* 50: 142-146
- Pendleton, R. G., Rasheed, A., Sardina, T., Tully, T., Hillman, R. (2002). Effects of Tyrosine Hydroxylase Mutants on Locomotor Activity in *Drosophila*: A Study in Functional Genomics. *Behavior Genetics* 32(2): 89-94
- Penta, J. S., Johnson, F. M., Wachsman, J. T., Copeland, W. C. (2001). Mitochondrial DNA in human malignancy. *Mutation Research/Reviews in Mutation Research* 488(2): 119-133
- Piazzesi, A., Da Re, C., Biscontin, A., Doimo, M., Mazzotta, G., Zordan, M. A., Grapputo, A., Tosatto, S., Salviati, L., Zeviani, M., Bernardi, P., De Pittà, C., Costa, R. (2014). Larval phenotype and rescue by the two human homologs *SLC25A33* and *SLC25A36* of an adult-lethal

knockout of the *Drosophila melanogaster* mitochondrial deoxynucleotide transporter *drim2*. *Paper in Preparation*

Piazzesi, A., Megighian, A., Sandrelli, F., Zordan, M. A. (2014). Social interaction in *Drosophila melanogaster* is influenced by visual acuity and by dopamine levels. *Paper in Preparation*

Politis, M., Piccini, P., Pavese, N., Brooks, D. J. (2008). Evidence of dopamine dysfunction in the hypothalamus of patients with Parkinson's disease: an in vivo 11C-raclopride study. *Experimental Neurology* 214: 112-116

Ponka, P. (1997). Tissue-Specific Regulation of Iron Metabolism and Heme Synthesis: Distinct Control Mechanisms in Erythroid Cells. *Blood* 89(1): 1-25

Prezant, T. R., Agopian, J. V., Bohlman, C., Bu, X., Öztas, S., Qiu, W.-Q., Arnos, K. S., Cortopassi, G. A., Jaber, L., Rotter, J. I., Shohat, M., Fischel-Ghodsian, N. (1993). Mitochondrial ribosomal RNA mutation associated with both antibiotic-induced and non-syndromic deafness. *Nature Genetics* (4): 289-294

Puffer, E. B., Lomneth, R. B., Sarkar, H. K., Singh, B. R. (2001). Differential Roles of Developmentally Distinct SNAP-25 Isoforms in the Neurotransmitter Release Process. *Biochemistry* 40: 9374-9378

Purves, D., Augustine, G. J., Fitzpatrick, D., Katz, L. C., LaMantia, A.-S., McNamara, J. O., Williams, S. M. (2001). Neuroscience, 2nd Edition. *Sunderland (MA): Sinauer Associates* available at: <http://www.biog1445.org/demo/09/synthesispackaging.html>

Ramadan, H., Alawi, A. A., Alawi, M. A. (1993). Catecholamines in *Drosophila melanogaster* (wild type and ebony mutant) decuticularized retinas and brains. *Cell Biology International* 17(8): 765-771

Rao, S. S., Stewart, B. A., Rivlin, P. K., Vilinsky, I., Watson, B. O., Lang, C., Boulianne, G., Salpeter, M. M., Deitcher, D. L. (2001). Two distinct effects on neurotransmission in a temperature-sensitive SNAP-25 mutant. *The EMBO Journal* 20(23): 6761-6771

Reiter, L. T., Potocki, L., Chien, S., Gribskov, M., Bier, E. (2001). A Systematic Analysis of Human Disease-Associated Gene Sequences In *Drosophila melanogaster*. *Genome Research* 11(6): 1114-1125

Remy, P., Doder, M., Lees, A., Turjanski, N., Brooks, D. (2005). Depression in Parkinson's disease: loss of dopamine and noradrenaline innervation in the limbic system. *Brain* 128(6): 1314-1322

Richardson, D. R., Lane, D. J. R., Becker, E. M., Huang, M. L.-H., Whitnall, M., Rahmanto, Y. S., Sheftel, A. D., Ponka, P. (2010). Mitochondrial iron trafficking and the integration of iron metabolism between the mitochondrion and cytosol. *PNAS* 107(24): 10775-10782

- Riemensperger, T., Völler, T., Stock, P., Buchner, E., Fiala, A. (2005). Punishment prediction by dopaminergic neurons in *Drosophila*. *Current Biology* 15(21): 1953-1960
- Risinger, C., Blomqvist, A. G., Lundell, I., Lambertsson, A., Nässel, D., Pieribone, V. A., Brodin, L., Larhammar, D. (1993). Evolutionary conservation of synaptosome-associated protein 25 kDa (SNAP-25) shown by *Drosophila* and *Torpedo* cDNA clones. *The Journal of Biological Chemistry* 268: 24408-24414
- Rizo, J., Südhof, T. C. (2002). SNAREs and MUNC18 in Synaptic Vesicle Fusion. *Nature Reviews Neuroscience* 3: 641-653
- Saada, A. (2009). Fishing in the (deoxyribonucleotide) pool. *Biochemical Journal* 422: e3-e6
- Saada, A., Shaag, A., Mandel, H., Nevo, Y., Eriksson, S., Elpeleg, O. (2001). Mutant mitochondrial thymidine kinase in mitochondrial DNA depletion myopathy. *Nature Genetics* 29:342–344
- Saha, S., Chant, D., McGrath, J. (2007). A systematic review of mortality in schizophrenia: is the differential mortality gap worsening over time? *Archives of General Psychiatry* 64: 1123-1131
- Salviati, L., Sacconi, S., Mancuso, M., Otaegui, D., Camaño, P., Marina, A., Rabinowitz, S., Shiffman, R., Thompson, K., Wilson, C. M., Feigenbaum, A., Naini, A. B., Hirano, M., Bonilla, E., DiMauro, S., Vu, T. H. (2002). Mitochondrial DNA depletion and dGK gene mutations. *Annals of Neurology* 52(3):311–317.
- Samii, A., Nutt, J. G., Ransom, B. R. (2004). Parkinson's Disease. *The Lancet* 363(9423): 1783-1793
- Sánchez, E., Lobo, T., Fox, J. L., Zeviani, M., Winge, D. R., Fernández-Vizarra, E. (2013). LYRM7/MZM1L is a UQCRC1 chaperone involved in the last steps of mitochondrial Complex III assembly in human cells. *Biochimica et Biophysica Acta – Bioenergetics* 1827(3): 286-293
- Sanchèz-Martinèz, A., Luo, N., Clemente, P., Adàn, C., Hernández-Sierra, R., Ochoa, P., Fernández-Moreno, M. Á., Kaguni, L. S., Garesse, R. (2006). Modelling human mitochondrial diseases in flies. *Biochimica et Biophysica Acta* 1757(9-10): 1190-1198
- Scheffler, I. E. (1999). Chapter 2: Evolutionary Origin of Mitochondria. *John Wiley & Sons, Inc.* DOI: 10.1002/0471223891.ch2
- Schneider, J., Dickinson, M. H., Levine, J. D. (2012). Social structures depend on innate determinants and chemosensory processing in *Drosophila*. *PNAS* 109(Suppl 2): 17174-17179
- Schwarz, T. (2006). Transmitter Release at the Neuromuscular Junction. *International Review of Neurobiology* 75: 105-144
- Sell, C., Dumenil, G., Deveaud, C., Miura, M., Coppola, D., DeAngelis, T., Rubin, R., Efstratiadis, A., Baserga, R. (1994). Effect of a null mutation of the insulin-like growth factor I

receptor gene on growth and transformation of mouse embryo fibroblasts. *Molecular and Cell Biology* 14: 3604-3612

Semitink, J., van den Heuvel, L., DiMauro, S. (2001). The genetics and pathology of oxidative phosphorylation. *Nature Reviews Genetics* 2: 342-352

Sifroni, K. G., Damiani, C. R., Stoffel, C., Cardoso, M. R., Ferreira, G. K., Jeremias, I. C., Rezin, G. T., Scaini, G., Schuck, P. F., Dal-Pizzol, F., Streck, E. L. (2010). Mitochondrial respiratory chain in the colonic mucosal of patients with ulcerative colitis. *Molecular and Cellular Biochemistry* 342: 111-115

Simon, A. F., Chou, M.-T., Salazar, E. D., Nicholson, T., Saini, N., Metchev, S., Krantz, D. E. (2012). A simple assay to study social behaviour in *Drosophila*: measurement of social space within a group. *Genes, Brain and Behaviour* 11(2): 243-252

Simon, J. C., Dickinson, M. H. (2010). A New Chamber for Studying the Behavior of *Drosophila*. *PLoS One* 5(1): e8793

Smith, P. M., Fox, J. L., Winge, D. R. (2012). Biogenesis of the cytochrome *bc*₁ complex and role of assembly factors. *Biochimica et Biophysica Acta – Bioenergetics*. 1817(2): 276-286

Stumpf, J. D., Copeland, W. C. (2011). Mitochondrial DNA replication and disease: insights from DNA polymerase γ mutations. *Cellular and Molecular Life Sciences* 68: 219-233

Suomi, S. J. (1997). Early determinants of behaviour: evidence from primate studies. *British Medical Bulletin* 53(1): 170-184

Swanson, J. M., Flodman, P., Kennedy, J., Spence, M. A., Moyzis, R., Schuck, S., Murias, M., Moriarity, J., Barr, C., Smith, M., Ponser, M. (2000). Dopamine genes and ADHD. *Neuroscience and Biobehavioral Reviews* 24: 21-25

Tempel, B. L., Livingstone, M. S., Quinn, W. G. (1984). Mutations in the dopa decarboxylase gene affect learning in *Drosophila*. *PNAS* 81: 3577-3581

"The Nobel Prize in Physiology or Medicine 1933". *Nobelprize.org*. Nobel Media AB 2013. Web. 18 Dec 2013. Available at: <http://www.nobelprize.org/nobel_prizes/medicine/laureates/1933/index.html>

Thibault, S. T., Singer, M. A., Miyazaki, W. Y., Milash, B., Dompe, N. A., Singh, C. M., Bucholz, R., Demsky, M., Fawcett, R., Francis-Lang, H. L., Ryner, L., Cheung, L. M., Chong, A., Erickson, C., Fisher, W. W., Greer, K., Hartouni, S. R., Howie, E., Jakkula, L., Joo, D., Killpack, K., Laufer, A., Mazzotta, J., Smith, R. D., Stevens, L. M., Stuber, C., Tan, L. R., Ventura, R., Woo, A., Zakrajsek, I., Zhao, L., Chen, F., Swimmer, C., Kopczynski, C., Duyk, G., Winberg, M. L. Margolis, J. (2004). A complementary transposon tool kit for *Drosophila melanogaster* using *P* and *Piggybac*. *Nature Genetics* 36(3): 283-289

- Thompson, P. M., Sower, A. C., Perrone-Bizzozero, N. I. (1998). Altered levels of the synaptosomal associated protein SNAP-25 in schizophrenia. *Biological Psychiatry* 43(4): 239-243
- Tiranti, V., Jaksch, M., Hofmann, S., Galimberti, C., Hoertnagel, K., Lulli, L., Freisinger, P., Bindoff, L., Gerbitz, K. D., Comi, G.-P., Uziel, G., Zeviani, M., Meitinger, T. (2001). Loss-of-Function Mutations of SURF-1 Are Specifically Associated with Leigh Syndrome with Cytochrome *c* Oxidase Deficiency. *Annals of Neurology* 46(2): 161-166
- Toivonen, J. M., O'Dell, K. M. C., Petit, N., Irvine, S. C., Knight, G. K., Lehtonen, M., Longmuir, M., Luoto, K., Touraille, S., Wang, Z., Alziari, S., Shah, Z. H., Jacobs, H. T. (2001). *Technical knockout*, a Drosophila Model of Mitochondrial Deafness. *GENETICS* 159(1): 241-254
- Van Dyck, E., Jank, B., Ragnini, A., Schweyen, R. J., Duyckaerts, C., Sluse, F., Foury, F. (1995). Overexpression of a novel member of the mitochondrial carrier family rescues defects in both DNA and RNA metabolism in yeast mitochondria. *Molecular and General Genetics* 246(4): 426-436
- Van Goethem, G., Dermaut, B., Lofgren, A., Martin, J.-J., Van Broeckhoven, C. (2001). Mutation of POLG is associated with progressive external ophthalmoplegia characterized by mtDNA deletions. *Nature Genetics* 28:211–212
- Van Os, J., Kapur, S. (2009). Schizophrenia. *The Lancet* 374: 635-645
- Venda, L. L., Cragg, S. J., Buchman, V. L., Wade-Martins, R. (2010). A-Synuclein and dopamine at the crossroads of Parkinson's disease. *Trends in Neurosciences* 33(12): 559-568
- Vilinsky, I., Stewart, B. A., Drummond, J., Robinson, I., Deitcher, D. L. (2002). A Drosophila SNAP-25 Null Mutant Reveals Context-Dependent Redundancy With SNAP-24 in Neurotransmission. *Genetics* 162(1): 259-271
- Vispaa, I., Fellman, V., Vesa, J., Dasvarma, A., Hutton, J. L., Kumar, V., Payne, G. S., Makarow, M., Van Coster, R., Taylor, R. W., Turnbull, D. M., Suomalainen, A., Peltonen, L. (2002). GRACILE syndrome, a lethal metabolic disorder with iron overload, is caused by point mutations in BCS1L. *American Journal of Human Genetics* 71: 863-876
- Wang, L., Munch-Petersen, B., Sjöberg, A. H., Hellman, U., Bergman, T., Jörnvall, H., Eriksson, S. (1999). Human thymidine kinase 2: molecular cloning and characterisation of the enzyme activity with antiviral and cytostatic nucleoside substrates. *FEBS Lett.* 443(2): 170–174
- White, K. E., Humphrey, D. M., Firth, F. (2010). The dopaminergic system in the ageing brain of *Drosophila*. *PLoS ONE* 5(1): e8793
- Wilson, M. C. (2000). Colomba mouse mutant as an animal model of hyperkinesia and attention deficit hyperactivity disorder. *Neuroscience & Biobehavioural Reviews* 24: 51-57

- Wittchen, H. U., Jacobi, F., Rehm, J., Gustavsson, A., Svensson, M., Jönsson, B., Olesen, J., Allgulander, C., Alonso, J., Faravelli, C., Fratiglioni, L., Jennum, P., Lieb, R., Maercker, A., van Os, J., Preisig, M., Salvador-Carulla, L., Simon, R., Steinhausen, H.-C. (2011). The size and burden of mental disorders and other disorders of the brain in Europe 2010. *European Neuropsychopharmacology* 21(9): 655-679
- Wittkopp, P. J., True, J. R., Carroll, S. B. (2002). Reciprocal functions of the *Drosophila* Yellow and Ebony proteins in the development and evolution of pigment patterns. *Development* 129: 1849-1858
- Wright, T. R. F. (1987). The genetics of biogenic amine metabolism, sclerotization and melanisation in *Drosophila melanogaster*. *Advanced Genetics* 24: 127-222
- Yoon, H., Zhang, Y., Pain, J., Lyver, E. R., Lesuisse, E., Pain, D., Dancis, A. (2011). Rim2, a pyrimidine nucleotide exchanger, is needed for iron utilization in mitochondria. *Biochemical Journal* 440(1): 137-146
- Young, C. E., Arima, K., Xie, J., Hu, L., Beach, T. G., Falkai, P., Honer, W. G. (1998). SNAP-25 deficit and hippocampal connectivity in schizophrenia. *Cerebral Cortex* 8: 261-268
- Yuan, J., Lipinski, M., Degtarev, A. (2003). Diversity in the Mechanisms of Neuronal Cell Death. *Neuron* 40(2): 401-413
- Zhang, B., Stewart, B. (2010). Electrophysiological Recording from *Drosophila* Larval Body-Wall Muscles. *Cold Spring Harbor Protocols* doi:10.1101/pdb.prot5487
- Zhang, Z., Huang, L., Shulmeister, V. M., Chi, Y.-I., Kim, K. K., Hung, L.-W., Crofts, A. R., Berry, E. A., Kim, S.-H. (1998). Electron transfer by domain movement in cytochrome *bc₁*. *Nature* 392: 677-684
- Zordan, M. A., Cisotto, P., Benna, C., Agostino, A.m Rizzo, G., Piccin, A., Pegoraro, M., Sandrelli, F., Perini, G., Tognon, G., De Caro, R., Peron, S., te Kronniè, T., Megighian, A., Reggiani, C., Zeviani, M., Costa, R. (2006). Post-transcriptional Silencing and Functional Characterization of the *Drosophila melanogaster* Homolog of *Surfl*. *GENETICS* 172(1): 229-241
- Zubieta-Calleja, G., Paulev, P.-E. (2004). *New Human Physiology: 2nd Edition*. University of Copenhagen and Panum Institute of Medical Physiology, Copenhagen. ISBN: 87-984078-0-5

APPENDIX I: **SOLUTION RECIPES**

Cornmeal-yeast-agar medium

Ingredient	Amount (for 4L medium)	Source
Cornmeal	288 gr	Genessee Scientific
Sucrose	317.2 gr	N/A
Yeast	200 gr	Sigma-Aldrich
Agar Type II	34 gr	Apex™
Propionic Acid	12 mL	Sigma-Aldrich
Tegosept (2gr/10mL EtOH)	54 mL	Genessee Scientific

HL3A

Reagent	Final Concentration	Source
KCl	5.1 mM	RP Normapur™
MgCl ₂	42 mM	Fluka
NaCl	69.8 mM	Sigma-Aldrich
Sucrose	115 mM	Sigma-Aldrich
Trehalose	1.1 mM	Sigma-Aldrich

PBS

Reagent	Final Concentration	Source
NaCl	137mM	Sigma-Aldrich
KCl	2.68mM	RP Normapur™
Na ₂ HPO ₄	10.14mM	Sigma-Aldrich
KH ₂ PO ₄	1.76mM	Sigma-Aldrich

20% PFA Stock (in PBS)

Reagent	Final Concentration	Source
Paraformaldehyde	20%	Sigma-Aldrich
NaOH	1.5 mM	Carlo Erba Reagents

0.3% PBST

Reagent	Final Concentration	Source
NaCl	137mM	Sigma-Aldrich
KCl	2.68mM	RP Normapur™
Na ₂ HPO ₄	10.14mM	Sigma-Aldrich
KH ₂ PO ₄	1.76mM	Sigma-Aldrich
Triton-X 100	0.3%	Sigma-Aldrich

0.05% PBST

Reagent	Final Concentration	Source
NaCl	137mM	Sigma-Aldrich
KCl	2.68mM	RP Normapur™
Na ₂ HPO ₄	10.14mM	Sigma-Aldrich
KH ₂ PO ₄	1.76mM	Sigma-Aldrich
Triton-X 100	0.05%	Sigma-Aldrich

1% PBSTA

Reagent	Final Concentration	Source
NaCl	137mM	Sigma-Aldrich
KCl	2.68mM	RP Normapur™
Na ₂ HPO ₄	10.14mM	Sigma-Aldrich
KH ₂ PO ₄	1.76mM	Sigma-Aldrich
Triton-X 100	0.05%	Sigma-Aldrich
Bovine Serum Albumin	1%	Sigma-Aldrich

0.1% PBSTA

Reagent	Final Concentration	Source
NaCl	137mM	Sigma-Aldrich
KCl	2.68mM	RP Normapur™
Na ₂ HPO ₄	10.14mM	Sigma-Aldrich
KH ₂ PO ₄	1.76mM	Sigma-Aldrich
Triton-X 100	0.05%	Sigma-Aldrich
Bovine Serum Albumin	0.1%	Sigma-Aldrich

Seahorse Program

Step	Command	Duration	Step	Command	Duration
1	Calibrate	0 min	10	Inject 20mM Glucose	0 min
2	Mix	2 min	11	Repeat Step 6-9 (3X)	19.5 min
3	Wait	2 min	12	Inject 5µM Rotenone and Antimycin	0 min
4	Repeat Step 2 and 3 (3X)	12 min	13	Repeat Step 6-9 (3X)	19.5 min
5	Measure	1.5 min	14	Inject HL3A	0 min
6	Mix	3 min	15	Repeat Step 6-9 (3X)	19.5 min
7	Wait	2 min	16	Inject HL3A	0 min
8	Measure	1.5 min	17	Repeat Step 6-9 (3X)	19.5 min
9	Repeat Step 6-9	7.5 min	18	End Program	

Iron Extraction Buffer

Reagent	Final Concentration	Source
Tris	10mM	Sigma-Aldrich
NaCl	137mM	Sigma-Aldrich
Triton-X 100	1%	Sigma-Aldrich
Glycerol	1%	Carlo Erba Reagents

TAE (50X Stock)

Reagent	Final Concentration	Source
Glacial Acetic Acid	951mM	Carlo Erba Reagents
Tris-Base	2M	Sigma-Aldrich
EDTA	50mM	Sigma-Aldrich

1% Agarose Gel

Reagent	Final Concentration	Source
Glacial Acetic Acid	19.02 mM	Carlo Erba Reagents
Tris-Base	0.04M	Sigma-Aldrich
EDTA	1mM	Sigma-Aldrich
Agarose	1%	Sigma
EtBr	5µg/ml	Sigma

DNA Extraction Buffer

Reagent	Final Concentration	Source
Tris-HCl pH 8.2	10mM	Sigma-Aldrich
EDTA	2mM	Sigma-Aldrich
NaOH	25mM	Carlo Erba Reagents

Modified TAE (50X Stock)

Reagent	Final Concentration	Source
Glacial Acetic Acid	951mM	Carlo Erba Reagents
Tris-Base	2M	Sigma-Aldrich
Na ₂ EDTA	5mM	Sigma-Aldrich

Modified TAE 1% Agarose Gel

Reagent	Final Concentration	Source
Glacial Acetic Acid	19.02mM	Carlo Erba Reagents
Tris-Base	0.04M	Sigma-Aldrich
Na ₂ EDTA	0.1mM	Sigma-Aldrich
Agarose	1%	Sigma
EtBr	5µg/ml	Sigma

SOC Medium

Reagent	Final Concentration	Source
Tryptone	2%	Sigma-Aldrich
Yeast Extract	0.5%	Sigma-Aldrich
NaCl	10mM	Sigma-Aldrich
KCl	2.5mM	RP Normapur TM
MgCl ₂	10mM	Sigma-Aldrich
MgSO ₄	10mM	Sigma-Aldrich
Glucose	20mM	Sigma-Aldrich

LB Broth

Reagent	Final Concentration	Source
N-Z-Case [®] Plus	1%	Fluka
Yeast Extract	0.5%	Sigma-Aldrich
NaCl	171 mM	Sigma-Aldrich

LB Agar

Reagent	Final Concentration	Source
N-Z-Case [®] Plus	1%	Fluka
Yeast Extract	0.5%	Sigma-Aldrich
NaCl	171 mM	Sigma-Aldrich
Agar	2%	Sigma-Aldrich

RIPA Buffer

Reagent	Final Concentration	Source
Tris-HCl pH 8.0	10mM	Sigma-Aldrich
NaCl	200mM	Sigma-Aldrich
Triton X-100	1%	Sigma-Aldrich
SDS	0.1%	Sigma-Aldrich
Na deoxycholate	1%	Sigma-Aldrich
NaF	0.05M	Sigma-Aldrich

Protein Extraction Buffer

Reagent	Final Concentration	Source
Hepes pH 7.5	20mM	Sigma-Aldrich
KCl	100mM	Sigma-Aldrich
Glycerol	5%	Carlo Erba Reagents
EDTA	10mM	Sigma-Aldrich
Triton X-100	0.1%	Sigma-Aldrich
DTT	1 mM	Sigma-Aldrich
PMSF	0.5 μ M	Sigma-Aldrich
Apoprotein	20 μ g/mL	Sigma-Aldrich
Leupeptin	10 μ M	Sigma-Aldrich
Pepstatin A	2 μ g/mL	Sigma-Aldrich

TBST

Reagent	Final Concentration	Source
Tris HCl pH 7.5	0.01M	Sigma-Aldrich
NaCl	0.14M	Sigma-Aldrich
Tween-20	0.05%	Sigma-Aldrich

MOPS Running Buffer (20X Stock)

Reagent	Final Concentration	Source
MOPS	1M	Sigma-Aldrich
Tris Base	1M	Sigma-Aldrich
SDS	69.3mM	Sigma-Aldrich
EDTA	20.5mM	Sigma-Aldrich

5X Blocking Buffer

Reagent	Final Concentration	Source
Tris HCl pH 7.5	0.01M	Sigma-Aldrich
NaCl	0.14M	Sigma-Aldrich
Tween-20	0.05%	Sigma-Aldrich
Non-Fat Powdered Milk	5%	Nestle®

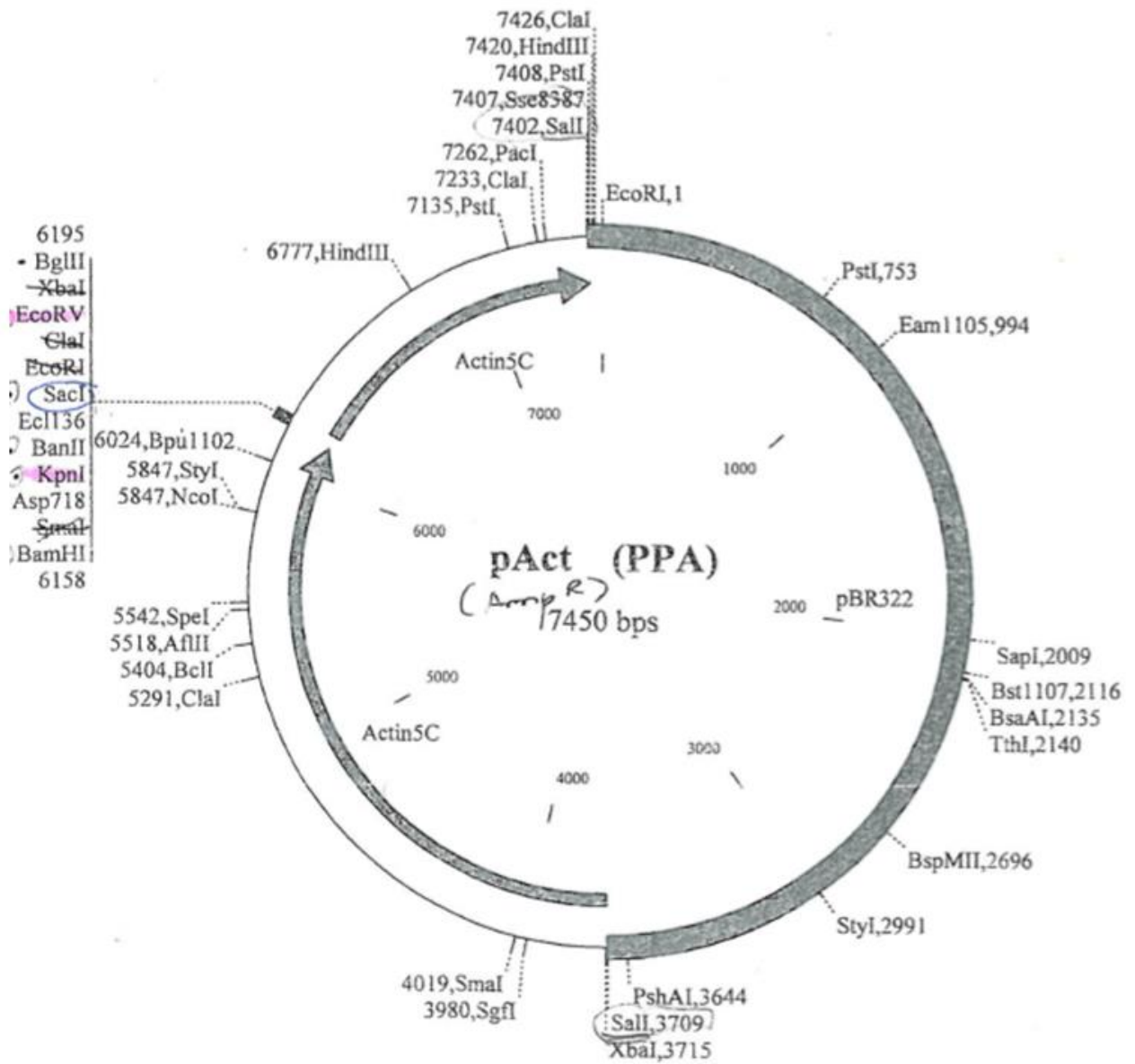
Transfer Buffer

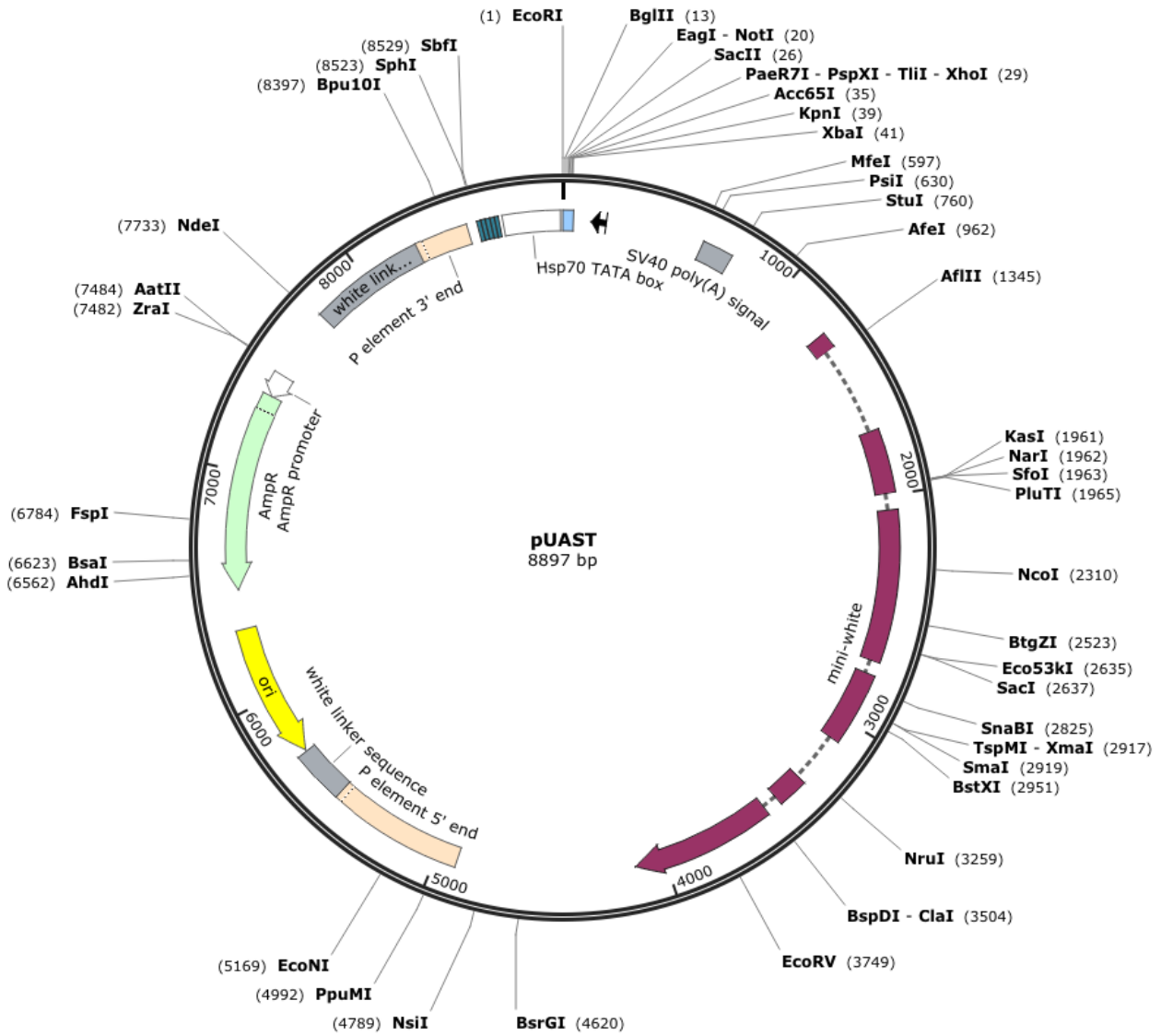
Reagent	Final Concentration	Source
Bicine	50mM	Sigma-Aldrich
Bis-Tris	50mM	Sigma-Aldrich
EDTA	2.05mM	Sigma-Aldrich
Methanol	10%	Sigma-Aldrich

ECL

Reagent	Final Concentration	Source
Tris-HCl pH 8.5	0.1 M	Sigma-Aldrich
Cumaric Acid (0.2mM in DMSO)	0.44 μ M	Sigma-Aldrich
Luminol (2.25mM in DMSO)	11.25 μ M	Sigma-Aldrich
H ₂ O ₂ (30%)	0.009%	Sigma-Aldrich

APPENDIX II: **VECTOR MAPS**





Source: www.snapgene.com